

# **Molecular Genetic Analysis of Primary Congenital Glaucoma in Indian Population**

**THESIS**

Submitted in partial fulfilment  
of the requirements for the degree of  
**DOCTOR OF PHILOSOPHY**

by

**KIRANPREET KAUR**

Under the Supervision of  
**Dr. Subhabrata Chakrabarti**



**BIRLA INSTITUTE OF TECHNOLOGY AND SCIENCE  
PILANI (RAJASTHAN) INDIA**

**2008**



**BIRLA INSTITUTE OF TECHNOLOGY & SCIENCE  
PILANI RAJASTHAN**

**CERTIFICATE**

This is to certify that the thesis entitled “**Molecular Genetic Analysis of Primary Congenital Glaucoma in Indian Population**” which is submitted by **Kiranpreet Kaur**, ID No. **2003PHXF424**, for award of Ph.D. degree of the institute, embodies original work done by her under my supervision.

**Date:**

**DR. SUBHABRATA CHAKRABARTI**

**Scientist**

**Kallam Anji Reddy Molecular**

**Genetics Laboratory**

**L V Prasad Eye Institute**

**Hyderabad**



**BIRLA INSTITUTE OF TECHNOLOGY & SCIENCE  
PILANI RAJASTHAN**

**CERTIFICATE**

This is to certify that the thesis entitled “**Molecular Genetic Analysis of Primary Congenital Glaucoma in Indian Population**” which is submitted by **Kiranpreet Kaur**, ID No. **2003PHXF424**, for award of Ph.D. degree of the institute, embodies my original work.

**Date:**

**KIRANPREET KAUR  
ID No.2003PHXF424  
Kallam Anji Reddy Molecular  
Genetics Laboratory  
L V Prasad Eye Institute  
Hyderabad**

*DEDICATED TO MY PARENTS*



## ACKNOWLEDGMENTS

I bow my head in reverence to the Almighty who has given me the strength and helped me to get through the whole task of my thesis.

I feel immense pleasure to extend my particular debt of gratitude to my supervisor, "**Dr. Subhabrata Chakrabarti**" for helping and guiding me throughout my course of thesis. My heartfelt thanks to you Sir for helping me achieve this.

I extend my heartfelt gratitude to Prof. **D. Balasubramanian**, Director of Research, L.V Prasad Eye Institute. He is a walking source of inspiration to me. It was an opportunity of a lifetime for me to have worked with research group headed by him.

I thank **Dr Mandal** for his support in collecting the patient samples and in the clinical evaluation of *PCG* families.

I extend my heartfelt thanks to **Dr. G.N. Rao**, for letting me work at this amazing institution of achievement - L V Prasad Eye Institute. Only a visionary like him could have shaped this institution of excellence in our country.

I also thank the other faculty members, **Dr. Geeta K Vemuganti, Dr. Chitra Kannibiran, Dr. Inderjeet Kaur, Dr. Savitri Sharma, Dr. Usha Gopinathan, Dr. Ashok K Reddy and Prof Rammaiah** for being patient with me and helping me during my stay at L V Prasad Eye Institute.

I thank **Prof. Ravi Prakash**, Dean Research and Consultancy Division, **Mr SD Pohekar, Mr SS Deshmukh, Mr Dinesh and Mr. Sharad Shrivastava** of BITS Pilani, for guiding me with various procedures, and rules and regulations of BITS.

**Mr. Koteswara, Mr. Shiva** and **Mr. Kumar** from the Information Systems Dept. for all those wonderful posters, they made for me for presentations at various conferences, **Mr. Jobi Kurien** and **Mr. Avinash** from Medical Records Dept, for their help in pulling out the MRD files. Special thanks to the whole staff of clinical biochemistry for their kind help in the collection of blood samples during the course of my study.

I thank **Mr. Krishnaiah** from the Biostatistics Department, for helping me in the statistical analysis.

The financial support received from **CSIR/UGC** as JRF and SRF fellowships is greatly acknowledged.

Finally I also take the opportunity to thank my friends from lab and outside lab for their support.

My special thanks to my best friend **Anees** for her support and love. Her company was a great support for me to cope with the tough times.

Last but not the least; I am highly grateful to '**My Parents**'. I bow my head to them. I could not have asked for more loving and inspiring parents. My heartfelt thanks to my twin sister, "**Kamal**", for her unconditional support and love. I am thankful to God for blessing me with the best sister in this world. I also thank my brother -in-law "**Ananath**", my younger brother "**Preet**" and his wife "**Manjeet** for being patient while listening to my problems and for their valuable suggestions and support.

My special thanks to the **PCG patients** and their families who played a major role in my thesis by providing their samples.

---

**ABSTRACT**

Primary Congenital Glaucoma (PCG) is the most common form of childhood blindness caused by an unknown developmental defect of the trabecular meshwork (TM) and anterior chamber angle. PCG is inherited in an autosomal recessive manner. Three loci have been linked to PCG at 2p21 (*GLC3A*), 1p36 (*GLC3B*) and 14q24.3 (*GLC3C*), of which, the *GLC3A* harbors cytochrome P4501b1 (*CYP1B1*) gene. The proportion of PCG-associated *CYP1B1* mutations varies from 13.3%-100% globally. However, the function of *CYP1B1* in PCG pathogenesis is yet unknown. Several studies have demonstrated that majority of the PCG cases are partially or completely unlinked to *CYP1B1* suggesting the involvement of other candidate genes in the disease pathogenesis. But the genetic bases of such cases are yet to be unveiled. To address these issues, the present study was designed to understand the spectrum of *CYP1B1* mutations in a cohort of Indian PCG patients, explore the involvement of two glaucoma associated genes (*MYOC* and *FOXC1*) in PCG cases that are unlinked to *CYP1B1* and undertake a genotype-phenotype correlation.

The study protocol was approved by Institutional Review Board and adhered to the guidelines of Declaration of Helsinki. Based on a stringent inclusion and exclusion criteria, consecutively diagnosed unrelated PCG cases (n=301) from 12 different states of India, presenting at the L.V. Prasad Eye Institute from January 2001-December 2006 along with unaffected normal controls (n=157) were enrolled. Blood samples were collected from patients and controls with prior informed consent. The coding regions of three candidate genes (*CYP1B1*, *MYOC* and *FOXC1*) were amplified by the polymerase chain reaction (PCR) and screened for mutations by a combination of SSCP, dHPLC and

resequencing. The allele and genotype frequencies were calculated by the gene counting method. The association of SNPs with the disease was determined by  $\chi^2$  test and odds ratios for the alleles and genotypes with 95% confidence intervals. Further analysis was done with the SPSS statistical software (version 14.0). Analysis of disease outcome was examined with respect to IOP, and computed by the Kaplan-Meier product limit method. Univariate analysis was performed using Cox's proportional hazard model to determine the hazards probabilities of IOP with the disease prognosis.

*CYP1B1* screening led to the identification of 38 different mutations in 43.8% (132/301) cases, of which 25 were novel. Among the patients with *CYP1B1* mutations, 24.3% (73/301) were homozygous, 5.9% (18/301) compound heterozygous and 13.6% (41/301) were heterozygous for *CYP1B1* mutations, respectively. The Arg368His was the most prevalent mutation identified in 20.9% (63/301) cases. To the best of our knowledge the current study reports the largest series of PCG cases screened so far. The proportion of *CYP1B1* mutation in our patient cohort was similar to those reported from Brazil (50%), Turkey (42.9%) and France (48.4%). Majority of the identified mutations were missense (73.7%), similar to Australian (70.0%), Turkish (75%), Kuwait (75%) and Indonesian (75%) PCG populations. Of the 301 PCG cases screened for *CYP1B1*, 169 cases (56.1%) did not harbor any *CYP1B1* mutation. A similar scenario was observed in other PCG populations from Brazil (50%), Japan (63.6%), Morocco (65.6%), France (51.6%), Turkey (57.1%) and Mexico (66.7%).

There were no significant differences between cases with and without *CYP1B1* mutation with respect to IOP at presentation ( $p = 0.16$ ) and mean corneal diameter ( $p = 0.18$ ). No significant association was noted between Arg368His mutation and the severity of the

disease based on age at onset ( $p= 0.87$ ), corneal diameter ( $p= 0.3$ ) and IOP at presentation ( $p= 0.41$ ). Genotype phenotype correlation data revealed that cases with *CYP11B* mutation had poor prognosis in terms of IOP reduction following surgical intervention up to one year, compared to cases that did not harbor *CYP11B* mutation ( $p= 0.038$ ). However, no significant difference ( $p>0.05$ ) was observed between the cases with and without *CYP11B* mutations, in terms of IOP reduction, after 1 year of surgical intervention.

PCG cases with either heterozygous *CYP11B* mutation ( $n=41$ ) or without any mutation ( $n=169$ ) were screened for two candidate (*MYOC* and *FOXC1*) genes. Screening of *MYOC* led to the identification of 2 heterozygous mutations (Gln48His and Tyr479His) in 4.3% (9/210) cases. The frequency of *MYOC* mutations in PCG was comparable to the global frequency of *MYOC* mutations (3-5%) in POAG cases. The Gln48His was the most prevalent mutation identified in 3.8% (8/210) cases. It has also been identified in other forms of glaucoma in Indian population. The digenic inheritance of *CYP11B* and *MYOC* was observed in one PCG family. To the best of our knowledge, this is the first report on the involvement of *MYOC* in a small proportion of cases that also suggested the possible digenic inheritance of *CYP11B* and *MYOC* in PCG. The patient with both *CYP11B* and *MYOC* mutations exhibited a relatively severe phenotype with respect to IOP at presentation compared to cases that exhibited only *MYOC* mutations. The severity of the disease in case of digenic inheritance could be due to the effect of two mutant alleles of two different genes.

*FOXC1* screening revealed 5 novel heterozygous mutations (His128Arg, Cys135Tyr, g.1086delC, g.1155-1163del9 and g.1947dup25) in 2.4% (5/210) families. The co-inheritance of *FOXC1* with *CYP1B1* mutations were observed in two PCG families, but a clear-cut digenic pattern could not be established. To the best of our knowledge, this is the first report on the involvement of *FOXC1* that accounted for a small proportion of cases. The patients with different *FOXC1* mutations showed similar clinical manifestations.

The present study provides information on the mutation spectrum of three candidate genes (*CYP1B1*, *MYOC* and *FOXC1*) in PCG cases where they jointly accounted for 48% (145/301) of PCG. The data obtained from the present study provides a better understanding on the genetic basis of PCG in the Indian context. This could be useful in developing an inexpensive diagnostic tool for screening the prevalent mutations in the predisposed families.

## TABLE OF CONTENTS

<b>CHAPTER 1: INTRODUCTION</b>	1-8
<b>CHAPTER 2: LITERATURE REVIEW</b>	
2.1. Glaucoma	9
2.2. Aqueous humour	9
2.2.1 Composition of aqueous humour	10
2.2.2 Functions of Aqueous humour	11
2.2.3 Drainage of Aqueous humour	11
2.3 Trabecular Meshwork	13
2.4 Classification of Glaucoma	15
2.4.1 Based on etiology	15
2.4.2 Based on mechanism	17
2.5 Epidemiology of OAG and ACG	20
2.6 Developmental glaucoma	21
2.6.1 Primary Congenital Glaucoma	21
2.6.2 Developmental glaucomas with associated anomalies	21
2.7 Primary Congenital Glaucoma	21
2.7.1 Prevalence of PCG worldwide	24
2.7.2 Pathogenesis of PCG	24
2.7.3 Genetics of PCG	26
2.7.4 Candidate loci/genes in PCG	26
2.7.4.1 <i>GLC3A</i>	26
2.7.4.2 Candidate gene screening	29
2.7.4.3 <i>GLC3B</i>	30
2.7.4.4 <i>GLC3C</i>	32
2.8 Cytochrome P450 1B1 ( <i>CYP1B1</i> )	34
2.8.1 Nomenclature and families of CYP450	35
2.8.2 Functions of P450	36
2.8.3 Isolation and Characterization of <i>CYP1B1</i>	37
2.8.3.1 Characterization of <i>CYP1B1</i> promoter	39
2.8.4 Association CYP450 with other diseases	41
2.8.5 Expression of CYP450 in ocular tissues	42
2.8.6 Use of <i>Cyp1b1</i> knockout mice in order to determine its role in PCG pathogenesis	44
2.8.7 Potential role of <i>CYP1B1</i> in development through retinoic acid mediated signaling	45
2.8.8 Mutation spectrum of <i>CYP1B1</i> worldwide	46
2.8.9 Prevalent mutations in <i>CYP1B1</i>	53
2.8.10 Clustering of prevalent <i>CYP1B1</i> mutations on common haplotype backgrounds	54
2.8.11 <i>CYP1B1</i> in other forms of glaucoma	58
2.8.12 Interaction of <i>CYP1B1</i> with other genes	59
2.8.13 Histological abnormalities in PCG	60
2.8.14 <i>CYP1B1</i> mutations with PCG pathogenesis	64
2.8.15 <i>in silico</i> studies on <i>CYP1B1</i> mutations	64
2.8.16 <i>in vitro</i> studies on <i>CYP1B1</i> mutations	65
2.8.17 Mislocalization of <i>CYP1B1</i> proteins	66
2.9 Hypothesis for the possible role of <i>CYP1B1</i> in PCG pathogenesis	66
2.10 MYOCILIN	67
2.10.1 <i>MYOC</i> expression in human tissues	68

2.10.2 <i>MYOC</i> mutations in glaucoma	68
2.10.3 Uniqueness of Q48H in Indian Glaucomas	72
2.10.4 Models for <i>MYOC</i> association with Glaucoma	73
2.11 Forkhead boxC1 ( <i>FOXC1</i> )	74
2.11.1 Expression of <i>FOXC1</i> in human tissues	76
2.11.2 <i>FOXC1</i> in ocular anomalies	77
2.12 Genotype Phenotype correlation with respect to <i>CYP11B1</i> mutations	81
2.13 Conclusion	83
<b>CHAPTER 3: MATERIALS AND METHODS</b>	
3.1 Enrollment of Patients and Controls	85
3.2 Clinical Examination	85
3.2.1 Slit Lamp examination	85
3.2.2 Tonometry	86
3.2.3 Gonioscopy	87
3.2.4 Ophthalmoscopy	88
3.3 Inclusion criteria for PCG cases	88
3.3.1 Rationale for the parameters in the inclusion criteria	88
3.4 Exclusion criteria for PCG cases	90
3.5 Enrollment of controls	91
3.6 Clinical and Demographic features of PCG cases	91
3.6.1 State-wise distribution of cases	91
3.6.2 Age at onset	92
3.6.3 Family history and consanguinity	92
3.6.4 Gender	93
3.7 Sample Collection	93
3.8 Molecular Analysis	93
3.8.1 Extraction of Genomic DNA	93
3.8.1.1 Protocol for DNA extraction	93
3.8.2 Quantification of genomic DNA	95
3.8.3 Amplification of candidate genes by polymerase chain reaction (PCR)	96
3.8.4 Confirmation of PCR amplification by agarose gel electrophoresis	98
3.8.4.1 Preparing of gel	98
3.8.4.2 Loading and running of the gel	99
3.8.5 Mutation detection	99
3.8.5.1 Single stranded conformation polymorphism (SSCP)	100
3.8.5.1.1 Protocol for SSCP	101
3.8.5.1.1.1 Preparing of samples	101
3.8.5.1.1.2 Gel electrophoresis	101
3.8.5.1.1.3 Protocol for Silver staining	103
3.8.5.2 Denaturing High Performance liquid chromatography (dHPLC)	103
3.8.5.2.1 Protocol for dHPLC	104
3.8.5.3 Bi-directional Automated Sequencing	107
3.8.5.3.1 Purification of amplicons	108
3.8.5.3.2 Sequencing PCR	109
3.8.5.3.3 Precipitation of sequencing PCR products	110
3.8.5.3.3.1 Protocol for precipitation	110
3.8.5.3.4 Electrophoresis	111
3.8.5.3.5 Data analysis	113
3.8.5.3.5.1 Multiple sequence alignment	113



3.8.5.3.5.2 SIFT Scores	113
3.8.5.3.5.3 Characterization of variants	114
3.8.5.4 PCR based restriction digestion	114
3.8.5.4.1 Protocol for Restriction digestion	117
3.8.5.4.2 Gel electrophoresis	117
3.9.5.4.3 Detection	117
3.8.6 Statistical analysis	118
<b>CHAPTER 4: RESULTS</b>	
4.1 Demographics of the PCG cases enrolled	119
4.2 Mutational analysis of <i>CYP11B1</i>	120
4.2.1 Distribution of cases and controls for screening	120
4.2.2 Screening of <i>CYP11B1</i>	121
4.2.3 Location of mutations in <i>CYP11B1</i> protein	127
4.2.4 Description of <i>CYP11B1</i> mutations in PCG patients	128
4.2.5 Conservation of the residues	157
4.2.6 Single nucleotide polymorphisms in <i>CYP11B1</i>	160
4.2.6.1 Distribution of <i>CYP11B1</i> SNPs in different categories	160
4.2.7 <i>CYP11B1</i> involvement in PCG cases worldwide	168
4.2.7.1 Arg368His-the prevalent mutation	168
4.3 Genotype Phenotype of <i>CYP11B1</i> mutations	169
4.3.1 Comparison with respect to mean IOP	170
4.3.2 Univariate Cox regression analysis	171
4.3.3 Survival analysis	171
4.4 Screening of other candidate genes	173
4.4.1 Mutational analysis of <i>MYOC</i>	173
4.4.1.1 Denaturing high performance liquid chromatography (dHPLC) for Gln48His	173
4.4.1.2 Synonymous changes in <i>MYOC</i>	175
4.4.1.3 Conservation of the residues	178
4.4.1.4 Segregation of <i>MYOC</i> mutations in PCG families	179
4.4.1.5 Digenic inheritance of <i>CYP11B1</i> and <i>MYOC</i> in PCG	181
4.4.2 Mutational analysis of <i>FOXC1</i>	183
4.4.2.1 <i>FOXC1</i> mutations identified in PCG	183
4.4.2.2 Segregation of <i>FOXC1</i> mutations	190
4.4.2.3 Conservation of the residues	198
4.4.2.4 <i>FOXC1</i> polymorphisms	198
4.5 Overall involvement of the candidate genes in PCG	200
<b>CHAPTER 5: DISCUSSION</b>	201
<b>CHAPTER 6: CONCLUSIONS OF THE STUDY</b>	229
<b>CHAPTER 7: SPECIFIC CONTRIBUTIONS OF THE STUDY</b>	233
<b>CHAPTER 8: LIMITATIONS OF THE STUDY</b>	235
<b>CHAPTER 9: FUTURE SCOPE OF THE STUDY</b>	236

<b>REFERENCES</b>	237
<b>ANNEXURE I</b>	254
<b>ANNEXURE II</b>	255
<b>ANNEXURE III</b>	256
<b>ANNEXURE IV</b>	257
<b>LIST OF PUBLICATIONS</b>	258
<b>LIST OF PRESENTATIONS</b>	260
<b>LIST OF AWARDS</b>	261
<b>BRIEF BIOGRAPHY OF THE CANDIDATE</b>	262
<b>BRIEF BIOGRAPHY OF THE SUPERVISOR</b>	263

## LIST OF TABLES

<b>Table No.</b>	<b>Title</b>	<b>Page</b>
Table 2.1	Prevalence studies of Glaucoma in Indian population	20
Table 2.2	Corneal diameter in children: normal and glaucomatous eyes	22
Table 2.3	Worldwide distribution of <i>CYP1B1</i> mutations	47
Table 2.4	Distribution of different types of <i>CYP1B1</i> mutations worldwide	51
Table 2.5.	Prevalent mutations in various PCG populations across the globe	54
Table 2.6	Distribution of PCG associated <i>CYP1B1</i> mutations across different populations on various haplotype backgrounds	56
Table 2.7	<i>CYP1B1</i> in adult onset OAG worldwide	58
Table 2.8	Correlation of <i>CYP1B1</i> mutations, slit lamp findings and histological abnormalities	63
Table 2.9	Structural analysis of PCG associated mutation in <i>CYP1B1</i>	64
Table 2.10	Worldwide distribution of <i>MYOC</i> mutations	70
Table 2.11	Distribution of Q48H mutation in Indian population	72
Table 2.12	Worldwide spectrum of <i>FOXC1</i> mutations identified in different anterior segment anomalies	78
Table 3.1	Worldwide distribution of mean IOP	89
Table 3.2	State- wise distribution of the PCG cases	92
Table 3.3	Distribution of the cases with respect to age of onset	92
Table 3.4	Primer sequences used to amplify the coding region of <i>CYP1B1</i>	96
Table 3.5	Reagents used in PCR reaction	97
Table 3.6	The methods used for the screening of candidate genes	100
Table 3.7	The reagents used for the sequencing PCR	109
Table 3.8	Various restriction enzymes used to screen the variations in candidate genes.	115
Table 3.9	Reagents used for Restriction digestion	117
Table 4.1	Comparison of demographic features of cases from different states and in comparison to AP	120
Table 4.2	Description of the PCG cases screened	121
Table 4.3	Different <i>CYP1B1</i> mutations in Indian PCG patients	121
Table 4.4	Mutations identified in Exon II of <i>CYP1B1</i>	123
Table 4.5	Mutations identified in Exon III of <i>CYP1B1</i>	125
Table 4.6	Mutations in the various domains of CYP1B1 protein	127
Table 4.7	Clinical features of patients with Tyr81Asn mutation	131

## LIST OF TABLES

Table 4.8	Clinical features of patients with Gly61Glu mutation	135
Table 4.9	Clinical features of patients with Arg368His mutation	140
Table 4.10	Clinical features of patients with Arg390Cys mutation	145
Table 4.11	Clinical features of patients with Arg390His mutation	147
Table 4.12	Single nucleotide polymorphisms (SNPs) in <i>CYP1B1</i> gene	160
Table 4.13	Allele frequency distribution of <i>CYP1B1</i> SNPs in [CYP1B1 (+)] cases and controls	162
Table 4.14	Genotype frequency distribution of <i>CYP1B1</i> SNPs in [CYP1B1 (+)] cases and controls	163
Table 4.15	Allele frequency distribution of <i>CYP1B1</i> SNPs in [CYP1B1 (-)] cases and controls	164
Table 4.16	Genotype frequency distribution of <i>CYP1B1</i> SNPs in [CYP1B1 (-)] cases and controls	165
Table 4.17	Allele frequency distribution of <i>CYP1B1</i> SNPs in cases with <i>CYP1B1</i> mutations and cases without <i>CYP1B1</i> mutations	166
Table 4.18	Genotype frequency distribution of <i>CYP1B1</i> SNPs in cases with <i>CYP1B1</i> mutations and cases without <i>CYP1B1</i> mutations	167
Table 4.19	Distribution of PCG cases screened for <i>CYP1B1</i>	168
Table 4.20	Distribution of PCG cases with Arg368His mutation	168
Table 4.21	Comparison of clinical features among the patients with R368H mutation	169
Table 4.22	Comparison between the cases with and without R368H mutation	169
Table 4.23	The t-test analysis for [CYP (+)] and [CYP (-)] cases with respect to IOP	170
Table 4.24	The Univariate Cox regression analysis for PCG cases	171
Table 4.25	Clinical features of patients with <i>MYOC</i> mutations	175
Table 4.26	Distribution of <i>FOXC1</i> gene variations in PCG patients.	186
Table 4.27	Clinical features of patients with <i>FOXC1</i> mutations	189
Table 4.28	Allele frequency of <i>FOXC1</i> polymorphisms	199
Table 4.29	Genotype frequency of <i>FOXC1</i> polymorphisms	199
Table 4.30	The overall involvement of candidate genes screened in PCG	200
Table 5.1	Worldwide distribution of homozygous, heterozygous and compound heterozygous <i>CYP1B1</i> mutations	207
Table 5.2	Distribution of recurrent <i>CYP1B1</i> mutations	211
Table 5.3	Comparison of clinical features among the patients with compound heterozygous <i>CYP1B1</i> mutations with the case with digenic inheritance	221

## LIST OF FIGURES

Figure no.	Title	Page
Figure 2.1	Schematic representation of aqueous humor outflow	10
Figure 2.2	Schematic diagram of the aqueous humor outflow through trabecular meshwork	12
Figure 2.3	The three layers of the trabecular meshwork	15
Figure 2.4	Diagrammatic representation of the drainage structures in POAG	18
Figure 2.5	Diagrammatic representation of the drainage structures in ACG	19
Figure 2.6	Haab's striae	23
Figure 2.7a	Corneal edema	23
Figure 2.7b	Epiphora	23
Figure 2.7c	Blepharospasm	24
Figure 2.8	Intermarker distance of the 14 STRs used for linkage analysis	28
Figure 2.9	The <i>GLC3A</i> critical region with the various candidate genes	30
Figure 2.10	Intermarker distance of the 14 STRs used for linkage analysis	32
Figure 2.11	Intermarker distance of the 6 STRs used for linkage analysis	33
Figure 2.12	Schematic representation various domains in <i>CYP1B1</i>	35
Figure 2.13	A schematic diagram showing the genomic organization of <i>CYP1B1</i> gene	40
Figure 2.14	Comparison of <i>CYP1B1</i> expression human fetal and adult ocular tissues	43
Figure 2.15	Spatio-temporal expression of <i>Cyp1b1</i> expression in various mouse ocular tissues	43
Figure 2.16	Comparison of anterior chamber angle structures (histological level) in wild type and <i>Cyp1b1</i> <sup>-/-</sup> mice	44
Figure 2.17	Comparison of anterior chamber angle structures (ultrastructural level) in wild type and <i>Cyp1b1</i> <sup>-/-</sup> mice	45
Figure 2.18	Worldwide distribution of <i>CYP1B1</i> mutations in cytosolic and other domains of the protein	52
Figure 2.19	Severe goniodysgenesis	61
Figure 2.20	Light micrograph of trabeculectomy specimen showing moderate goniodysgenesis	61
Figure 2.21	Light micrograph of trabeculectomy specimen showing the mild goniodysgenesis.	62
Figure 2.22	Schematic representation of Human Myocilin protein	68
Figure 2.23	Showing the various domains of FOXC1 protein	76
Figure 3.1A	Gonioscopic picture of an open angle	87
Figure 3.1B	Gonioscopic picture of a closed angle	87
Figure 3.2A	Normal optic nerve	88
Figure 3.2B	Glaucomatous optic nerve with increased cup to disc ratio	88
Figure 4.1	Distribution of cases with <i>CYP1B1</i> mutations and without <i>CYP1B1</i> mutations	122
Figure 4.2	Schematic representation of the <i>CYP1B1</i> gene with the novel mutations	127
Figure 4.3	Electropherograms showing the nine novel mutations identified in exon II of <i>CYP1B1</i> in PCG cases	153
Figure 4.4	Electropherograms showing the six novel mutations identified in exon III in PCG cases	155
Figure 4.5	Multiple sequence alignment showing the conservation of wild type residues (in the blocks) in exon II in different cytochrome families across various species	158
Figure 4.6	Multiple sequence alignment showing the conservation of wild type residues (in the blocks) in exon III in different cytochrome families across various species	159

---

Figure 4.7	Survival curve analysis for IOP in [CYP (+)] and [CYP (-)] cases	172
Figure 4.8	Heteroduplex peaks obtained in patients with heterozygous. Gln48His mutation	174
Figure 4.9	Schematic representation of the <i>MYOC</i> gene	175
Figure 4.10	Electropherograms showing the six <i>MYOC</i> variations found in PCG cases	177
Figure 4.11	Multiple sequence alignment of MYOC protein	178
Figure 4.12	The segregation of Q48H mutation in four PCG families as indicated by PCR based restriction digestion on a 9% polyacrylamide gel	180
Figure 4.13	The segregation of <i>CYP1B1</i> and <i>MYOC</i> mutation in PCG 095 family by PCR based restriction digestion on a 9% polyacrylamide gel	182
Figure 4.14	Schematic representation of the <i>FOXC1</i> gene	183
Figure 4.15	Electropherograms showing the two missense mutations identified in <i>FOXC1</i>	187
Figure 4.16	Electropherograms showing the two deletions and one duplication mutation identified in <i>FOXC1</i>	188
Figure 4.17	The <i>FOXC1</i> missense (His128Arg) mutation in PCG209 family	191
Figure 4.18	The <i>FOXC1</i> missense (Cys135Tyr) mutation in PCG216 family	192
Figure 4.19	The segregation of g.1086delC mutation in <i>FOXC1</i> in PCG 100 family by PCR based restriction digestion on a 9% polyacrylamide gel	194
Figure 4.20	Segregation of a <i>FOXC1</i> frameshift (g.1947dup25) mutation in PCG044 family	195
Figure 4.21	Segregation of a <i>FOXC1</i> deletion (g.1155delAAA) mutation in PCG196 family	197
Figure 4.22	Multiple sequence alignment of human FOXC1 protein across other members of the FOX family in humans and other species	198
Figure 5.1	The involvement of <i>CYP1B1</i> mutations in various populations across the globe	204

## ABBREVIATIONS

µg	Microgram
µl	Microlitre
µM	Micromolar
A	Adenine
bp	Basepair
C	Cytosine
cDNA	Complementary DNA
DMSO	Dimethylsulphoxide
dNTPs	deoxy nucleotide triphosphates
dup	Duplication
G	Guanine
Ins	Insertion
IOP	Intraocular pressure
JOAG	Juvenile open angle glaucoma
kDa	Kilodalton
PAC	Primary angle closure
PACG	Primary angle closure glaucoma
PAGE	Polyacrylamide gel electrophoresis
PCG	Primary congenital glaucoma
PCR	Polymerase chain reaction
POAG	Primary open angle glaucoma
RFLP	Restriction fragment length polymorphism
rpm	Revolutions per minute
SNP	Single nucleotide polymorphism
T	Thymine
TM	Trabecular meshwork
EDTA	Ethylenediaminetetraacetic acid
TAE	Tris acetate EDTA
SDS	Sodium dodecylsulphate
Tris	2-amino-2-(hydroxymethyl)propane-1,3-diol
PBS	Phosphate buffered saline
SSCP	Single stranded conformational polymorphism

dHPLC	denaturing high performance liquid chromatography
C:D	cup to disc ratio
FHD	Forkhead domain
RGC	retinal ganglion cell
TEAA	triethylammonium ion
PS-DVB	polystyrene-divinylbenzenepolymeric beads
DTH	digitally high
DTN	digitally normal
DTL	digitally low
FFL	fixing and following light
PLPR	Perception and projection of light
OD	right eye
OS	left eye
OU	both eyes
CF	counting fingers
TRAB & TRAB	Trabeculectomy and Trabeculotomy
AD	Activation domain



---

## CHAPTER 1: INTRODUCTION

Glaucoma comprises a group of clinically and genetically heterogeneous optic neuropathies characterized by an excavation of the optic disc and progressive alteration of the visual field, which if left untreated, results in an irreversible blindness (Shields *et al.*, 2005).

It is the second leading cause of blindness worldwide that accounts for 12.3% (4.4 million people) of global blindness (Resnikoff *et al.*, 2004). It has been estimated that by the year 2010, around 60.5 million people worldwide will be affected with glaucoma, which includes open angle glaucoma (OAG) and angle closure glaucoma (ACG). Over 8.4 million people will be bilaterally blind from primary glaucoma in 2010 and this figure will rise to 11.1 million by 2020 (Quigley *et al.*, 2006).

The population based epidemiological study, in the Indian state of Andhra Pradesh, estimated that blindness due to glaucoma accounts for 8.2% of overall blindness in this state (Dandona *et al.*, 2001). Primary Open Angle Glaucoma (POAG) has been reported to be the most common type of glaucoma in Southern India with a prevalence of 0.41%- 2.56% (Jacob *et al.*, 1998, Dandona *et al.*, 2000, Ramakrishnan *et al.*, 2003, Vijaya *et al.*, 2005).

Glaucomas are classified into primary and secondary based on their etiology and alterations in the aqueous humour dynamics (Shields *et al.*, 2005). Based on etiology the glaucomas are classified as primary and secondary. In primary glaucomas the causal events are largely confined to the anterior chamber angle or conventional outflow pathway with no contribution from other ocular or systemic disorders (Shields *et al.*, 2005). On the other hand secondary glaucomas are associated with other ocular or systemic abnormalities and may be responsible for the alteration in

aqueous humor dynamics such as inflammations, neovascular glaucoma, lens induced glaucoma, pigmentary and pseudoexfoliation glaucomas. Based on mechanisms, the glaucomas are classified on the basis of alterations in the anterior chamber angle of the eye. There are two forms of glaucoma in this category, i.e, POAG and primary angle closure glaucoma (PACG) (Shields *et al.*, 2005). In POAG, there is an increased resistance to the outflow of aqueous humour due to obstruction at the trabecular meshwork (TM) whereas, PACG is an anatomical disorder of the anterior segment of the eye characterized by permanent closure of part of the filtration angle as a result of the iris apposition to the TM (Ritch *et al.*, 1996).

A third category of glaucomas called the developmental glaucomas, are associated with developmental anomalies of the eye that are present at birth (Mandal and Netland, 2006). Developmental glaucomas are classified into two groups on the basis of their clinical presentation and association with other anomalies: a) Primary congenital glaucoma (PCG), which is an ocular developmental anomaly that occurs due to the obstruction in the drainage of the aqueous humor outflow caused by the maldevelopment of TM and anterior chamber angle, b) Developmental glaucomas, which are associated with other ocular anomalies like Axenfeld- Rieger syndrome (ARS), Peter's anomaly, aniridia etc (Shields *et al.*, 2005).

PCG is the most common form of childhood blindness caused by an unknown developmental defect of the TM and anterior chamber angle. It is characterized by raised intraocular pressure (IOP), buphthalmos, corneal enlargement, breaks in the Descemet's membrane (Haab's Striae), photophobia and epiphora (Mandal and Netland 2006).

The prevalence of PCG ranges from 1 in 1250 among the Gypsies of Slovakia (Gencik *et al.*, 1989), 1 in 2500 in the Saudi Arabian populations (Bejjani *et al.*, 1998) and between 1 in 10,000 and 12,000 in the Western populations (Gencik *et al.*, 1982). According to British infantile and childhood glaucoma (BIG) Eye study, the incidence of PCG in Great Britain is 1 in 18,500 live births whereas it is 1 in 30,200 in the Republic of Ireland (Papadopoulos *et al.*, 2007). In the Indian state of Andhra Pradesh it has been estimated to be 1 in 3300 live births that account for 4.2% of all childhood blindness (Dandona *et al.*, 1998).

Generally, PCG is inherited as an autosomal recessive disorder and majority of the cases are sporadic without a family history. Rare pseudodominant inheritance has also been documented in families with high rate of inbreeding and multiple consanguinity (Bejjani *et al.*, 1998). Three candidate loci have been mapped to PCG by linkage analysis at 2p21 (*GLC3A*; Stoilov *et al.* 1997), 1p36 (*GLC3B*; Akarsu *et al.*, 1996) and 14q24.3 (*GLC3C*; Stoilov *et al.*, 2002b), of which the *GLC3A* locus colocalizes the CytochromeP4501B1 (*CYP1B1*; OMIM 601771) gene (Stoilov *et al.* 1997).

Identification of *CYP1B1* as candidate gene in PCG is the first example in which mutations in a member of the cytochrome p450 superfamily have shown to be associated with a primary development defect (Stoilov *et al.*, 1997). However, the function of *CYP1B1* in aqueous humour and its association with PCG pathogenesis is yet unknown (Doshi *et al.*, 2006). *CYP1B1* protein expresses in various human ocular tissues like cornea, ciliary body, iris and retina. At the mRNA level, *CYP1B1* was identified as one of the glaucoma candidate genes to be expressed in the TM (Tomarev *et al.*, 2003). Interestingly, an increased *CYP1B1* expression has been observed in the fetal eyes compared to adult eyes. Thus, *CYP1B1* in the eye may be

metabolizing an important substrate that might play a key role in the development and maturation of ocular tissues (Doshi *et al.*, 2006).

More than 70 PCG-associated *CYP11B1* mutations have been identified in different ethnic groups (<http://www.hgmd.cf.ac.uk/ac/index.php>). The proportion of *CYP11B1* mutations varies from 13.3%-100% globally. The highest frequency of mutations has been observed in the Slovakian Gypsies (100%), followed by the Saudi Arabian (92%) populations (Plasilova *et al.*, 1999 and Bejjani *et al.*, 2000). The proportion of *CYP11B1* mutations ranges from 20-70% among the PCG population of Iran, Brazil, Indonesia and Japan (Chitsazian *et al.*, 2007, Stoilov *et al.*, 2002, Sitorus *et al.*, 2003, Mashima *et al.*, 2001). In a preliminary study on a cohort from Indian population, *CYP11B1* mutations were observed in 37.5% PCG cases (Reddy *et al.*, 2004).

Majority of the *CYP11B1* mutations are missense that ranges from 9.5% - 88.7 (Bejjani *et al.*, 2000, Mashima *et al.*, 2001, Curry *et al.*, 2004, Chitsazian *et al.*, 2007, Bagiyeva *et al.*, 2007, Dimasi *et al.*, 2007, Alfdhli *et al.*, 2006). These missense mutations affect the amino acid residues located either in the hinge region or the conserved core structures of the cytosolic domain of the protein. These mutations, therefore, are expected to interfere with fundamental properties of the protein such as folding, heme binding, substrate accommodation and interaction with the redox partner (Stoilov *et al.*, 2001, Achary *et al.*, 2006). Among the various missense mutations, G61E is the most frequent among Saudi Arabians (Bejjani *et al.*, 2000), 4340delG among Brazilians (Stoilov *et al.*, 2002), E387K among Slovakian Gypsies (Plasilova *et al.*, 1999), and R368H among the the Indian PCG patients (Reddy *et al.*, 2004), respectively. Based on the haplotypes constructed with six *CYP11B1* intragenic SNPs (-13T/C, R48G, A119S, V432L, and D449D), it was observed that the 'C-G-G-T-A' is the most common haplotype associated with different *CYP11B1* mutations in

ethnically different populations (Bejjani *et al.*, 2000, Mashima *et al.*, 2001, Stoilov *et al.*, 2002, Curry *et al.*, 2004, Sena *et al.*, 2004, Chakrabarti *et al.*, 2006).

*CYP1B1* is also implicated in juvenile and adult onset forms of glaucoma (Melki *et al.* 2004, Acharya *et al.* 2006). The percentage of *CYP1B1* mutations in POAG/JOAG ranged between 4.5% - 23.3% (Melki *et al.* 2004, Acharya *et al.* 2006, Lopez-Garrido *et al.*, 2006, Chakrabarti *et al.*, 2007, Kumar *et al.*, 2007). The association of *CYP1B1* mutations with these glaucomas suggests that it is an important candidate gene for all glaucomas worldwide (Chakrabarti *et al.*, 2007).

*CYP1B1* has also been reported to co-segregate with Myocilin (*MYOC*; OMIM 601652, a candidate gene for Primary Open Angle Glaucoma) in juvenile onset open angle glaucoma through a digenic mechanism suggesting that *CYP1B1* may be a modifier of *MYOC* expression and that these two genes might act through common biochemical pathways (Vincent *et al.* 2002). In a glaucoma family of East Indian (Guyanese) origin, it was observed that the individuals with both *CYP1B1* (R368H) and *MYOC* (G399V) mutations had juvenile form of open angle glaucoma with mean ages of onset at 27 years, whereas individuals with only *MYOC* (G399V) mutation had adult onset glaucoma with a mean ages of onset at 51 years. Based on this, it was suggested that congenital glaucoma and juvenile glaucoma are allelic variants of *CYP1B1* and that *CYP1B1* and *MYOC* might act through common biochemical pathways (Vincent *et al.* 2002).

*MYOC* expression has been demonstrated in various ocular like TM, sclera, iris, cornea, ciliary body, retina and optic nerve (Tamm *et al.*, 2002). Around 70 different glaucoma associated mutations have been reported in *MYOC* worldwide (Gong *et al.*, 2004). Mutations in *MYOC* are associated with most of the familial forms of JOAG

and 2-5% of adult-onset POAG cases ([www.myocilin.com](http://www.myocilin.com)). The most common *MYOC* mutation observed across different populations is the Gln368Stop mutation (Fingert *et al.*, 1999). The Gln48His was the predominant mutation identified in Indian population. This mutation has been identified in both JOAG (Ramprasad *et al.*, 2005), POAG (Mukhopadhyay *et al.*, 2002, Sripriya *et al.*, 2004, Chakrabarti *et al.*, 2005, Kumar *et al.*, 2007) and PCG cases (Kaur *et al.*, 2005). Gln48His has not yet been reported from any other population, suggesting its uniqueness to glaucomas in India. Although causality of all glaucoma phenotypes cannot be ascribed to the Gln48His mutation alone, it is likely that Gln48His mutation a potential risk factor towards disease predisposition.

While *MYOC* mutations are associated with adult and juvenile glaucomas in different populations, the function of *MYOC* protein in aqueous humour physiology is not known (Tamm *et al.*, 2002). It has been suggested that *MYOC* facilitates the aqueous humour outflow through the TM. Also it has a protective role against stress (Johnson *et al.*, 2000). However, *Myoc*<sup>-/-</sup> mice neither developed any symptoms of glaucoma nor any anterior chamber angle abnormalities at the ultrastructural level (Kim *et al.*, 2001). Various in vitro studies have shown that mutant *MYOC* forms insoluble aggregates that are not secreted and accumulate intracellularly indicating that its accumulation in the cytoplasm or in the extracellular matrix causes an obstruction in the normal aqueous humor outflow (Caballero *et al.*, 2000, Jacobson *et al.*, 2001, Gobeil *et al.*, 2004.).

Another interesting candidate, Forkhead box C1 (*FOXC1*; OMIM 601090) is a member of winged helix/forkhead family of transcription factors and is associated with various anterior segment anomalies like Axenfeld anomaly, Reiger anomaly, Axenfeld- Reiger anomaly (ARA), iris hypoplasia, iridogoniodysgenesis and aniridia

(Granadino *et al.*, 2000, Komatireddy *et al* 2003, Saleem *et al* 2003, Mortemousque *et al* 2004, Murphy *et al.* 2004, Weisschuh *et al.* 2006, Fuse *et al.* 2007). Almost half of these cases lead to glaucoma (Shields *et al.*, 1985). *FOXC1* expresses in various ocular tissues like trabecular meshwork, optic nerve head, choroid, ciliary body, cornea, iris, retina and lens. Moreover, histologically, the mice with heterozygous null allele (*Foxc1*<sup>+/-</sup>) were found to have anterior segment abnormalities such as small or absence of Schlemm's canal, iris hypoplasia, displaced Schwalbe's line similar to human ARA and congenital glaucoma patients (Smith *et al* 2000). So far 37 different mutations have been reported in *FOXC1* that are associated with various anterior segment anomalies, of which majority have been identified in forkhead domain (FHD) of the protein (<http://www.hgmd.cf.ac.uk/ac/all.php>). Also, *FOXC1* has been suggested to play an important role in the development of various ocular tissues including the aqueous humor drainage structures (Smith *et al.*, 2000). A preliminary screening of *FOXC1* in 6 PCG cases (Nishimura *et al.*, 1998) did not reveal any mutations. However, the *FOXC1* mutations were identified in 4 families with different anterior segment defects (Axenfeld anomaly =1, Reiger's anomaly =2, spectrum of anterior chamber defects like iris hypoplasia, embryotoxon, Reiger's anomaly and Axenfeld anomaly=1). Additionally, *FOXC1* mutations (g.1792-1793delCT and W152X) were identified in two families with Axenfeld Reiger's syndrome (Cella *et al.*, 2006), where the patients presented with glaucoma. These observations suggest the possible involvement of *FOXC1* mutations in different glaucoma phenotypes.

Although *CYP1B1* is the only candidate gene linked to PCG, the exact role of *CYP1B1* mutations with PCG pathogenesis is yet unknown (Doshi *et al.*, 2006). *CYP1B1* expresses in various human ocular tissues like cornea, ciliary body, iris and

retina. Also the *Cyp11b1* knockout (*Cyp11b1*<sup>-/-</sup>) mice showed various histological abnormalities (small Schlemm's canal, attachments of iris over cornea, basal lamina extending from cornea over TM) suggesting the possible role of *CYP11B1* in the development of these ocular structures (Libby *et al.*, 2003). *CYP11B1* has also been shown to metabolize the two step oxidative synthesis of retinoic acid (RA) from retinol (Chambers *et al.*, 2007), which is known to regulate morphogenesis during embryogenesis. Based on these observations, it was suggested that *CYP11B1* might play an important role in development via RA mediated signaling pathways (Chambers *et al.*, 2007). In several populations, majority of the PCG cases are partially or completely unlinked to *CYP11B1* (Mashima *et al.*, 2001, Stoilov *et al.*, 2002a, Sitorus *et al.*, 2003, Reddy *et al.*, 2004, Sena *et al.*, 2004, Alfadhli *et al.*, 2006, Dimasi *et al.*, 2007, Bagiyeva *et al.*, 2007, Messina-Bass *et al.*, 2007) suggesting the involvement of other candidate genes in the disease pathogenesis. But the genetic bases of such cases are yet to be unveiled. To the best of our knowledge, there are no studies in the existing literature that have addressed this question. Based on these lacunae, the present study was designed to understand the spectrum of *CYP11B1* mutations in a cohort of Indian PCG patients, explore the association of other candidate genes with PCG and undertake a genotype-phenotype correlation. The specific objectives were:

1. To estimate the frequency, distribution and mutation spectrum of *CYP11B1* in PCG cases in a cohort from India.
2. To understand the involvement of other candidate genes in PCG cases that are either heterozygous or do not harbor any *CYP11B1* mutation.
3. To undertake a genotype phenotype correlation based on IOP reduction following surgical intervention, in cases with and without *CYP11B1* mutations and to understand its role in disease prognosis.



---

## CHAPTER 2: LITERATURE REVIEW

### 2.1 GLAUCOMA

Glaucoma comprises a heterogeneous group of optic neuropathies characterized by an excavation of the optic disc and progressive alteration of the visual field (Shields *et al.*, 2005). It is associated with a gradual loss of retinal ganglion cells (RGCs) and their axons that affect the connections between eye and brain (Flammer *et al.*, 2003). The loss of RGCs leads to gradual enlargement of the optic cup, which is a small depression in the optic nerve head (the site where the axons of RGCs converge and then leave the eye). The loss of RGCs also lead to the formation of blind spots (scotomas) in the visual field, which in turn leads to a decrease in visual function (Flammer *et al.*, 2003). The formation of scotomas begins in the peripheral field and gradually progresses towards centre the resulting in complete blindness (Flammer *et al.*, 2003).

Glaucomas are usually associated with raised IOP. IOP is a function of the balance between the rate of production of aqueous humor (inflow) and the rate of drainage (outflow) in the eye (Flammer *et al.*, 2003).

### 2.2 AQUEOUS HUMOR

Aqueous humor is a clear transparent fluid produced by the ciliary body behind the iris. As the fluid is secreted, it flows across the back of the iris through the pupil into the anterior chamber, which is a compartment between cornea and the iris (Fig 2.1).

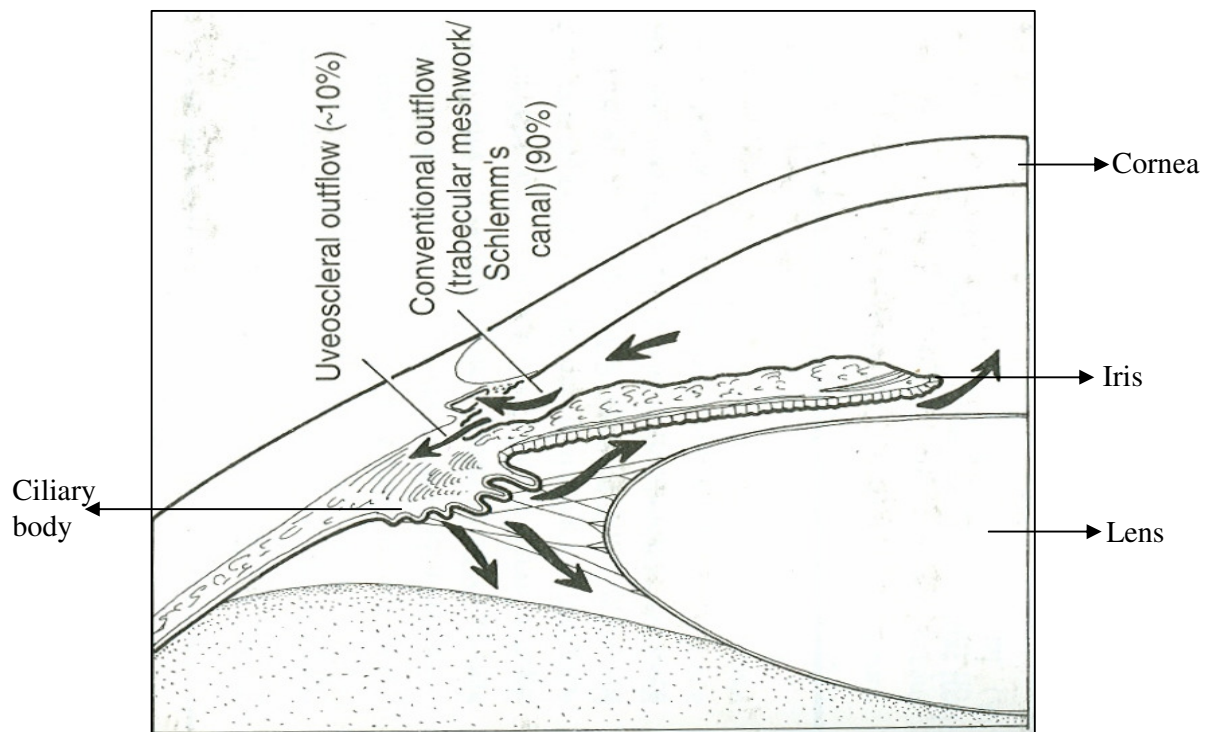


**Figure 2.1:** Schematic representation of aqueous humor outflow  
(Adapted from Epstein DL. *Glaucoma* 4<sup>th</sup> ed. Baltimore, MD: Williams & Wilkins; 1997:p19)

### 2.2.1 Compositions of aqueous humor

Aqueous humor of both anterior and posterior chamber is slightly hypertonic when compared to plasma. It is acidic with a pH of 7.2 in the anterior chamber. The two most striking characteristics of aqueous humor are, a) a marked excess of ascorbate, which is 15 times greater than that of arterial plasma. b) a marked deficit of protein (0.02% in aqueous humor compared to 7% in plasma). It also has free amino acids (ratio of aqueous humor to plasma ranges from 0.08 to 3.14) and sodium hyaluronate (Shields *et al.*, 2005).

### **2.2.2 Functions of aqueous humor**

1. The aqueous fluid serves two important functions in the eye (Shields *et al.*, 2005).
  - a) It nourishes the area around the iris and behind the cornea.
  - b) The continuous production of aqueous humor creates pressure in the eye known as intraocular pressure (IOP), which maintains the shape of the eye.

### **2.2.3 Drainage of the Aqueous humor**

To maintain a normal IOP, the aqueous humor drains out of the eye through the anterior chamber angle (the junction of the cornea and the iris). The drainage of the fluid occurs through two channels:-

**2.2.3.1) Trabecular Meshwork (TM) pathway:** In this pathway the aqueous humor in the iridocorneal angle drains out of the eye through the TM. After passing through the TM, aqueous humor drains through a conduit in the sclera called the canal of Schlemm, then into other tiny conduits and finally into small blood vessels on the surface of the eye to the blood circulatory system of the body (Fig 2.2). Trabecular outflow pathway accounts for 70%- 95% of the aqueous humor outflow within the eye. The TM plays a major role in providing resistance to the flow. The rate of ocular outflow and thus the IOP is mainly determined by the aqueous humor production by the ciliary epithelium and its drainage through the TM (Shields *et al.*, 2005).

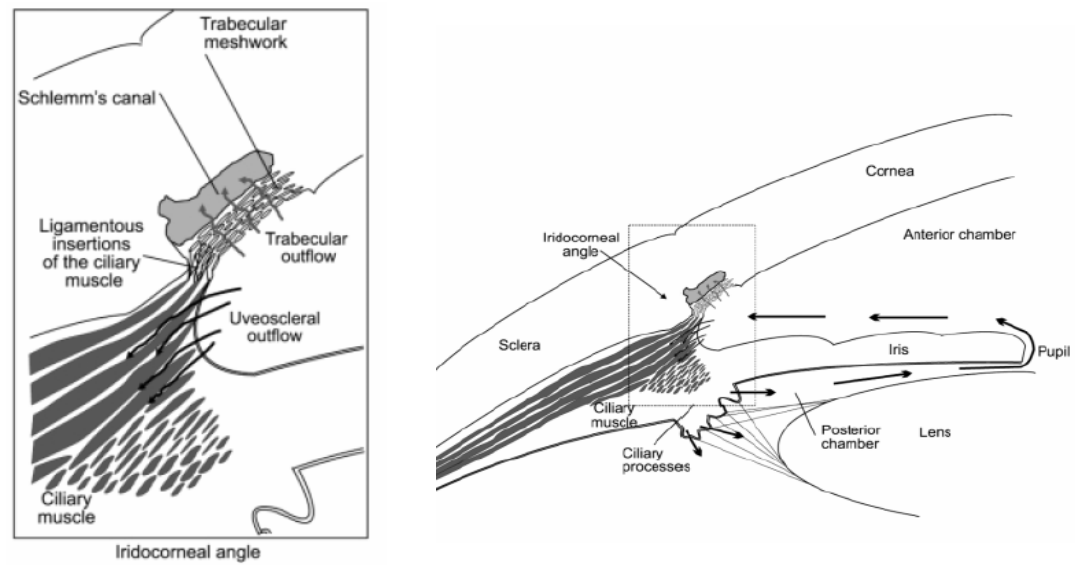


**Figure 2.2:** Schematic diagram of the aqueous humor outflow through trabecular meshwork ( Adapted from Llobet *et al.*, 2003; 18: 205-209.).

2.2.3.2) *The uveoscleral pathway:* It is located behind the TM and is also known as the unconventional pathway. Aqueous humor passes through the root of the iris and interstitial spaces of the ciliary muscle to reach the suprachoroidal space. From there it passes to episcleral tissue via scleral pores surrounding the ciliary blood vessels and nerves, vessels of the optic nerve membranes or directly through the collagen substance of the sclera and then probably it drains into the venous circulation of the body. Around 5-30% of the fluid flows out through this channel (Shields *et al.*, 2005).

Since majority (70%-95%) of the aqueous humor flows out of the eye through the trabecular pathway, it is important to study the various features of this tissue.

### 2.3 TRABECULAR MESHWORK (TM)

TM is a sponge like porous network present at the junction between the cornea and the iris. This porous tissue extends from scleral spur to the Schwalbe's ring with a width of 750  $\mu\text{m}$  and consists of connective tissue beams, which are arranged as superimposed perforated sheets (Bron *et al.*, 1997). Only higher primates and humans have a developed TM. Lower order primates and other mammals have a reticular meshwork, which covers a broader area of the sclera. In these species the anterior chamber angle is filled with radial interlacing strands of the pectinate ligament. In the course of primate evolution, the pectinate ligaments have gradually reduced and the ciliary body is unified. The morphologic and functional division into three or four different portions is probably the result of evolution (Ritch *et al.*, 1996).

The Ultrastructural studies of TM have shown that it contains three differentiated layers (Shields *et al.*, 2005)

1. *Uveal meshwork*: it is the innermost portion of TM and closest to the anterior chamber. It is formed by prolongations of connective tissue arising from the iris and ciliary body and is covered by endothelial cells. The individual cords of the uveal trabeculae have a diameter of 4-6  $\mu\text{m}$  in the mid region, being thicker posteriorly and narrower anteriorly. The intertrabecular spaces range between 20-75  $\mu\text{m}$ . This layer does not offer much resistance to aqueous humor outflow because of its large intercellular spaces (Fig.2.3).
2. *Corneoscleral meshwork*: This layer extends from the scleral spur to the anterior wall of the scleral sulcus. It consists of sheets of trabeculae that are perforated by pelliptical openings. The thickness of these sheets ranges from 5-12  $\mu\text{m}$  with the intertrabecular space ranges from 5-20  $\mu\text{m}$ . There are

approximately 8-10 trabecular layers with a total width of 120-150  $\mu\text{m}$ . The size of the openings decreases as the trabecular sheets approach the Schlemm's canal. This layer provides more resistance to the aqueous humor outflow in comparison to the uveal meshwork due to the higher organization and the narrow intercellular spaces (Fig.2.3).

3. *Juxtacalicular tissue* (cribriform meshwork): It is the outermost portion of TM. It is in direct contact with the inner wall of endothelial cells from Schlemm's canal. It consists of a layer of connective tissue lined on either side by endothelium. The outer endothelial layer comprises the inner wall of Schlemm's canal while the inner layer is continuous with the remainder of the trabecular endothelium. The thickness of this layer ranges from 2-20  $\mu\text{m}$  and consists of 2-5 layers of loosely arranged cells, embedded in the extracellular matrix. This layer provides the maximum resistance to the aqueous humor outflow due to the narrowest intercellular spaces of this layer when compared to other two layers (Fig.2.3).

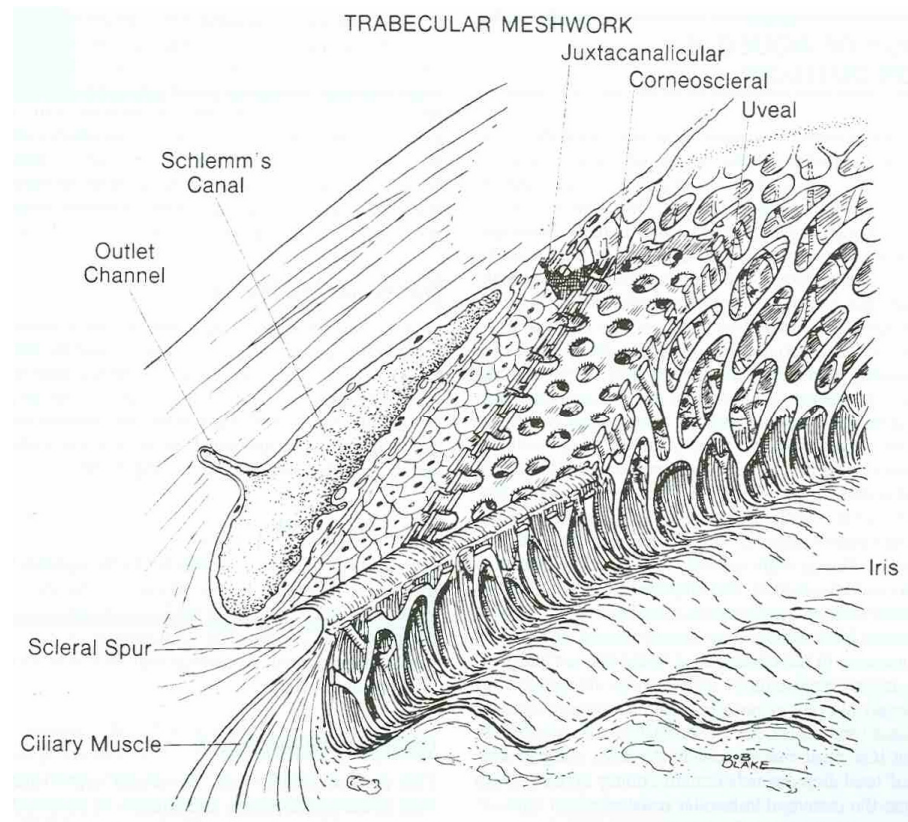


**Figure 2.3:** The three layers of the trabecular meshwork

(Shields MB. Textbook of glaucoma. 5<sup>th</sup> edition. Baltimore; Williams & Wilkins. 2005: p20).

## 2.4 CLASSIFICATION OF GLAUCOMAS

Glaucomas are commonly classified on the basis of

- a) Etiology, i.e., factors causing the alteration in aqueous humor dynamics.
- b) Mechanisms that are associated with the alteration in the structures involved with aqueous drainage

### 2.4.1 Based on etiology

- a) *Primary glaucomas*: In this category the causal events are largely confined to the anterior chamber angle or conventional outflow pathway. Apparently there is no contribution from other ocular or systemic disorders. These cases are typically

bilateral and may have a genetic basis. Example: Primary open angle glaucoma (POAG), Primary angle closure glaucoma (PACG) (Shields *et al.*, 2005).

- b) *Secondary glaucomas*: These are associated with other ocular or systemic abnormalities and may be responsible for the alteration in aqueous humor dynamics. They may be either unilateral or bilateral and acquired from secondary conditions such as inflammations, neovascular glaucoma, lens induced glaucoma etc (Shields *et al.*, 2005). The inflammatory glaucomas occur mostly due to the inflammation of uvea or iris, which results in the infiltration and dysfunction of the TM by inflammatory material such as WBC aggregates, macrophages, lymphocytes and fibrin causing a diminished outflow of aqueous humor. The neovascular glaucoma is commonly associated with the conditions like retinal vein obstruction and diabetic retinopathy. The swollen lens (due to cataract or a traumatic rupture of lens capsule) obliterates the drainage angle by forcing the root of iris against the cornea. Apart from these the release of pigment granules or the exfoliate material in the anterior chamber angle results in the pigmentary and pseudoexfoliation glaucomas, respectively (Shields *et al.*, 2005).

The concept of primary and secondary classification of glaucomas represents a lack of understanding of the pathophysiological mechanisms underlying glaucoma. Furthermore, glaucomas caused by developmental anomalies do not fit into either category (Shields, 2005).



### **2.4.2 Based on mechanisms**

The glaucomas are grouped with respect to the configuration of the iridocorneal angle in the anterior chamber of the eye: a third group, which did not fit into either of the two types, are developmental glaucomas (Shields *et al.*, 2005).

*a) Primary Open angle glaucoma (POAG):* It is the form of glaucoma in which the iridocorneal angle is normal and the obstruction of the outflow may be located within or distal to the TM in the Schlemm's canal or along the aqueous drainage system (Fig. 2.4). The majority of primary glaucomas (60%-70%) are of open angle type and is also known as chronic open angle glaucoma (Vincent *et al.*, 1997). The elements obstructing aqueous humor outflow pathway may be located on the anterior side of the TM (pre-trabecular mechanisms) or distal to the meshwork in Schlemm's canal (post-trabecular mechanism).

- i) Pre-trabecular mechanism: a translucent membrane extends across the open iridocorneal angle, leading to the obstruction of aqueous outflow.
- ii) Trabecular mechanism: the obstruction to the aqueous outflow is located within the TM.
- iii) Post trabecular mechanism: the obstruction to the aqueous outflow results from increased resistance in Schelmm's canal due to collapse or absence of clogging of the canal (Shields *et al.*, 2005).

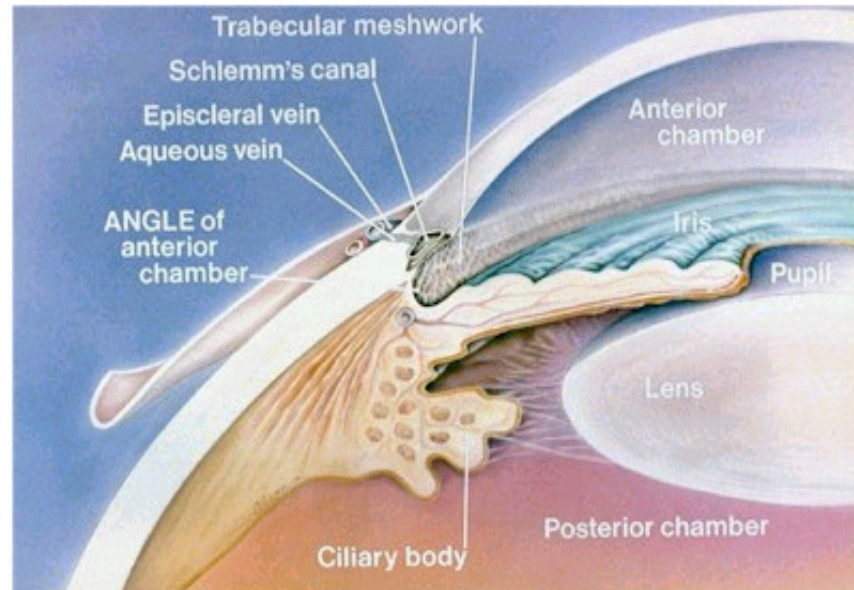


**Figure 2.4:** Diagrammatic representation of the drainage structures in POAG (<http://www.umkc-efkc.org/diseases/glaucoma/poag.htm>)

Normal tension glaucoma is a type of OAG where the cupping of the optic nerve head, loss of the retinal nerve fiber layer and visual field defects are similar to those seen in POAG. But the IOP always remains at  $\leq 21$  mm of Hg (Flammer *et al.*, 2003).

*b) Primary Angle closure glaucoma (PACG):* In this form of glaucoma, the anterior chamber is shallow and aqueous outflow is blocked by the root of the iris, which lies in apposition to the TM or peripheral cornea (Fig. 2.5). As a result the peripheral iris may either be pulled (anterior mechanism) or pushed (posterior mechanism) into this position. In the anterior mechanism, an abnormal tissue bridges the anterior chamber angle and subsequently undergoes contraction, pulling the peripheral iris into the iridocorneal angle. In the posterior mechanism, the pressure behind the iris, lens or vitreous causes the peripheral iris to be pushed into the anterior chamber angle, which occurs with or without the papillary block

(Shields *et al.*, 2005). Due to the shallow anterior chamber and a narrow filtration angle, a functional block resulting in the build-up of pressure in the posterior chamber, which results to a forward shift of the iris and closure of the anterior chamber angle (Ritch *et al.*, 1996).

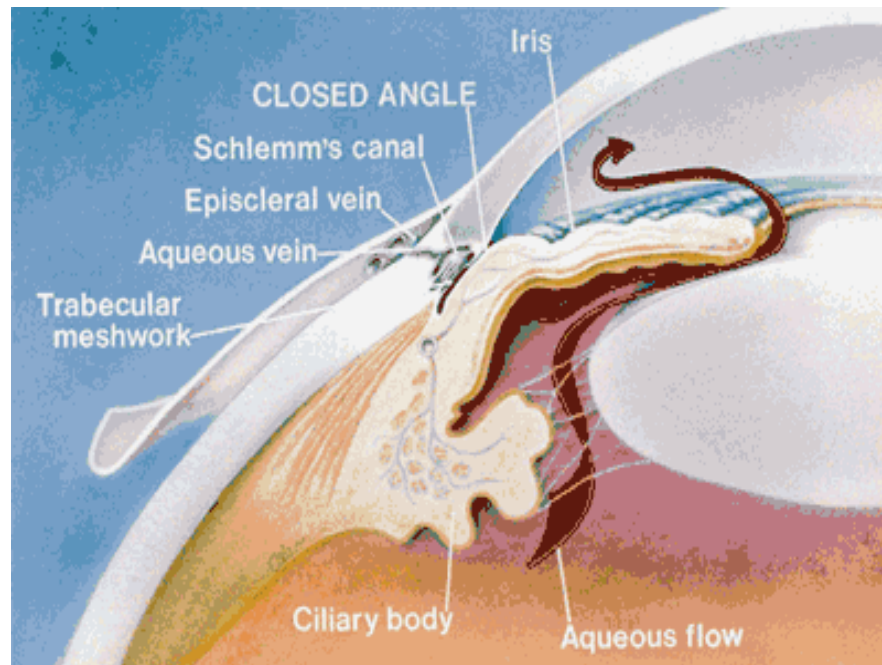


**Figure. 2.5:** Diagrammatic representation of the drainage structures in ACG

(<http://www.flei.com/Eye-Diseases-glaucoma.htm>)

Various anatomical factors like short eye, smaller corneal diameter, a shallow anterior chamber and a relative anterior positioning of the lens-iris diaphragm etc. predispose to PACG, which is divided into three clinical subtypes:

- i) Subacute or intermittent angle closure glaucoma, which generally occurs in individuals with shallow anterior chamber and occludable angles.
- ii) Acute primary angle-closure glaucoma, which is caused by a sudden occlusion of the entire angle with a resultant acute rise in IOP.
- iii) Chronic angle closure glaucoma, which is characterized by chronic rise in IOP in the eye having synechial closure over at least 180 degrees.

## 2.5 EPIDEMIOLOGY OF OAG AND ACG

Bilateral blindness would account for 4.5 million people with OAG and 3.9 million with PACG in the year 2010 that would rise to 5.9 and 5.3 million people by 2020, respectively. It is estimated that 2010, 74% of those with glaucoma will be POAG cases and 26% will be ACG. The mean prevalence for OAG worldwide in 2010 is estimated to be 1.96%, while that for ACG it is 0.69% (Quigley *et al.*, 2006).

The prevalence percentages of different glaucomas in India as reported by different epidemiological studies are given in Table 2.1. The prevalence percentages of POAG ranged from 0.41% - 3.79%. On the other hand the prevalence for PACG ranged from 0.5% - 4.32%.

**Table2.1:** Prevalence studies of Glaucoma in Indian population

Region	Name of the study	POAG prevalence	PACG prevalence	Reference
South India	APEDS (Andhra Pradesh Eye Disease Study)	2.56%	-	Dandona <i>et al.</i> , 2000
South India	ACES (Aravind comprehensive eye study)	1.7%	0.5%	Ramakrishnan <i>et al.</i> , 2003
South India	CGS (Chennai glaucoma study)	3.79%	-	Vijaya <i>et al.</i> , 2005
South India	VES (Vallore eye study)	0.41%	4.32%	Jacob <i>et al.</i> , 1998
East India	WBGs (West Bengal glaucoma study)	2.7%	-	Raychoudhuri <i>et al.</i> , 2005
North India		37%	63%	Das <i>et al.</i> , 2001

## 2.6 DEVELOPMENTAL GLAUCOMAS

These glaucomas are associated with developmental anomalies of the eye that are present at birth (Mandal and Netland, 2006). Developmental glaucomas are classified into two groups on the basis of their clinical presentation and association with other anomalies:

**2.6.1 Primary Congenital Glaucoma (PCG):** It is the most common form of childhood blindness caused by a developmental defect of the TM and anterior chamber angle (Mandal and Netland., 2006).

**2.6.2 Developmental glaucomas with associated anomalies:** A number of ocular conditions that are the result of an abnormal differentiation of neural crest cells are also reported to be associated with glaucomas. One of these forms is Axenfeld- Rieger syndrome (ARS). It is an autosomal dominant developmental disorder characterized by a prominent anteriorly displaced Schwalbe's line, insertion of iris processes in the stroma, hypoplasia of the iris, corectopia and pseudopolyopia etc . Around 50% of these patients develop glaucoma, which generally appears in childhood or early adulthood. Peter's anomaly that includes the defects of the ear and auditory system orofacial system. Aniridia is a bilateral developmental disorder characterized by the congenital absence of normal iris, are some commonly observed anterior segment anomalies that are associated with glaucoma (Shields *et al.*, 2005)

## 2.7 PRIMARY CONGENITAL GLAUCOMA

Primary Congenital glaucoma (PCG) is an ocular developmental anomaly occurs due to the obstruction in the drainage of the aqueous humor outflow caused by the maldevelopment of TM and anterior chamber angle. (Mandal and Netland, 2006).

PCG manifests during neonatal or early infantile period and is characterized by following clinical features (Mandal and Netland., 2006).

- a) *Elevated IOP*: the mean IOP in newborn infants is  $9.59 \pm 2.3$  mm of Hg and it increases to  $13.95 \pm 2.49$  mm of Hg by the age of 7 to 8 years and remain constant through the middle teenage years. The normal intraocular pressure in infants is slightly lower than in an adult but 21 mm of Hg remains a useful upper limit (Mandal and Netland, 2006).
- b) *Megalocornea*: The horizontal corneal diameter in normal newborns ranges from 9.5 mm – 10.5 mm. the corneal diameter increases by about 0.5 mm to 1.0 mm in the first year of life (Table 2.2). A corneal diameter greater than 12 mm of Hg in the first year of life is highly suggestive of glaucoma (Mandal and Netland, 2006). Also the asymmetry in diameter between the two corneas or a corneal diameter of 13 mm or more at any age is a strong indicator for ocular abnormality (DeLuise *et al.*, 1983).

**Table 2.2:** Corneal diameter in children: normal and glaucomatous eyes (Shaffer and Weiss.1970)

Age	Corneal diameter (horizontal, in mm)	
	Normal	Suspicious for possible glaucoma
Birth – 6 months	9.5 – 11.5	> 12
1-2 years	10-12	>12.5
Older child	$\leq 12$	>13

- c) *Haab's striae*: These are the ruptures in the Descemet's membrane, which occurs due to high IOP. These ruptures can be visualized under slit lamp as opaque lines characteristically oriented horizontally or concentric to the limbus (Fig.2.6).

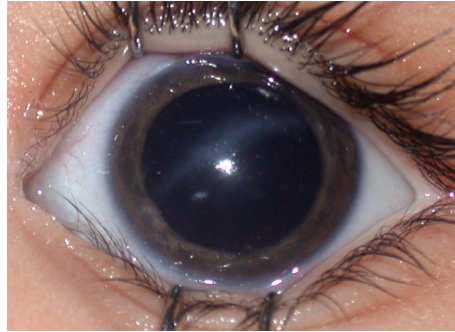


**Figure 2.6** Haab's striae

Apart from this triad there are few corroborating factors in PCG that includes

- a) *Corneal edema*: occurs due to the elevated IOP and results in corneal haze (Fig. 2.7a).
- b) *Photophobia* : it is hypersensitivity of the patients to light, which occurs due to corneal edema.
- c) *Ephiphora*: it is excessive tearing in PCG that occurs due to hypersensitivity to light (Fig.2.7b).
- d) *Blepharospasm*: it is involuntary contraction of the eye muscles that results in the squeezing of the eyelids. It manifests due to photophobic nature of the patients (Fig.2.7c).



**Figure.2.7a** Corneal edema  
*Mandal and Netland. 2006*

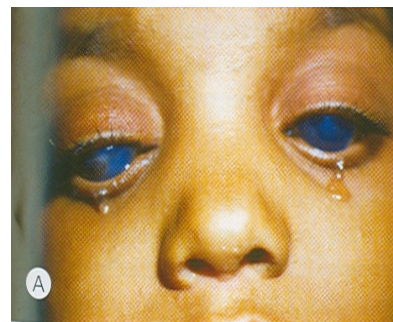


**Figure.2.7b** Epiphora  
*Mandal and Netland. 2006*



**Figure. 2.7c** Blepharospasm  
*Mandal and Netland. 2006*

### ***2.7.1 Prevalence of PCG worldwide***

The prevalence of PCG ranges from 1 in 1250 to 1 in 20,000 with the highest (1 in 1250) among the Gypsy population of Slovakia (Gencik *et al.*, 1989), 1 in 20,000 in the Western populations (Gencik *et al.*, 1982). The high rate of inbreeding and consanguinity among the Slovakian Gypsies accounted for high prevalence of PCG. According to the APEDS, the prevalence of PCG was estimated to be 1 in 3300 live births that accounted for 4.2% of overall childhood blindness (Dandona *et al.*, 1998). Since this study was carried out on rural and semi urban population of Andhra Pradesh, it was suggested that other epidemiological studies on other parts of India and on a large sample size would give a good estimate of the prevalence of childhood blindness (Dandona *et al.*, 1998).

### ***2.7.2 Pathogenesis of PCG***

Various hypotheses have been given about the pathogenesis of PCG on the basis of both histological and ultrastructural observations on the specimens from the anterior chamber angle during trabeculectomy or trabeculotomy. These include:



- a) Barkan's membrane theory: According to this theory the aqueous humor outflow is blocked by an impermeable endothelial membrane, which covers the anterior chamber angle and leads to increase in IOP. (Barkan.1955)
- b) Maumenee and coworkers have suggested that it is the abnormal insertion of the ciliary muscle fibres that would interfere with the increase in the filtration area produced by the scleral spur. (Maumenee *et al.*, 1958).
- c) Shaffer (1955) observed the existence of an abnormal insertion of the iris in the endothelial TM.
- d) Anderson and coworkers had carried out the electron microscopic studies on the TM of infantile glaucoma patients and observed that the TM was not completely uncovered and exposed to the anterior chamber because of the iris and anterior ciliary body overlapped a portion of the TM, which is equivalent to the seventh or eighth month of the fetal development. He attributed this to the excessive formation of collagenous beams within the TM, which prevents normal posterior sliding of the uveal tissues during the formation of the anterior chamber angle (Anderson .1981).

Apart from these the presence of amorphous and fibrous materials in the endothelial TM and incomplete development of SC was identified in congenital glaucoma patients.

Recent study carried out by Rojas and coworkers (2006) compared the trabeculectomy specimens of congenital glaucoma patients with those obtained from the normal human eyes, both at histological and ultrastructural level, in an attempt to determine the pathogenic mechanisms of the disease. Based on the observations like

accumulation of amorphous material in TM, insertion of iris in TM, bulky endothelial cells in SC, increase in the size of trabeculae, the authors had suggested that abnormalities in the TM structure result in the disease pathogenesis, which do not always parallel an abnormal development of SC.

### **2.7.3 Genetics of PCG**

The genetic basis of the disease was based on the segregation of PCG phenotype in families (Sarfarazi and Stoilov.2000). Grilos in 1836 observed for the first time the endemic occurrence of PCG in the Jewish population of Algiers (Sarfarazi and Stoilov.2000). Later Jungken in 1842 suggested that PCG is an autosomal recessive disorder based on its inheritance pattern in a Swedish family (Sarfarazi and Stoilov.2000). The high rate of concordance among monozygotic and discordance among the dizygotic twins also provided an additional genetic basis for PCG (Gencik *et al.*, 1989). The autosomal recessive mode of inheritance was also supported by prevalence of consanguinity among the affected families and is the most common mode of inheritance reported in various studies (Stoilov *et al.*, 2002a). However, pseudodominance has been observed in some pedigrees due to high rate of consanguinity and inbreeding in certain ethnic groups (Stoilov *et al.*, 2002a).

### **2.7.4 Candidate loci/genes in PCG**

Three chromosomal loci have so far been implicated in PCG on - *GLC3A* at 2p21-22 (Stoilov *et al.* 1997), *GLC3B* at 1p36.2-36.1 (Akarsu *et al.*, 1996) and *GLC3C* at 14q24.3 (Stoilov *et al.*, 2002b).

#### **2.7.4.1 *GLC3A***

The first genetic locus (*GLC3A*) for PCG was mapped by Sarfarazi and co-workers in 1995 based on their study on 17 Turkish families comprising of 113 individuals that

included 79 offsprings, of which 40 were affected with PCG (Sarfarazi *et al.*, 1995). These families had a diagnosis of bilateral PCG within first 6 months of birth without any other associated abnormality. Each family had 2-4 affected sibs with parents being normal and belonged to the same genetic background. Karyotyping by G-banding was normal in these individuals. they carried out a genome wide scan on 17 different chromosomes using 126 short tandem repeat (STRs) markers. Linkage analysis revealed lod scores of 2.33 for D2S406 ( $\theta = 0.16$ ) and 1.96 for D2S405 ( $\theta = 0.16$ ) on 2p in 11 out of 17 families. To refine the locus further, a two-point linkage analysis was carried out with 14 different STR markers (Fig 2.8) within an interval of 29.8 cM between these two markers in all the families. A strong linkage was noted in 11 families with maximum lod scores of 6.48, 5.38 and 5.40 for D2S177, D2S1346, D2S1348, respectively, with no recombination. The remaining 6 families did not exhibit linkage to these markers indicating the presence of some other locus in the genome, thereby exhibiting genetic heterogeneity of the disease condition. But lod scores among these families was  $<-2$  suggestive of total exclusion. In order to determine genetic heterogeneity among 17 families linkage analysis was carried out with D2S1788, D2S1325, D2S177, D2S1346 and D2S1348 markers. No significant heterogeneity among them was attributed to the non informativeness of these markers in the unlinked families

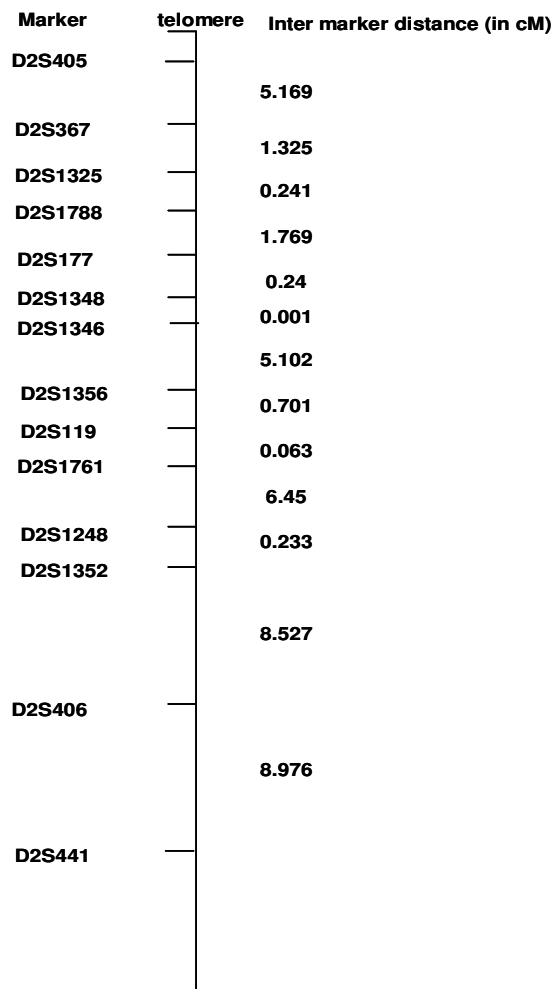


**Figure 2.8:** Intermarker distance of the 14 STRs used for linkage analysis.

On the other hand 85% of the families showed homogeneity to the three linked markers (D2S177/D2S1346/D2S1348) indicating this region (2p21-22) to be the major locus for PCG. This region was termed as *GLC3A* locus, where 'GLC' is the designated symbol for glaucoma, '3' congenital glaucoma and 'A' to designate the first mapped locus in PCG (Sarfarazi *et al.*, 1995).

Haplotypes constructed by using 14 STRs and recombinant events among the affecteds positioned *GLC3A* centromeric to the three tightly linked markers D2S367,

D2S1788 and D2S1325, and telomeric to D2S1356. Further multipoint linkage analysis and the haplotype construction using 8 markers (D2S367, D2S1788, D2S1325, D2S177, D2S1346, D2S1348, D2S1356 and D2S119) linked to *GLC3A*, in 6 consanguineous families revealed crossovers that placed the *GLC3A* at an interval of 2.01 cM between D2S177 and D2S1325 on 2p21 (Sarfarazi *et al.*, 1995).

Another such study on 7 PCG families belonging to Roman populations was carried out by Plasilova and co-workers in 1998 (Plasilova *et al.*, 1998). Homozygosity mapping was done to identify the disease locus. They genotyped a panel of 8 samples of unrelated affected persons with 160 autosomal STRs from the Weber (version 6a) and Weissenbach set (Dib *et al.*, 1996) but could not find any linkage. Later on they carried out the linkage analysis with four STR markers at the 2p21 region and observed significant lod scores with all of them. The highest lod score (8.18) was observed at  $\theta = 0$  with D2S1346. Based on this and recombination events, the disease locus was mapped at an interval of 8 cM between D2S1788 and D2S1356. The results were confirmed by multipoint linkage analysis with the highest lod scores at D2S1346 (9.469) and D2S2328 (9.569). Genetic homogeneity in all these families was attributed to endogamy and high rate of inbreeding (Plasilova *et al.*, 1998).

#### ***2.7.4.2 Candidate gene screening***

On mapping *GLC3A* for PCG, Sarfarazi and co-workers in 1995 established the critical region for the identification of the candidate gene using YAC (Yeast artificial chromosome) screening and radiation hybrid mapping. On the basis of STS (sequence tagged sites) and EST (expressed sequence tags) maps of the human genome, the position of various STR markers linked to *GLC3A* was refined (Stoilov *et al.*, 1997). The critical region for *GLC3A* harbored two genes, Human cytochrome P4501B1 (*CYP1B1*), and protein kinase, interferon-inducible double stranded RNA- activated

gene (*PRKR*) and a guanine nucleotide exchanger factor for RAS (*hSOS1*) flanking D2S1346. The splicing factor, Arginine/serine-rich, 7 (*SFRS7*) gene was also mapped within the critical region by BLAST search (Fig. 2.9). As the pathophysiology of PCG was unknown and there was no prior evidence of an association of these genes to the disease phenotype, all of these were considered as potential candidates. The coding region of these genes was screened by direct sequencing. The template used in the study was cDNA obtained by reverse transcription of the total RNA from human skin fibroblasts. Direct sequencing excluded *hSOS1* and *PRKR* as the candidates as no variation was observed in these genes. However three different frameshift mutations (2 deletions and one insertion) in *CYP1B1* were detected in three families that segregated in the affected individuals and were absent in 470 normal chromosomes.

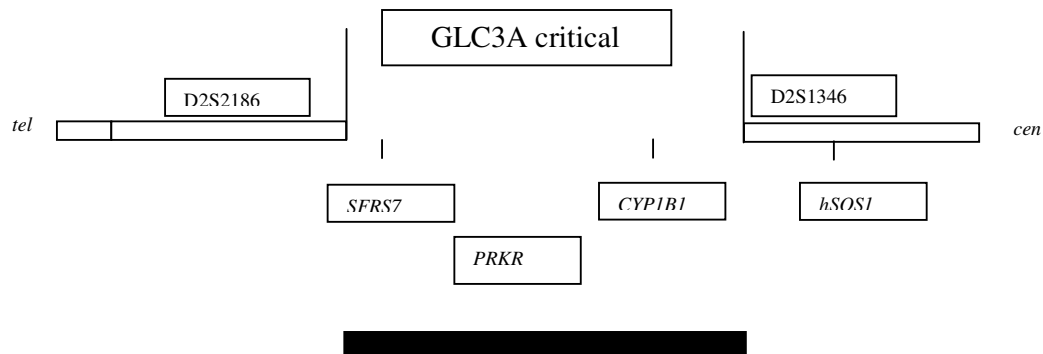


**Figure 2.9:** The *GLC3A* critical region with the various candidate genes (Stoilov *et al.*, 1997).

#### 2.7.4.3 *GLC3B*

The second PCG locus was mapped to 1p36.2-36.1 by Akarsu and co-workers in 1996. Their study on 8 PCG families comprising of 37 offsprings, of whom 17 were affected, did not reveal linkage to *GLC3A*. A whole genome scan was carried out on

these families with 126 STRs. Two-point linkage analysis was done with medium-density markers followed by saturating the region of linkage with tightly linked markers (Fig 2.10). The markers, D1S1635, D1S228, D1S507, D1S407 and D1S1368, on 1p36 exhibited high lod scores in 4 out of 8 families. Further refining of the locus was done by two-point linkage analysis of 17 STRs from 1p36.2-1p36.1 region. The maximum lod score was obtained with D1S2834 (4.510) and D1S402 (4.157). Recombination events placed the disease locus centromeric to D1S1193 and telomeric to D1S2728 and crossover events positioned it between two sets of tightly linked markers: D1S1597/D1S489/D1S228 and D1S1176/D1S507/D1S407 at an interval of ~ 3 cM, which was named as *GLC3B*. The position of *GLC3B* was confirmed and the significant heterogeneity indicated the existence of another locus for PCG. The 1p36.2-1p36.1 has been reported to be a GC-rich region (Saccone *et al.*, 1992) and harbors a number of tumor suppressor genes. These genes are associated with various malignancies but so far, none of them have segregated with PCG.

Marker	telomere	Inter marker distance (in cM)
D1S1635		1.64
D1S489		0.521
D1S1597		0.203
D1S228		0.478
D1S2834		0.564
D1S507		0.132
D1S2728		0.03
D1S402		0.019
D1S1176		0.66
D1S436		1.342
D1S170		0.004
MFAP2		0.772
D1S1592		1.008
D1S1368		

**Figure 2.10:** Intermarker distance of the 14 STRs used for linkage analysis.

#### 2.7.4.4 *GLC3C*

The third locus for PCG was mapped to 14q24.3 and was named as *GLC3C* (Stoilov *et al.*, 2002b). This study was carried out on a five generation consanguineous family with 13 individuals, of which 4 were affected. On exclusion of *GLC3A* and *GLC3B* in this family, a whole genome scan was done with 235 STRs. This led to the identification of homozygosity with only marker (D14S53) at 14q in the all the



affecteds. The results were refined using a set of 6 STRs in that region (Fig.2.11), which revealed the homozygosity of the haplotype (constructed by those STRs) in all the affecteds. Based on the results, *GLC3C* was placed within a 2.9 cM region between D14S61 and D14S1000. Seven known genes have been identified in the *GLC3C* candidate region: Neurexin 3A, Nuclear Receptor ERBB2, KIAA0759, Glutathione Transferase Zeta 1, Maleylacetoacetate Isomerase, Serine Palmitoyl Transferase Subunit II and Alk B protein Homologue. These genes would be the next targets for screening studies in order to determine their association with the disease phenotype.

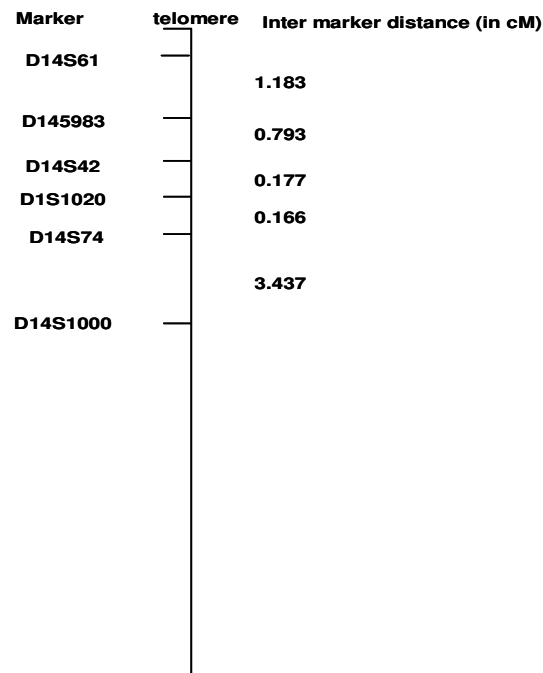


**Figure 2.11:** Intermarker distance of the 6 STRs used for linkage analysis.

However, the linkage of PCG families to either *GLC3B* or *GLC3C* has not been replicated by any other study.

Only the *GLC3A* locus harboring the human cytochrome P4501B1 gene (*CYP1B1*) has been characterized (Stoilov *et al.*, 1997). So far around 70 *CYP1B1* mutations

---

have been implicated in PCG among various ethnic groups (<http://www.hgmd.cf.ac.uk/ac/index.php>).

## 2.8 CYTOCHROME P4501B1 (*CYP1B1*; 2p21-2p22)

Cytochrome P450 (CYP450) is a superfamily of closely related hemeproteins found throughout the phylogenetic spectrum of plants and animals. The term CYP450 arises from the presence of a heme group and their maximum absorption at 450nm, which is unique for these proteins and serves as their signature (Hasler *et al.*, 1999). Cytochrome P450 proteins have an average mass of approximately 50 kDa. These are mostly membrane bound, anchored to the endoplasmic reticular membrane or the inner mitochondrial membrane with few soluble forms found in bacteria (Stoilov *et al.*, 2001). Structurally they consist of:

- a) Hydrophobic amino terminal region: It contains a membrane insertion sequence and a stop transfer sequence. It functions as an anchor in the membrane determining the topological orientation of the cytochrome (Fig.2.12).
- b) Proline rich region: Following the amino terminal region is the proline-rich hinge region. It imparts flexibility between the transmembrane region and the globular catalytic part of the protein that resides in the cytosol. This flexibility may be necessary to orient the cytosolic portion of the molecule with respect to the membrane for substrate access and for the interaction with the appropriate electron transfer partner (Murray *et al.*, 2001).
- c) Carboxyl terminal portion: It consists of a set of conserved core structures and signature sequences (Fig.2.12). These structures include a number of  $\alpha$  helices and  $\beta$  sheets and a "meander region" that are necessary for the heme binding ability of the protein. The conserved core structure is formed of a four helix bundle ('D', 'E',

T' and 'L'), helices 'J' and 'K', two sets of  $\beta$  sheets and a coil called the meander.

These regions comprise:

- i) The heme - binding loop, containing the most characteristic P-450 consensus protein sequence (Phe-X-X-Gly-X-Arg-X-Cys-X-Gly), located on the proximal face of the heme just before the 'L' helix. The conserved cysteine serves as the fifth ligand to the heme iron.
  - ii) The absolutely conserved Glu-X-X-Arg motif in the 'K' helix, on the proximal side of heme that is probably needed to stabilize the core structure.
  - iii) The central part of the 'I' helix containing another consensus considered as the P450 signature sequence (Ala/Gly-Gly-X-Asp/Glu-Thr-Thr/Ser).
- d) **Substrate binding region:** It is a less conserved region between the hinge region and conserved core structure. This region is associated with certain variable and flexible sites, which help in the catalytic reaction of the enzyme (Stoilov *et al.*, 2001).

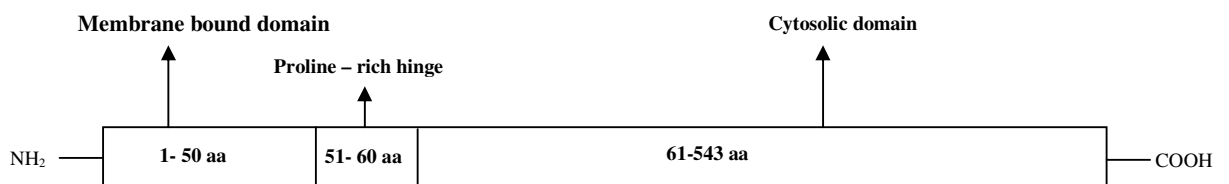


**Figure 2.12** Schematic representation various domains in CYP1B1

### 2.8.1 Nomenclature and families of CYP450

The superfamily of cytochrome P450 consists of about 1200 individual genes along with 310 mammalian forms. This includes forms from bacteria to yeast and other

primitive eukaryotes to simple plants and trees. The P450 proteins are categorized into families and subfamilies on the basis of their sequence homology. Sequences with > 40% identity at the amino acid level belong to the same family, whereas, the sequences with > 55% identity are grouped in the same subfamily. The families of CYP are designated by an arabic numeral ranging from 1-51 (e.g. CYP1). Subfamilies are designated by a letter ranging from A to W (e.g. CYP1B) and members in the subfamilies by an arabic numeral from 1-22 (e.g. CYP1 B1). There are 17 mammalian families of CYP450, of which families 2, 3 and 4 contain endoplasmic reticulum enzymes for xenobiotic metabolism and exhibit the greatest variability. There are 52 different forms of CYP450 in the human genome, of which 15 are in family 2, 4 in family 3 and 11 in family 4. Thus more than half of cytochrome P450 families contain single members, each presumably affecting a specific task related to homeostasis in the organism (Werck-Reichhart *et al.*, 2000).

### **2.8.2 Function of P450s**

- 1) P450 proteins are monooxygenases or mixed function oxidases, which catalyses the oxidation of various endogeneous substrates like steroids and fatty acids and exogeneous compounds like drugs (Hasler *et al.*, 1999).
- 2) P450s are the important xenobiotic metabolizing enzymes involved in the metabolism and detoxification of various drugs, environmental chemicals and carcinogens (Hasler *et al.*, 1999).

Drug metabolizing CYPs belong to three families - CYP1, CYP2 and CYP3. For example, CYP1A2 participates in the oxidation of paracetamol and theophylline in human liver (Gu *et al.*, 1992). CYP2C8 and CYP2C9 metabolises tobutamide, phenytoin, tosemide etc. CYP2E1 oxidises nitrosamines and metabolises general anesthetics such as sevoflurane and halothane. CYP3A4 is active on cyclosporin

macrolide antibiotics and anticancer agents like taxol (Guengeric *et al.*, 1991). Polycyclic aromatic hydrocarbons (PAHs) and arylamines are the various xenobiotic chemicals metabolized by CYP450s (Hasler *et al.*, 1999).

Cytochrome P450 1B1 (CYP1B1) is the only member in the CYP1B subfamily and shares 40% homology with two members in the CYP1A subfamily (CYP1A1 and CYP1A2) (Murray *et al.*, 2001).

### ***2.8.3 Isolation and characterization of CYP1B1***

CYP1B1 was first isolated by Sutter *et al.* (1994). They constructed a cDNA library from human neonatal foreskin keratinocyte cell line. The cDNA library was treated with 2,3,7,8-tetrachlorodibenzo-p-dioxin TCDD for 6 hours and the responsive clones were isolated by differential hybridization (Sutter *et al.*, 1994). Based on the results of the differential hybridization, 5 clones responsive to TCDD were selected, one of the clone was identified as CYP1A1, two each of plasminogen activator inhibitor-2 (PAI-2) and interleukin-1B (IL-B) genes, respectively.

The cDNA inserts of the two uncharacterized clones were used as probes to screen the library by colony hybridization and identified a set of 8 overlapping clones covering the full cDNA sequence (Sutter *et al.*, 1994) and led to the identification of the 5'terminal and 3'terminal sequences of the *CYP1B1* gene.

Human *CYP1B1* gene has been mapped to chromosome 2 by screening the human /rodent somatic cell hybrids , containing one or more human chromosomes, with the primer set specific to the 3'-untranslated region of clone 1 cDNA sequence. The amplified product (490bp) was observed in the hybrids containing human chromosome 2, hence locating human *CYP1B1* on the same (Sutter *et al.*, 1994).

In order to determine other members of CYP1B subfamily southern blot analysis of human genomic DNA, digested with restriction endonucleases *HindIII*, *PstI*, *EcoRI* and *SacI*, was done using a single cDNA probe corresponding to the 5'-portion of the CYP open reading frame. Hybridization results of all the four restriction endonucleases revealed only a single band indicating the presence of a single gene for CYP1B1 (Sutter *et al.*, 1994). CYP1B1 was found to express in other tissues such as heart, brain, placenta, testis, lung, liver, skeletal muscle, kidney, spleen, thymus, ovary, small intestine, colon and peripheral blood leukocytes by northern blot analysis with the highest expression in the kidney.

Another study to characterize *CYP1B1* was carried out by Tang *et al* (1996). They screened 950,000 colonies of human genomic and identified a 5.1 kb cDNA sequence of CYP1B1 along with an additional 3 kb DNA sequence upstream to the cDNA sequence. Comparison of the sequences of the clones with the complete cDNA sequence of *CYP1B1* led to identification of three exons of 371bp, 1044 bp and 3707 bp in length along with two introns of 390 and 3032 bp, respectively (Fig. 2.13). Unlike the other CYP family members the coding region of *CYP1B1* was identified to start in the 5' end of the second exon and termination within the third exon. They also confirmed the existence of a single member of the CYP1B subfamily by southern blot analysis of human genomic DNA digested with 4 restriction endonucleases, *EcoRI*, *PstI*, *SacI* and *HindIII*, using the cDNA probes corresponding to the three exons of *CYP1B1*. The position of *CYP1B1* on chromosome 2 was also refined by fluorescent *in situ* hybridisation (FISH) also confirmed the localization of human *CYP1B1* to 2p21-22.

---

### 2.8.3.1 Characterization of *CYP1B1* promoter

The characterization of the 5' flanking region for the various functional modalities like TATA box, enhancer sequences and transcription initiator site was done by the progressive 5'-3' deletions and 3'-5' deletions in the region between -2300 nucleotide to -164 nucleotide (Wo *et al.*, 1997). The various deleted fragments were inserted into pCAT promoter followed by the transfection of the constructs into human squamous cell carcinoma (SCC12) cell line. Effect of the deletions on the expression of the reporter gene (Chloremphenicol Acetyl Transferase [CAT] ) downstream of the deleted fragment was tested, which revealed the region between -164 to + 25 as the active promoter sequence. Two enhancer sequences were identified between -2300 to -1356 and -1022 to -835 nucleotides. The *CYP1B1* promoter was found to contain the TATA like sequence from -33 to -28 nucleotide position instead of the consensus TATA box. S1 nuclease mapping (Berk *et al.*, 1977) and primer extension analysis (Sambrook *et al.*, 1989) methods were used to determine the transcription initiation site (TIS) of *CYP1B1* at 27 nucleotides downstream from a TATA- like box. Two Sp1 binding sites were identified at -84 and -68 nucleotide positions, respectively (Fig.2.13).

The promoter sequence of *CYP1A1* contains DNA response elements (DREs). TCDD binds to the core recognition sequences within these DREs with the help of two proteins, aromatic hydrocarbon receptor (AhR) and aromatic hydrocarbon receptor nuclear translocator (ARNT). These two proteins belong to the basic helix loop helix family of transcription factors. The interaction of this complex with the DRE activates the transcription of the target gene (Whitlock *et al.*, 1990, Dolwick *et al.*, 1993). The sequence analysis of the 3 kb 5' flanking region of *CYP1B1* cDNA found to harbor 9 DRE motifs. The DRE motif responsible for TCDD response was determined by the

5'-3' and 3'-5' progressive deletions in the -2300 to +1500 region. The various deleted fragments were inserted into pCAT promoter followed by the transfection of the constructs into human squamous cell carcinoma (SCC12) cell line. Effect of TCDD on the expression of the reporter gene (Chloremphenicol Acetyl Transferase [CAT] ) downstream of the various deleted fragments was tested which revealed that the deletion fragments proximal to -1200 and distal to -835 were not responsive to TCDD indicating this region (-1200 to -835) as the dioxin responsive element (Tang *et al.*, 1996).

The *CYP1B1* gene is transcriptionally activated by polycyclic aromatic hydrocarbons (Ah) which act via Ah receptor complex. The most potent activator of *CYP1B1* is dioxin. Dioxin-responsive elements as well as multiple xenobiotic responsive elements have been identified in the 5' regulatory region of *CYP1B1*. The activation involves a specialized receptor called Ah receptor, which binds to Ah. This complex in turn with the help of another protein, called Ah receptor nuclear translocator, reaches the nucleus and activates gene transcription (Murray *et al.*, 2001).

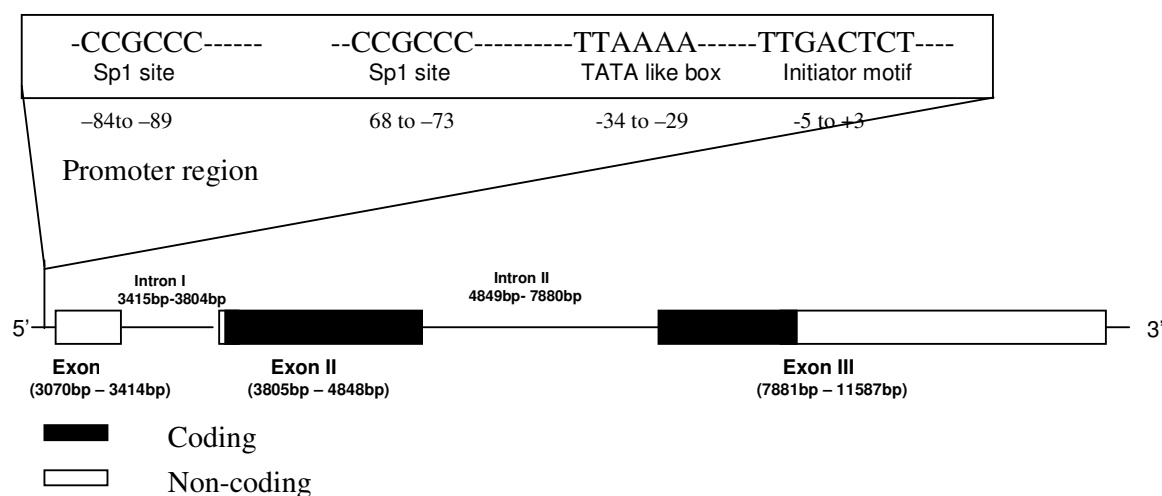


**Figure 2.13** Diagram showing the genomic organization of *CYP1B1* gene (Tang *et al.*, 1996; Wo *et al.*, 1997).



---

#### 2.8.4 Association CYP1B1 with other diseases

CYP1B1 has the highest catalytic activities towards several polycyclic aromatic hydrocarbons like dibenzopyrene-11, 12-diol, dibenzochrysene-11, 12-diol, benzophenanthrene-3, and several aryl amines including 2-aminoanthracene, 6-aminochrysene etc. These chemicals are the most potent inducers of mammary tumors and lung cancers (Shimada *et al.*, 1996).

Apart from these exogenous compounds CYP1B1 is also involved in the metabolism of endogenous steroids like 17 $\beta$  estradiol. CYP1B1 adds the hydroxyl group at 4<sup>th</sup> carbon position of this estrogen unlike the other CYPs (CYP1A1) which hydroxylates it at the 2<sup>nd</sup> position. The 2-OH and 4-OH metabolites of the estrogen are oxidized to semiquinones and quinines that induce single strand breaks and cause oxidative DNA damage. A significantly higher expression with elevated 4-hydroxy estradiol production has been found in various tumor tissues like breast, uterus, prostate, lung etc than in the normal tissues.

Four single nucleotide polymorphisms (SNPs) in CYP1B1 (R48G, A119S, and V432L) exhibits altered kinetics with significantly increased  $K_m$  and lowered  $V_{max}$  values for hydroxylation of estradiol (Shimada *et al.*, 2001, Akillu *et al.*, 2002). These SNPs show significant associations with various cancers with respect to the genotypic and allelic frequencies in patients than controls. For instance the mutant S119 allele frequency has been reported to be significantly higher in prostate cancer, breast and lung cancer patients (Tanaka *et al.*, 2002, Watanabe *et al.*, 2000), while the wild type V432 allele is associated with breast cancer in Turkish population and Caucasian populations. However Chinese population exhibits a higher frequency of mutant L432 allele as opposed to V432 allele (Zheng *et al.*, 2000). The A119 residue lies within the putative active site region of CYP1B1 and the R48, L432 are on surface of the

enzyme that might be important for binding to its redox partners. Hence alterations in these residues are likely to affect the activity of the enzyme and may influence the susceptibility of individuals towards endogenous and exogenous carcinogens (Lewis *et al.*, 2003).

### ***2.8.5 CYP1B1 expression in ocular tissues***

CYP1B1 protein expresses in various human ocular tissues like cornea, ciliary body, iris, retina etc. However, no expression has been identified in TM. Interestingly, an increased CYP1B1 expression has been identified in the fetal eyes studied in comparison to the adult eyes (Fig 2.14). This observation makes it tempting to speculate that CYP1B1 in the eye metabolizes an important substrate that plays a key role in the development and maturation of ocular tissues (Doshi *et al.*, 2006). However, an entirely opposite scenario has been observed in the mouse ocular tissues. According to a study carried out to look for the spatio-temporal expression of CYP1B1 in mouse eye ontogeny revealed that the expression increases with age (Choudhary *et al.*, 2007). They have observed the highest CYP1B1 expression at the adult stage (6 months) of mice (Fig 2.15). Based on the observations of these two studies, it can be suggested that CYP1B1 expression pattern is different in the two species. The involvement of CYP1B1 in the development of human ocular tissues can be speculated but its role in mice ocular tissue development is questionable.

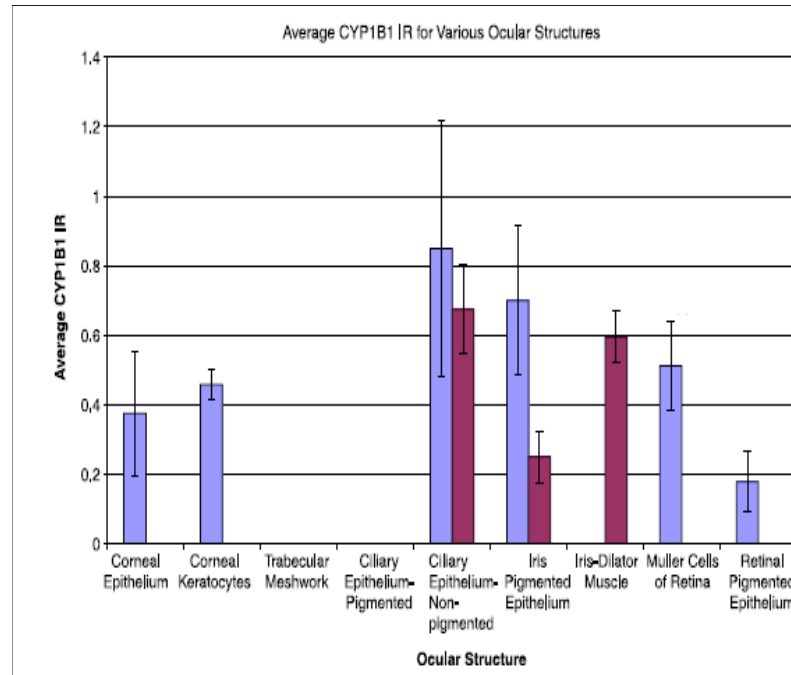


**Figure 2.14:** Comparison of CYP1B1 expression human fetal and adult ocular tissues (Doshi *et al.*, 2006)

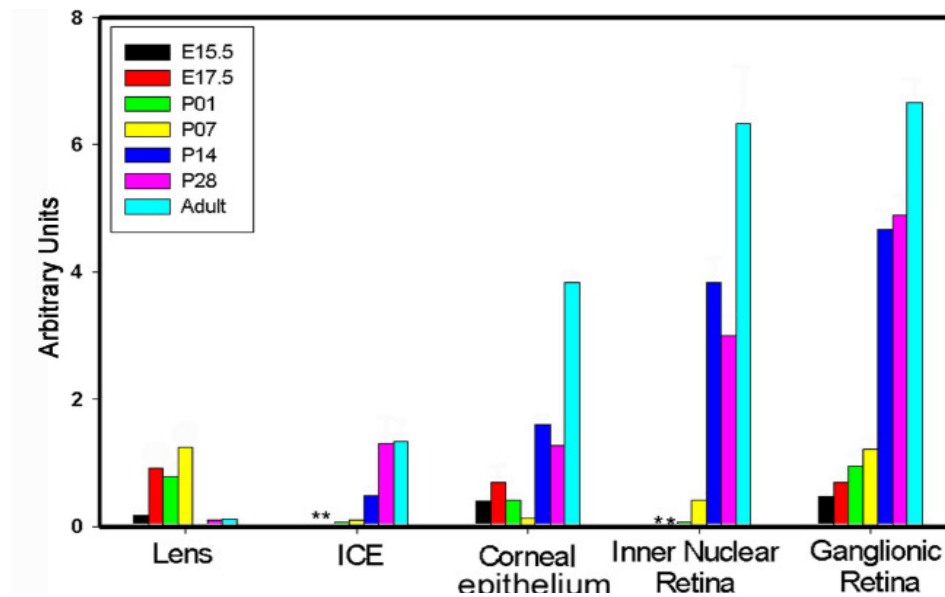


**Figure 2.15:** Spatio-temporal expression of Cyp1b1 expression in various mouse ocular tissues (Choudhary *et al.*, 2007)

### 2.8.6 Use of CYP1B1 knock out mice to determine its role in PCG pathogenesis

To investigate the role of *CYP1B1* in PCG, *Cyp1b1* knockout (*Cyp1b1*<sup>-/-</sup>) mice were created by targeted gene disruption in embryonic stem cells (Butters *et al.*, 1999). However, gross examination of the eyes of the *Cyp1b1*<sup>-/-</sup> mice did not show any evidence of glaucoma. Also the behavioral comparisons between the *Cyp1b1*<sup>-/-</sup> and wild type mice on the basis of their response to light and dark revealed that the animals were not blind. In addition no systemic abnormalities in the *Cyp1b1*<sup>-/-</sup> mice suggested that *CYP1B1* is not required for mammalian development (Butters *et al.*, 1999).

Similarly, the *Cyp1b1*<sup>-/-</sup> mice created by Libby and coworkers (2003) showed no gross abnormalities with their IOP indistinguishable from the wild type mice. However, the histological and electron microscopic analysis revealed abnormalities in the eyes of *Cyp1b1*<sup>-/-</sup> mice and not in the wild type ones (Figs 2.16 & 2.17). These abnormalities included

- a) Small /absent Schlemm's canal.
- b) Basal lamina extending from the cornea over the TM.
- c) Attachments of iris to TM and peripheral cornea.

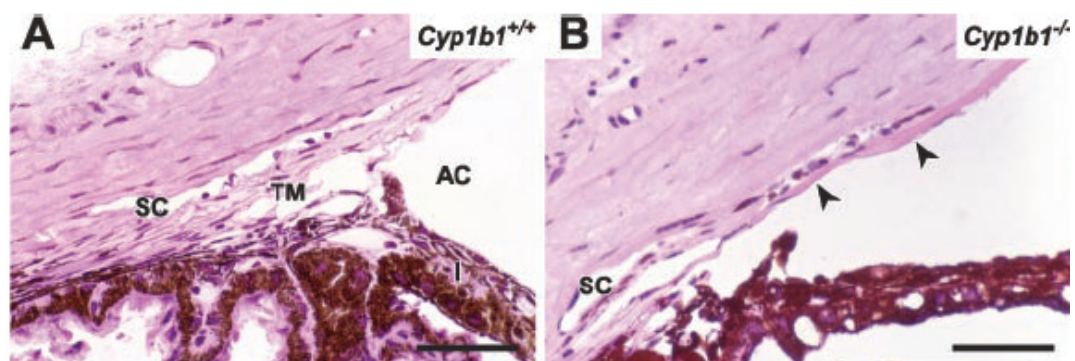


**Figure 2.16.** Comparison of anterior chamber angle structures (histological level) in wild type and *Cyp1b1*<sup>-/-</sup> mice (adapted from Libby *et al.* 2003). A) Well formed angle structures in wild type mice. B) Angle abnormalities in *Cyp1b1*<sup>-/-</sup> mice. Hypoplastic TM. Material resembling Descemet's membrane (shown by arrow heads) abnormally covers a portion of TM.

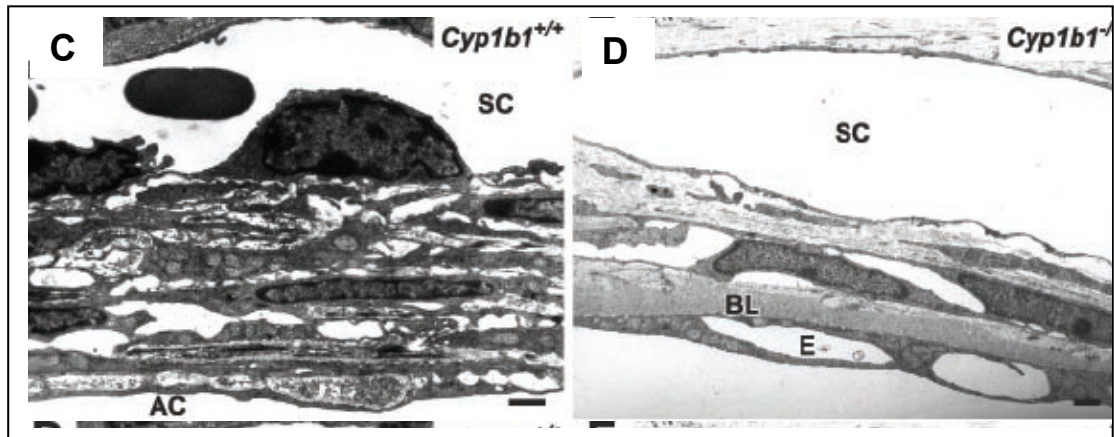


**Figure 2.17** Comparison of anterior chamber angle structures (ultrastructural level) in wild type and *Cyp1b1*<sup>-/-</sup> mice (adapted from Libby *et al.* 2003). C) There is an endothelial –lined SC and a robust TM with numerous well formed trabecular beams in the wild type mice. D) In *Cyp1b1*<sup>-/-</sup> mice, the endothelial lining of SC is attenuated and there is only a single trabecular beam. Access to TM and SC is blocked by a thick basal lamina. The inner aspect of the basal lamina is covered with abnormal cells resembling endothelial cells.

Based on these observations, it was suggested that even though the *Cyp1b1*<sup>-/-</sup> mice did not show the classical PCG features, the anterior chamber angle abnormalities in the *Cyp1b1*<sup>-/-</sup> mice revealed the potential role of *CYP1B1* in the development of these structures (Libby *et al.*, 2003).

### ***2.8.7 Potential role of CYP1B1 in development through Retinoic acid mediated signaling***

CYP1B1 has been shown to metabolize the two step oxidative synthesis of retinoic acid (RA) from retinol (Chambers *et al.*, 2007). RA is a ligand for various nuclear receptor proteins and is known to regulate morphogenesis by providing positional information to cells during embryogenesis. The two step oxidative synthesis of RA can be metabolized by various retinaldehyde dehydrogenases (RALDH) like RALDH-1, RALDH-2 and RALDH-3. In order to correlate the RA synthesis by CYP1B1, a study by Chambers and coworkers (2007) has been carried out in chick with a focus on the regions, which are rich in RA production and CYP1B1 synthesis but are deficient in

RALDH expression. The authors have studied the ectopic expression of CYP1B1 and in turn its affect on the transcription of developmental genes, which are known to be regulated by RA. The study revealed that ectopic expression of CYP1B1 resulted in the downregulation of two such developmental genes, i.e, Shh (sonic hedgehog homolog of drosophila)- regulates the vertebrate organogenesis and Nkx6.1 (NK homobeobox family 6)- involved in the development of beta cells in endocrine pancreas and is a crucial regulator of motor neurons progenitor domains. Based on these observations it was suggested that CYP1B1 might play an important role in the development via RA mediated signaling pathways (Chambers *et al.*, 2007).

#### **2.8.8 Mutation spectrum of CYP1B1 worldwide**

A total of 70 distinct mutations (<http://www.hgmd.cf.ac.uk/ac/index.php>) in *CYP1B1* have been described in PCG in different ethnic groups (Table 2.3) and populations indicating the genetic heterogeneity of the condition, of which G61E (Bejjani *et al.*, 2000), E387K (Plasilova *et al.*, 1999) and R368H (Reddy *et al.*, 2003) were the predominant mutations identified in Saudi Arabia, Slovakian Gypsies and Indian population, respectively. *CYP1B1* mutations in PCG populations ranges from 20% in Japanese (Mashima *et al.*, 2001), 33.3% in Indonesians (Sitorus *et al.*, 2003), 50% among the Brazilians (Stoilov *et al.*, 2002 a) to almost 100% among the Saudi Arabians (Bejjani *et al.*, 1998) and Slovakian Gypsies (Plasilova *et al.*,1999). The high prevalence of this disease in the latter two populations is attributed to consanguinity and inbreeding.

**Table2.3:** Worldwide distribution of *CYP1B1* mutations

S. no.	Nucleotide position	Amino acid change	Type of mutation	Exon	Population	Reference
1	g.3775insA	----	Frameshift	II	India	Panicker <i>et al.</i> , 2002
2	g.3860C>T	Q19X	Nonsense	II	Brazil	Stoiov <i>et al.</i> , 2002
3	g.3928delG	----	Frameshift	II	India	Present study
4	g.3905-3927del23	----	Frameshift	II	India	Reddy <i>et al.</i> , 2003
5	g.3964delC	----	Frame shift	II	Japan	Mashima <i>et al.</i> , 2001
6	g. 3972 C>T	A56V	Missense	II	India	Present study
7	g.3976G>C	W57C	Missense	II	Hispanic	Stoilov <i>et al.</i> , 1998
8	g.3896G>A	W57X	Nonsense	II	Brazil	Stoilov <i>et al.</i> , 2002
9	g.3988delA	----	Frameshift	II	Iran	Chitsazian <i>et al.</i> , 2007
10	g.4035 T>C	L77P	Missense	II	Saudi Arabia	Bejjani <i>et al.</i> , 2000
11	g.4046 T>A	Y81N	Missense	II	India	Present study
12	g.4048C>A	Y81X	Nonsense		Iran	Chitsazian <i>et al.</i> , 2007
13	g.4055 G>T	V84F	Missense	II	India	Present study
14	g.4148 G>C	A115F	Missense	II	India	Reddy <i>et al.</i> , 2004
15	g.4154C>T	R117W	Missense	II	Turkey	Bagiyeva <i>et al.</i> , 2007
16	g.4200 T>G	M132R	Missense	II	India	Reddy <i>et al.</i> , 2004
17	g.4236 A>C	Q144P	Missense	II	India	Reddy <i>et al.</i> , 2004
18	g.4236A>G	Q144R	Missense	II	India, Spain	Chakrabarti <i>et al.</i> , 2007 Lopez-Garrido <i>et al.</i> , 2006
19	g.4322G>A	E173R	Missense	II	Iran	Chitsazian <i>et al.</i> , 2007
20	g.4339delG	----	Frameshift	III	Morocco	Belmouden <i>et al.</i> , 2002
21	g.4380A>T	D192V	Missense	II	Japan	Mashima <i>et al.</i> , 2001
22	g.4383C>T	P193L	Missense	II	India	Reddy <i>et al.</i> , 2004
23	g.4397G>A	V198I	Missense	II	Japan	Mashima <i>et al.</i> , 2001
24	g.4410C>A	A202D	Missense	II	Iran	Chitsazian <i>et al.</i> , 2007

25	g.4449G>T	S215I	Missense	II	Indonesia	Sitorus <i>et al.</i> ,2003
26	g.4490G>A	E229K	Missense	II	Iran, India, France, Turkey	Reddy <i>et al.</i> ,2003, Panicker <i>et al.</i> , 2004, Kumar <i>et al.</i> , 2007, Acharya <i>et al.</i> , 2006, Melki <i>et al.</i> , 2004, Colomb <i>et al.</i> , 2003, Bagiyeva <i>et al.</i> , 2007, Chitsazian <i>et al.</i> ,2007
27	g.4499G>C	G232R	Missense	II	France	Colomb <i>et al.</i> ,2003
28	g.4520 A>C	S239R	Missense	II	India	Reddy <i>et al.</i> ,2003
29	g.4547C>T	Q248X	Missense	II	France	Colomb <i>et al.</i> ,2003
30	g.4611-4619dup9	----	Frameshift	II	Iran	Chitsazian <i>et al.</i> , 2007
31	g. 4645 C>A	C280X	Nonsense	II	India, Japan	Mashima <i>et al.</i> , 2001, present study
32	g.4646G>T	E281X	Frameshift	II	Turkey	Stoilov <i>et al.</i> , 1998
33	g.4673-4674insC		Frameshift	II	Iran	Chitsazian <i>et al.</i> , 2007
34	g.4677A>G	D291G	Missense	II	Iran	Chitsazian <i>et al.</i> ,2007
35	g.4763G>T	V320L	Missense	II	Japan	Mashima <i>et al.</i> , 2001
36	g. 4776insAT		Frameshift	II	Japan	Mashima <i>et al.</i> , 2001,
37	g.4791G>T	G329V	Missense	II	Japan, Iran, Turkey	Mashima <i>et al.</i> , 2001, Chitsazian <i>et al.</i> ,2007, Bagiyeva <i>et al.</i> , 2007
38	g.4791G>T	G329D	Missense	II	Australia	Dimasi <i>et al.</i> , 2007
39	g.4793G>T	A330F	Missense	II	Japan	Ohtake <i>et al.</i> , 2003
40	g.4793 G>A	A330T	Missense	II	India	Present study
41	g.7900 C>T	Arg355Stop	Nonsense	III	Turkey, India	Michels-Rautenstrauss <i>et al.</i> , 2001, present study
42	g. 7900-7901 del2	----	Frameshift -	III	Indian	Reddy <i>et al.</i> , 2004
43	g.7927G>A	V364M	Missense	III	Japan, Indonesia	Mashima <i>et al.</i> , 2001,



						Sitorus <i>et al.</i> ,2003
44	g.7934G>T	G365W	Missense	III	USA	Stoilov <i>et al.</i> , 1998
45	g.7934delG	----	Frameshift	III	Iran	Chitsazian <i>et al.</i> , 2007
46	g.7939C>T	R368C	Missense	III	Iran	Chitsazian <i>et al.</i> ,2007
47	g.7940G>A	R368H	Missense	III	India, SaudiArabia,Brazil, Turkey, Kuwait, Iran	Reddy <i>et al.</i> ,2003, Panicker <i>et al.</i> , 2004 Panicker <i>et al.</i> , 2002 Chakrabarti <i>et al.</i> , 2006 Bejjani <i>et al.</i> , 2000 Stoilov <i>et al.</i> , 2002 Bagiyeva <i>et al.</i> , 2007 AlFadhli <i>et al.</i> , 2006 Chitsazian <i>et al.</i> , 2007
48	g.7957G>A	D374N	Missense	III	Saudi Arabia	Bejjani <i>et al.</i> , 2000 Bejjani <i>et al.</i> , 1998
49	g.7971C>T	P379L	Missense	III	Turkey	Stoilov <i>et al.</i> , 1998
50	g.7996G>A	E387K	Missense	III	Brazil France	Stoilov <i>et al.</i> , 2002 Colomb <i>et al.</i> , 2003
51	g.8006G>A	R390H	Missense	III	India, Iran,France,	Reddy <i>et al.</i> , 2004, Chitsazian <i>et al.</i> , 2007, Melki <i>et al.</i> , 2004
52	g.8005 C>A	R390S	Missense	III	Saudi Arabia	Bejjani <i>et al.</i> , 2000
53	g.8005 C>T	R390C	Missense	III	India	Reddy <i>et al.</i> ,2003
54	g.8033T>G	I399S	Missense	III	France	Colomb <i>et al.</i> ,2003
55	g.8035C>T	P400S	Missense	II	Australia	Dimasi <i>et al.</i> , 2007
56	g.8037-8046 dup10	----	Frameshift	III	-- Brazil, USA, British, Turkey, France, Germany, UK, Costa Rica Iran, Australia	Stoilov <i>et al.</i> , 2002 Sena <i>et al.</i> , 2004 Colomb <i>et al.</i> , 2003 Stoilov <i>et al.</i> , 1998 Michels-Rautenstrauss <i>et</i>

						<i>al.</i> , 2001 Chavarria Soley <i>et al.</i> , 2003 Chitsazian <i>et al.</i> , 2007 Dimasi <i>et al.</i> , 2007
57	g.8147 C>T	P437L	Missense	III	Turkey, Brazil, India	Stoilov <i>et al.</i> ,1998, Stoilov <i>et al.</i> ,2002, Reddy <i>et al.</i> ,2003
58	g.8148-8152 de5 *	----	Frameshift	III	India	Present study
59	g.8162C>G	P442R	Missense	III	Iran	Chitsazian <i>et al.</i> , 2007
60	g.8165C>G	A443G	Missense	III	Brazil,France	Stoilov <i>et al.</i> , 2002 Rautenstrauss <i>et al.</i> , 2001
61	g.8168G>A	R444Q	Missense	III	Japan	Mashima <i>et al.</i> , 2001
62	g.8182delG	----	Frameshift	III	Brazil	Stoilov <i>et al.</i> , 2002
63	g.8214-8215del2	----	Frameshift	-III	Brazil	Stoilov <i>et al.</i> , 2002
64	g.8227T>C	S464P	Missense	III	India	Present study
65	g.8234 G>A	G466D	Missense	III	India	Reddy <i>et al.</i> , 2003
66	g. 8242C>T	R469W	Missense	III	Saudi Arabia, Turkey, Iran	Bejjani <i>et al.</i> , 2000 Stoilov <i>et al.</i> ,1998 Chitsazian <i>et al.</i> , 2007
67	g. 8333A>G	E499G	Missense	III	Japan	Mashima <i>et al.</i> , 2001
68	g.8341delA	----	Frameshift	III	Iran	Chitsazian <i>et al.</i> , 2007
69	g.8354-8373delA	----	Frameshift	III	Iran	Chitsazian <i>et al.</i> , 2007
70	g.8393 A>G	Asn519Ser	Missense	III	India	Present study

Majorities of mutations reported in *CYP1B1* are missense (Table 2.4), which affect the amino acid residues located either in the hinge region or the conserved core structures in the cytosolic region (Fig 2.18). These mutations, therefore, are expected to interfere with fundamental properties of the protein such as folding, heme binding, substrate accommodation and interaction with the redox partner (Stoilov *et al.*, 2001). Among the various missense mutations, G61E (Bejjani *et al.*, 2000), E387K (Plasilova *et al.*, 1999) and R368H (Reddy *et al.*, 2003) are the most predominant mutant alleles in Saudi Arabian, Slovakian Gypsies and Indian populations, respectively (Table 2.5). However, insertions have been identified only in Japanese and Turkish populations. The wide spectrum of mutations identified in *CYP1B1* suggested allelic heterogeneity of the condition. Moreover, mutations have been identified throughout the gene indicating that there are no hot spot regions in the *CYP1B1*. Most of the *CYP1B1* mutations have been identified in the cytosolic domain of the protein.

**Table 2.4:** Distribution of different types of *CYP1B1* mutations worldwide

Population	Type of mutation					Cases without <i>CYP1B1</i> mutation
	Missense	Nonsense	Deletion	Duplication	Insertion	
Saudi Arabia (n=62)	55 (88.7%)	-	2 (3.2%)	-	-	5 (8.1%)
Brazil (n=52)	5 (9.6%)	3 (5.8%)	16 (30.8%)	4 (7.8%)	-	
Iran (n=104)	81 (77.9%)	1 (0.96%)	4 (3.84%)	3 (2.9%)	1 (0.96%)	14 (13.5%)
Australia (n=37)	8 (21.6%)	1 (2.7%)	1 (2.7%)	1 (2.7%)	-	26 (70%)
Japan (n=65)	10 (15.4%)	1 (1.5%)	1 (1.5%)	-	3 (4.6%)	50 (76.9%)
Turkey (n= 35)	13 (37.1%)	-	-	1 (2.9%)	1 (2.9%)	20 (57.1%)
Ecuador (n=15)	2 (13.3%)	-	1 (6.7%)	-	-	12 (80%)

Kuwait (n=17)	11 (64.7%)	1 (5.9%)	-	-	-	5 (29.4%)
Indonesia & Europe (n=21)	5 (23.8%)	1 (4.8%)	2 (9.5%)	-	-	13 (61.9%)
Morocco (n=32)	9 (28.1%)	-	4 (12.5%)	-	-	19 (59.4%)
France (n=31)	6 (19.4%)	9 (29.0%)	2 (6.5%)	-	-	14 (45.2%)
Mexico (n=12)	4 (33.3%)	-	-	1 (8.3%)	-	7 (58.3%)
US & Brazil (n=21)	2 (9.5%)	-	2 (9.5%)	2 (9.5%)	-	15 (71.4%)
Egypt (n=10)	3 (30%)	-	-	-	-	7 (70%)

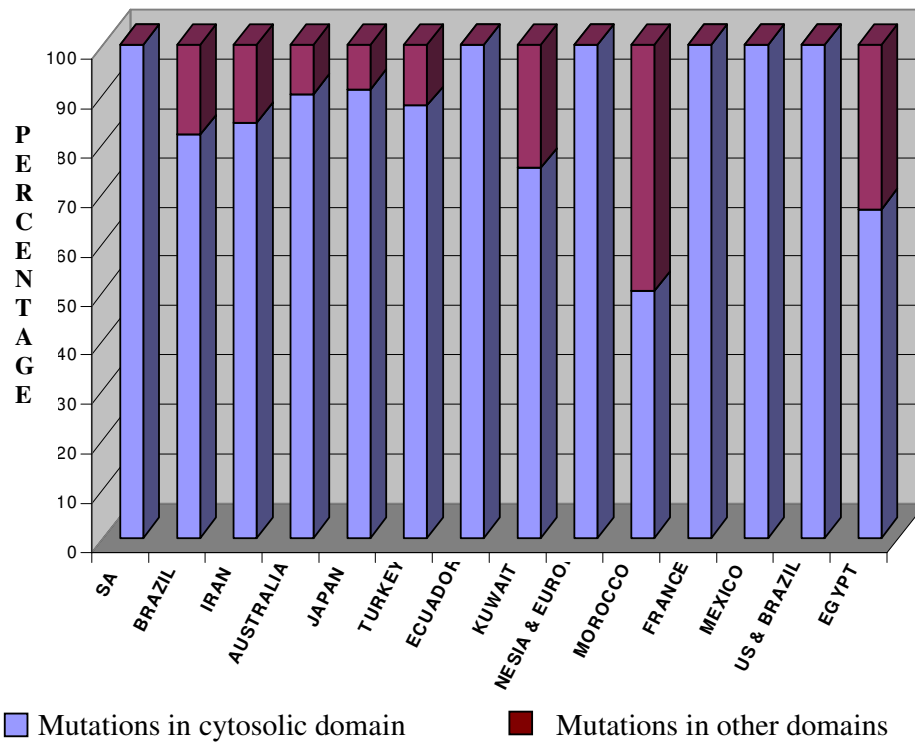


**Figure 2.18:** Worldwide distribution of *CYP11B1* mutations in cytosolic and other domains of the protein

### **2.8.9 Prevalent mutations in *CYP1B1***

Among the various *CYP1B1* mutations in PCG populations across the globe, G61E was the prevalent mutation identified in 69.3% (43/62) of Saudi Arabian and 29% (30/104) of Iranian cases, respectively (Table 2.5). Apart from G61E, the R390H and R368H mutations were also identified at a higher frequency (20.1% and 10.6%, respectively) in Iranian patients. In both the populations the G61E mutation has occurred on a single haplotype background (C-C-G-G-T-A), constructed on the basis of six SNPs in *CYP1B1* (-13T/C, R48G, A119S, V432L, D449D and N453S), suggesting the occurrence of this mutation through a common founder in both the populations. In Saudi Arabian population 44.2% (19/43) of the patients with G61E did not manifest the disease at presentation, indicating the incomplete penetrance of this mutation. In the Iranian population, 26 out of the 29 cases with G61E were bilateral with an age of onset within 3 months of life. The IOP was raised in 26 cases at presentation whereas readings were not available for the other three cases. However, no comparison was made between the cases with G61E and cases with other mutations with respect to severity of the disease.

E387K was the only mutation identified in all the 20 PCG cases from Slovakia (Table 2.5) suggesting that it might have occurred through a single ancestral mutational event. The common haplotype (T-G-T-C-C-A) background of the patients harboring the mutation further confirmed the founder effect of E387K mutation in this population.

Among the Brazilian population 4340delG was the most predominant mutation identified in 23% (12/52) of the cases screened (Table 2.5). This mutation had occurred on a common haplotype background (C-G-G-T-A), constructed on the basis of five SNPs in *CYP1B1* (R48G, A119S, V432L, D449D and N453S), in 11 out of 12

cases. This suggested the founder effect of 4340delG mutation in Brazilian population. All the patients with 4340delG were bilateral cases with an age of onset within first month of life and IOP ranged between 25-55 mm of Hg. The patients had undergone multiple surgical interventions with an average of 2.6 in the left eye and 2.8 in the right eye.

The R368H mutation was the predominant *CYP1B1* mutant allele identified in PCG (Table 2.5). However, no association of severity of disease phenotype was established with this mutation (Reddy *et al.*, 2003).

**Table 2.5:** Prevalent mutations in various PCG populations across the globe

<i>Prevalent mutation</i>	<i>Population</i>	<i>Number of patients screened</i>	<i>Cases with prevalent mutation</i>	<i>Reference</i>
G61E	Saudi Arabia	62	43 (69.3%)	Bejjani <i>et al.</i> , 2000
	Iran	104	30 (29%)	Chitsazian <i>et al.</i> , 2007
	Turkey	35	5(14.3%)	Bagiyeva <i>et al.</i> , 2007
	Kuwait	17	9 (52.9%)	Alfadhli <i>et al.</i> , 2006
4339delG	Morocco	32	9 (28.1%)	Belmouden <i>et al.</i> , 2002
4340delG	Brazil	52	12 (23%)	Stoilov <i>et al.</i> , 2002
R444Q	Australia	37	2 (5.4%)	Dimasi <i>et al.</i> , 2007
	Japan	65	3 (4.6%)	Mashima <i>et al.</i> , 2001
	Japan	65	4 (6.2%)	Mashima <i>et al.</i> , 2001
V364M	Indonesia & Europe	21	4 (19%)	Sitorus <i>et al.</i> , 2003
8037-8046dup10	USA + Brazil	21	2 (9.5%)	Sena <i>et al.</i> , 2004
R368H	India	138	25 (18%)	Reddy <i>et al.</i> , 2003
E387K	Slovakia	20	20 (100%)	Plasilova <i>et al.</i> , 1999

#### **2.8.10 Clustering of prevalent *CYP1B1* mutations on common haplotype backgrounds**

Haplotypes have been generated with the five intagenic SNPs (R48G, A119S, V432L, D449D and N453S) from different PCG populations and it was identified that the “C-C-G-G-T-A” as the most prevalent haplotype among PCG cases with *CYP1B1*

mutations (Table 2.6). The frequency of “C-G-G-T-A” haplotype was found to be higher in [CYP1B1 (+)] cases than controls and [CYP1B1 (-)] cases, indicating a possible association with *CYP1B1* mutations (Chakrabarti *et al.*, 2006). On the other hand, the “G-T-C-C-A” was the most common haplotype among the [CYP1B1 (-)] cases and controls in comparison to [CYP1B1 (+)] cases (Chakrabarti *et al.*, 2006). As shown in Table 2.6 most of the common mutations from different populations were found to cluster on the same haplotype background. Since it is very unlikely that a specific haplotype would favor the occurrence of a specific mutation, the clustering of mutations from different geographical regions on the same haplotype background is therefore suggestive of their common founder effects. It is very unlikely that the same mutation would have arisen several times during the course of evolution. Therefore, the occurrence of same mutation on the common haplotype background in different geographical regions is probably because of the human migration. For example, the E387K mutation, which is the prevalent mutation among the Slovakian Roms (Plasilova *et al.*, 1999), was observed at a low frequency among patients in United States and Brazil (Sena *et al.*, 2004). However, in all the three populations E387K has been observed on the “G-T-C-C-A” haplotype background. This indicates that migrant Roms probably might have carried this mutation to these countries. Similarly the immigrants from Saudi Arabia to India might have carried the G61E mutation, which is the prevalent mutation in Saudi Arabian population and found to be associated with “C-G-G-T-A” haplotype in both the populations (Chakrabarti *et al.*, 2006).

**Table 2.6** Distribution of PCG associated *CYP11B1* mutations across different populations on various haplotype backgrounds

<b>HAPLOTYPE</b>	<b>India</b>	<b>Algeria</b>	<b>Morocco</b>	<b>Rome</b>	<b>Portugal</b>	<b>S.Arabia</b>	<b>Japan</b>	<b>USA</b>	<b>Ecuador</b>	<b>Brazil</b>
<b>C-G-G-T-A</b>	<b>R368H</b>					R368H				R368H
	A115P	g.4340delG	g.4340 del G							
	G466D									W57X
	G61E		G61E			<b>G61E</b>			G61E	
	g.3905del23						g.3964delC			
	g.8037bpdup10							g.8037bp dup10		g.8037bp dup10
	E229K						D192V			7901del13
	R469W, P437L					R469W	R444Q	SNF268 del		P437L
						SNF268del			g.4340 delG	<b>g.4340 delG</b>
<b>C-G-C-C-A</b>	R390C									
	S239R								R390C	
	P437L									
	C280X						C280X			
	R355X						g.4776ins AT			
	R390S									
	g.3928delG									
<b>G-T-C-C-A</b>	g.3835insA									



	E229K								
	g.1409del2			<b>E387K</b>		g.4238del 10		E387K	E387K
	P437L								
	g.7900del2								
	Y81N								
<b>C-G-C-C-G</b>	R390H				g.8182 delG				g.8182 del G
	M132R					L77P			

**Bold letters – predominant mutations in different populations**

In a similar way, C-G-G-T-A was identified as a risk haplotype in cases of POAG and PACG with *CYP1B1* mutations (Chakrabarti *et al.*, 2007). On the other hand, G-T-C-C-A haplotype, which was largely associated with the unaffected controls and PCG cases without *CYP1B1* mutations (Chakrabarti *et al.*, 2006), was similar in frequency in POAG and PACG cases with *CYP1B1* mutations and controls (Chakrabarti *et al.*, 2007). Also, similar to the findings in PCG, most of the prevalent mutations observed in POAG and PACG cases were clustered on C-G-G-T-A background (Chakrabarti *et al.*, 2007).

### 2.8.11 *CYP1B1* in other forms of glaucoma

*CYP1B1* has also been implicated in juvenile and adult onset forms of glaucoma, from various ethnic groups as shown in Table 2.7. The association of *CYP1B1* mutations with adult onset glaucomas ranged from 1.3% - 6.0 % (Table 2.7). The involvement of *CYP1B1* in POAG and PCG indicates that it is an important gene in different forms of glaucoma and its association with these glaucomas should be explored further to elucidate its involvement in disease pathogenesis.

**Table 2.7:** *CYP1B1* in adult onset OAG worldwide

Population	Type of glaucoma	No. of patients	Cases with <i>CYP1B1</i>	Prevalent mutation	Cases with prevalent mutation	Reference
French	POAG	236	11 (4.6%)	A443G	3 (1.3%)	Melki <i>et al.</i> , 2004
Indian	POAG	200	9 (4.5%)	S515L	4 (2%)	Acharya <i>et al.</i> , 2006
Indian	POAG	251	27 (10.8%)	R368H	10 (4.7%)	Kumar <i>et al.</i> , 2007
Indian	POAG	104	18 (17.3%)	R368H	6 (5.8%)	Chakrabarti <i>et al.</i> , 2007
	JOAG	30	7 (23.3%)		2 (2.2%)	
	PACG	90	10 (11.1%)		5 (5.6%)	
Spain	POAG	82	9 (10.9%)	Y81N	5 (6.0%)	Lopez-Garrido <i>et al.</i> , 2006

### **2.8.12 Interaction of *CYP1B1* with other genes**

*MYOC*, a candidate gene for juvenile and adult onset forms of primary open angle glaucoma, and has been suggested to be involved with *CYP1B1* through digenic mechanism in a glaucoma family of East Indian (Guyanese) origin. Based on their observations, the authors have suggested that congenital glaucoma and juvenile glaucoma are allelic variants of *CYP1B1* and that *CYP1B1* and *MYOC* might act through common biochemical pathways with *CYP1B1* acting as a modifier for *MYOC* (Vincent *et al.*, 2002).

*CYP1B1* has also been reported to interact with tyrosinase (*Tyr*) gene. *Tyr* is a candidate gene for ocular albinism that codes for a protein, which converts tyrosine to L-dopa that are precursors of catecholamines and are important regulators in development. *Tyr* has been identified as a modifier in iridocorneal angle defects present in *CYP1B1* knock-out mice. It has been observed that mice lacking both *CYP1B1* and *Tyr* had severe iridocorneal angle malformations than those lacking only *CYP1B1* (Libby *et al.*, 2003). Also some albinos are reported to have anterior segment dysgenesis and congenital glaucoma suggesting the possible role of *Tyr* in congenital glaucoma. It has been hypothesized that *Tyr* affects the angle development through modulation of L-dopa as treatment of L-dopa was found to prevent the severe angle dysgenesis present in mice lacking both *CYP1B1* and *Tyr*.

The TYR did not show any association with human PCG patients. Bidinost and coworkers (2006) have carried out a genome wide scan on 97 individuals from 17 Saudi Arabian families. Of these 97 individuals, 58 had homozygous or compound heterozygous mutations in *CYP1B1*. Thirty three of these 58 individuals were affected whereas 25 did not manifest clinical features of PCG. Along with these 58 individuals, 39 normal individuals (normal parents and siblings with one or no mutant *CYP1B1* alleles) were also

included. Genome wide scan did not show any significant evidence for a co-segregating locus. Besides, the screening of whole TYR gene by direct sequencing did not reveal any mutations in the gene. On the basis of these findings the authors had suggested that TYR is not a modifier for CYP1B1 mutations in humans. And the possible role of TYR in normal human eye development is different from that in the mouse model due to some yet unidentified differences between mice and humans.

### **2.8.13 Histological abnormalities in PCG**

Recently, Hollander and coworkers (2006) tried to correlate *CYP1B1* mutations with the degree of angle dysgenesis observed histologically and disease severity in terms of age at diagnosis, difficulty in controlling IOP, in 6 congenital glaucoma patients. Based on the histological findings the cases were divided into three categories:

- 1) Severe goniodysgenesis highlighted by agenesis of SC, hypoplasia of TM (Fig.2.19)
- 2) Moderate goniodysgenesis characterized by the presence of a band of collagenous tissue in TM (Fig 2.20.)
- 3) Mild goniodysgenesis associated with the deposition of a mucopolysaccharide material in juxtacanalicular tissue (Fig.2.21).

The correlation of *CYP1B1* mutations with histological findings, slit lamp observations etc., is shown in Table 2.8. The observations of this study (Hollander *et al.*, 2006) suggest that *CYP1B1* mutations can be classified based on the histological findings, which can be used to correlate these mutations with the severity of disease.

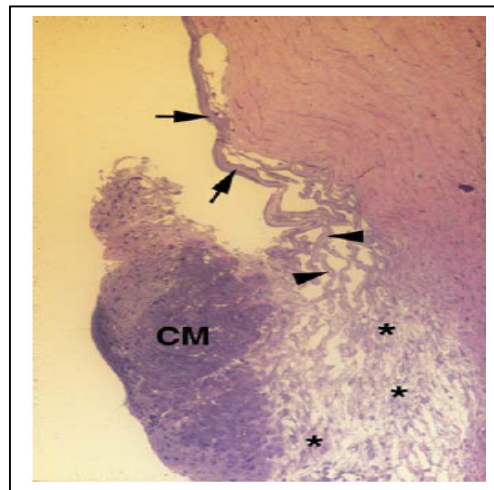


**Figure 2.19:** Severe goniodysgenesis: Light micrograph of trabeculectomy specimen showing the anterior chamber angle structures. Only a few elements of uveal cords (marked by arrows) and corneal scleral meshwork (marked by arrowheads) are present. The ciliary muscle (CM) is prominent and separated from the sclera (marked by asterisk).

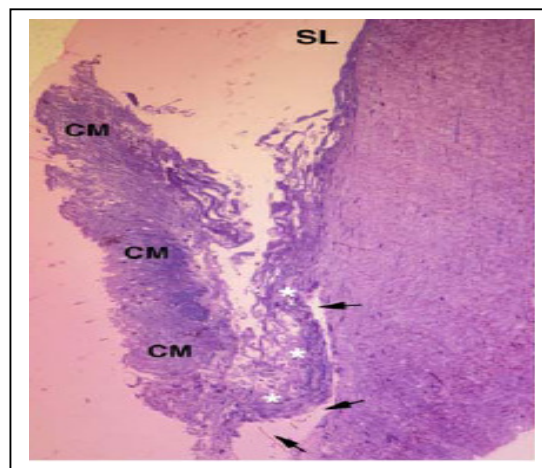


**Figure 2.20:** Light micrograph of trabeculectomy specimen showing moderate goniodysgenesis. Schwalbe's line (SL) is pointed out anteriorly and a prominent ciliary muscle (CM) posteriorly. A very well developed SC is present (marked by arrows). The TM is disorganized and the juxtacanalicular tissue has a thickened tissue pointed out (marked by asterisk).

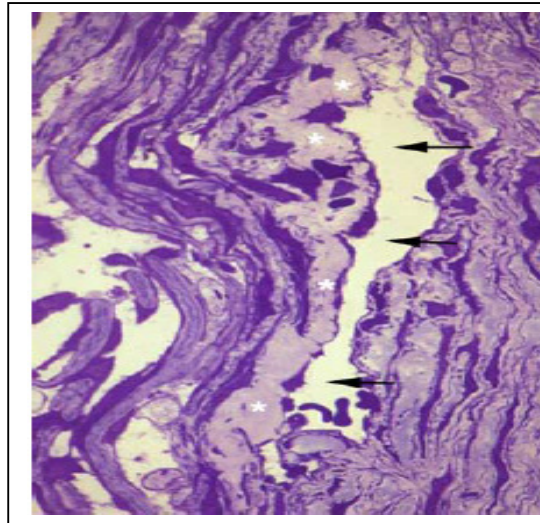


**Figure 2.21** : Light micrograph of trabeculectomy specimen showing the mild goniodysgenesis. Well formed Schlemm's canal (marked by arrows) and the juxtacanalicular tissue (marked by asterisk). There is a dense granular tissue within the the juxtacanalicular tissue.

**Table 2.8:** Correlation of *CYP1B1* mutations, slit lamp findings and histological abnormalities

<i>Cases</i>	<i>Goniodysgenesis</i>	<i>Age at diagnosis</i>	<i>CYP1B1 mutation</i>	<i>Slit lamp findings</i>	<i>Gonioscopy</i>	<i>Angle abnormalities based on histological observations</i>	<i>Outcomes</i>
Case-1	Severe goniodysgenesis	Since birth	R390H & R117P	Corneal edema	Open angle, iris insertion	SC agenesi s, prominent uveoscleral pathway	IOP under control after multiple surgeries
Case-2	Severe goniodysgenesis	Since birth	4340delG & C209R	Corneal edema	Open angle	SC agenesi s, prominent uveoscleral pathway	IOP under control after multiple surgeries
Case-3	Moderate goniodysgenesis	6 months	R368H & G61E	Corneal enlargement, edema, Haab's striae	Open angle, flat iris insertion	Connective tissue band in the juxtacanalicular tissue	IOP under control after single surgery followed by medication
Case-4	Moderate goniodysgenesis	8 months	No mutation	Corneal edema & enlargement	Open angle	Connective tissue band in the juxtacanalucular tissue	IOP under control after single surgery followed by medication
Case-5	Moderate goniodysgenesis	7 months	E229K	Corneal edema, Haab's striae	Open angle, flat iris insertion, iris hypoplasia	Connective tissue in corneo-scleral meshwork	IOP under control after single surgery followed by medication
Case-6	Mild goniodysgenesis	4 months	No mutation	Corneal enlargement, haab's striae	Open angle, flat iris insertion	Amorphous material in juxtacanalicular tissue	IOP under control by medication

(Adapted from Hollander et al., 2006)

### 2.8.14 *CYP1B1* mutations with PCG pathogenesis

The exact role of *CYP1B1* in the development of eye and its association with PCG is not known. Various in silico and in vitro studies have been carried out to determine the impact of the mutations in *CYP1B1* on the structure and function of the protein. The findings of these studies can help in a better understanding of the association of *CYP1B1* with the disease pathogenesis.

### 2.8.15 In-silico studies on the *CYP1B1* mutations

Among the 70 different mutations identified in *CYP1B1*, 8 have been studied in-silico for their possible impact on the protein structure and hence its function (Achary *et al.*, 2006). The human CYP1b1 structure was modeled by means of comparative modeling using the X-ray structure of CYP2c9 as the template. The wild type and mutant structures were the subjected to long molecular dynamics simulations. The effects produced by the various mutations studied are summarized in Table 2.9.

**Table 2.9:** Structural analysis of PCG associated mutation in *CYP1B1*

<b>Mutation</b>	<b>Location</b>	<b>Effect on protein</b>
A115P	Close proximity to the heme binding region (HBR)	Restricts conformational freedom, precludes the hydrogen bonding
M132R	HBR	Potentially harming the H-bond interaction with HBR
Q144P	Close to the HBR	Potentially break the continuity of the c-helix, inhibits the interaction with other amino acids
P193L	N-cap position of the E-helix	Affect stability of the e-helix thereby affecting the packing in this region
S239R	Close to substrate access channel (SAC)	Affects the substrate and dynamics of the SAC region
R368H	Between the J and K helices	Affects interaction with other amino acids
G466D	Middle of the heme-binding loop (HBL)	Affects interaction with reductase protein



### **2.8.16 In vitro studies on CYP1B1 mutations**

The first study to determine the effect of *CYP1B1* mutations on the stability and function of the protein was carried out by Jansson and coworkers (2001). The authors have studied the effect of two missense mutations (G61E and R469W) on the stability and enzymatic activity of CYP1B1. The constructs of wild type and two mutants were transformed into *E. coli* DH5 $\alpha$  cells. Membrane fragments (both wild type and mutants) of *E. coli* (source of Cyp1b1) were incubated at 40C for 48 hrs to determine the stability of the protein. It was observed that G61E mutant had lost 60% of the stability. However, the R469W retained about 80% of the stability after 48hrs when compared to the wild type. The effect of the mutants on the function of protein was determined by an enzymatic assay where membrane fragments of *E. coli* were incubated with various steroids like testosterone, progesterone, estradiol etc. it was observed that both the mutant proteins had decreased metabolic activity (50%- 70%) for all the three substrates when compared to the wild type protein.

Similarly Bagiyeva and coworkers (2007) have compared the enzymatic activity of the two mutants (R117W and G329V) proteins with wild type. It was done by transfecting the HEK293T (African Green monkey kidney cell line) cells with wild type or mutant proteins. The enzymatic activity was determined by using P450-Glo kit assay that is devised to measure the in vivo conversion of modified Luciferin – CEE (Luciferin 6' chloroethyl ether) into luciferin substrate, which is then secreted to the medium and quantifiable by standard luciferase assay. No difference in the expression levels of wild type and mutant proteins was observed. However, the decreased enzymatic activity of mutant proteins was identified in comparison to the wild type protein. On the basis of these results it was suggested that the slow CYP1B1 traffic through ER in case of mutant

CYP1B1 contribute to the lower enzyme activity. This in turn could lead to the pathogenesis of PCG cases with *CYP1B1* mutations (Bagiyeva *et al.*, 2007).

#### ***2.8.17 Mislocalization of CYP1B1 mutant proteins***

CYP1B1 has been localized to cellular organelles like endoplasmic reticulum (ER) and mitochondria. Bagiyeva and coworkers (2007) have looked for the localization of two mutant CYP1B1 (R117W and G329V) proteins compared to the wild type. The authors showed that the wild type protein first localized to ER and then translocated to mitochondria. No localization in Golgi body was identified. In comparison to the wild type protein, an increased amount of mutant protein was detected in ER, whereas the localization in the mitochondria was decreased. This suggested a partial ER-retention or decreased trafficking through the ER. Also some of the G329V mutant protein was mislocalized to Golgi body (Bagiyeva *et al.*, 2007).

### **2.9 HYPOTHESIS FOR THE POSSIBLE ROLE OF CYP1B1 IN PCG PATHOGENESIS**

Although the exact function of *CYP1B1* protein in the eye is still unclear but from the fact that *CYP1B1* is a monooxygenase, two possible scenarios are expected for its role in the development of the eye (Stoilov *et al.*, 2001):

- a) *CYP1B1* is involved in the generation of some morphogen that plays an important role for the development of trabecular meshwork and other components in the outflow system by regulating the spatial and temporal expression of genes controlling the anterior chamber angle development. Hence the mutations in *CYP1B1* might result in the absence of the morphogen, which in turn alters the expression of genes.

b) Alternatively, *CYP11B* eliminates some active morphogen and prevents its signal capacity from dispersing beyond the specific cells upon which it must act. Hence the mutations in *CYP11B* might result in the accumulation of this metabolite producing toxic effects, which in turn may lead to developmental arrest.

But the absence of the orthologous enzyme in mouse (knockout mouse) did not show any evidence of glaucoma. This might be due to the less sensitivity of methods used to evaluate glaucomatous changes in the mouse. In addition, the mouse phenotype may differ from humans, since the anterior chamber angle has undergone evolutionary changes very recently as evident from the presence of typical trabecular meshwork in humans and higher apes as opposed to a reticular type meshwork in lower organisms (Gonzalez *et al.*, 2003, Stoilov *et al.*, 2001).

Apart from *CYP11B* two other candidate genes, i.e, Myocilin (*MYOC*) and Forkhead box C1 transcription factor (*FOXC1*) were also selected for screening.

### **2.10 MYOCILIN (*MYOC*) (LOCUS: *GLC1A* ON 1q23-25; OMIM # 601652)**

This gene is also termed as trabecular meshwork induced glucocorticoid receptor (*TIGR*) as it over expresses due to the induction of glucocorticoid to the cells. It consists of three exons that code for an mRNA of about 2.5 kb that encompasses a 57-kDa glycoprotein of 504 amino acids (Kubota *et al.*, 1998).The protein has two domains - a myosin like domain near the 'N' terminal and olfactomedin like domain near the 'C' terminal (Fig 2.22) (Johnson *et al.*, 2000). The 'N' terminal region consists of elements like leucine zipper and multiple sites for glycosylation and phosphorylation (Johnson *et al.*, 2000).

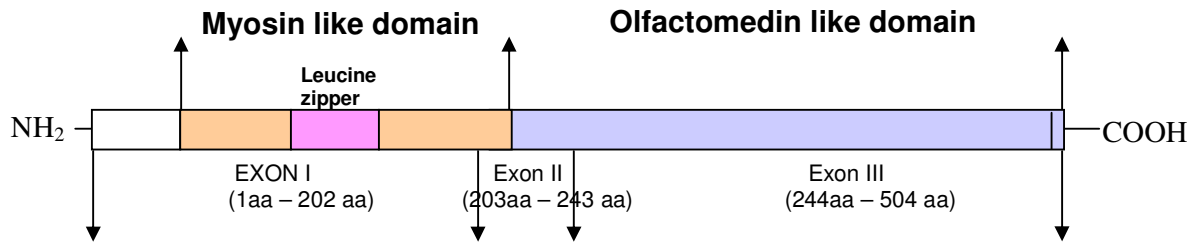


**Figure 2.22** Schematic representation of Human Myocilin protein

### 2.10.1 MYOC expression in human tissues

*MYOC* expression has been demonstrated in various ocular and non-ocular tissues. The ocular tissues include TM, sclera, iris, cornea, ciliary body, retina and optic nerve. Its expression has been noted in heart, skeletal muscle, stomach, thyroid, bone marrow, prostate, intestine, lung, pancreas and lymph node. (Johnson *et al.*, 2000). While *MYOC* has been reported as a secretory protein, various immunocytochemical studies on TM cells have also localized it to intracellular vesicles associated with cytoskeleton motor which reflects its normal processing during secretion.

### 2.10.2 MYOC mutations in glaucoma

Mutations in *MYOC* are associated with most of the familial forms of JOAG and 3%-4% of adult-onset POAG cases and normal tension glaucoma (Gong *et al.*, 2004). Most of these mutations are present in the olfactomedin domain of the protein. The domain is highly conserved among the species like fish, frog, rat, mouse and human, which supports its functional significance (Gong *et al.*, 2004).

Apart from this *MYOC* has also been reported to have an association with other forms of glaucoma like primary angle closure glaucoma, normal tension glaucoma and pigmentary glaucoma. Faucher *et al* screened *MYOC* in individuals with various forms of glaucoma

other than 'typical' POAG and identified mutations in three such individuals with angle closure glaucoma (Q368X), mixed mechanism glaucoma (R126W) and pigmentary glaucoma (A445V), respectively (Faucher *et al.*, 2002). Similarly, Vincent *et al.* (2002) reported two *MYOC* mutations, T293K and G399V, in two cases of pigmentary glaucoma and mixed mechanism glaucoma, respectively. These mutations have also been observed in the patients affected with POAG and JOAG. Table 2.10 shows the predominant mutations identified in *MYOC* from different populations.

*MYOC* has also been reported to co-segregate with *CYP1B1* in juvenile onset open angle glaucoma through a digenic mechanism in a glaucoma family of East Indian (Guyanese) origin (Vincent *et al.* 2002).it was observed that individuals with both *CYP1B1* (R368H) and *MYOC* (G399V) mutations had juvenile form of open angle glaucoma with mean age of onset at 27 years, whereas individuals with only *MYOC* (G399V) mutation had adult onset glaucoma with a mean age of onset at 51 years. Based on these observations it was suggested that *CYP1B1* may be a modifier of *MYOC* expression and that these two genes might act through common biochemical pathways. However, no study has looked for the association of *MYOC* mutations in PCG.

**Table 2.10:** Worldwide distribution of *MYOC* mutations

<i>Population</i>	<i>Phenotype</i>						<i>Cases with MYOC mutation</i>	<i>Predominant mutation (%)</i>	<i>Reference</i>
	POAG	PACG	PCG	XFG	OHT	PG			
India	56	-	-	-	-	-	4 (7.1%)	Q48H (5.3%)	Mukhopadhyay <i>et al.</i> , 2002
	107						2 (1.8)	G367R, T377M	Kanagavalli <i>et al.</i> , 2003
	100						2 (2%)	Q48H (2%)	Sripriya <i>et al.</i> , 2004
	200	200					5 (2.5%)	Q48H (2.5%)	Chakrabarti <i>et al.</i> , 2005
	100						2 (2%)		Rose <i>et al.</i> , 2007
	315						7 (2.2%)	Q368X (0.63%)	Bhattacharjee <i>et al.</i> , 2007
	251						2 (0.8%)	Q48H (0.8%)	Kumar <i>et al.</i> , 2007
				72			4 (5.5%)	Q48H (5.5%)	Kaur <i>et al.</i> , 2005
China	201						3 (1.5%)		Pang <i>et al.</i> , 2002
	91						1 (1.1%)		Lam <i>et al.</i> , 2000
Japan	114 (NTG) + 119 (POAG)						1 (0.9%)		Mabuchi <i>et al.</i> , 2001
	107						3 (2.8%)		Fingert <i>et al.</i> , 1999
	140						4 (2.8%)		Kubota <i>et al.</i> , 2000
	50						2 (4%)		Suzuki <i>et al.</i> , 1997
	171						5 (2.9%)		Ishikawa <i>et al.</i> , 2004
	80 (NTG)						2 (2.5%)		Izumi <i>et al.</i> , 2003
Korea	45						2 (4.4%)		Yoon <i>et al.</i> , 1999
IOWA	727						31 (4.3%)	Q368X (2.2%)	Fingert <i>et al.</i> , 1999

USA	25(JOAG)+49(POAG)						9 (36%) + 2 (4%)	Q368X (2.7%), V426F (2.7%)	Shimizu <i>et al.</i> , 2000
	POAG (393)+ JOAG (47)+NTG (84)			60	83	66	17 (2.3%)	Q368X (1.5%)	Alward <i>et al.</i> , 2002
	29						5 (17.2%)	Q368X (10.3%)	Allingham <i>et al.</i> , 1998
Australia	390						11 (2.8%)		Fingert <i>et al.</i> , 1999
Canada	157						5 (3.1%)		Fingert <i>et al.</i> , 1999
Germany	341						11(3.2%)		Michels-Rautenstrauss <i>et al.</i> ,2002
Sweden	200			200			1(0.5%)		Jansson <i>et al.</i> ,2003
Ghana	90						4 (4.4%)	R342K (2.2%), D340N (2.2%)	Challa <i>et al.</i> ,2002
France	237						17 (7.5%)	Q368X (5%)	Melki <i>et al.</i> , 2003
Spain	79						8 (7.5%)		Vazquez <i>et al.</i> , 2000
Brazil	25						7 (28%)	C433R (28%)	Vasconcellos <i>et al.</i> , 2000
Taiwan	48(JOAG)						1 (12.5%)	R46X (6.25%)	Yen <i>et al.</i> ,2007
Morocco	57						1 (1.7%)	T377M (1.7%)	Melki <i>et al.</i> ,2003
African	312						8 (2.6%)	E352K (0.64%)	Fingert <i>et al.</i> ,1999
Switzerland	117						10 (8.5%)	Q368X (4.3%)	Mataftsi <i>et al.</i> ,2001

### 2.10.3 Uniqueness of Gln48His in Indian glaucomas

Among the various mutations identified in *MYOC*, Gln48His was the predominant mutation identified in Indian population. This mutation has been identified in different forms of glaucoma (Table 2.11). For the first time it was identified in two sporadic cases of JOAG and in an adult-onset POAG case from eastern India (Mukhopadhyay *et al.*, 2002). Later this change was also noted in a JOAG family and in a sporadic POAG case from northern and southern India, respectively (Sripriya *et al.*, 2004). The Gln48His mutation has also been identified in several other studies on Indian POAG patients (Ramprasad *et al.*, 2005, Kumar *et al.*, 2007). Apart from JOAG and POAG cases, this mutation has been reported as a predominant *MYOC* mutation in Indian PCG cases (Kaur *et al.*, 2005, Chakrabarti *et al.*, 2005). These observations clearly establish that Gln48His is a common mutation among Indian glaucoma patients but has not yet been reported from any other population.

**Table 2.11:** Distribution of Gln48His mutation in Indian population

Region	Phenotype	Cases with <i>MYOC</i> mutations	Prevalence of Gln48His mutation	Reference
East India	POAG (n= 56)	4 (7.14%)	3 (5.3%)	Mukhopadhyay <i>et al.</i> , 2002
South India, North India	POAG (n=100)	2 (2%)	2 (2%)	Sripriya <i>et al.</i> , 2004
South India	PCG (n= 72)	4 (5.5%)	4 (5.5%)	Kaur <i>et al.</i> , 2005
South India + East India	POAG (n= 200)	5 (2.5%)	5 (2.5%)	Chakrabarti <i>et al.</i> , 2005
South India	POAG (n=24)	1 (4.1%)	1 (4.1%)	Ramprasad <i>et al.</i> , 2005
South India	POAG (n=251)	2 (0.8%)	2 (0.8%)	Kumar <i>et al.</i> , 2007



#### **2.10.4 Models for MYOC association with Glaucoma**

The models for glaucoma pathogenesis associated with *MYOC* indicate its accumulation in the cytoplasm or in the extracellular matrix causing an obstruction in the normal aqueous humor outflow. One such model given by Kim *et al.* (2001) suggests that *MYOC* mutations causing glaucoma are gain of function mutations. The heteromultimerization of mutant and wild type proteins would lead to the accumulation of aberrant *MYOC* products in the extracellular matrix thereby impeding the normal outflow of the aqueous humor. This results in the elevation of IOP along with the degeneration of the neuronal cells. A similar model given by Jacobson *et al.* (2001) examined the expression of normal and mutant myocilin in cultured TM cells (TM cell line) and in non ocular cells (human lung carcinoma cell line) as well as in the aqueous humor of glaucoma patients with or without *MYOC* mutations. They observed that normal myocilin was secreted from the cultured cells whereas a little or no myocilin was secreted from cells expressing mutant forms of *MYOC*. They also found that cotransfection of cultured cells with normal and mutant myocilin leads to suppression of normal myocilin secretion indicating the interaction of mutant protein with the normal protein. This in turn prevents secretion of the latter from cell to the extracellular matrix resulting in accumulation of these complexes within the secretory compartments of TM cells, which would interfere with the normal function of these cells, i.e., the flow of aqueous humor. These models have been supported by observations in various studies e.g. Morissette *et al.* (1998) reported the development of juvenile glaucoma in individuals harboring heterozygous missense mutations, whereas homozygotes for the same mutations were found to be asymptomatic. Based on these results authors suggested that homoallelic complementation may be responsible for restoration of myocilin function. Also Lam *et al.* (2000) found an elderly woman homozygous for a nonsense mutation (Arg46Stop) to be clinically normal. No myocilin

secretion was observed in this individual suggesting that truncated myocilin might be more susceptible to intracellular degradation. The same phenotypic observations in the mice homozygous and heterozygous for a null mutation in *MYOC* suggests that disease causing mutations in *MYOC* are gain of function mutations.

### **2.11 FORKHEAD BOX C1 (*FOXC1*) (6p25; OMIM# 601090)**

*FOXC1* (Forkhead box C1) is a member of winged helix/forkhead family of transcription factors. This family of transcription factors is distinguished by a highly conserved 110 amino acids DNA binding domain, known as forkhead domain (FHD). This FHD was first identified as a region of homology between *Drosophila Melanogaster* protein forkhead and rat hepatocyte nuclear factor 3 protein. Forkhead domains are evolutionary conserved and exists in wide range of species from yeast to humans. The nomenclature of the proteins is done using FOX (fork head box) as a prefix followed by a capital letter indicating the subfamily and then a number, which indicates the position of the protein within the subfamily. For example in *FOXC1*, FOX is for forkhead domain, C is the subfamily and 1 indicates it as the first member of the subfamily C (Granadino *et al.*, 2000).

*FOXC1* gene is located on 6p25 with open reading frame of 1,659 bp and one exon codes for a protein of 553 amino acids (Nishimura *et al.*, 1998). The *FOXC1* protein contains the following mentioned regions, which are critical for its activity as a transcription factor (Fig. 2.23).

a) *Activation domains*: The transcription activation by *FOXC1* is mediated by two activation domains- activation domain-1 (AD-1) and activation domain -2 (AD-2) spans from residues 1-51- and 466-553, respectively. AD-2 serves as a general transcription factor capable of activating transcription from a number of transcription

factors, whereas AD-1 is responsible for activation of FOXC1 specific target genes (Berry *et al.*, 2002).

b) *Nuclear localization signal*: The forkhead domain proteins are transported to the nucleus through the nuclear localization signal (NLS). It is an amino acid sequence, which acts like a tag on the exposed surface of the protein. The sequence is recognized by nuclear transporter receptors in the cytoplasm of the cells and help in confining a specific protein to the nucleus through the nuclear pore. Most of the NLS consist of basic amino acids. These amino acids are either present at a stretch or are more complex bipartite type with two basic clusters separated by variable spacer. FOXC1 like other forkhead proteins, has a distinct class of bipartite NLS, which is located at both ends of the FHD. The NLS at the N-terminal of the forkhead domain (NLS-N) is located just in front and at the beginning of the helix H1 spanning from 77- 93 residues. This is a highly conserved region among all fork head factors. The NLS-C terminal to the forkhead domain (NLS-C) is located within the W2 wing. The region is not a well conserved region and shows the highest sequence variability. It spans from 168-176 amino acids of the protein (Berry *et al.*, 2002).

c) *Forkhead domain (FHD)*: It is a 110 amino acid long evolutionary conserved DNA binding domain, which folds in a particular three dimensional structure with three  $\alpha$  helices and three  $\beta$  strands, assemble to form a compact hydrophobic core. Two regions of the domain, the W1 and W2 wings, display random coil structures that project out of the hydrophobic core. The fork head domain is a variant of the helix turn helix motif that it differs in the length of the turn connecting the helix two (H2) and helix three (H3). Forkhead proteins bind to DNA as monomers. A consensus sequence of seven nucleotides – 5' (A/G)-(T/C)-(C/A)-AA-(C/T)-A 3' has been identified to be

present in the DNA sequences recognized by many forkhead factors. Sequences flanking this core sequence are specific for each factor, which allows the specificity of binding between different forkhead factors. However, some forkhead factors can bind to the same DNA sequence and vice versa, i.e, the same factor can bind several DNA sequences but with different affinities (Berry *et al.*, 2002).

d) *Inhibitory domain/ phosphorylation domain*: FOXC1 protein contains an inhibitory domain located at amino acids from 215-366. This region has been shown to reduce the activity of transcriptional activation domains and serves to modulate the FOXC1 transcriptional activity. FOXC1 is a phosphoprotein and the activity of inhibitory domain may be regulated by phosphorylation.

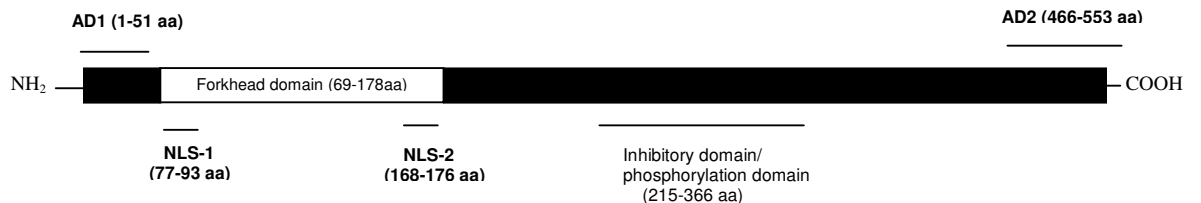


**Figure 2.23:** Showing the various domains of FOXC1 protein (Berry *et al.*, 2002)

### 2.11.1 Expression of FOXC1 in human tissues

Expression of FOXC1 has been observed in both ocular and non-ocular tissues. Among the ocular tissues the maximum expression was identified in trabecular meshwork followed by optic nerve head, choroids/RPE and ciliary body. However, cornea, iris and optic nerve showed the lower expression with the least detected in retina and lens. A comparatively lower expression has been observed in the non-ocular tissues like liver, muscle, lung, heart, pancreas and brain (Wang *et al.*, 2001).

### 2.11.2 *FOXC1* in ocular anomalies

*FOXC1* expression has been identified in the periocular mesenchyme cells that give rise to ocular drainage structures like iris, cornea and TM (Wang *et al.*, 2001). Also *FOXC1*<sup>-/-</sup> mice were found to die with hemorrhagic hydrocephalus with several skeletal, cardiovascular and ocular abnormalities including the absence of anterior chamber and open eyelids at birth. In addition to this, *FOXC1* mutations have also been reported to have association with various anterior segment anomalies like axenfeld reiger anomaly (ARA), Peter's anomaly etc., which lead to glaucoma in 50% of affected cases (Shields *et al.*, 1985). These findings indicate the potential role of *FOXC1* in the development of ocular tissues including the aqueous humor drainage structures. Moreover, mice heterozygous for *Foxc1* null allele (*Foxc1*<sup>+/-</sup>) were found to have anterior segment abnormalities similar to human patients with ARA and congenital glaucoma at the histological level (Smith *et al.*, 2000). These abnormalities included small or absent Schlemm's canal, aberrantly developed trabecular meshwork, iris hypoplasia, severely eccentric pupils and displaced schwalbe's line (Smith *et al.*, 2000). Table 2.12 shows the worldwide distribution of *FOXC1* mutations identified in different ocular abnormalities. Majority of the mutations identified in *FOXC1* were associated with both ocular and nonocular abnormalities. *FOXC1* being a transcription factor, might play an important role in the development of various non ocular tissues. Hence, any mutation could result in the mal-development of these tissues.

**Table 2.12:** Worldwide spectrum of *FOXC1* mutations identified in different anterior segment anomalies

<i>S. no.</i>	<i>Genomic DNA position</i>	<i>Mutations</i>	<i>Position in protein</i>	<i>Type of mutation</i>	<i>Ocular features</i>	<i>Non ocular features</i>	<i>Reference</i>
1	g.1078 CAG>TAG	Q2X	AD-1	Nonsense	ARA		Komatireddy <i>et al.</i> , 2003,
2	g.1100-1121ins22		AD-1	Frameshift	Axenveld anomaly		Nishimura <i>et al.</i> , 2001, Kawase <i>et al.</i> , 2001
3	g.1141 CAG>TAG	Q23X	AD-1	Nonsense	Iris hypoplasia, displaced pupils		Mirzayans <i>et al.</i> , 2000
4	g.1167-1176del10		AD-1	Frameshift	ARA		Mears <i>et al.</i> , 1998
5	g.1173-1182del10		AD-1	Frameshift	Axenveld anomaly		Nishimura <i>et al.</i> , 2001
6	g.1190-1197del8		AD-1	Frameshift	RA		Nishimura <i>et al.</i> , 2001
7	g.1217 TCG>TAG	S48X	AD-1	Nonsense	Iridocorneal adhesions, posterior embrotoxion		Weisschuh <i>et al.</i> , 2006
8	g.1227-1236del11		AD-1	Framesift	RA		Nishimura <i>et al.</i> ,1998
9	g.1309 CCG>ACG	P79T	FHD	Missense	ARS		Suzuki <i>et al.</i> , 2001
10	g.1310 CCG>CTG	P79L	FHD	Missense	RA		Nishimura <i>et al.</i> , 2001
11	g.1310 CCG>CGG	P79R	FHD	Missense	Iridocorneal adhesions, poeterior embryotoxon	Microganthia	Weisschuh <i>Net al.</i> , 2006
12	g.1312-1315insC		FHD	Frameshift	ARA		Nishimura <i>et al.</i> , 2001
13	g.1319 AGC>ACC	S82T	FHD	Missense	Posterior embryotoxon, congenital galaucoma		Mears <i>et al.</i> , 1998

14	g.1327 GCG>CCG	A85P	FHD	Missense	Hazy megalocornea, posterior embryotoxon, iris hypoplasia, corectopia, early onset glaucoma	Atrial septal defects, aortic stenosis, pulmonary stenosis	Fuse <i>et al.</i> , 2007
15	g.1328 CTC>TTC	L86F	FHD	Missense	Iris hypoplasia, iridocorneal adhesions in the angle, mild corectopia, congenital glaucoma	Short stature, obesity, myocardial infarction, dental abnormalities	Saleem <i>et al.</i> , 2003
16	g.1335 ATC>ATG	I87M	FHD	Missense	Corectopia, glaucoma, goniodysgenesis, iris strands, posterior embryotoxon	Deafness, heart anomalies	Mears <i>et al.</i> , 1998
17	g.1336insG		FHD	Frameshift	ARA		Kawase <i>et al.</i> , 2001
18	g.1346 ATC>ACC	I91T	FHD	Missense	ARA		Mortemousque <i>et al.</i> , 2004
19	g.1346 ATC>AGC	I91S	FHD	Missense	Iris hypoplasia with severe early onset glaucoma		Kawase <i>et al.</i> , 2001
20	g.1409 TTC>TCC	F112S	FHD	Missense	RA and iris hypoplasia		Nishimura <i>et al.</i> , 1998, Honkanen <i>et al.</i> , 2003
21	g.1418 TAC>TCC	Y115S	FHD	Missense	Iridocorneal adhesions, posterior embryotoxon, iris hypoplasia	Mild ear deafness	Weisschuh <i>et al.</i> , 2006
22	g.1441 CAG>TAG	Q123X	FHD	Nonsense	ARA		Komatireddy <i>et al.</i> , 2003
23	g.1452 ATC>ATG	I126M	FHD	Missense	Axenfeld anomaly and glaucoma		Nishimura <i>et al.</i> , 1998
24	g.1454 CGC>CAC	R127H	FHD	Missense	Iris hypoplasia with severe early onset glaucoma		Kawase <i>et al.</i> , 2001
25	g.1462 CTC>TTC	L130F	FHD	Missense	ARS		Ito <i>et al.</i> , 2007

26	g.1466 TCG>TTG	S131L	FHD	Missense	RA and glaucoma		Nishimura <i>et al.</i> , 1998
27	g.1511-1527del17		FHD	Frameshift	Posterior embryotoxon, congenital glaucoma		Fuse <i>et al.</i> , 2007
28	g.1520 GGC>GAC	G149D	FHD	Missense	Iridocorneal adhesions, posterior embryotoxon, corectopia	Hypospadias, heart defect	Weisschuh <i>et al.</i> , 2006
29	g.1530 TGG>TGA	W152X	FHD	Nonsense	ARA		Cella <i>et al.</i> , 2006
30	g.1555 ATG>GTG	M161V	FHD	Missense	Iridocorneal adhesions, posterior embryotoxon, iris hypoplasia	Umbilicus, middle ear deafness	Weisschuh <i>et al.</i> , 2006
31	g.1556 ATG>AAG	M161K	FHD	Missense	ARA		Komatireddy <i>et al.</i> , 2003, Panicker <i>et al.</i> , 2002
32	g.1567 GGC>CGC	G165R	FHD	Missense	Iris stroma hypoplasia, posterior embryotoxon, corectopia, glaucoma		Murphy <i>et al.</i> , 2004
33	g.1580 CGG>CCG	R169P	FHD	Missense	Iris hypoplasia, hypertelorism, corneal opacity	Abnormal papillary function, hearing loss	Murphy <i>et al.</i> , 2004
34	g.1792-1793delCT		Inhibitory domain	Frameshift	ARA		Cella <i>et al.</i> , 2006
35	g.1814delG		Inhibitory domain	Frameshift	Posterior embryotoxon, iris hypoplasia	Hypertelorism, umbilicus	Weisschuh <i>et al.</i> , 2006
36	g.2585delT		AD-2	Frameshift	Iris hypoplasia		Weisschuh <i>et al.</i> , 2006
37	g.2656delA		AD-2	Frameshift	Axenfeld anomaly		Nishimura <i>et al.</i> , 2001



## 2.12 GENOTYPE PHENOTYPE CORRELATION WITH RESPECT TO *CYP1B1* MUTATIONS

In spite of a number of PCG associated mutations in *CYP1B1*, there are only few evidences of direct correlation of the mutant genotype with the disease phenotype. There are a handful of reports, which demonstrated the association of some mutations with the severity of the disease. One such report is from Brazilian population where the most prevalent mutation (4340delG), identified in 21 out of 52 (20.2%) of the PCG cases, exhibited a severe phenotype. The clinical evaluation of 12 individuals with this mutation revealed that all were bilateral cases, with an early onset of the disease ( $\leq 1$  month) and with a maximum IOP ranging between 25 to 55 mm of Hg. These patients had poor response to surgery (number of surgeries up to six with an average of 2.6 in left eye and 2.8 in right eye) when compared to those who did not have this mutation (average of 1.5 in left eye and 1.4 in right eye) (Stoilov *et al.*, 2002a).

On the other hand there are some reports about the variable expression of the disease phenotype. For example, four affected individuals in an American PCG family were found to be compound heterozygotes for the E387K and 268del SNF. But only two of them manifested a severe form of the disease with IOP of 25mm of Hg and 28 mm Hg in the right and left eye, respectively, and corneal edema, whereas, the other two did not show any symptoms till their mid teenage (Sena *et al.*, 2004).

Two PCG patients along with a JOAG case from Costa Rica were reported to harbor the same homozygous (g.8037-8046dup) mutation (Soley *et al.*, 2003). These patients had a maximum IOP of 22 mm Hg and 24 mm Hg, respectively. The Cup to Disc ratio (C/D ratio) in the former was 0.3 (right eye) and 0.4 (left eye), while it was 0.5 (right eye) and 0.4 (left eye) in the latter, respectively, at the time of presentation. The former patient had

two surgeries in the right eye and six surgeries in the left eye whereas the latter one had two surgeries in both the eyes. The JOAG case had a maximum IOP of 26 mm Hg and C/D ratio of 0.6 and 0.5 in the right and left eye, respectively. All the three cases did not harbor any *MYOC* mutation. The presence of the same mutated allele resulting in manifestation of the disease symptoms at different ages indicates the possible relationship between the genotype and the environmental factors.

A study from our centre on 146 Indian PCG patients screened for 6 different mutations (Ins376 A, P193L, E229K, R390C, G61E and R368H) tried to correlate the genotype of the patients to disease severity (Panicker *et al.*, 2004). The most severe phenotype was defined as the presence of IOP >30 mm Hg with a corneal diameter of >13 mm, C/D ratio >0.8, severe corneal edema and presence of Haab's striae. Accordingly, a severity index was prepared that included corneal diameter, IOP, C/D ratio, corneal clarity and last recorded visual acuity as the parameters to grade the diseased phenotype as severe, moderate or mild. Cases with frameshift mutation (ins376A) had the worst phenotype followed by those with homozygous R390C mutation. In addition 80% of the cases with E229K, 72% with R368H, 66.7% with G61E and 62.5% with P193L exhibited a severe phenotype in at least one eye. However, no mutations have been assigned to other grades of severity.

A study on the Arab-Bedouin PCG cases determined the prognostic factors for surgical outcomes in cases intervened within first three months of birth (Levy *et al.*, 2005). The initial measure of outcome was based on surgical intervention, which was considered as success when normal IOP (<21mm Hg) was attained without any anti-glaucoma medication. The final outcome was considered as success when IOP was between 5 – 21 mm Hg at the end of 2 years follow-up without anti-glaucoma medication irrespective of

the number of surgical interventions. It was suggested that IOP before surgical procedure was an independent predictive factor for the final outcome. Family history was a poor prognostic factor for the final outcome. A higher IOP and C/D ratio were found to be associated with the failure of first surgical procedure. It was observed that among patients with a failure in first outcome, the initial IOP was high ( $40.47 \pm 11.06$ ) when compared to the group with lower IOP ( $34.14 \pm 4.95$ ) where it was a success. However, mean age at intervention ( $17 \pm 20$  days), corneal diameter ( $12.62 \pm 0.98$ ) and C/D ratio ( $0.41 \pm 0.16$ ) did not show any association with the final outcome.

### **2.13 CONCLUSION**

PCG is clinically and genetically a heterogeneous condition with only *CYP11B1* as the candidate gene known till date. The PCG associated mutations in *CYP11B1* have been reported worldwide. The exact role of this gene in the pathophysiology of the disease is not known. However, various *in vitro* and *in-silico* studies have shown the pathogenic nature of the identified mutations. Even though there are studies about the extensive screening of *CYP11B1* in PCG from various populations worldwide. But the genetic basis of cases without any mutation in *CYP11B1* is lacking. Since PCG is a congenital disorder, early and reliable diagnosis is vital, so that appropriate and prompt medical and surgical interventions can be initiated in time. This could prevent unwanted visual loss. Based on these available facts the present study was conducted as an attempt towards better understanding of the genetic mechanisms in PCG.

The data obtained from the current study would provide information on the mutation spectrum of three candidate genes (*CYP11B1*, *MYOC* and *FOXC1*) in the Indian PCG population, which can be used to understand the molecular genetic defects underlying PCG. It may be helpful in developing a reliable diagnostic method for screening of

prevalent mutations identified in these candidate genes at the population level that can help in better prognosis of the disease in the predisposed families.

---

## CHAPTER 3: MATERIALS AND METHODS

### 3.1 Enrollment of patients and controls

The study protocol adhered to the guidelines of the Declaration of Helsinki and was approved by the Institutional Review Board. Consecutively diagnosed unrelated PCG cases (n=301), presenting at the L.V. Prasad Eye Institute from January 2001-January 2006 from 12 different states along with normal individuals without any signs and symptoms of glaucoma at presentations as controls (n=157), were enrolled.

### 3.2 Clinical examination

Clinical examination included slit lamp biomicroscopy, applanation tonometry, gonioscopy (where corneal clarity permitted) and ophthalmoscopy. General anesthesia (Savoflorane) was used in younger age groups (<5 years) and where required. PCG was diagnosed independently by two glaucoma surgeons with expertise in congenital glaucoma and an inter-observer agreement based on kappa statistics was established. Cases that did not meet the clinical criteria even by one clinician were excluded. Unrelated normal individuals (n=157) without any signs and symptoms of PCG (mentioned in section 3.5), at presentation, were also recruited for the study. The mean age at presentation the of control individuals was  $54.2 \pm 12.8$  years.

#### 3.2.1 Slit lamp examination:

This examination was done with a portable hand-held slit lamp (Carl Zeiss Meditec Inc. Dublin, CA, USA). It was done under general anesthesia, which would provide the opportunity to thoroughly examine the eye. Anesthesia was administered in the operating room, by an experienced anesthetist. The slit lamp examination was done to access the corneal findings, which were judged with magnification and stereopsis.

The corneal findings included the corneal clarity, presence of corneal edema, breaks in the Descemet's membrane (Haab's striae) and corneal enlargement.

### **3.2.2 Tonometry:**

Tonometry measures the intraocular pressure (IOP) by subjecting the eye to force. It was done by touching the prism of the tonometer to the surface of cornea that flattens the cornea or the degree of corneal indentation produced by a fixed force (Ritch *et al.*, 1996). Tonometry was performed with a Perkins hand held applanation tonometer (Haag-Streit, USA). The tear film of the patient was stained with fluorescein. The prism of the tonometer was positioned in front of the apex of the cornea. When the prism touched the apex of cornea, the two semicircles were seen, which represent the fluorescein-stained tear film touching the upper and lower halves of the prism. The dial of the slit lamp was then adjusted such that the inner edges of the two semicircles just touch indicating the perfect flattening of cornea. The IOP was then determined by reading the number on the dial and multiplying by 10. (Kanski, 2003). The Goldmann applanation tonometry is based on the Imbert-Fick law, which states that the pressure within a sphere (P) is roughly equal to the external force (F) needed to flatten a portion of the sphere divided by area (A) of the sphere, which is flattened.

$$P = F/A$$

The outer diameter of the prism of the applanation tonometer, which touches the surface of the cornea, is 3.06 mm. This diameter corresponds to an area of 7.35 mm<sup>2</sup>.

Based on the Imbert-Flick law, the pressure applied by the prism was calculated as

$$P = F/7.35 \text{ mm}^2$$

The IOP in mm of Hg was then interpreted as ten times the contact pressure in grams (Nema and Nema 2002). For example if external force applied is 14, the IOP in mm of Hg can be calculated as

$$P = 14/7.35$$

$$P = 1.9 \text{ mm}^2$$

$$\text{or, } P = 1.9 \times 10 = 19 \text{ mm of Hg}$$

### 3.2.3 Gonioscopy:

Gonioscopy was done to view the anterior chamber angle structures and to estimate the width of the chamber. Direct visualization of anterior chamber is not possible through an intact cornea because the light emitted from the angular structures undergoes total internal reflection. The goniolens (4M and 2M lens, Volk Optical inc., Mentor, OH, USA) solves this problem by replacing the cornea –air interface with a new interface, which has a refractive index greater than that of cornea and tears (Kanski, 2003). Koeppe 14 to 16 mm goniolens with a Barkan light and a hand-held binocular microscope (Carl Zeiss Meditec Inc. Dublin, CA, USA) was used to view the anterior chamber angle. Figs. 3.1A and 3.1B show the open and closed iridocorneal angles viewed by Goniolens.

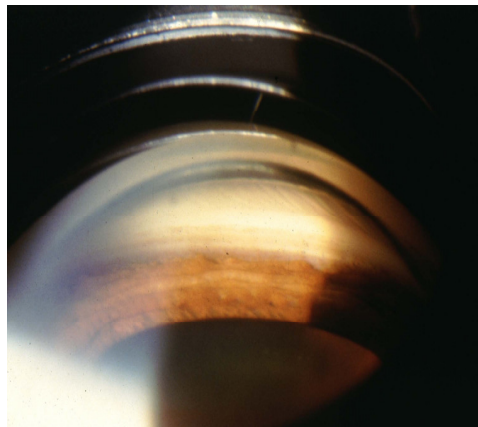


Figure 3.1A) Gonioscopic picture of an open angle

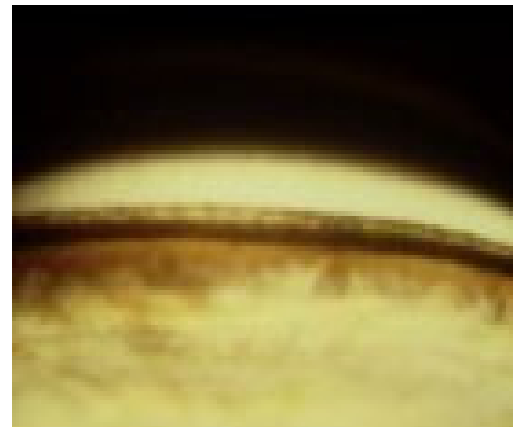


Figure 3.1B) Gonioscopic picture of a closed angle

([www.optometricglaucomasociety.org/EJSupp/Gonio.html](http://www.optometricglaucomasociety.org/EJSupp/Gonio.html))

### 3.2.4 Ophthalmoscopy:

Ophthalmoscopy was done to evaluate the optic disc. It was done under general anesthesia through a semi-dilated pupil. Hand held ophthalmoscope was used to obtain monocular clues of optic nerve head cupping. Figs 3.2A and 3.2B show the normal versus glaucomatous optic nerve.



Figure 3.2A) Normal optic nerve

([www.aafp.org/afp/20030501/1937.html](http://www.aafp.org/afp/20030501/1937.html))

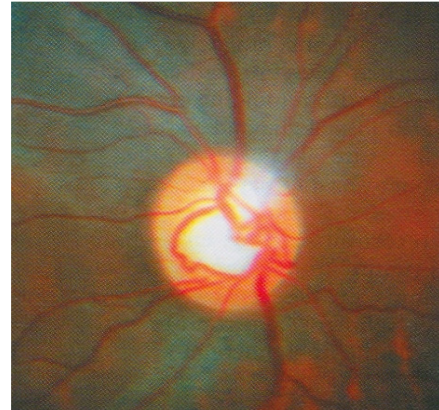


Figure 3.2B) Glaucomatous optic nerve with increased cup to disc ratio (Mandal and Netland.2006)

### 3.3 Inclusion criteria for PCG cases

PCG cases were enrolled based on the following inclusion criteria:

- 1 Corneal diameter >12.0 mm
2. Intra ocular pressure (>21mm of Hg) and/or
3. Haab's striae

#### 3.3.1 Rationale for the parameters in the inclusion criteria

1) The horizontal corneal diameter in newborn ranges from 9.5 to 10.5 mm, which enlarges by 0.5 to 1.0 mm in the first year of life. Based on this the horizontal corneal diameter >12 mm is considered as a risk factor for congenital glaucoma (Shaffer and Weiss.1970).



2) The cut off value for IOP in cases was based on the study carried out by Leydhecker and coworkers (1958). The authors have measured the IOP of 10,000 persons with no known eye disease in the age group 10-69 years. They obtained a distribution of pressures that resembled a Gaussian curve, but was skewed towards the higher pressures. Based on their findings they divided the individuals into two groups. The large “normal” group and smaller group with the individuals with high IOP but without any established glaucomatous optic nerve damage. In the normal group, the mean IOP was  $15.5 \pm 2.57$  mm of Hg. Two standard deviation (2SD) above the mean IOP was approximately 20.5 mm of Hg. Based on this value the cases with IOP  $>21$  mm of Hg were enrolled for the study. Several other studies have been carried out to determine the IOP in normal individuals in their respective populations (Table 3.1). As shown in the table the mean IOP of these studies ranged between 13.4mm of Hg- 17.8 mm of Hg.

**Table 3.1:** Worldwide distribution of mean IOP

Population	Number of samples	Age (in years)	Mean IOP (mm of Hg)	Reference
Japan	8126	$\geq 40$	$13.4 \pm 3.1$	Shiose <i>et al.</i> , 1986
Australia	4744	$\geq 40$	$14.7 \pm 3.5$	Weih <i>et al.</i> , 2001
Australia	3654	49- 97	$16.1 \pm 2.9$	Mitchell <i>et al.</i> , 1996
Barbados	4601	40-84	$17.8 \pm 3.5$	Leske <i>et al.</i> , 1997
Iran	3833	$\geq 10$	$14.5 \pm 2.6$	Hashemi <i>et al.</i> , 2005
Korea	13212	20-84	$15.5 \pm 3.1$	Lee <i>et al.</i> , 2002
US	4856	43-84	$15.3 \pm 3.2$	Klein <i>et al.</i> , 1992
South Africa	1005	$>40$	$13.9 \pm 3.4$	Rotchford <i>et al.</i> , 2002
India	300	20-70	$15.3 \pm 1.57$	Gupta <i>et al.</i> , 1971

The mean IOP in children in the Indian population was found to be  $12.02 \pm 3.74$  mm of Hg based on the study carried out on 810 eyes of 405 children of age

ranged between 0-12 years. The IOP showed an increasing trend and approached the adult levels by 12 years of age (Sihota *et al.*, 2006).

- 3) Haab's striae are the tears in the Descemet's membrane, which occur due to the raised IOP (Fig.2.6). These tears may be single or multiple and are characteristically visible as opaque lines on the cornea, oriented horizontally or concentric to the limbus.

Corneal edema, epiphora and blepharospasm are the three corroborating factors in PCG

### **3.4 Exclusion criteria for PCG cases**

The cases belonging to either of the categories mentioned below were excluded from the study

1. Patients with iris and lens changes.
2. Patients with other ocular pathologies like Axenfeld Rieger's anomaly, aniridia, Peter's anomaly etc. that can manifest along with congenital glaucoma.
3. Patients with any history of mechanical traumas or injury in the eye.

The detailed family history of the patients was documented in the form of a pedigree on the basis of guidelines given by Bennett and coworkers (1995). The segregation of the disease, its mode of inheritance, consanguinity in the family, ages at onset, number of affecteds in the family along with their geographical identities were recorded.

### **3.5 Enrollment of controls**

One hundred and fifty seven normal individuals were enrolled as controls on the basis of following inclusion criteria

1. Age more than 5 years.
2. No family history of glaucoma and other ocular disease.
3. Cup to disc ratio (<0.4:1). This cut off value was based on the study carried out by Carpel and coworkers (1981), where they determined the cup to disc ratio in 580 normal individuals in the age group of 4-91 years. The IOP in all the individuals was less than or equal to 18 mm of Hg. The mean cup to disc ratio in the individuals examined was 0.38. The authors had also examined 289 of these 580 individuals with direct ophthalmoscope and identified the mean cup to disc ratio of 0.28. Based on these findings, the normal cup to disc ratio was considered as equal to or less than 0.4.
4. IOP <18 mm of Hg. The cut off value for IOP in cases was based on the study carried out by Leydhecker and coworkers (1958) as mentioned in the inclusion criteria for cases.

### **3.6 Clinical and Demographic features of PCG cases**

#### ***3.6.1 State-wise distribution of cases***

The patients in the study cohort belonged to 12 different states of India (Table 3.2). The highest number of patients were from Andhra Pradesh (n=203) followed by Maharashtra (n=40) and West Bengal (n=18). Majority (93.3%) of the cases (281/301) were sporadic in nature while the rest had a family history of the disease with more than one affected individual.

**Table 3.2:** State-wise distribution of the PCG cases

Serial number	State	Cases enrolled (n=301)
1	Andhra Pradesh (AP)	203 (67.4%)
2	Bihar	5 (1.6%)
3	Gujarat	5 (1.6%)
4	Jharkhand	2 (0.7%)
5	Karnataka	12 (4.0%)
6	Kerala	2 (0.7%)
7	Maharashtra	40 (13.2%)
8	Madhya Pradesh	3 (1.0%)
9	Orissa	7(2.3%)
10	Rajasthan	1 (0.3%)
11	Uttar Pradesh	3 (1.0%)
12	West Bengal	18 (6.0%)

### 3.6.2 Age at onset

Most (71.7%) of the children (216/301) had a congenital onset of PCG. The remaining cases had between 1 month to 3 years (Table 3.3).

**Table3.3:** Distribution of the cases with respect to age of onset

S. No.	Age at onset	Number of families (n= 301)
1	At birth	216 (71.7%)
2	0-1 month	11 (3.6%)
3	1-6 months	48 (15.9%)
4	6months-1 year	17 (5.6%)
5	1- 3 year	9 (3.0%)

### 3.6.3 Family history and Consanguinity

Majority (99.6%) of the cases (300/301) were sporadic in nature. The family history was observed in one PCG family, where one of the parents was also affected. Consanguinity was observed in 42.8% (129/301) cases, and the highest rate of consanguinity was observed among patients from Andhra Pradesh, 32.2% (97/301).

### **3.6.4 Gender**

There was not much difference in the number of affected male [56.1 % (169/301)] and female [43.8% (132/301)] probands in the cohort of 301 cases suggesting no gender specificity in PCG.

### **3.7 Sample collection**

Around 2-4 ml blood sample was collected from the probands, their relatives and normal controls by venipuncture in heparanized-coated vacutainers with prior informed consent. The blood samples of most of the probands were collected during examination under general anesthesia.

### **3.8 Molecular analysis**

#### **3.8.1 Extraction of Genomic DNA**

Genomic DNA was extracted by the standard phenol chloroform method that uses phenol and chloroform to separate proteins from DNA (Sambrook *et al.*, 1989). The composition of the stock solutions is given in Annexure-I.

##### **3.8.1.1 Protocol for DNA extraction**

1. Equal volume (4 ml) of 1X Phosphate Buffer Saline (PBS) solution was added to it. The solution was mixed thoroughly by swirling and inverting the tube until the solution became homogeneous. PBS is a hypotonic solution that helps in the lysis of red blood cells (RBCs).
2. The solution was spun at 3000 revolutions per minute (rpm) for 10 minutes.
3. Reddish brown pellet was formed at the bottom of the tube. The supernatant was removed with the help of a pasture pipette.
4. The pellet was resuspended in 4 ml of PBS and centrifugation was done at 3000 rpm for another 10 minutes and the supernatant was aspirated.

5. This procedure was repeated 2-3 times until the pellet became clear indicating the complete lysis of RBCs and aggregation of WBCs at the bottom of the tube.
6. 3 ml of extraction buffer (Annexure I), 15  $\mu$ l of Proteinase K (Banglore Genei, Bangalore, India) and 6  $\mu$ l of Rnase (Banglore Genei, Bangalore, India) was added to the white pellet obtained.
7. The pellet was resuspended in the solution with the help of pasteur pipette and the solution was kept in water bath (Julabo, Shake Temp- SW22, Germany) for incubation at 37°C overnight.
8. On incubation the solution was clear and equal volume of saturated phenol (Ambion, Texas, USA) was added (~3.5 ml) to it. The solution was mixed thoroughly by swirling the tube. Centrifugation was done at 4500 rpm for 10 minutes to separate the aqueous phase at lower layer from the organic phase at upper layer. Phenol degrades the protein into peptides that aggregate to form an interphase between these two phases.
9. The aqueous phase was transferred to a fresh 15 ml tarson tube and equal volume of phenol and chloroform (Qualigens Fine Chemicals, Mumbai, India) (3 ml) in the ratio of 1:1 was added. The solution was mixed thoroughly and centrifuged at 4500 rpm for 10 minutes.
10. The aqueous phase was transferred to a fresh tarson tube and equal volume of chloroform (~2 ml) was added. Chloroform plays a dual role in protein denaturation and removes phenol residues in the solution.
11. Centrifugation was done at 4500 rpm for 10 minutes and the aqueous phase was transferred to a fresh tube. 6  $\mu$ l of ammonium acetate was added along with 2 volumes of chilled 100% ethanol (Qualigens Fine Chemicals, Mumbai, India) (4

ml). Ammonium acetate and absolute alcohol dehydrates DNA resulting in its precipitation.

12. The precipitated DNA was transferred to a fresh 1ml-ependorf tube and washed with 70% ethanol twice to remove any remnants of salts and air dried.
13. The air dried DNA was dissolved in 500 $\mu$ l of double distilled water and kept at 37°C for 2-3 hours.

### 3.8.2 Quantification of the Genomic DNA by UV spectrophotometer

The concentration of genomic DNA extracted was done in a UV spectrophotometer (UV-1601, Shimadzu, Japan). The instrument is based on the principle of Beer-Lambert law (1954), which states that absorbance of a wavelength is proportional to the concentration of absorber and thickness of the layer.

To estimate the concentration of DNA, 10  $\mu$ l of the sample was transferred to a fresh eppendorf tube and diluted 100 times with double distilled water. Quantification was done in a UV spectrophotometer (UV-1601, Shimadzu, Japan) by taking the readings at wavelength 260 nm and 280 nm. The reading at 260 nm calculates the concentration of DNA in the sample. An optical density (OD) value of 1 corresponds to ~ 50 ng/ $\mu$ l for the double stranded DNA. The OD ratio at 260 nm and 280 nm provides an estimate of purity of the DNA. A pure DNA sample would have OD<sub>260</sub>/OD<sub>280</sub> values of 1.8. If this value is <1.8, it indicates contamination with protein or phenol whereas a value of >1.8 indicates an RNA contamination in the sample.

The concentration of DNA was calculated using the formula

$$\text{Concentration} = \text{OD}_{260} \times 50 \text{ (concentration of double stranded DNA at OD}_{260} \text{ value of 1)} \times 100 \text{ (dilution factor)}$$

### 3.8.3 Amplification of candidate genes by polymerase chain reaction (PCR)

The coding regions of the three candidate genes (*CYP11B1*, *MYOC* and *FOXC1*) were amplified using the gene specific primers (Table.3.4). All the PCR reactions were set up in GeneAmp PCR system 9700 (Foster City, CA). A 25 µl PCR reaction was set up with the reagents mentioned in Table 3.5.

**Table 3.4:** Primer sequences used to amplify the coding region of *CYP11B1*

Gene	Exon	Primer sequence (5'- 3')	Gene fragment amplified	Amplicon size (bp)	MgCl <sub>2</sub> (mM)	Annea- ling (°C)
<i>CYP11B1</i>	II	CYP-1F CTCCAGAGAGTCAGCTCCG CYP-1R GGGTCGTCGTGGCTGTAG	g.3676bp-4461bp	786 *	2.5	56.5
	II	CYP- 2F GATGCGCAACTTCTTCACG CYP- 2R CTA CTCCGCCTTTTCAGA	g.4318bp-4905bp	648 *	2.5	56.5
	III	CYP- 3F GCTCACTTGCTTTTCTCTCT CYP- 3R AAATTTTCAGCTTGCCTCTTG	g.7841bp-8943bp	653	2.5	58
<i>MYOC</i>	I	MYOC -1F GGCTGGCTCCCCAGTATATA MYOC-1R GATGACTGACATGGCCTGG-	g.538bp-873bp	334	2.5	62
	I	MYOC-2F GAGTGGCCGATGCCAGTATAC MYOC-2R TAGGAGAAAGGGCAGGCAGG	809bp-1364bp	576	2.5	62
	II	MYOC-3F AACATAGTCAATCCTTGGGCC MYOC-3R TAAAGACCATGTGGGCACAA	g.14486bp-14719bp	223	2.5	60.5
	III	MYOC-4F TTATGGATTAAGTGGTGCTTCG MYOC-4R AGCATCTCCTTCTGCCATT	g.16519bp- 17388bp	880	2.5	56.5
<i>FOXC1</i>	I	FOXC1-1F CCCGGACTCGGACTCGGC FOXC1-1R AAGCGGTCCATGATGAACTGG	g.982bp-1409bp	427 *	1.0	60
	I	FOXC1-2F CGGCATCTACCAGTTCATCAT FOXC1-2R TCTCCTCCTTGTCCTTACC	g.1380bp-1630bp	220 *	2.5	62
	I	FOXC1-3F GAGAACGGCAGCTTCTCTG FOXC1-3R TGTCGGGGCTCTCGATCTT	g.1561bp-1858bp	298 *	1.0	53
	I	FOXC1-4F AGATCGAGAGCCCCGACA FOXC1-4R GCAGCGACGTCATGATGTTG	g.1841bp-2026bp	184 *	2.0	60



I	FOXC1-5F CAACATCATGACGTCGCTG FOXC1-5R TTGCAGGTTGCAGTGGTAGGT	g.1982bp-2268bp	262 *	1.0	62
I	FOXC1-6F GGCCAGAGCTCCCTCTACA FOXC1-6R GTGACCGGAGGCAGAGAGTA	g.2140bp-2384bp	245 *	1.0	61.5
I	FOXC1-7F TCACCAGCAGCAGCTCGT FOXC1-7R ACTCGAACATCTCCCGCA	g.2382bp-2611bp	231	1.0	54
I	FOXC1-8F TCACAGAGGATCGGCTTGAA FOXC1-8R CTGCTTTGGGGTTCGATTTA	g.2609bp-2615bp	165	2.0	62

\*10X DMSO was used

*CYP11B* GenBank Accession number: U56438

(<http://www.ncbi.nlm.nih.gov/entrez/viewer.fcgi?db=nucleotide&id=1663555>)

*MYOC* (Ensembl Human Gene :ENSG00000034971)

([http://www.ensembl.org/Homo\\_sapiens/geneseqview?db=core;gene=ENSG00000034971](http://www.ensembl.org/Homo_sapiens/geneseqview?db=core;gene=ENSG00000034971))

*FOXC1* (Ensembl Human Gene : ENSG00000054598)

([http://www.ensembl.org/Homo\\_sapiens/geneseqview?db=core;gene=ENSG00000054598](http://www.ensembl.org/Homo_sapiens/geneseqview?db=core;gene=ENSG00000054598))

**Table 3.5:** Reagents used in PCR reaction

Serial no.	Reagents	Concentrations	Total volume
1	Genomic DNA	50 ng – 100 ng	1 µl – 2µl
2	10X PCR buffer		2.5 µl
3	dNTPs	200 uM	2.5 µl
4	Forward primer	5µm-12.5 pm	1µl -2.5 µl
5	Reverse primer	5µm-12.5 pm	1µl -2.5 µl
6	Taq polymerase (1U/µl)	1U	1 µl
7	Total volume		25 µl

*Amplification conditions*

1 Initial denaturation	94°C – 3 minutes
2. Denaturation	94°C – 30 seconds
3. Annealing	X <sup>0</sup> – 30 seconds (Table 3.4)
4. Extension	72°C – 30 to 45 seconds
steps 2-4	30-35 cycles
5 Final extension	72°C – 5 minutes
6. Final hold	4°C – 5 minutes

**3.8.4 Confirmation of the PCR amplification by agarose gel electrophoresis**

PCR products were run on 1.5% agarose gel to determine their amplification and quality (Annexure II).

**3.8.4.1 Preparing of gel**

1. An appropriate quantity of agarose (to make it 1.5%) was added to electrophoresis buffer (1X Tris Borate EDTA- TAE) in a glass flask.
2. The flask was then swirled once and heated for 2-3 minutes to in a microwave oven to boil the agarose.
3. Boiled agarose was cooled to a 50°C- 55°C by keeping at room temperature for ~ 5 minutes.
4. Ethidium Bromide (USB, Amersham Biosciences, New Jersey, USA) was added (final concentration 1µg/ml) to the agarose solution and the flask was gently swirled for even mixing.
5. The gel was poured in the casting apparatus with an inserted comb.
6. The gel was allowed to solidify for 15-20 minutes.
7. The comb was removed gently from the gel plate on solidification.

#### **3.8.4.2 Loading and running of the gel**

1. The gel plate was placed in the electrophoresis tank (USB, Amersham Biosciences, New Jersey, USA).
2. 1X Tris –Acetate-EDTA (TAE) buffer was poured to completely immerse the agarose gel in the buffer.
3. PCR products were mixed with 1 ul of loading buffer (6X) (MBI Fermentas, Lithuania) and were loaded with a micropipette into the wells along with a marker comprising of 100-bp ladder a (MBI Fermentas, Lithuania) for sizing. The PCR reaction mix without genomic DNA (negative control) was also loaded.
4. The gel was run for approximately half an hour at a voltage supply of 10V/cm till bromophenol migrated at least half the distance through the gel.
5. The gel was removed from the tank and visualized under a UV transilluminator (UV Tec, Cambridge, UK).

#### **3.8.5 Mutation detection**

The amplicons were then screened for detection of variants by either of the following methods (Table 3.6)

1. Single Strand Conformation Polymorphism (SSCP)
2. Denaturing high performance liquid chromatography (dHPLC).
3. Bi-directional sequencing

**Table 3.6:** The methods used for the screening of candidate genes

Gene	Coding Region	Screening method
<i>CYP11B1</i>	Exon II (g.3806bp-4848 bp)	Bidirectional sequencing
	Exon III (g.7881bp-11587 bp)	
<i>MYOC</i>	Exon II (g.9186bp-9321bp)	SSCP
	Exon I (g.601bp-1203bp)	Bidirectional sequencing
	Exon III (g.10883bp-11668bp)	
<i>FOXC1</i>	Forkhead domain (g.1279bp-1608bp)	Bidirectional sequencing
	Rest of the coding region (g.601bp-1278bp & g.1609bp-2733bp)	SSCP

*CYP11B1* GenBank Accession number: U56438

(<http://www.ncbi.nlm.nih.gov/entrez/viewer.fcgi?db=nuccore&id=1663555>)

*MYOC* (Ensembl Human Gene :ENSG00000034971)

([http://www.ensembl.org/Homo\\_sapiens/geneseqview?db=core;gene=ENSG00000034971](http://www.ensembl.org/Homo_sapiens/geneseqview?db=core;gene=ENSG00000034971))

*FOXC1* (Ensembl Human Gene : ENSG00000054598)

([http://www.ensembl.org/Homo\\_sapiens/geneseqview?db=core;gene=ENSG00000054598](http://www.ensembl.org/Homo_sapiens/geneseqview?db=core;gene=ENSG00000054598))

### 3.8.5.1 Single Strand Conformation Polymorphism (SSCP)

It is an electrophoretic method to determine variants in a DNA fragment based on differential mobility of the single stranded DNA. Single stranded DNA (ssDNA) is unstable due to the absence of its complimentary strand. The ssDNA experience intra - strand base pairing based on the complimentary sequences present within the ssDNA, resulting in the formation of secondary conformations (Orita *et al.*, 1990). The secondary conformers are largely based on their sequences of the DNA as well on the fragment length. The denaturation time, snap chilling prior to loading, buffer concentration, temperature (25°C /4°C), percentage of the polyacrylamide gel and voltage at which the electrophoresis is carried out and the glycerol concentration can affect the formation of secondary conformations by ssDNA. Even a single nucleotide variation could result in a differential conformation that can be detected due to differences in mobility in the gel. The DNA fragments of length  $\leq 200$  bp can be screened for variation with

sensitivity of 90%. However, for the fragments of length between 200-400bp the sensitivity decreases to 80% (Hayashi. 1991).

### **3.8.5.1.1 Protocol for SSCP**

#### ***3.8.5.1.1.1 Preparation of samples:***

PCR products were mixed with 95% formamide loading buffer (in a ratio of 1:2; PCR product: Formamide) and denatured at 95°C for 5 minutes. The denatured PCR products were snap chilled in ice to prevent reannealing of the complementary strands.

#### ***3.8.5.1.1.2 Gel electrophoresis:***

It was performed in an electrophoretic unit (Hoefer SE 600 Series, electrophoretic unit, Amersham Biosciences, San Francisco, USA). The details about the preparation of the reagents are given in Annexure III.

- a) Glass plates (20X16cm) were cleaned with isopropanol. The plates were separated from each other by spacers (1.5mm thick) and fixed on the gel stand with the help of screws from the sides and rubber gasket at the bottom.
- b) 20 ml of 20% acylamide solution (39: 1; acrylamide: bisacrylamide) (Sigma - Aldrich, St. Louis, USA), 2.5 ml of 10X Tris BoricEDTA (TBE), 2.5 ml of glycerol, 300µl of 10 % Ammonium persulphate (APS) (Sigma Chemical Co. St. Louis, MO, USA and 30 µl of Tetramethylethylenamine (TEMED) (USB, Amersham Biosciences, NJ, USA). Final volume was adjusted to 50 ml with autoclaved distilled water. APS is the source of persulphate radicals. TEMED catalyses the

formation of free radicals from these ions, which in turn initiates the polymerization of acrylamide with bis-acrylamide.

- c) The gel solution was poured immediately between the plates. Combs (1.5mm thick) were inserted and the gel was left for about 45 minutes to polymerize.
- d) On polymerization, the combs were removed. The wells formed were flushed with distilled water to remove any un polymerised acrylamide.
- e) Upper buffer tank was fixed to the top of the plates, which was then placed in the lower buffer tank.
- f) 0.5X TBE was poured in the upper and lower buffer tanks of the electrophoretic unit and a pre- run was done for 15 minutes before loading the samples. This was done to remove any air bubbles and other particles from the gel.
- g) The denatured PCR products along with a non-denatured PCR product, for confirming the denaturation of samples, were loaded in the gel and electrophoresed overnight at 70 volts at room temperature. When the gels were run at 4<sup>0</sup>C, electrophoresis was done at 110 volts. Since the mobilities of single stranded DNA were temperature dependent, the gels were electrophoresed at two different temperatures (4<sup>0</sup>C and room temperature), which helped in the detection of variants.
- h) On electrophoresis the plates were removed from the apparatus and separated from each other. The gel was transferred to a glass tray for washing in double distilled water.
- i) Silver staining method of the gels. This method is based on the principle that silver ion (Ag<sup>+</sup>) in silver nitrate is reduced to the atomic state (Ag) in the presence of sodium hydroxide (NaOH). The silver atoms get

impregnated on the DNA molecules and on oxidation make them visible as bands on the gel.

#### **3.8.5.1.1.3 Protocol for silver staining**

- a) Gels were rinsed in the fixative solution (Annexure III) for 30 seconds and washed in autoclaved distilled water.
- b) The gels were stained in 0.2 % silver nitrate solution (Annexure III) for 10-15 seconds followed by two subsequent washes in autoclaved distilled water.
- c) The gels were transferred to a tray containing the developing solution (Annexure III) and kept on a shaker (Amersham Pharmacia Biotech San Francisco, USA) at 5 revolutions per minute until the DNA bands were visible.
- d) The gels were washed with autoclaved distilled water and photographed on a UVI Doc gel documentation system (UVI Tec, Cambridge, UK).

The variants obtained as band shifts were compared to the band pattern of denatured and non-denatured control samples and checked for difference in the band pattern.

#### **3.8.5.2 Denaturing High Performance Liquid Chromatography (dHPLC)**

It is a chromatographic method for detecting variations in a DNA sequence, based on heteroduplex formation under partial denaturing conditions (Oefner *et al.*, 1995). Heteroduplexes are the DNA fragments that contain mismatched bases and form as a result of base pairing of the single stranded mutated DNA with a single stranded wild type DNA. The two strands will not form hydrogen bonds at the variation site because the base pairs are mismatched and hence the heteroduplex gives different melting properties than homoduplex along with a different eluting time (Oefner *et al.*, 1995)

In dHPLC, the separation of nucleic acids is based on the principle of reverse phase ion exchange chromatography. The stationary phase is the nonpolar C18 alkylated, polystyrene – divinylbenzene polymeric (PS-DVB) beads, which are packed in column called DNASep cartridge. The mobile phase consists of a combination of buffers that elute the DNA.

The separation of DNA molecules is achieved by means of a TEAA- a hydroorganic eluent (Annexure IV) that forms an amphiphilic ion (triethylammonium ion) and a small, hydrophilic counter-ion (acetate). TEAA acts as a bridging molecule between DNA and the stationary phase. Hydrophobic groups (ethyl groups) of TEAA interact with the hydrophobic C-18 chains on the PS-DVB beads whereas the positively charged groups (triethylammonium ions) interact with the negatively charged phosphate backbone of DNA. On the other hand acetonitrile is an organic compound that competes with the TEAA for the hydrophobic interactions with the hydrophobic C-18 chains on the PS-DVB beads and in turn helps in the elution of DNA molecules. The elution of DNA molecules is governed by electrostatic interaction between the positive surface potential generated by triethylammonium ions adsorbed at the stationary phase and the negative potential generated by the phosphate groups of the sugar- phosphate backbone of DNA. The heteroduplex fragments are less stable than perfectly matched duplices and hence less number of acetonitrile molecules are required to disrupt the interactions between DNA fragments and the stationary phase. Therefore, the heteroduplex fragments elute faster than the homoduplex at same percentage (25%) of acetonitrile.

#### ***3.8.5.2.1 Protocol for dHPLC***

1. The amplicons were denatured at 95°C for 5 minutes.



2. The denatured PCR products were then gradually cooled to ~ 65°C. This allows the DNA fragments with to form heteroduplex.
3. The PCR products were loaded in the sample tray of the dHPLC machine (Wave: Nucleic acid fragment analysis system Transgenomics Inc., Omaha, NE).
4. Melting temperature was calculated from WAVEMAKER™ software (version 4.1). Melting point was determined on the basis of Fiman and Friere implementation of Poland's algorithm (Steger *et al.*, 1994), which calculates the probability that a base is in the helical duplex form or the non-helical single stranded form. Separation of the homoduplex DNA depends on a greater proportion of the non- helical form in the vicinity of the mismatched bases. If the location of the base change is known the percent helicity at that base can be calculated by filling the base position unlike the average percent helicity in case of the unknown variation.
5. Washing of syringe: The syringe was washed with solution D (8% acetonitrile).
6. Purging of the pump: It was done by pressing Manual Set on the L7100 keypad. The percentages of the buffers (A - 34%, B - 33% and D- 33%) were set, to make the total of 100%, along with the pump flow rate (0.9 ml/min) and pressure settings.
7. The sample sheet was prepared with information about the location of each sample in the sample tray, volume of each sample, number of injections for each sample, type of application e.g., mutation detection, the name of the file containing the length and sequence of the given DNA fragment, oven temperature etc.

8. The samples were run in Wave Analyzer with a time period of 8.8 minutes per sample. This time period included the following steps:

- a) Equilibration time (3 minutes): This involved the equilibration of the DNASep cartridge with Buffer A (50%) and Buffer B (50%) (Annexure II).
- b) Loading time (0.1-0.5 minutes): The PCR product was picked up by the syringe to the DNASep cartridge. The percentage of buffer B used for loading was slightly lower than that used at the start of the linear gradient. This drop in percentage allowed the non-retained components (dNTPs, primers, and buffers) in the PCR product to pass through so that they do not influence the separation of heteroduplex from homoduplex.
- c) Gradient duration (4.5 minutes): The length of the time over which the percentage of buffer B increases linearly. This increase is 2 percent per minute as selected by slope field. The slope field indicates change in percentage of buffer B per minute, which is set according to the length of the fragment screened. It is 2% per minute for mutation detection system.
- d) Clear duration (0.5 minute): The time at which the percentage of buffer B remains at 100% to clean high molecular weight DNA, i.e., genomic DNA.

9. The variants were obtained as heteroduplex peaks in the form of chromatograms.

### 3.8.5.3 Bi-directional Automated Sequencing

This method of DNA sequencing uses the property of dideoxynucleotides (ddNTPs) that are the analogs of dNTPs and lack a hydroxyl group at the 2' and 3' carbon position. Hence, a ddNTP can be incorporated into a growing DNA chain by forming a phosphodiester bond between its 5' carbon atom and the 3' carbon of the previously incorporated dNTP but cannot form a phosphodiester bond at its 3' carbon atom thereby causing the abrupt termination of chain synthesis. Hence it is also called as the chain termination method (Sanger *et al.*, 1975).

In automated DNA sequencing method four ddNTPs are labelled with different fluorescent dyes and hence all the four reaction products can be loaded in a single lane. During electrophoresis as the individual DNA fragment migrates through the gel the laser beam hits the fluorophore that in turn fluoresce at a specific wavelength. Although each of the four fluorescent dyes emits their maximum fluorescence at a different wavelength, there is some overlap in the emission spectra between them. The matrix file is created to compensate for this spectral overlap. This file is created by multicomponent analysis, which is a process to isolate the signal from each dye so that there is as little noise as possible. The precise spectral overlap between the four dyes is measured by running DNA fragments labeled with each of the dyes in separate injections through a capillary. These dye labeled DNA fragments are called matrix standards. The matrix files give the normalized fluorescence of the dyes in each virtual filter. The virtual filters allow the detection of light intensity in four non-overlapping regions on a CCD camera. Each region corresponds to a wavelength range that contains the maximum emission of an ABI prism dye. The maximum value of 1 is set for the dye specific filter e.g., blue filter has value of 1 for blue dye. The values for other dyes in the filter are less than 1 that represents the amount of spectral

overlap observed for each dye. The raw data of the sequences were obtained through the data collection software (version 3.0). The raw data was analyzed with the ABI prism DNA SEQUENCING ANALYSIS software (version 3.7, Applied Biosystems, Foster city, CA). The electropherograms obtained were compared with sequence obtained from the Gen Bank database (<http://www.ncbi.nlm.nih.gov/>).

#### **3.8.5.3.1 Purification of the amplicons**

The amplicons were purified using ultra clean™ PCR clean up DNA purification kit (MO BIO laboratories, CA.) in the following steps according to manufacturer's guidelines:

- a) The amplicons were mixed with 5 volumes of the SPIN BIND SOLUTION and the solution was transferred to the spin filter unit followed by centrifugation at 13000 rpm for 10-30 seconds.
- b) The liquid flow through was decanted from the eppendorf tube.
- c) SPIN CLEAN BUFFER (300 ul) was added to the spin filter followed by a centrifugation at 13000 rpm for 10-30 seconds.
- d) The flow through was discarded and spin filter unit was centrifuged again for 1 minute.
- e) The spin filter was transferred to a new collection tube.
- f) ELUTION BUFFER (50 ul) was added to the spin filter followed by a centrifugation at 13000 rpm for 1 minute.
- g) The eluted DNA in the collection buffer was precipitated by adding 2 ul of 5M sodium hydroxide and 100 ul of absolute ethanol and spinning at 13000 rpm for 5 minutes.
- h) The supernatant was aspirated and the DNA pellet was air dried.
- i) On drying DNA was dissolved in 15 ul of autoclaved distilled water.

The cleaned PCR product was then subjected to the sequencing PCR.

A reaction mixture (10 µl) was made using the following reagents listed in Table 3.7.

The sequencing PCR causes the linear amplification of one of the strands based on the primer used (forward or reverse). As the ddNTPs incorporate randomly in the growing chain, the final PCR product is a collection of labeled DNA fragments of different lengths with a common 5' end.

### 3.8.5.3.2 Sequencing PCR

The sequencing PCR was performed in the thermal cycler (Gene Amp, PCR system 9700, Applied Biosystems) under the following conditions.

- a) Initial denaturation at 94°C for 2 minutes
- b) Denaturation at 94°C for 10 seconds
- c) Annealing of primers at 50°C for 6 seconds
- d) Extension at 60°C for 4 minute.

Steps 'b-d' were repeated for 30 cycles.

- e) Final hold at 4°C for 5 minutes

**Table 3.7:** The reagents used for the sequencing PCR

<i>Serial number</i>	<i>Reagent</i>	<i>Volume</i>
1	3 pmol of primer (forward/reverse)	1 µl
2	BigDye terminator (version 3.1)	2 µl
3	10X sequencing buffer	1 µl
4	Purified PCR product	1-3 µl
5	Autoclaved distilled water	Adjusted to make the final volume of 10 µl

### **3.8.5.3.3 Precipitation of sequencing PCR products**

The sequencing PCR products were precipitated using 3M sodium acetate and absolute ethanol and washed with 70% ethanol. The precipitated products were dissolved in 15µl of Hi-Dye formamide (ABI 310, Applied Biosystems, Foster city, CA).

#### **3.8.5.3.3.1 Procedure for precipitation**

a) A master mix was made as follows:

3M sodium acetate (pH 4.6) 3ul

(Qualigens Fine Chemicals, Mumbai, India)

Ethanol 250ul

- b) The volume of the PCR product after cycle sequencing reaction was made up to 100ul with autoclaved water, transferred to 1.5ml centrifuge tube and 253ul of the above master mix was added to each tube.
- c) Contents of the tube were mixed thoroughly and centrifuged immediately at a speed of 12,000 rpm for 20 min at room temperature.
- d) The orientation of the tubes was marked as a precautionary measure for the subsequent steps.
- e) The supernatant was carefully decanted and to each tube 250ul of 70% ethanol was added.
- f) The tubes were spun at 14,000 rpm on a tabletop centrifuge for 10 min and the supernatant was carefully decanted.
- g) The 70% ethanol wash step was repeated without inverting the tubes this time.
- h) The supernatant was aspirated and the pellet was air dried.

- i) The pellet was resuspended in 10ul of HiDi formamide (Applied Biosystems, Foster city, CA, USA) and vortexed.
- j) The sample was then transferred to 0.5ml 310 auto-sampler tubes and capped with septa.
- k) The tubes were tapped once and spun down gently.
- l) The contents of the tube were checked for air bubbles.

#### **3.8.5.3.4. Electrophoresis**

These amplicons were electrophoresed, using the following procedures:

- a) The injection syringe was rinsed with distilled water.
- b) The POP 6 (Applied Biosystems, Foster city, CA, USA) polymer was brought to room temperature and a small amount (~0.6 ml) of the polymer was gently drawn into syringe for priming.
- c) The capillary was first connected to the pump block and then positioned in the vertical track of the detector, by opening laser detector door and was arranged such that the central portion of the capillary window would rest over the laser detector window. The end of the capillary was adjusted so that it was positioned directly below the opening of the glass syringe.
- d) The capillary and the cathode were adjusted in such a way that the capillary protrudes beyond the electrode by a maximum of 0.5 mm (the anode was always kept immersed in the electrophoresis buffer while the cathode, located above the auto-sampler was placed in the sample during electrophoresis).
- e) The injection syringe was then loaded with polymer (~0.5 ml) carefully without introducing any air bubbles.

- f) Meanwhile the 10X Genetic analyzer EDTA buffer (Applied Biosystems, Foster city, CA, USA) was diluted to 1X concentration with deionised water to use in the run. The anode buffer reservoir was filled with the 1X Genetic analyzer EDTA buffer and placed on the pump block.
- g) The auto-sampler consists of two 4 ml vials and a 1.5 ml eppendorf tube with the lid clipped off. The first vial was filled with 1X Genetic analyzer EDTA buffer and the second one was filled with de-ionised water for the purpose of washing. The wastes produced during the run were collected into the eppendorf tube.
- h) The samples were denatured at 95°C for 3 minutes and immediately kept on ice till loading.
- i) The denatured samples were loaded in the sample tray, which was placed on the auto-sampler of the automated DNA sequencer (ABI 310, Applied Biosystems, Foster city, CA).
- j) The sample sheet was created that contained the information about the sample name and its position in the tray.
- k) The information regarding the orders for running of samples, number of injections to be made from each sample, running conditions like duration of injection, temperature of the plate, running time of the sample.
- l) The samples were electrophoresed for 60-120 minutes depending on their fragment length.
- m) The raw data were collected and stored in the computer's hard drive by Data collection software (ABI 310 Data Collection Software). The raw data were visualized by opening the raw data window from the window menu, which showed the data detected as the samples passed through the capillary window.



Re-sequencing was independently repeated multiple times to confirm the observed variations.

#### **3.8.5.3.5. Data analysis**

The raw data was analyzed with the ABI prism<sup>R</sup> DNA SEQUENCING ANALYSIS software (version 3.7. Applied Biosystems, Foster city, CA).

a) The sequence analysis software (version 3.7) was opened to set the start and end points.

b) The auto analysis function was used to analyse and the results were obtained in the form of electropherograms. The DNA sequencing analysis software analyses the raw data collected by the Data collection software. The analysis software has data utility program, which helps to make and copy matrices to correct for the spectral overlap of the fluorescent labels. The sequence analysis software identifies and tracks the sample lanes of the gel and subsequently normalizes and integrates raw data into a chromatogram of the final sequence.

c) The sequences were compared to the wild type gene sequence obtained from GENBANK (<http://www.ncbi.nlm.nih.gov/>).

##### **3.8.5.3.5.1 Multiple sequence alignment**

The CLUSTAL W software analysis (<http://www.ebi.ac.uk/clustalw/>) was used for multiple sequence alignment to determine the conservation of the residues mutated based on the homology of the residues across different species.

##### **3.8.5.3.5.2 The SIFT (sorting intolerant from tolerant) scores**

The SIFT (sorting intolerant from tolerant) software was also used to predict the effect of the variation on the protein's function, based on homology search

and the physical properties of amino acids. For calculating the SIFT scores, the protein sequence of the candidate gene was downloaded from GENBANK in the Fasta format. The mutated residues were then compared to the wild type residues in order to determine the affect of the mutations on the protein. This SIFT scores suggested the pathogenic nature of the mutation.

#### ***3.8.5.3.5.3 Characterization of the variants***

The variants were characterized as mutation or polymorphism based on the following criteria: a) co-segregation of the variant with the disease phenotype, b) its absence in the unaffected controls and c) conservation of the wild type residue across different species.

#### **3.8.5.4 PCR-based Restriction digestion**

PCR based restriction digestion was used to confirm nucleotide variants, and for screening normal controls for the observed variation. It was also used to ascertain the segregation of mutations in other family members. This method utilizes restriction endonuclease (RE) digestion to identify the variations in a given DNA sequence (Table 3.8). RE recognizes a specific DNA sequence (4-8 bp long) called the recognition site and digests the DNA at a given site within or flanking the sequence. Any sequence variation at a specific DNA region either creates or abolishes the recognition site. This in turn produces a difference in the fragments generated by the endonuclease and is termed as restriction fragment length polymorphism (RFLP). It was used to confirm the variations and for screening normal control individuals in order to confirm the variation as a mutation.

**Table 3.8:** Various restriction enzymes used to screen the variations in candidate genes.

Gene	Mutation/Polymorphism	Restriction enzyme (+)/ (-)	Restriction cutting site	Product size (bp)	Allele sizes (bp)			Digestion temperature (°C)	Obtained from
					Wild type	Het	Mut		
CYP11B1	G61E	<i>Taq</i> I(+)	t/cga	786	627, 84,75	627, 309, 318, 84, 75	627, 309, 318, 84, 75	65	MBI
	Y81N	<i>Hae</i> II (-)	rgcgc/y	786	298, 294, 90, 76, 28	592, 298, 294, 90, 76, 28	592, 90, 28	37	MBI
	M132R	<i>Nla</i> III (-)	catg/	786	293, 162, 133, 100, 57, 41	293,233, 162, 133, 100, 57, 41	293,233, 162, 57, 41	37	MBI
	L181P	<i>Cfr</i> 10I (+)	r/ccggy	648	508, 140	508, 420, 140, 88	420, 140, 88	37	MBI
	P193L	<i>Eco</i> 81I (+)	cc/tnagg	648	648	648, 523, 125	523, 125	37	MBI
	E229K	<i>Eam</i> 140I (-)	ctcttc(1/4)/	648	648	586, 348, 62	586, 62	37	MBI
	H279P	<i>Cfr</i> 13I (+)	g/gncc	648	350, 207, 49, 36, 6	350, 332, 207, 49, 36, 18, 6	332, 207, 49, 36, 18, 6	37	MBI
	C280X	<i>Dde</i> I (+)	c/tnag	648	427, 162, 59	552, 427, 263, 164, 162, 59	552, 68, 28	37	MBI
	206del Serine	<i>Pag</i> I(-)	t/catga	648	489, 159	648, 489, 159	648	37	MBI
	A330T	<i>Hae</i> II (-)	rgcgc/y	648	423,129, 68, 28	552, 423, 129, 68, 28	552,	37	MBI
R355X	<i>Xho</i> I (-)	c/tcgag	653	327, 267, 59	327, 326, 267, 59	327, 326	37	MBI	
R368H	<i>Taa</i> I (-)	can/gt	653	402, 152, 99	402, 251, 152, 99	402, 251	65	MBI	
R390C	<i>Hin</i> 6I (-)	g/cgc	653	489, 164	653, 489, 164	653	37	MBI	
R390S	<i>Hin</i> 6I (-)	g/cgc	653	489, 164	653, 489, 164	653	37	MBI	

	R390S	<i>Hin6I</i> (-)	g/cgc	653	489, 164	653, 489, 164	653	37	MBI
<i>MYOC</i>	Q48H	<i>AccI</i> (-)	gt/mkac	334	271, 63	334, 271, 63	334	37	NEB
<i>FOXC1</i>	L130F	<i>MnII</i> (-)	cctc(7/6)/	220	163, 52, 5	215, 163, 52, 5	215, 5	37	NEB
	C135Y	<i>RsaI</i> (+)	g/tac	220	220	220,155, 65	155, 65	37	MBI
	V547I	<i>AccI</i> (-)	gt/mkac	165	104, 61	165, 104, 61	165	37	NEB
	g.1927dup25 bp	<i>Hin6I</i> (+)	g/cgc	184	72, 64, 33, 15	72, 64, 58, 33, 15	72, 64, 58, 15	37	MBI
	g.1086delC	<i>PauI</i> (-)	g/cgcgc	427	347, 100	427, 347, 100	427	37	MBI
	g.1164- g.1172del9	<i>Not I</i> (-)	gc/ggccgc	427	248, 178	427, 248, 179	427	37	NEB

(-) indicates the abolition of site, (+) indicates the creation of site, r= purines (A, T), y=pyrimidines (C, T), m= A+C, k= G+T, MBI - the MBI fermentas, NEB -

New England Biolabs

#### 3.8.5.4.1 Protocol for Restriction digestion

1. The information regarding the creation or abolition of the restriction site of an endonuclease was obtained from WEB CUTTER 2

(<http://www.firstmarket.com/cutter/cut2.html>). The enzymes with a recognition sequence of 6-8 nucleotides and 1-3 cutting site were selected.

2. The amplicons are incubated overnight in the water bath with the required enzyme (2-3 units) and 1X buffer specific to the RE at the required temperature (Table 3.9).

**Table 3.9** Reagents used for Restriction digestion

S.No	Reagents	Stock concentration	Working concentration	Total volume for one reaction (ul)
1	Compatible buffer	10X	1X	1-1.5
2	Enzyme	10U/ul	2-3 U/ul	0.2-0.3
3	Template (PCR product)	-	50-100ng	2-4 ul
4	Milli Q	-	Adjusted the reaction volume to 10-15 ul	Made up to the reaction volume (10-15 ul)

#### 3.8.5.4.2 Gel electrophoresis

It was performed in the electrophoretic unit (Hoefer SE 600 Series, electrophoretic unit, Amersham Biosciences, San Francisco, USA). The details about the preparation of the reagents are given in Annexure III. The protocol of gel electrophoresis was the same as mentioned earlier for SSCP (section 3.8.5.1) with minor modifications. The digested amplicons were loaded along with a digested control sample, an undigested amplicon and a 100bp ladder (MBI Fermentas, Lithuania) on the gel.

#### 3.8.5.4.3 Detection

1) On electrophoresis the plates were removed from the apparatus and stained with ethidium bromide.

- 2) The gels were visualized under the UV Transilluminator (UV Tec, Cambridge, UK).
- 3) The digestion pattern of the patient samples was compared to controls along with digested and undigested product to determine the genotypes.
- 4) The genotypes were further cross-validated by a masked observer randomly. Any discrepancies with respect to genotyping were resolved by repeating the experiments on the same samples.

### **3.8.6 Statistical analysis**

The allele and genotype frequencies were calculated by using the gene counting method. Further statistical analysis was done by using the SPSS statistical software (version 14.0).

---

## CHAPTER 4: RESULTS

### 4.1 DEMOGRAPHICS OF THE PCG COHORT STUDIED

Three candidate genes (*CYP11B1*, *MYOC* and *FOXC1*) were screened in a cohort of 301 clinically diagnosed and consecutively enrolled PCG cases and 157 controls in an attempt to understand their mutation spectrum in India and their association with disease pathogenesis. The male to female ratio in our patient cohort was 1.3:1. The mean age of onset was  $2.01 \pm 5.3$  months and the age at intervention was  $23.5 \pm 46.0$  months, respectively. Majority (93.3%) of the cases (281/301) were sporadic in nature without a family history, while the rest (6.7%) were familial with more than one affected individual. Consanguinity was observed in 42.8% (129/301) cases.

Majority (67.8%) of the cases (204/301) belonged to Andhra Pradesh (AP) due to the location of L.V. Prasad Eye Institute, a tertiary eye care centre in that area. Also the high rate of consanguinity and inbreeding would have contributed to the high prevalence of PCG in AP. Hence the distribution of demographic and clinical parameters have been shown with respect to the overall distribution of cases and also separately for AP in Table 4.1.

**Table 4.1:** Comparison of demographic features of cases from different states and in comparison to AP

Parameters		Number of cases (overall) n=301	Number of cases in AP n=204
A) Consanguinity	Overall	129/301(42.8%)	97/204 (47.5%)
	i) First cousin	i) 70/129 (54.3%)	i) 48/97 (49.5%)
	ii) Second cousin	ii) 15/129 (11.6%)	ii) 9/97 (9.3%)
	iii) Uncle niece	iii) 44/129 (34.1%)	iii) 40/97 (41.2%)
B) Non- consanguinity		172/301 (57.1%)	107/204 (52.5%)
Gender	a) Males	169/301 (56.1%)	105/204 (51.5%)
	b) Females	132/301 (43.8%)	99/204 (48.5%)
Age at onset	At birth	216/301 (71.7%)	146/204 (71.6%)
	0-1 month	11/301 (3.6%)	6/204 (2.9%)
	1-6 months	48/301 (15.9%)	33/204 (16.2%)
	6months-1 year	17/301 (5.6%)	11/204 (5.4%)
	1- 3 year	9/301 (3.0%)	8/204 (3.9%)

## 4.2 MUTATIONAL ANALYSIS OF *CYP1B1*

### 4.2.1 Distribution of cases and controls for screening

Cytochrome P450B1 gene (*CYP1B1*) is the only candidate gene implicated in PCG. Around 70 different mutations have been identified in *CYP1B1* to be associated with PCG from different populations (<http://www.hgmd.cf.ac.uk/ac/index.php>). Among the 301 PCG cases enrolled, 80 cases were screened for *CYP1B1* in an earlier study (Reddy *et al.*, 2003). In this study, a total of 120 PCG cases were screened, of which 80 were screened by direct sequencing whereas 40 cases were screened by PCR based restriction digestion for 6 mutations (ins376A, G61E, P193L, E229K, R368H and R390C). The present study therefore included the remaining (n=221) cases, which included 188 newly enrolled cases and 33 cases of the previous study (Reddy *et al.*, 2003), which were either heterozygous or did not harbor any mutation after PCR based restriction digestion (Table 4.2). All these cases along with 157 unrelated normal control subjects were screened for the entire coding region of *CYP1B1* (exon II and exon III) by resequencing in the present study. For screening *MYOC* and *FOXC1*, cases that were either heterozygous (n=41) or did not harbor any mutation in *CYP1B1* (n=169) were screened.



**Table 4.2:** Description of the PCG cases screened

<i>Study</i>	<i>Cases enrolled</i>	<i>Cases screened by direct sequencing</i>	<i>Cases not screened by direct sequencing</i>
Previous study (Reddy <i>et al.</i> , 2003)	120	80	40
Present study	188	221 (188 + 33* of Reddy <i>et al.</i> , 2003)	-

\* 33 out of 40 samples (Reddy *et al.*, 2003.) that were heterozygous or without any mutation in *CYP1B1* were screened by direct sequencing in the present study

#### 4.2.2 Screening of *CYP1B1*

Thirty three different mutations were identified in 90 patients (40.7%), of which 15 were novel. These mutations included 6 frameshift (5 deletions and 1 duplication), 2 nonsense and 25 missense mutations (Table 4.3). The details of these mutations are given in Tables 4.4 and 4.5. Among to the novel mutations, 9 were identified in exon II and 6 in exon III, respectively that included 3 deletions and 12 missense mutations (Fig.4.2). Among the 90 patients with *CYP1B1* mutations, 48.8% (44/90) were homozygous, 34.4% (31/90) heterozygous and 16.6% (15/90) were compound heterozygous for the mutations, respectively (Fig.4.1). Arg368His was the most predominant mutation identified in 46.7% (42/90) cases.

**Table 4.3:** Different *CYP1B1* mutations identified in Indian PCG patients

Serial no.	Type of mutation	No. of different mutations
1	Missense	25 (75.7%)
2	Deletion	5 (15.2%)
3	Nonsense	2 (6.0%)
4	Duplication	1 (3.0%)

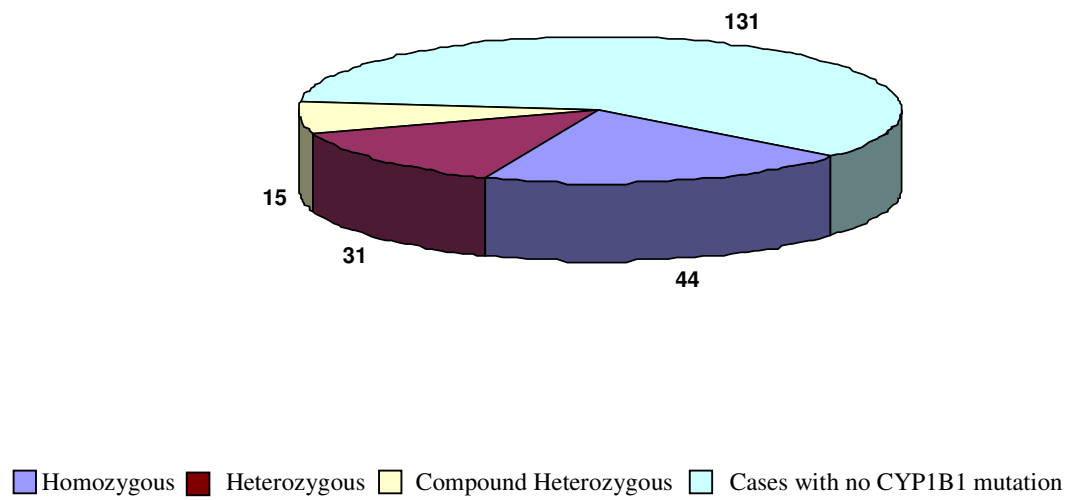


**Figure 4.1:** Distribution of cases with *CYP1B1* mutations and without *CYP1B1* mutations

**Table 4.4:** Mutations identified in Exon II of *CYP11B1*

S.No	Nucleotide change	Codon change	Amino acid change	Frequency (n= 90)	SIFT score	Affect on protein	Previously observed in other populations	References
1	g. 3972 C>T	GCG>GTG	Ala56Val *	1 (1.1%)	0.06	Tolerated	Present study	
2	g.3987G>A	GGA>GAA	Gly61Glu	1 (1.1%)	0.00	Affect protein function	Saudi Arabia, Ecuador, Turkey, Morocco, Egypt, Iran	Bejjani <i>et al.</i> , 2000 Stoilov <i>et al.</i> , 1998 Belmouden <i>et al.</i> , 2002 Curry <i>et al.</i> , 2004 El-Ashry <i>et al.</i> , 2007 Chitsazian <i>et al.</i> , 2007
3	g.4046 T>A	TAC>AAC	Tyr81Asn	6 (6.6%)	0.00	Affect protein function	France (in POAG patients)	Melki <i>et al.</i> , 2004
4	g.4055 G>T	GTT>TTT	Val84Phe*	1 (1.1%)	0.00	Affect protein function	Present study	
5	g.4095 T>C	CTG>CCG	Leu97Pro*	1 (1.1%)	0.00	Affect protein function	Present study	
6	g.4196 A>C	AGC>CGC	Ser131Arg*	1 (1.1%)	0.00	Affect protein function	Present study	
7	g.4200 T>G	ATG>AGG	Met132Arg	1 (1.1%)	0.00	Affect protein function	Indian	Reddy <i>et al.</i> , 2004
8	g.4347 T>C	CTG>CCG	Leu181Pro*	1 (1.1%)	0.00	Affect protein function	Present study	
9	g.4383 C>T	CCG>CTG	Pro193Leu	1 (1.1%)	0.01	Affect protein function	Indian	Paniker <i>et al.</i> , 2002

10	g.4491 G>A	<b>GAA&gt;AAA</b>	Glu229Lys	11 (12.2%)	0.10	Tolerated	Indian, Lebanon, France, Iran, Australia	Paniker <i>et al.</i> , 2002 Michels-Rautenstrauss <i>et al.</i> , 2001 Colomb <i>et al.</i> , 2003 Chitsazian <i>et al.</i> , 2007 Dimasi <i>et al.</i> , 2007
11	g.4520 A>C	<b>AGC&gt;CGC</b>	Ser239Arg	2 (2.2%)	0.00	Affect protein function	Indian	Reddy <i>et al.</i> , 2004
12	g.4641 A>C	<b>CAC&gt;CCC</b>	His279Pro*	1 (1.1%)	0.00	Affect protein function	Present study	
13	g. 4645 C>A	<b>TGC&gt;TGA</b>	Cys280Stop	2 (2.2%)	-	-	Japan	Mashima <i>et al.</i> , 2001
14	g.4793 G>A	<b>GCC&gt;ACC</b>	Ala330Thr*	1 (1.1%)	0.00	Affect protein function	Present study	
15	g.3928 del G *	-	-	1 (1.1%)	-	-	Present study	
16	g.4421- 4423del3*	-	-	1 (1.1%)	-	-	Present study	

\* Novel mutations

*CYP11B1* GenBank Accession number: U56438 (<http://www.ncbi.nlm.nih.gov/entrez/viewer.fcgi?db=nucore&id=1663555>)

**Table 4.5:** Mutations identified in Exon III of *CYP11B1*

S. No	Nucleotide change	Codon change	Amino acid change	Frequency (n= 90)	SIFT score	Affect on protein	Previously observed in other populations	References
1	g.7900 C>T	CGA>TGA	Arg355Stop	2 (2.2%)	-	-	Turkey	Michels-Rautenstrauss <i>et al.</i> , 2001
2	g.7940 G>A	CGT>CAT	Arg368His	42 (46.7%)	0.00	Affect protein function	Saudi Arabia, Brazil Iran, Australia	Bejjani <i>et al.</i> , 2000 Stoilov <i>et al.</i> , 2002 Chitsazian <i>et al.</i> , 2007 Dimasi <i>et al.</i> , 2007
3	g.7949 G>T	TGT>TTT	Cys371Phe*	1 (1.1%)	0.06	Tolerated	Present study	
4	g.8005 C>A	CGC>AGC	Arg390Ser	1 (1.1%)	0.00	Affect protein function	Saudi Arabia, France	Bejjani <i>et al.</i> , 2000
5	g.8005 C>T	CGC>TGC	Arg390Cys	7 (7.7%)	0.00	Affect protein function	Indian, Ecuador	Reddy <i>et al.</i> , 2003 Curry <i>et al.</i> , 2004
6	g.8006 G>A	CGC>CAC	Arg390His	6 (6.6%)	0.00	Affect protein function	Pakistan Iran	Stoilov <i>et al.</i> , 1998 Chitsazian <i>et al.</i> , 2007
7	g.8147 C>T	CCG>CTG	Pro437Leu	2 (2.2%)	0.00	Affect protein function	Brazil, Turkey	Stoilov <i>et al.</i> , 2002 Stoilov <i>et al.</i> , 1998
8	g.8162 C>T	CCA>CTA	Pro442Leu*	1 (1.1%)	0.02	Affect protein function	Present study	
9	g.8165 C>G	GCT>GGT	Arg443Gly	1 (1.1%)	0.00	Affect protein function	Brazil	Stoilov <i>et al.</i> , 2002
10	g.8227 T>C	TCA>CCA	Ser464Pro*	1 (1.1%)	0.01	Affect protein function	Present study	

11	g.8242 C>T	CGG>TGG	Arg469Trp	1 (1.1%)	0.00	Affect protein function	Saudi Arabia, British, Turkey, Iran	Bejjani <i>et al.</i> , 2000, Stoilov <i>et al.</i> , 1998, Chitsazian <i>et al.</i> , 2007
12	g.8264 C>A	TCT>TAT	Ser476Tyr*	1 (1.1%)	0.00	Affect protein function	Present study	
13	g.8393 A>G	AAT>AGT	Asn519Ser*	1 (1.1%)	0.82	Tolerated	Present study	
14	g.8037 dup TCATGCCACC	-	-	1 (1.1%)	-	-	Brazil, USA, British, Turkey, France, Germany, UK, Costa Rica, Iran, Australia	Stoilov <i>et al.</i> , 2002, Sena <i>et al.</i> , 2004, Colomb <i>et al.</i> , 2003, Stoilov <i>et al.</i> , 1998, Michels-Rautenstrauss <i>et al.</i> , 2001, Chavarria Soley <i>et al.</i> , 2003, Chitsazian <i>et al.</i> , 2007, Dimasi <i>et al.</i> , 2007
15	g.7900delCG	-	-	1 (1.1%)	-	-	Indian	Reddy <i>et al.</i> , 2004
16	g.8148delGGAGA*	-	-	1 (1.1%)	-	-	Present study	
17	g.8214del2AG	-	-	1 (1.1%)	-	-	Brazil	Stoilov <i>et al.</i> , 2002

## \* Novel mutations

*CYP11B* GenBank Accession number: U56438 (<http://www.ncbi.nlm.nih.gov/entrez/viewer.fcgi?db=nucore&id=1663555>)

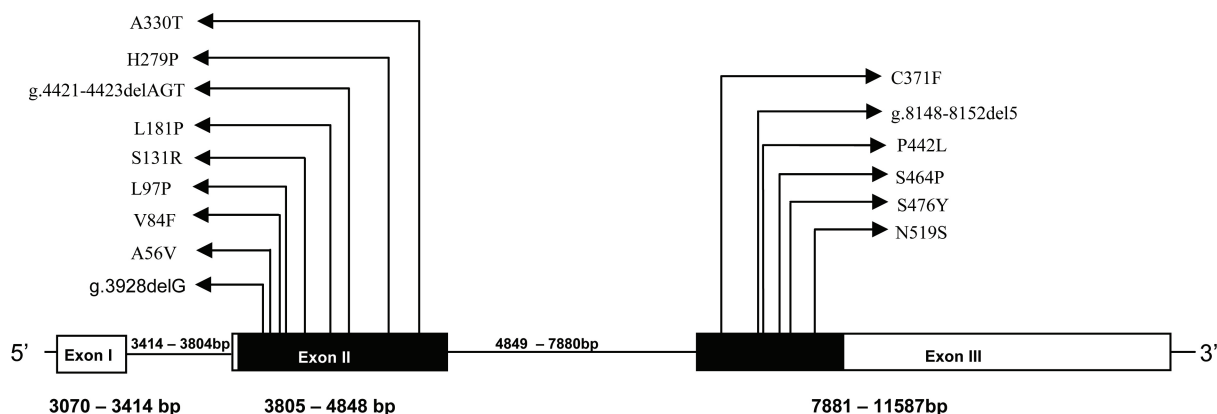


**Figure 4.2:** Schematic representation of the *CYP1B1* gene with the novel mutations. The filled boxes represent the coding region whereas the open boxes represent the untranslated region of the gene. The novel mutations identified in the present study are indicated by arrows.

#### 4.2.3 Location of the mutations in the *CYP1B1* protein

Among the 33 mutations, 30 (90.9%) were identified in the cytosolic domain, 2 (6.0%) in the proline rich region and 1 (3.0%) in the membrane bound domain of the protein, respectively (Table 4.5). Of the 15 novel mutations, 13 were identified in the cytosolic domain, while the remaining were in the membrane bound N-terminal region and the proline-rich hinge region. These mutations in the cytosolic region may affect the catalytic activity of the protein.

**Table 4.5:** Mutations in the various domains of *CYP1B1* protein

<i>S. No</i>	<i>Mutation</i>	<i>Domain</i>
1	g.3928delG	Membrane bound domain
2	Ala56Val	Proline rich region
3	Gly61Glu	Proline rich region
4	Tyr81Asn	Cytosolic domain
5	Val84Phe	Cytosolic domain

6	Leu97Pro	Cytosolic domain
7	Ser131Arg	Cytosolic domain
8	Met132Arg	Cytosolic domain
9	Leu181Pro	Cytosolic domain
10	Pro193Leu	Cytosolic domain
11	Glu229Lys	Cytosolic domain
12	Ser239Arg	Cytosolic domain
13	His279Pro	Cytosolic domain
14	Cys280Stop	Cytosolic domain
15	Ala330Thr	Cytosolic domain
16	g.4421delSer	Cytosolic domain
17	Arg355Stop	Cytosolic domain
18	Arg368His	Cytosolic domain
19	Cys371Phe	Cytosolic domain
20	Arg390Ser	Cytosolic domain
21	Arg390Cys	Cytosolic domain
22	Arg390His	Cytosolic domain
23	Pro437Leu	Cytosolic domain
24	Pro442Leu	Cytosolic domain
25	Ala443Gly	Cytosolic domain
26	Ser464Pro	Cytosolic domain
27	Arg469Trp	Cytosolic domain
28	Ser476Tyr	Cytosolic domain
29	Asn519Ser	Cytosolic domain
30	g.8037dupTCATGCCACC	Cytosolic domain
31	g.7900delCG	Cytosolic domain
32	g.8148delGGAGA	Cytosolic domain
33	g.8214delAG	Cytosolic domain

#### 4.2.4 Description of *CYP1B1* mutations in PCG patients

The electropherograms of all the mutations are shown in Fig 4.3 and 4.4. The clinical features of the patients with *CYP1B1* mutations are mentioned below.

1. g.3928delG: A homozygous deletion of ‘G’ at position g.3928 resulted in a frameshift at codon 41 and premature termination after 17 amino acids at codon 59 in a single consanguineous PCG (PCG305) family. The proband with this mutation had onset of the disease since birth and was intervened at the age of 2 months. He presented with raised IOP (30 and 32 mm of Hg in the right and left eye, respectively) in both the eyes, which was reduced to 12 and 14 mm of Hg in the right and left eye, respectively on surgical treatment. Both the parents



---

were heterozygous for the mutation and did not exhibit any signs of glaucoma at presentation.

2. Ala56Val and Asn519Ser : A heterozygous change from cytosine to thymine at position g.3972 resulted in the replacement of Alanine by Valine at codon 56 in a single non-consanguineous PCG (PCG254) family. The proband with Ala56Val was also heterozygous for a substitution of adenine to guanine at position g.8393 resulting in the replacement of Asparagine by Serine at codon 519, which forms a part of the cytosolic domain of CYP1B1 protein. The proband had a bilateral manifestation of the disease with onset at birth and was intervened at 3 months of age. He had megalocornea (14.5 and 13.5 mm in the right and left eye, respectively) and increased C:D ratio (0.7) at presentation. The IOP was under control (12 mm of Hg) on surgery with a visual acuity of 20/84. The proband's father was heterozygous for the Asn519Ser mutation and did not show any signs of glaucoma at presentation; the mother's DNA sample was not available for analysis.
  
3. Gly61Glu : A homozygous substitution of guanine by adenine at position g.3987 resulted in the replacement of Glycine to Glutamic acid at codon 61 in a single consanguineous PCG (PCG302) family. The proband had bilateral manifestation with onset of the disease since birth and was intervened at 9 days after birth. The proband presented with raised IOP (28 and 30 mm of Hg in the right and left eye, respectively) and megalocornea (12.5 mm in both eyes) in both eyes. Following the surgical intervention, his IOP reduced to 16 and 13 mm of Hg in the right and left eye, respectively. The DNA samples of the parents were not available for analysis.

- 
4. Tyr81Asn: A substitution of thymine by adenine at position g.4046 resulted in the replacement of Tyrosine to Asparagine at codon 81 in 6 PCG families. The proband of 2 families (PCG318 and PCG340) were homozygous, 3 heterozygous (PCG104, PCG338 and PCG350) and one was compound heterozygous (PCG281) with another missense mutation (Cys371Phe). Five patients had bilateral PCG whereas one patient (PCG340) manifested the disease only in his left eye. The details about the clinical features are mentioned in Table 4.7. The segregation analysis of the homozygous Tyr81Asn mutation in PCG340 family revealed that both the parents were heterozygous for the mutant allele. But, in PCG318 family, proband's mother was homozygous and father was heterozygous for the mutant allele. In PCG104, the mother carried the heterozygous mutant allele whereas father did not harbor the change. In the PCG338 family, the proband inherited the mutant allele from his father while his mother did not harbor the change. The DNA samples of parents of the proband in PCG350 family were unavailable for analysis. In the PCG281 family, the proband inherited the Tyr81Asn mutation from his mother and Cys371Phe from his father. The parents of the probands in all these PCG families did not manifest any signs of glaucoma at presentation.

**Table 4.7:** Clinical features of the patients with Tyr81Asn mutation

ID	Onset	Age at intervention	Genotype		^C/NC	IOP at presentation *OD;OS (mm of Hg)	IOP at final follow-up *OD;OS (mm of Hg)	C: D ratio at presentation OD;OS	Corneal diameter at presentation *OD;OS (mm)
			Allele1	Allele2					
PCG104	20 days	7 months	Tyr81Asn	wt	NC	24 ;25	10;11	0.2;0.2	14;14
PCG281	Since birth	2 months	Tyr81Asn	Cys371Phe	NC	28;26	12;14	NA	14;13
PCG318	Since birth	10 days	Tyr81Asn	Tyr81Asn	C	28;28	8;8	NA	13;13
PCG338	Since birth	3 months	Tyr81Asn	wt	C	34;30	8;12	0.5;0.5	14;14
PCG340	Since birth	45 days	Tyr81Asn	Tyr81Asn	C	12;30	12;10	0.2;0.2	11;14
PCG350	7 months	20 days	Tyr81Asn	wt	C	32;32	<21;<21	NA	17;17

^C – consanguineous; NC- non-consanguineous

\*OD- right eye, OS- left eye

NA-not available

- 
5. Val84Phe: A heterozygous change from guanine to thymine at position g.4055 resulted in the replacement of Valine by Phenylalanine at codon 84 in a single non-consanguineous PCG (PCG212) family. The proband with this mutation was also heterozygous Arg368His mutation. The proband had bilateral manifestation since birth and, diagnosed elsewhere and was under treatment. She came to our centre for further management and presented with raised IOP (22 and 28 mm of Hg in the right and left eye, respectively) and increased C:D ratio (0.7:1 and 0.8:1 in the right and left eye, respectively) at the age of 7 years. On surgery the IOP was reduced to 18 mm of Hg in both eyes and her visual acuity was 20/25 and perception and projection of light in the right and left eye, respectively. The proband inherited the Val84Phe mutation from her mother and Arg368His mutation from her father; both the parents did not manifest any signs of glaucoma at presentation.
  
  6. Leu97Pro & Ser131Arg: A heterozygous change from thymine to cytosine at position g.4095 resulted in the replacement of Leucine by Proline at codon 97 in a single non-consanguineous PCG (PCG358) family. The proband with this mutation was also heterozygous for a substitution of adenine to cytosine at position g.4196 resulting in the replacement of Serine by Arginine at codon 131. The proband had bilateral manifestation of the disease since birth and presented with raised IOP (32 and 38 mm of Hg in the right and left eye, respectively) and megalocornea (13.5 mm in both eyes) at the age of 2 months. On surgical intervention his visual acuity was 20/170 in the right eye, whereas he could not appreciate the nearby objects with his left eye. The proband inherited the Leu97Pro from his unaffected father who did not have any signs of glaucoma at presentation, while his mother's DNA sample was unavailable for analysis.

7. Met132Arg: A homozygous substitution from thymine to guanine at position g.4200 resulted in the replacement of Methionine by Arginine at codon 132 in a single consanguineous PCG (PCG205) family. The proband had bilateral manifestation of the disease since birth, was diagnosed elsewhere and was under treatment. He came to our centre for further management and presented with raised IOP (30 and 26 mm of Hg in the right and left eye, respectively), total cupping of 0.9:1 in both eyes and megalocornea (14 and 15 mm in the right and left eye, respectively) in both the eyes at the age of 12 years. On surgical intervention the IOP was <21 mm of Hg with a visual acuity of perception and projection of light in both the eyes. The proband's unaffected mother was heterozygous for the Met132Arg mutation, while his father's DNA sample was unavailable for analysis.
  
8. Leu181Pro: A homozygous change from thymine to cytosine at position g.4347 resulted in the replacement of Leucine by Proline at codon 181 in a single consanguineous PCG (PCG170) family. The proband had bilateral manifestation of disease since birth and presented at the age of 2 years with raised IOP (30 and 44 mm of Hg in the right and left eye, respectively) and megalocornea (14 mm in both eyes). Her IOP was >21 mm of Hg in the right eye with a visual acuity of fixing and following light in both the eyes on surgical intervention. Both the parents were heterozygous for the mutant allele and did not show any signs of glaucoma at presentation.
  
9. Pro193Leu: A heterozygous substitution of cytosine by thymine at position g.4383 resulted in the replacement of Proline to Leucine at codon 193 in a single non-consanguineous PCG (PCG131) family. The proband had a bilateral manifestation since birth and was intervened at the age of 16 months with high

---

IOP (30 mm of Hg), increased C:D ratio (0.6:1 and 0.7:1 in the right and left eye, respectively) and megalocornea (13.5 and 14 mm in the right and left eye, respectively) in both the eyes. On surgical intervention, the proband's IOP reduced to 11 and 13 mm of Hg in the right and left eye, respectively with a visual acuity of 20/170 in both the eyes on surgical intervention. The proband inherited the mutant allele from his unaffected mother who did not manifest any signs of glaucoma at presentation.

10. Glu229Lys: A substitution of guanine by adenine at position g.4491 resulted in the replacement of Glutamic acid to Lysine at codon 229 in 11 PCG families (Table 4.8). The probands of 10 families (PCG241, PCG279, PCG323, PCG326, PCG334, PCG341, PCG352, PCG354, PCG364 and PCG365) were heterozygous while one patient (PCG264) was compound heterozygous with another missense mutation (Ala443Gly). Seven cases had bilateral manifestation (PCG323, PCG326, PCG334, PCG352, PCG354, PCG364 and PCG365). The segregation analysis revealed that probands of 6 PCG families (PCG264, PCG279, PCG323, PCG334, PCG364 and PCG365) inherited the mutant allele from their mother. The mother of proband PCG326 did not harbor this change and his father's DNA sample was unavailable for analysis. In PCG341, the proband's father did not harbor the change and mother's DNA sample was unavailable for analysis. The parents of all these PCG families did not show any signs of glaucoma at presentation. The DNA samples of the parents from three PCG families (PCG241, PCG352 and PCG354) were unavailable for analysis.

**Table 4.8:** Clinical features of the patients with Glu229Lys mutation

ID	Onset	Age at intervention	Genotype		^C/NC	IOP at presentation *OD;OS (mm of Hg)	IOP at final follow-up *OD;OS (mm of Hg)	C: D ratio at presentation *OD;OS	Corneal diameter at presentation *OD;OS (mm)
			Allele 1	Allele 2					
PCG241	10 months	1 year	Glu229Lys	wt	C	38;14	37;14	0.9;0.3	NA
PCG279	Since birth	4 days	Glu229Lys	wt	NC	32;10	10;16	0.6;0.2	12;10
PCG323	1 year	5 years #	Glu229Lys	wt	NC	28;25	14;15	0.8;0.8	13.5;13
PCG326	2 years	3 years #	Glu229Lys	wt	NC	22;22	16;15	0.8;0.9	13;13.5
PCG334	6 months	6 months	Glu229Lys	wt	NC	28;28	12;12	0.5;0.5	13.5;13.5
PCG341	Since birth	3 years #	Glu229Lys	wt	C	36;12	7;16	0.8;0.3	15;13
PCG352	Since birth	2 months	Glu229Lys	wt	C	36;34	<21;<21	NA	15;15
PCG354	Since birth	1 month	Glu229Lys	wt	NC	25;27	7;9	0.5;0.6	13;13.5
PCG364	Since birth	1 month	Glu229Lys	wt	NC	30;28	34;16	0.2;0.2	12;12
PCG365	Since birth	4 months	Glu229Lys	wt	NC	20;33	8;10	0.3;0.3	13;14.5
PCG264	Since birth	3 months	Glu229Lys	Ala443Gly	NC	27;12	8;12	0.6;0.6	13;12

# Diagnosed elsewhere and was under treatment before coming to our centre for further management

wt- wild type

^C – consanguineous; NC- non-consanguineous

\* OD- right eye, OS- left eye

NA- not available

- 
11. Ser239Arg: A homozygous substitution of adenine by cytosine at position g.4520 resulted in the replacement of Serine to Arginine at codon 239 identified in 2 consanguineous (PCG147 and PCG250) families. Both the patients had bilateral manifestation of the disease since birth. The proband (PCG147) presented with digitally raised IOP in both the eyes at the age of 6 months. The other proband (PCG250) was intervened at the age of 2.5 months who had raised IOP (34 and 36 mm of Hg in the right and left eye, respectively) and megalocornea (13.5 and 13 mm in the right and left eye, respectively) in both the eyes. On surgical intervention the IOP was <21 mm of Hg with the visual acuity of fixing and following light in both the probands. The unaffected parents of PCG250 family were heterozygous for the mutant allele and did not manifest any signs of glaucoma at presentation. The DNA samples of both the parents in PCG147 family were unavailable for analysis.
12. g.4421delSer: A homozygous deletion of three bases (AGT) at position g.4421-4423 resulted in the deletion of an amino acid (Serine) at codon 206, in a single non-consanguineous PCG (PCG342) family. The proband had bilateral manifestation of the disease since birth and presented at 15 days after birth with raised IOP (23 mm of Hg and 28 mm of Hg in the right and left eye, respectively) in both the eyes. The C: D ratio was 0.8:1 in the right eye while the fundus of the left eye could not be assessed due to hazy view. She had poor prognosis with raised IOP of 24 mm of Hg in both eyes after surgery. The proband's mother was heterozygous for the mutant allele with no signs of glaucoma at presentation; her father's DNA sample was unavailable for analysis.



- 
13. His279Pro: A heterozygous change from adenine to cytosine at position g.4641 resulted in the replacement of Histidine by Proline at codon 279 in a single non-consanguineous PCG (PCG193) family. The proband was also heterozygous for a substitution of cytosine to adenine at g.4645 position resulting in Cys280Stop mutation. The proband had bilateral manifestation of disease since birth. The proband was diagnosed elsewhere and was under treatment. He came to our centre for further management and presented with raised IOP (24 mm of Hg in both eyes), megalocornea (13 mm in both eyes) and increased C:D ratio (0.7: in both eyes) at the age of 4 years. He had good prognosis on surgical treatment with reduction of IOP to 14 mm of Hg in both eyes along with a visual acuity of 20/80 in both the eyes. The proband inherited the His279Pro mutation from his mother and Cys280Stop mutation from his father; both the parents had no signs of glaucoma at presentation.
14. Cys280STop: A substitution of cytosine by adenine at position g.4645 resulted in the replacement of Cytosine by a stop codon at position 280. This nonsense mutation was identified in 2 families (PCG187 and PCG193), of which PCG193 had history of parental consanguinity. The proband of PCG187 was homozygous whereas the proband of PCG193 was compound heterozygous with another missense mutation (His279Pro). The patient with homozygous mutation had bilateral manifestation of the disease since birth and was intervened at 3 days of age with an IOP of 30 mm of Hg in the both eyes. On surgical intervention the IOP reduced to 19 mm of Hg in both the eyes. Both the parents carried the heterozygous mutant allele and did not exhibit any signs of glaucoma at presentation.

- 
15. Ala330Thr: A heterozygous change of guanine to adenine at position g.4793 resulted in the replacement of Alanine by Threonine at codon 330 in a single non-consanguineous PCG152 family. The proband had bilateral manifestation of the disease since birth and presented with raised IOP (24 mm of Hg in both eyes), megalocornea (12 mm) and increased C:D ratio (0.7:1) at the age of 1 month. The IOP reduced to 10 and 18 mm of Hg in the right and left eye, respectively with the visual acuity of fixing and following light on surgical intervention. The DNA samples of both the parents were unavailable for analysis.
16. Arg355Stop: A substitution of cytosine by thymine at position g.7900 resulted in the replacement of Arginine by a stop codon at position 355. This nonsense mutation was identified in 2 non-consanguineous (PCG265 and PCG369) families. One of the proband (PCG265) was homozygous and the other proband (PCG369) was compound heterozygous with another missense (Arg390His) mutation. Both the patients had bilateral manifestation since birth and were intervened within 1 month of age. The patient with the homozygous mutation presented with raised IOP (32 mm of Hg in both the eyes), increased C:D ratio (0.8:1 in both the eyes) and megalocornea (12.5 and 13.5 mm in the right and left eye, respectively) in both the eyes. On surgical intervention her IOP reduced to 12 mm of Hg in the right eye but could not be controlled in the left eye (28 mm of Hg). The visual acuity was fixing and following light in both the eyes. The proband with compound heterozygous mutation presented with IOP of 22 mm of Hg in both the eyes, which was reduced to 12 and 14 mm of Hg in the right and left eye, respectively, with a visual acuity of 20/260 in both the eyes. The proband (PCG369) inherited the Arg355Stop mutation from his mother and

Arg390His mutation from his father; both the parents did not have any signs of glaucoma at presentation. However, the DNA samples from the parents of PCG265 proband were unavailable for analysis.

17. Arg368His: A substitution of guanine by adenine at position g.7940 resulted in the replacement of Arginine by Histidine at codon 368. This mutation was the most prevalent mutation identified in our patient cohort. This mutation was seen in 42 cases, the details of which are provided in Table 4.8. The segregation analysis of this mutation could be ascertained in only 37 families (Table 4.9) whereas the DNA samples of the parents were unavailable in the remaining families. Among the 42 cases, 34 had bilateral manifestation of the disease. The clinical features of the patients are described in Table 4.9.

**Table 4.9:** Clinical features and segregation analysis of the patients with Arg368His mutation

ID	Genotype		onset	Age at intervention	^C/NC	IOP at presentation *OD;OS (mm of Hg)	IOP at final follow-up *OD;OS (mm of Hg)	C: D ratio at presentation *(OD;OS)	Corneal diameter at presentation *OD;OS (mm)	Mutation in mother's sample	Mutation in Father's sample
	Allele 1	Allele 2									
PCG95	Arg368His	wt	2 months	2 years	NC	38;36	16;14	0.4;0.3	12;12	Arg368His	wt
PCG100	Arg368His	wt	Since birth	4 months	C	11;11	18;20	0.9;0.9	10.5;11	wt	Arg368His
PCG166	Arg368His	wt	2 days	1 month	NC	26;26	33;33	0.9;0.9	NA	NA	NA
PCG171	Arg368His	Arg368His	Since birth	2 years	NC	22;24	16;16	NA	13;13	NA	NA
PCG176	Arg368His	wt	Since birth	3 months	NC	26;24	12;12	0.3;0.2	13.5;13	NA	NA
PCG178	Arg368His	wt	Since birth	8 days	C	32;32	28;10	NA;0.6	13.5;14	wt	Arg368His
PCG182	Arg368His	wt	Since birth	3 weeks	NC	24;22	10;10	0.3;0.3	12.5;12	Arg368His	wt
PCG185	Arg368His	Arg368His	Since birth	18 days	C	30;30	<21;<21	NA	12;12.5	Arg368His	Arg368His
PCG186	Arg368His	Arg368His	Since birth	1 month	C	26;28	<21;<21	NA	12;13	Arg368His	Arg368His
PCG188	Arg368His	wt	Since birth	7 months	NC	32;12	22;14	0.8;0.3	14.5;12.5	wt	Arg368His
PCG189	Arg368His	Arg368His	Since birth	15 days	C	36;32	12;14	0.2;0.2	12;11.5	Arg368His	Arg368His
PCG190	Arg368His	Arg390His	Since birth	8 months	NC	22;17	15;13	0.5;0.5	13.5;13.5	Arg368His	Arg390His
PCG196	Arg368His	wt	Since	7 months	NC	24;16	20;16	0.9;0.4	NA	Arg368His	wt

PCG200	Arg368His	wt	birth Since birth	8 days	C	24;24	12;12	NA	12;12	Arg368His	wt
PCG206	Arg368His	Arg390Cys	Since birth	4 days	C	34;12	17;14	NA	13;12	Arg390Cys	Arg368His
PCG212	Arg368His	Val84Phe	Since birth	7 years#	NC	22;28	18;18	0.7;0.8	NA	Val84Phe	Arg368His
PCG214	Arg368His	wt	3 years	3 years#	C	30;10	<21;<21	0.9;0.5	14;11.5	NA	Arg368His
PCG218	Arg368His	Arg368His	Since birth	7 years#	C	32;34	<21;<21	0.5;0.5	17;16	Arg368His	NA
PCG220	Arg368His	Arg390Cys	Since birth	1 month	C	30;36	14;24	0.2;0.3	12;14	Arg368His	Arg390Cys
PCG228	Arg368His	Pro442Leu	1 year	3 years#	NC	24;28	20;23	NA	15;15	Pro442Leu	Arg368His
PCG232	Arg368His	Arg368His	Since birth	15 days	C	28;32	24;21	NA	14;14	NA	NA
PCG235	Arg368His	Arg368His	Since birth	2 months	NC	26;28	10;10	0.4;0.2	12.5;12.5	Arg368His	Arg368His
PCG244	Arg368His	Arg368His	Since birth	1 month	C	28;33	8;10	0.2;0.3	13;13.5	Arg368His	Arg368His
PCG246	Arg368His	wt	Since birth	2 years	NC	26;10	10;14	0.3;0.1	14;12.5	wt	NA
PCG251	Arg368His	Ser464Pro	Since birth	1 year	NC	30;17	NA	0.8;0.7	14;11	NA	Arg368His
PCG258	Arg368His	Arg390Cys	Since birth	1 year	C	25;24	10;8	0.7;0.5	15;14.5	NA	Arg390Cys
PCG268	Arg368His	wt	6 months	6 months	NC	34;28	12;10	0.4;0.2	14;13	wt	Arg368His
PCG269	Arg368His	Arg368His	Since birth	4 years#	C	14;24	<21;<21	0.1;0.8	13.5;18	Arg368His	Arg368His
PCG272	Arg368His	wt	Since birth	9 days	NC	26;28	6;6	0.3;0.3	12;12	wt	Arg368His

PCG277	Arg368His	Arg368His	Since birth	2 months	C	14;14	NA	0.5;0.2	13;11.5	Arg368His	Arg368His
PCG283	Arg368His	wt	1 month	4 months	C	27;30	9;14	0.2;0.2	15;15	wt	Arg368His
PCG289	Arg368His	Arg368His	Since birth	9 days	NC	22;22	10;22	0.4;0.4	14;14	Arg368His	Arg368His
PCG298	Arg368His	Arg368His	Since birth	2 months	NC	26;28	16;16	0.2;0.2	13.5;13.5	Arg368His	Arg368His
PCG309	Arg368His	wt	Since birth	6 months	NC	14;32	<21;>21	0.3;0.9	12;16	NA	NA
PCG315	Arg368His	Arg368His	5 days	9 years#	C	46;28	38;12	NA;0.9	15;13	Arg368His	Arg368His
PCG320	Arg368His	Arg368His	1 month	4 months	NC	30;22	10;10	0.5;0.4	13.5;13.5	Arg368His	Arg368His
PCG328	Arg368His	Arg368His	Since birth	3 months	NC	24;26	12;12	0.2;0.2	12;12	Arg368His	Arg368His
PCG333	Arg368His	Arg368His	Since birth	3 months	NC	>21;>21	10;16	0.4;0.6	13;13	Arg368His	Arg368His
PCG339	Arg368His	wt	3 months	6 months	NC	30;28	16;22	0.9;0.4	13;13	wt	Arg368His
PCG362	Arg368His	Arg368His	Since birth	2 days	NC	32;34	16;17	0.5;0.7	14;13	Arg368His	Arg368His
PCG370	Arg368His	Arg368His	Since birth	1 day	NC	28;32	10;10	0.5;0.6	13;13.5	Arg368His	Arg368His
PCG373	Arg368His	Arg390His	Since birth	1 month	NC	8;16	16;22	0.6;0.6	14;14	Arg390His	Arg368His

#Diagnosed elsewhere and was under treatment before coming for further management; wt- wild type

^C – consanguineous; NC- non-consanguineous

\* OD- right eye, OS- left eye

& All the parent samples were heterozygous for their respective mutation

- 
18. Cys371Phe: A heterozygous change from guanine to thymine at position g.7949 resulted in the replacement of Cysteine by Phenylalanine at codon 371 in a single non-consanguineous PCG (PCG281) family. The proband with this mutation was also heterozygous for Tyr81Asn mutation. The proband had bilateral manifestation of disease since birth and presented with raised IOP (28 mm of Hg and 26 mm of Hg in the right and left eye, respectively) and megalocornea (14mm and 13 mm in the right and left eye, respectively) at the age of 2 months. The IOP reduced to 12 mm of Hg and 14 mm of Hg in the right and left eye, respectively on surgery. The proband inherited the Cys371Phe mutant allele from his father and Tyr81Asn mutant allele from his mother, respectively; both the parents did not manifest any signs of glaucoma at presentation.
19. Arg390Ser: A homozygous change from cytosine to adenine at position g.8005 resulted in the replacement of Arginine by Serine at codon 390 in a single consanguineous PCG (PCG271) family. The proband had bilateral manifestation of the disease since birth and presented with raised IOP (34 and 32 mm of Hg in the right and left eye, respectively), megalocornea and increased C:D ratio (0.7:1) at 1 day after birth. The IOP reduced to 14 mm of Hg in both the eyes and the visual acuity was fixing and following light on surgery. Both the unaffected parents were heterozygous for the mutant allele and did not manifest any signs of glaucoma at presentation.
20. Arg390Cys: A substitution of cytosine by thymine at position g.8005 resulted in the replacement of Arginine by Cysteine at codon 390 in 7 PCG families. The proband of 4 families (PCG180, PCG184, PCG273 and PCG295) were homozygous whereas 3 (PCG206, PCG220 and PCG258) were compound

heterozygous with another missense mutation (Arg368His). Six probands had bilateral manifestation and the clinical features of these patients with Arg390Cys mutation are mentioned in Table 4.9. The segregation analysis was ascertained in 6 families (PCG180, PCG206, PCG220, PCG258, PCG273, and PCG295). Both the parents of PCG180, PCG273 and PCG295 were heterozygous for the mutant allele. On the other hand, the probands of PCG 220 and PCG258 families inherited the Arg290Cys mutant allele from their respective fathers. The mother of the proband in family PCG220 was heterozygous for the other mutant allele (Arg368His); the DNA sample from the mother of the proband (PCG258) was unavailable for analysis. In PCG206, the proband inherited the Arg390Cys and Arg368His mutation from his mother and father, respectively. The parents of all these PCG families were unaffected without any signs of glaucoma at presentation.



**Table 4.10:** Clinical features of the patients with Arg390Cys mutation

ID	Genotype		Onset	Age at intervention	^C/NC	IOP at presentation *OD;OS (mm of Hg)	IOP at final follow-up *OD;OS (mm of Hg)	C: D ratio at presentation *OD;OS	Corneal diameter at presentation\$ *OD;OS (mm)
	Allele 1	Allele 2							
PCG180	Arg390Cys	Arg390Cys	Since birth	1 day	C	30;30	30;20	0.6;0.6	12;12
PCG184	Arg390Cys	Arg390Cys	Since birth	20 days	NC	26;28	13;14	0.1;0.1	12;12
PCG273	Arg390Cys	Arg390Cys	Since birth	1 year	NC	22;34	32;42	0.6;0.6	12.5;12.5
PCG295	Arg390Cys	Arg390Cys	Since birth	1 month	NC	26;24	34;18	0.3;0.3	11;11
PCG206	Arg390Cys	Arg368His	Since birth	9 days	C	34;12	17;14	NA	12;10.5
PCG220	Arg390Cys	Arg368His	Since birth	1 month	C	30;36	14;24	0.2;0.3	12;14
PCG258	Arg390Cys	Arg368His	Since birth	1 year	C	25;24	10;8	0.7;0.5	15;14.5

^C – consanguineous; NC- non-consanguineous

\*OD- right eye, OS- left eye

NA-not available

---

21. Arg390His: A substitution of guanine by adenine at position g.8006 resulted in the replacement of Arginine by Histidine at codon 390. This mutation was identified in 6 PCG families with bilateral manifestation of the disease. The proband of 3 families were homozygous (PCG119, PCG317 and PCG367) whereas 3 were compound heterozygous (PCG190, PCG369 and PCG373) with another mutation (Arg368His and Arg355Stop). The clinical features of the patients with Arg390Cys mutation are mentioned in Table 4.11. The segregation analysis was ascertained in 5 families (PCG190, PCG317, PCG367, PCG369 and PCG373) whereas the DNA samples from both the parents were unavailable in PCG119 family. The probands of PCG369 and PCG373 families inherited the Arg390His mutation from their respective mothers and the second mutant allele (Arg355Stop in PCG369 and Arg368His in PCG373) from their respective fathers. The proband of PCG190 inherited the Arg390His mutation from her father and Arg368His mutation from her mother, respectively. Both the parents of PCG317 and PCG367 families were heterozygous for the Arg390His mutation. The parents of all these PCG families did not exhibit any signs of glaucoma at presentation.

The codon “390” happens to be a mutant hot spot in the *CYP11B1* gene. Three different substitutions (Arg390Ser, Arg390Cys and Arg390His) were identified at this position that jointly accounted for 15.5% (14/90) cases.

**Table 4.11:** Clinical features of the patients with Arg390His mutation

ID	Onset	Age at intervention	Genotype		C/NC	IOP at presentation *OD;OS (mm of Hg)	IOP at final follow – up *OD;OS (mm of Hg)	C: D ratio at presentation *OD;OS	Corneal diameter at presentation *OD;OS (mm)
			Allele 1	Allele 2					
PCG119	Since birth	10 years#	Arg390His	Arg390His	C	14; <21	28;Pthisis bulbi	0.9;Pthisis bulbi	NA
PCG317	Since birth	6 days	Arg390His	Arg390His	NC	22;22	16;22	0.6;NA	12;13
PCG367	Since birth	2 days	Arg390His	Arg390His	NC	44;28	NA	NA	14;14
PCG190	Since birth	1 year	Arg390His	Arg368His	NC	22;17	15;13	0.8;0.6	13.5;13.5
PCG369	Since birth	2 days	Arg390His	Arg355stop	NC	>21;>21	12;12	0.3;0.3	11;11
PCG373	Since birth	1 day	Arg390His	Arg368His	NC	16;22	8;16	0.6;0.6	14;14

#Diagnosed elsewhere and was under treatment before coming for further management

^ C – consanguineous; NC- non-consanguineous

\* OD- right eye, OS- left eye

NA-not available

---

22. Pro437Leu: A homozygous change from cytosine to thymine at position g.8147 resulted in the replacement of Proline by Leucine at codon 437 in two consanguineous PCG (PCG140 and PCG224) families. Both the patients had bilateral manifestation of the disease since birth and were intervened within 3 years of age with raised IOP (28 mm of Hg in both the eyes [PCG140]; 24 and 42 mm of Hg in the right and left eye, respectively in [PCG224]) and megalocornea (12.5 mm [PCG140] and 16mm [PCG224], respectively) in both the eyes. The IOP reduced to 10mm of Hg [PCG140 and 12 mm of Hg [PCG224], respectively in both the patients at their final follow up. The parents of both the PCG140 and PCG224 families were heterozygous for Pro447Leu mutation and did not exhibit any signs of glaucoma at presentation.

23. Pro442Leu: A heterozygous change from cytosine to thymine at position g.8162 resulted in the replacement of Proline by Leucine at codon 442 in a non-consanguineous PCG (PCG228) family. The proband with this mutation was also heterozygous for Arg368His mutation. The proband had a bilateral manifestation of disease at 1 year of age and was diagnosed elsewhere. The proband was under treatment and came to our centre for further management. She presented with raised IOP (24 mm of Hg and 28 mm of Hg in the right and left eye, respectively) and megalocornea (15 mm in both the eyes) at 3 years of age. She had poor prognosis with slightly low IOP (20mm of Hg) in the right eye but 23 mm of Hg in and left eye, respectively, along with visual acuity of fixing and following light on surgery. The proband inherited the Pro442Leu mutation from her mother and Arg368His mutation from her father, respectively. Both the parents were unaffected without any signs of glaucoma at presentation.

24. Ala443Gly: A heterozygous substitution of cytosine to guanine at position g.8165 resulted in the replacement of Alanine by Glycine at codon 443 in a single non-consanguineous PCG (PCG264) family. The proband with this mutation was also heterozygous for Glu229Lys mutation. The patient had unilateral PCG since birth and presented with an IOP of 20 mm of Hg in his right eye at the age of 3 months. His IOP was 10 mm of Hg on surgical intervention with a visual acuity of 20/84. The proband inherited the mutant Ala443Gly allele from his father and Glu229Lys mutated allele from his mother, respectively. Both the parents were unaffected without any signs of glaucoma at presentation.

25. Ser464Pro: A heterozygous change from thymine to cytosine at position g.8227 resulted in the replacement of Serine by Proline at codon 464 in a single non-consanguineous PCG (PCG251) family. The proband with this mutation was also heterozygous for Arg368His mutation. The proband had a unilateral manifestation since birth and was diagnosed elsewhere at the age of 1 year. He was under treatment and came to our centre for further management. He presented with raised IOP (30 mm of Hg), megalocornea (14 mm) and increased C:D ratio (0.8:1) in his right eye at the age of 10 years. On surgery his visual acuity was perception and projection of light in the glaucomatous eye; it was 20/40 in the fellow eye. The proband inherited the Arg368His mutation from his father who did not have any signs of glaucoma at presentation whereas the mother's DNA sample was unavailable for analysis.

26. Arg469Trp: A heterozygous change from cytosine to thymine at position g.8242 resulted in the replacement of Arginine by Tryptophan at codon 469 in a

---

single consanguineous PCG (PCG195) family. The proband had bilateral manifestation of the disease since birth and presented with an IOP of 34 mm of Hg at the age of 5 days. His IOP was reduced to 16 and 10 mm of Hg in the right and left eye, respectively on surgical intervention but his visual acuity was 20/670 in both the eyes. The proband inherited the Arg469Trp mutated allele from his father whereas his mother did not harbor this change. Both the parents were unaffected without any signs of glaucoma at presentation.

27. Ser476Tyr: A heterozygous change from cytosine to adenine at position g.8264 resulted in the replacement of Serine by Tyrosine at codon 476 in a single non-consanguineous PCG (PCG70) family. The proband had bilateral manifestation of the disease since birth and was operated elsewhere. He came to our centre for further management and presented with IOP of 20 mm of Hg and C:D ratio of 0.8:1 in the right eye. The IOP in the left eye was 11 mm of Hg and fundus could not be assessed due to hazy view. The visual acuity was 20/20 in the right eye but there was no perception of light in the left eye. The DNA sample from the parents was unavailable for analysis. The patient was under medication and later lost to follow-up, hence the prognosis could not be ascertained.

28. g.7900delCG: A homozygous deletion of 2 bases (CG) at position g.7900 resulted in a frame shift at amino acid position 355 and led to the premature termination of the protein after 17 amino acids at codon 373. The mutation was identified in a single consanguineous PCG (PCG142) family. The proband had bilateral manifestation since birth and presented with raised IOP (36 and 34 mm of Hg, respectively) and megalocornea (12 mm) in both the eyes at the age of 1 month. On surgical intervention the IOP was <21 mm of Hg in both the eyes with a visual acuity of fixing and following light. Both the parents were

---

heterozygous for the mutant allele and did not exhibit any signs of glaucoma at presentation.

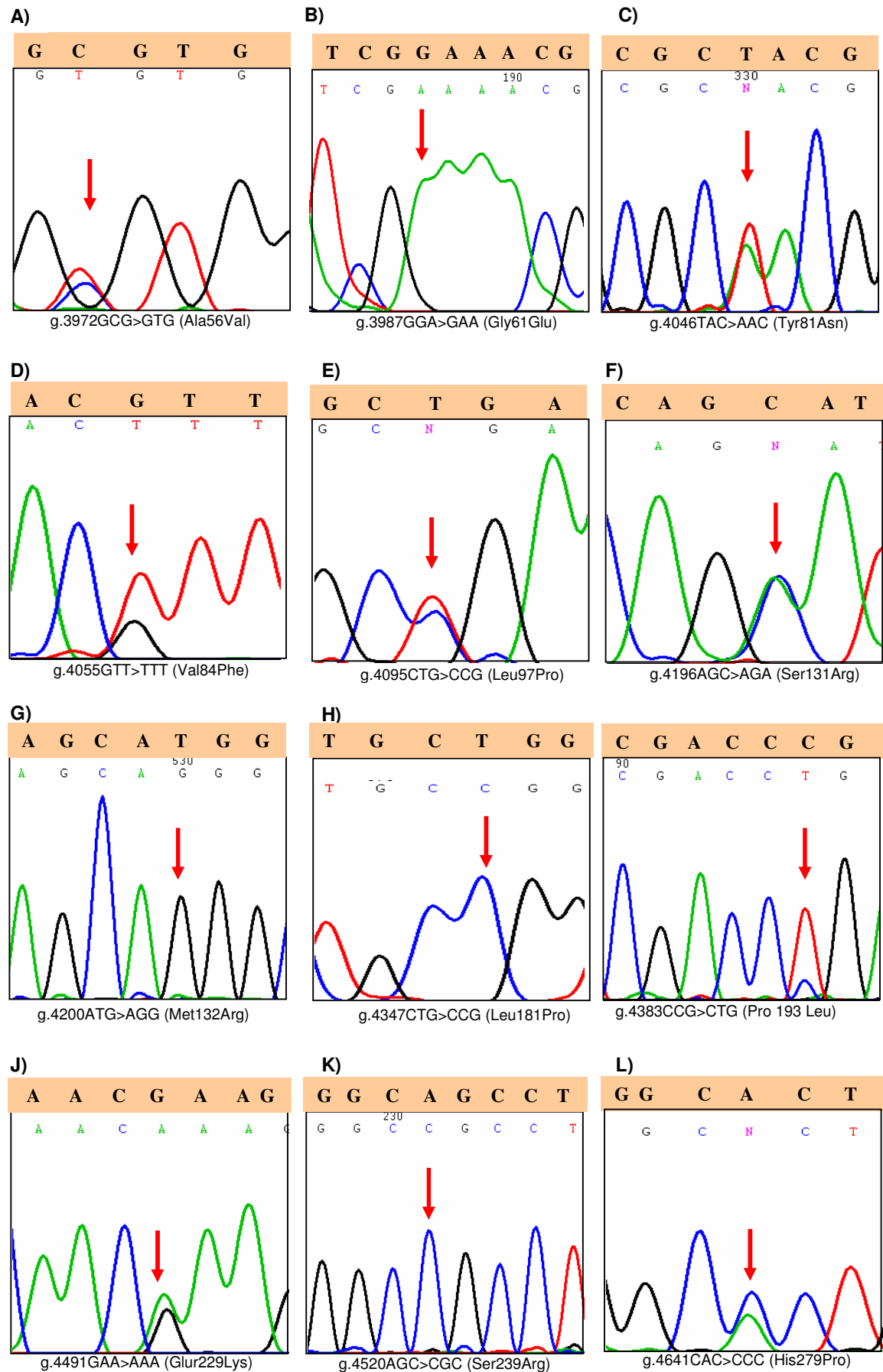
29. g.8037dupTCATGCCACC: A homozygous duplication of 10 bases (TCATGCCACC) at position g.8037 resulted in a frameshift at amino acid position 403 and led to the premature termination of the protein after 29 amino acids at codon 433. The mutation was identified in a single consanguineous PCG (PCG110) family. The proband had bilateral manifestation of disease since birth and presented at 5 days after birth with raised IOP (44 mm of Hg) and megalocornea (14mm). On surgery the IOP was >21 mm of Hg with a visual acuity of fixing and following of light. The DNA samples from the parents were unavailable for analysis.

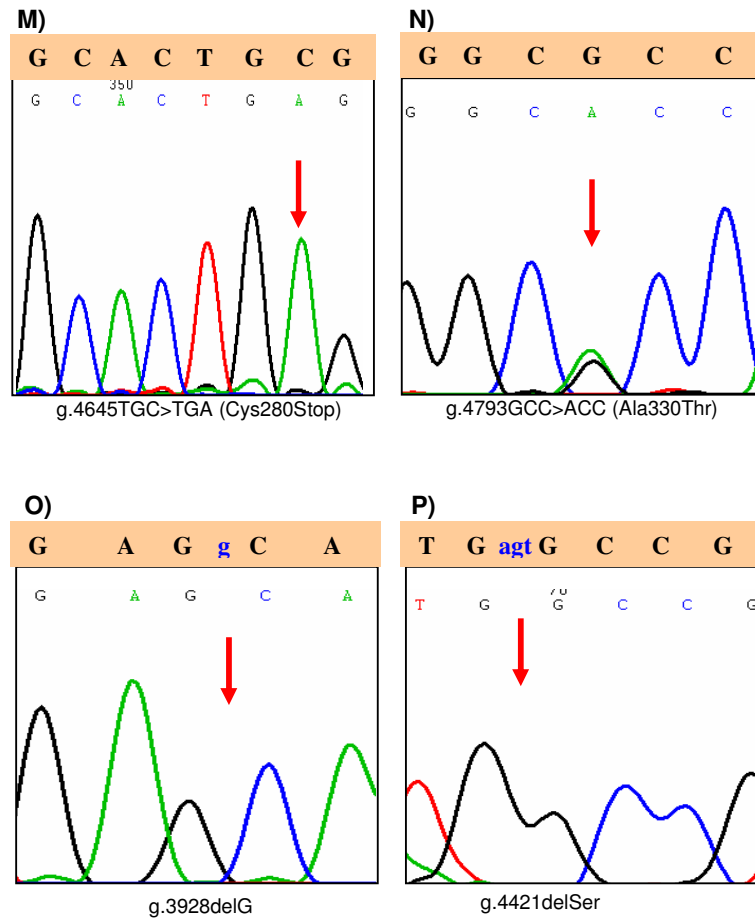
30. g.8148delGGAGA: A homozygous deletion of 5 bases (GGAGA) at position g.8148 resulted in a frameshift at amino acid position 438 that led to the premature termination of the protein at codon 439. The mutation was identified in a single consanguineous PCG (PCG238) family. The proband had bilateral manifestation of disease since birth and presented at the age of 3 months with raised IOP (24 and 26 mm of Hg in the right and left eye, respectively), megalocornea (12mm in both the eyes) and increased C:D ratio (0.6:1 in both the eyes). On surgical treatment her IOP reduced to 20 mm of Hg but the visual acuity was 20/960 in both the eyes. Both the parents were heterozygous for the mutant allele and did not show any signs of glaucoma at presentation.

31. g.8214delAG: A homozygous deletion of 2 bases (AG) at position g.8214 resulted in a frameshift at amino acid position 459 that led to the premature termination of the protein after 17 amino acids at codon 476. The mutation was

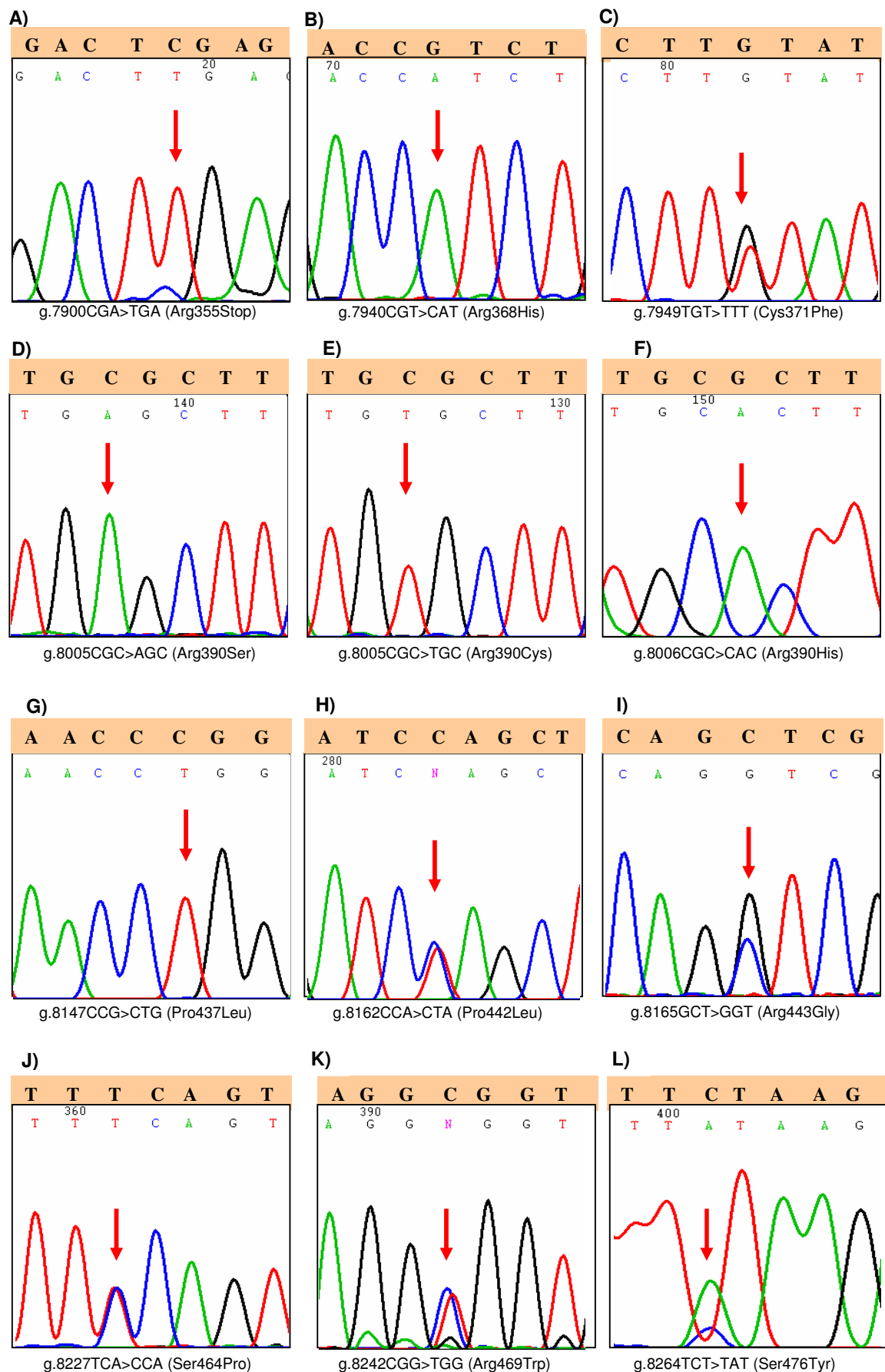
identified in a single consanguineous PCG (PCG357) family. The proband had bilateral manifestation of disease since birth and presented at the age of 3 months with raised IOP (30 and 32 mm of Hg in the right and left eye, respectively) and megalocornea (12 mm). On surgical treatment her IOP was >21 mm of Hg with a visual acuity of 20/960. Both the parents were heterozygous for the mutant allele and did not exhibit any signs of glaucoma at presentation.







**Figure 4.3:** Electropherograms showing the 16 mutations identified in exon II of *CYP11B1* in PCG cases. The sequence above the electropherogram in the shaded portion represents the wild type sequence. The arrow head indicates the site of change. **A)** A heterozygous substitution of GCG>GTG at g.3972, resulted in the Arg56Val mutation. **B)** A homozygous substitution of GGA>GAA at g.3987, resulted in the Gly61Glu mutation. **C)** A heterozygous substitution of TAC>AAC at g.4046, resulted in the Tyr81Asn mutation. **D)** A heterozygous substitution of GTT>TTT at g.4055, resulted in the Val84Phe mutation. **E)** A heterozygous substitution of CTG>CCG at g.4095, resulted in Leu97Pro mutation. **F)** A heterozygous substitution of AGC>AGA at g. 4196, resulted in Ser131Arg mutation. **G)** A homozygous substitution of ATG>AGG at g.4200, resulted in the Met132Arg mutation. **H)** A homozygous substitution of CTG>CCG at g.4347, resulted in Leu181Pro mutation. **I)** A heterozygous substitution of CCG>CTG at g.4383, resulted in Pro193Leu mutation. **J)** A heterozygous substitution of GAA>AAA at g.4491, resulted in Glu229Lys mutation. **K)** A homozygous substitution of AGC>CGC at g.4520, resulted in Ser239Arg mutation. **L)** A heterozygous substitution of CAC>CCC at g.4641, resulted in His279Pro mutation. **M)** A homozygous substitution of TGC>TGA at g.4645, resulted in Cys280Stop mutation. **N)** A heterozygous substitution of GCC>ACC at g.4793, resulted in Ala330Thr mutation. **O)** A homozygous deletion of G at g.3928 position resulted in the frame shift after amino acid position 40. **P)** A homozygous deletion of AGT at g.4421 resulted in a deletion of serine amino acid at position 206.



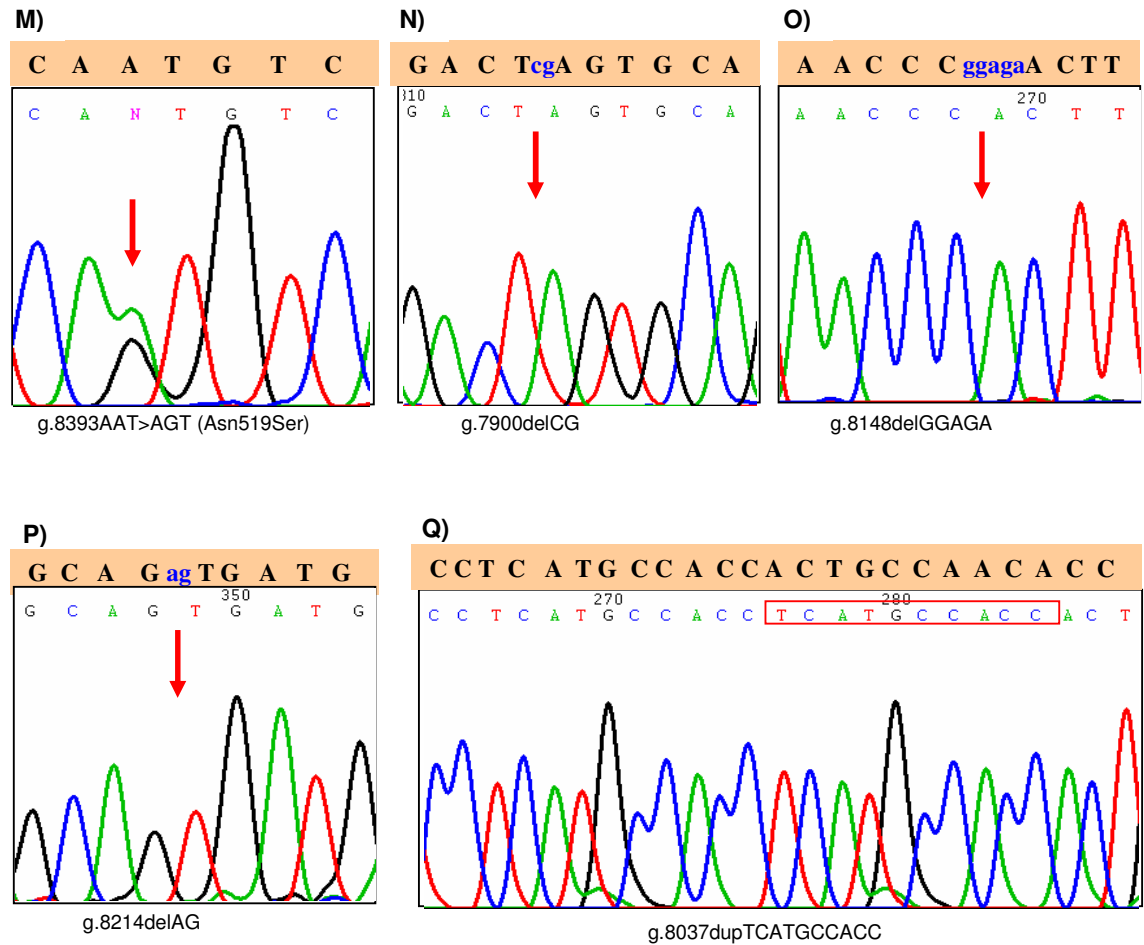


**Figure 4.4:** Electropherograms showing the 17 mutations identified in exon III in PCG cases. The sequence above the electropherogram in the shaded portion represents the wild type sequence. The arrow head indicates the site of change. **A)** A homozygous substitution of CGA>TGA at g.7900, resulted in the Arg355Stop mutation. **B)** A homozygous substitution of CGT>CAT at g.7940, resulted in the Arg368His mutation. **C)** A heterozygous substitution of TGT>TTT at g.7949, resulted in the Cys371Phe mutation. **D)** A homozygous substitution of CGC>AGC at g.8005, resulted in the Arg390Ser mutation. **E)** A homozygous substitution of CGC>TGC at g.8005, resulted in the Arg390Cys mutation. **F)** A homozygous substitution of CGC>CAC at g.8006, resulted in the Arg390His mutation. **G)** A homozygous substitution of CCG>CTG at g.8147, resulted in the Pro437Leu mutation. **H)** A heterozygous substitution of CCA>CTA at g.8162, resulted in the Phe442Leu mutation. **I)** A heterozygous substitution of GCT>GGT at g.8165, resulted in the Arg443Gly mutation. **J)** A heterozygous substitution of TCA>CCA at g.8227, resulted in Ser464Pro mutation. **K)** A heterozygous substitution of CGG>TGG at g.8242, resulted in Arg469Trp mutation. **L)** A heterozygous substitution of TCT>TAT at g.8264, resulted in Ser476Tyr mutation. **M)** A heterozygous substitution of AAT>AGT at g.8393, resulted in Asn519Ser mutation. **N)** A homozygous deletion of 2 bases (CG) at position g.7900 resulted in a frame shift at position 355. **O)** A homozygous deletion of 5 bases (GGAG) at position g.8148 resulted in a frame shift at codon 438. **P)** A homozygous deletion of 2 bases (AG) at position g.8214 resulted in a frame shift at codon 459. **Q)** A homozygous duplication of 10 bases (TCATGCCACC) at position g.8037 resulted in a frame shift at codon 403.

#### ***4.2.5 Conservation of the residues***

Multiple sequence alignment was done using Clustal W software ([www.expasy.ch](http://www.expasy.ch)) to determine the conservation of the wild type residues. Fifteen out of 33 missense mutations were found to be highly conserved whereas other mutations showed less conservation across species (Fig 4.5, 4.6). The SIFT score analysis revealed 30 mutations as pathogenic with an effect on protein function, whereas three mutations (Glu229Lys, Cys371Phe and Asn519Ser) were found to have no effect on the protein (Tables 4.4 and 4.5).

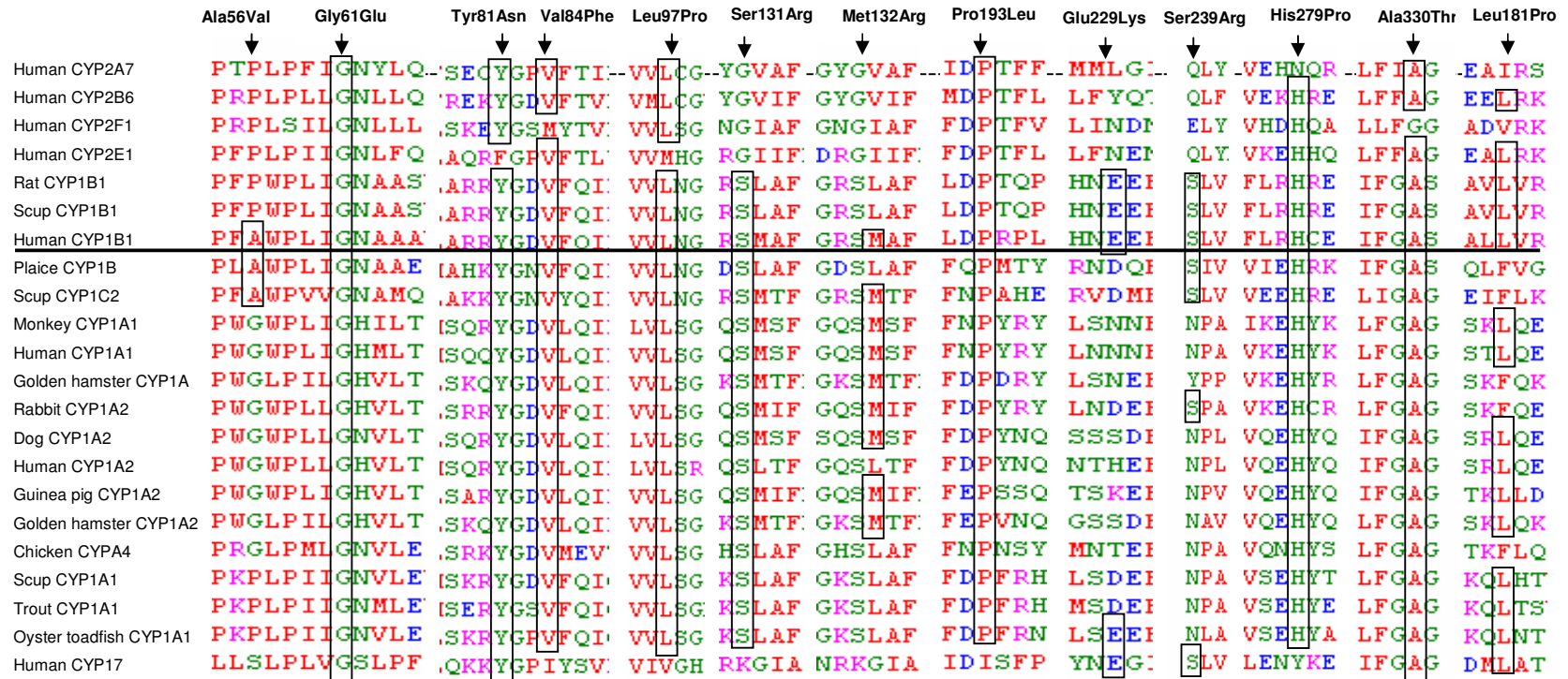


**Figure 4.5:** Multiple sequence alignment showing the conservation of wild type residues (in the blocks) in exon II in different cytochrome families across various species. The human CYP1B1 protein is underlined and wild type residues are blocked.

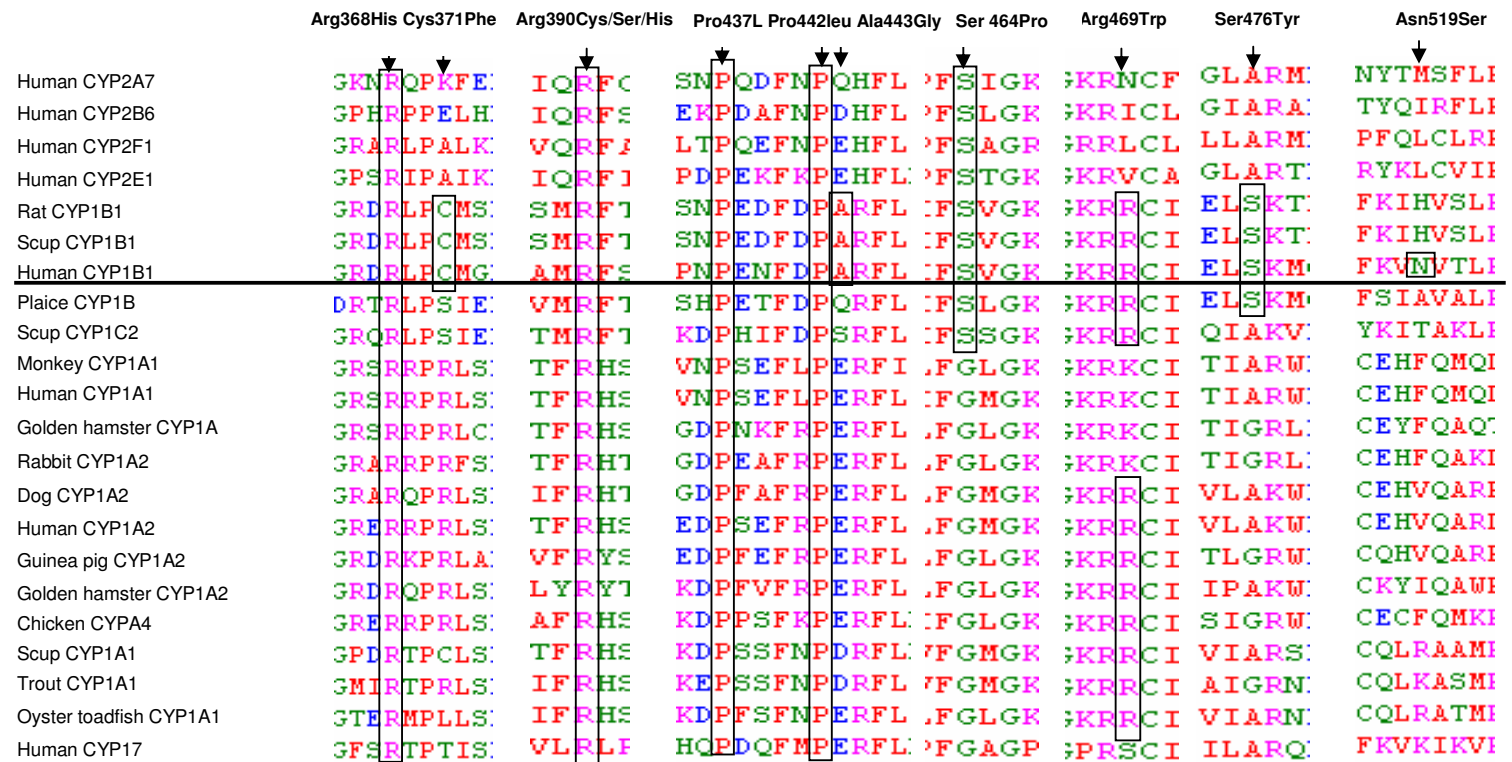


**Figure 4.6:** Multiple sequence alignment showing the conservation of wild type residues (in the blocks) in exon III in different cytochrome families across various species. The human CYP1B1 protein is underlined and wild type residues are blocked.

#### 4.2.6 Single nucleotide polymorphisms in *CYP1B1*

Six single nucleotide polymorphisms (SNPs) were identified in *CYP1B1* gene, of which one was in intron I and remaining five were in the coding region (Table 4.12).

**Table 4.12:** Single nucleotide polymorphisms (SNPs) in *CYP1B1* gene

<i>S.No.</i>	<i>Location</i>	<i>Nucleotide change</i>	<i>Amino acid change</i>	<i>dbSNP ID</i>
1	Intron I	-13T/C	—	rs2617266
2	Exon II	g. 3947 C>G	R48G	rs10012
3	Exon II	g. 4160 G>T	A119S	rs1056827
4	Exon III	g. 8131 G>C	V432L	rs1056836
5	Exon III	g. 8184 T>C	D449D	rs1056837
6	Exon III	g. 8195 A>G	N453S	rs1800440

##### 4.2.6.1 Distribution of *CYP1B1* SNPs in different categories

The patients were divided into two groups i.e., patients with *CYP1B1* mutation [*CYP1B1* (+)] and patients without *CYP1B1* mutation [*CYP1B1* (-)]. The distribution of allele and genotype frequencies of these groups was compared with each other and also with the control group (Tables 4.13 to 4.18).

##### a) [*CYP1B1* (+)] cases and controls

The allele and genotype frequencies of the four SNPs (rs10012, rs1056827, rs1056836 and rs1056837) were significantly different among the [*CYP1B1* (+)] cases compared to controls (Tables 4.13 and 4.14). The frequency of the heterozygous (A,G) genotype in rs1800440 SNP was significantly different between the two groups, which could be due to the large number of heterozygotes in the



control group The frequency of only homozygous (C,C) genotype in rs2617266 SNP was significantly different among the two groups (Table 4.14).

*b) [CYP1B1 (-)] cases and controls*

There were no significant differences in the distribution of allele frequencies between [CYP1B1 (-)] cases and control group (Tables 4.15 & 4.16).

*c) [CYP1B1 (+)] and [CYP1B1 (-)] cases*

The allele and genotype frequencies of the four SNPs (rs10012, rs1056827, rs1056836 and rs1056837) were significantly different between the [CYP1B1 (+)] and [CYP1B1 (-)] cases (Tables 4.17 & 4.18). The frequency of the heterozygous (A,G) genotype in rs1800440 SNP and the frequency of only homozygotes (C,C) in rs2617266 SNP were significantly different among the two groups in (Table 4.16) as in scenario “a”.

**Table 4.13:** Allele frequency distribution of *CYP1B1* SNPs in [CYP1B1 (+)] cases and controls

S. No	SNP	Allele	Allele frequency		p value	ODDS Ratio (95% CI)
			Patients with <i>CYP1B1</i> mutations (n= 132)	Controls (n= 102)		
1	-13T>C	T	0.18	0.44	0.0001	1
		C	0.82	0.56		3.6 (1.8-6.8)
2	R48G	C	0.78	0.58	0.002	1
		G	0.22	0.42		0.4 (0.2-0.7)
3	A119S	G	0.78	0.58	0.002	1
		T	0.22	0.42		0.4 (0.2-0.7)
4	V432L	G	0.49	0.2	0.0001	1
		C	0.51	0.8		0.26 (0.13-0.48)
5	D449D	T	0.49	0.2	0.0001	1
		C	0.51	0.8		0.26 (0.13-0.48)
6	N453S	A	0.91	0.83	0.09	1
		G	0.09	0.17		0.5 (0.2-1.1)

**Table 4.14:** Genotype frequency distribution of CYP1B1 SNPs in [CYP1B1 (+)] cases and controls

S. No	SNP	GENOTYPE	PATIENTS WITH CYP1B1 MUTATIONS (n=132)	CONTROLS (n=102)	p value	ODDS RATIO (95% CI)
1	-13T>C	T,T	13 (9.8%)	19 (18.6%)	—	1
		T,C	21 (15.8%)	51 (50%)	0.25	0.6 (0.3- 1.4)
		C,C	98 (74.2%)	32 (31.3%)	0.0001	4.5 (2.0 -10.1)
2	R48G	C,C	91 (68.9%)	35 (34.3%)	—	1
		C,G	24 (18%)	49 (48%)	0.0001	0.2 (0.1-0.3)
		G,G	17 (12.8%)	18 (17.6%)	0.008	0.4 (0.2-0.8)
3	A119S	G,G	91 (68.9%)	35 (34.3%)	—	1
		G,T	24 (18%)	49 (48%)	0.0001	0.2 (0.1-0.3)
		T,T	17 (12.8%)	18 (17.6%)	0.008	0.4 (0.2-0.8)
4	V432L	G,G	52 (39%)	5 (5%)	—	1
		G,C	26 (19.5%)	31 (30.4%)	0.0001	0.08 (0.03-0.23)
		C,C	54 (40.9%)	66 (64.7%)	0.0001	0.08 (0.03-0.2)
5	D449D	T,T	52 (39%)	5 (5%)	—	1
		T,C	26 (19.5%)	31 (30.4%)	0.0001	0.08 (0.03-0.23)
		C,C	54 (40.9%)	66 (64.7%)	0.0001	0.08 (0.03-0.2)
6	N453S	A,A	113 (85.6%)	72 (70.6%)	—	1
		A,G	14 (10.5%)	26 (25.5%)	0.002	0.3 (0.2-0.7)
		G,G	5 (3.8%)	4 (3.9%)	0.73	0.8 (0.2-3.0)

**Table 4.15:** Allele frequency distribution of *CYP1B1* SNPs in [CYP1B1 (-)] cases and controls

S. No	SNP	Allele	Allele frequency		p value	ODDS Ratio (95% CI)
			Patients without CYP1B1 mutations (n= 169)	Controls (n= 102)		
1	-13T>C	T	0.39	0.44	0.47	1
		C	0.61	0.56		1.2 (0.7-2.1)
2	R48G	C	0.57	0.58	0.88	1
		G	0.43	0.42		1 (0.6-1.8)
3	A119S	G	0.57	0.58	0.88	1
		T	0.43	0.42		1 (0.6-1.8)
4	V432L	G	0.19	0.2	0.86	1
		C	0.81	0.8		1 (0.5-2.1)
5	D449D	T	0.19	0.2	0.86	1
		C	0.81	0.8		1 (0.5-2.1)
6	N453S	A	0.83	0.83	1	1
		G	0.17	0.17		1 (0.5-2.1)

**Table 4.16** Genotype frequency distribution of *CYP1B1* SNPs in [CYP1B1 (-)] cases and controls

S. No	SNP	Genotype	Patients without <i>CYP1B1</i> mutations (n = 169)	Controls (n = 102)	p value	ODDS RATIO (95% CI)
1	-13T>C	T,T	36 (21.3%)	19 (18.6%)	—	1
		T,C	60 (35.5%)	51 (50%)	0.16	0.6 (0.3-1.2)
		C,C	73 (43.1%)	32 (31.3%)	0.6	1.2 (0.6-2.4)
2	R48G	C,C	63 (37.2%)	35 (34.3%)	—	1
		C,G	70 (41.4%)	49 (48%)	0.4	0.8 (0.5-1.4)
		G,G	36 (21.3%)	18 (17.6%)	0.8	1.1 (0.6-2.2)
3	A119S	G,G	63 (37.2%)	35 (34.3%)	—	1
		G,T	70 (41.4%)	49 (48%)	0.4	0.8 (0.5-1.4)
		T,T	36 (21.3%)	18 (17.6%)	0.8	1.1 (0.6-2.2)
4	V432L	G,G	11 (6.5%)	5 (5%)	—	1
		G,C	44 (26%)	31 (30.4%)	0.45	0.6 (0.2-2.0)
		C,C	114 (67.5%)	66 (64.7%)	0.7	0.8 (0.3-2.4)
5	D449D	T,T	11 (6.5%)	5 (5%)	—	1
		T,C	44 (26%)	31 (30.4%)	0.45	0.6 (0.2-2.0)
		C,C	114 (67.5%)	66 (64.7%)	0.8 (0.3-2.4)	0.7
6	N453S	A,A	118 (69.8%)	72 (70.6%)	—	1
		A,G	45 (26.6%)	26 (25.4%)	0.84	1.0 (0.6-2.0)
		G,G	6 (3.6%)	4 (3.9%)	0.89	0.9 (0.2-3.4)

**Table 4.17:** Allele frequency distribution of *CYP1B1* SNPs in [CYP1B1 (+)] and [CYP1B1 (-)] cases

S. No	SNP	Allele	Allele frequency		p value	ODDS RATIO (95% CI)
			Patients with <i>CYP1B1</i> mutations (n= 132)	Patients without <i>CYP1B1</i> mutations (n= 169)		
1	-13T>C	T	0.18	0.39	0.001	1
		C	0.82	0.61		2.9 (1.5-5.6)
2	R48G	C	0.78	0.57	0.002	1
		G	0.22	0.43		0.4 (0.2-0.7)
3	A119S	G	0.78	0.57	0.002	1
		T	0.22	0.43		0.4 (0.2-0.7)
4	V432L	G	0.49	0.19	0.0001	1
		C	0.51	0.81		0.24 (0.13-0.5)
5	D449D	T	0.49	0.19	0.0001	1
		C	0.51	0.81		0.24 (0.13-0.5)
6	N453S	A	0.91	0.83	0.09	1
		G	0.09	0.17		0.5 (0.2-1.1)

**Table 4.18:** Genotype frequency distribution of *CYP1B1* SNPs in [CYP1B1 (+)] and [CYP1B1 (-)] cases

S. No	SNP	Genotype	Patients with <i>CYP1B1</i> mutations (n=132)	Patients without <i>CYP1B1</i> mutations (n = 169)	p value	ODDS RATIO (95% CI)
1	-13T>C	T,T	13 (9.8%)	36 (21.3%)	—	1
		T,C	21 (15.8%)	60 (35.5%)	0.94	0.9 (0.4-2.2)
		C,C	98 (74.2%)	73 (43.2%)	0.0001	3.7 (1.8-7.5)
2	R48G	C,C	91 (68.9%)	63 (37.3%)	—	1
		C,G	24 (18%)	70 (41.4%)	0.0001	0.2 (0.13-0.4)
		G,G	17 (12.8%)	36 (21.3%)	0.0006	0.3 (0.2-0.6)
3	A119S	G,G	91 (68.9%)	63 (37.3%)	—	1
		G,T	24 (18%)	70 (41.4%)	0.0001	0.2 (0.13-0.4)
		T,T	17 (12.8%)	36 (21.3%)	0.0006	0.3 (0.2-0.6)
4	V432L	G,G	52 (39.1%)	11 (6.5%)	—	1
		G,C	26 (19.5%)	44 (26.0%)	0.0001	0.13 (0.06-0.3)
		C,C	54 (40.9%)	114 (67.4%)	0.0001	0.1(0.05-0.2)
5	D449D	T,T	52 (39.1%)	11 (6.5%)	—	1
		T,C	26 (19.5%)	44 (26.0%)	0.0001	0.13 (0.06-0.3)
		C,C	54 (40.9%)	114 (67.4%)	0.0001	0.1(0.05-0.2)
6	N453S	A,A	113 (85.6%)	118 (69.8%)	—	1
		A,G	14 (10.5%)	45 (26.6%)	0.0005	0.3 (0.2-0.6)
		G,G	5 (3.8%)	6 (3.6%)	0.82	0.9 (0.3-2.9)

#### 4.2.7 *CYP1B1* involvement in PCG cases world wide

*CYP1B1* screening in the present study led to the identification of 33 mutations in 40.7% (90/221) cases, the details of which are provided in Tables 4.3 and 4.4. Combining our results with the previous study (Reddy *et al.*, 2003), *CYP1B1* mutations were identified in 43.8% (132/ 301) of PCG cases (Table 4.19).

**Table 4.19:** Distribution of PCG cases screened for *CYP1B1*

Study	Cases screened (n)	Cases with homozygous mutation (n, %)	Cases with heterozygous mutations (n, %)	Cases with compound heterozygous mutations (n, %)	Cases with no mutations (n, %)
Present study	221	(44, 20%)	(31, 14.0%)	(15, 6.8%)	(131, 59.3%)
Previous study (Reddy <i>et al.</i> , 2003)	80	(29, 36.3%)	(10, 12.5%)	(3, 3.8%)	(38, 47.5%)
Overall	301	(73, 24.3%)	(41, 13.6%)	(18, 5.9%)	(169, 56.1%)

##### 4.2.7.1 *Arg368His* – the prevalent mutation

Similar to the previous study (Reddy *et al.*, 2003), *Arg368His* was the most prevalent mutation identified in the present cohort (Table 4.20).

**Table 4.20:** Distribution of PCG cases with *Arg368His* mutation

Study	Cases with <i>Arg368</i> mutation (n, %)	Cases with homozygous mutant allele (n, %)	Cases with heterozygous mutant allele (n, %)	Cases with compound heterozygous mutant allele (n, %)
Present study	(42, 46.6%)	(18, 42.9%)	(16, 38.0%)	(8, 19.0%)
Previous study (Reddy <i>et al.</i> , 2003)	(21, 50%)	(16, 76.2%)	(2, 9.5%)	(3, 14.3%)
Overall	(63, 47.7%)	(34, 53.9%)	(18, 28.6%)	(11, 17.5%)

The patients with homozygous, heterozygous and compound heterozygous *Arg368His* mutations were compared with respect to different clinical parameters. No significant difference was observed among the patients from these three groups (Table 4.21).



**Table 4.21:** Comparison of clinical features among the patients with Arg368His mutation

<i>Parameters</i>	<i>H</i> ( <i>n=34</i> )	<i>CH</i> ( <i>n=11</i> )	<i>H</i> ( <i>n=18</i> )	<i>P value</i> ( <i>H vs CH</i> )	<i>P value</i> ( <i>H vs h</i> )	<i>P value</i> ( <i>CH vs h</i> )
Mean age at onset (in months)	0.09±0.38	1.09±3.6	4.7±9.8	0.113	0.008	0.25
Mean IOP at presentation	30±5.5	29.9±7.2	28.2±7.2	0.96	0.32	0.53
Mean IOP at final follow up	16.8±5.7	20.5±6.9	17.5±7.3	0.10	0.7	0.32
Mean corneal diameter at presentation	13.5±1.5	13.5±1.2	13.5±1.5	0.92	0.95	0.88

H= homozygous, CH= compound heterozygous, h= heterozygous

\*P values are based on the t test for two independent samples

The same clinical parameters were analyzed between cases with Arg368His mutations and those with other *CYP1B1* mutations. There were no significant differences between these two groups (Table 4.22).

**Table 4.22:** Comparison of the clinical features between the cases with and without Arg368His mutation

<i>Parameters</i>	<i>With Arg368His mutation</i>	<i>With other CYP1B1 mutations</i>	<i>P value</i>
Mean age at onset (in months)	1.7 ± 5.7 (n= 63)	1.5 ± 4.6 (n= 70)	P= 0.87
Mean IOP at presentation	29.2 ± 6.4 (n= 58)	30.2 ± 6.8 (n= 65)	P= 0.41
Mean IOP at final follow up	20.18 ± 15.5 (n=45)	18.1 ± 7.5 (n=47)	P=0.43
Mean corneal diameter at presentation	13.4±1.4 (n=49)	13.1±1.3 (n=61)	P=0.3

\*P values are based on the t test for two independent samples

### 4.3 GENOTYPE - PHENOTYPE CORRELATION BETWEEN *CYP1B1* MUTATIONS AND IOP

Genotype phenotype correlation determines the association of a certain mutation (genotype) with the clinical abnormality (phenotype). We used the positive predictive value (PPV) to determine the frequency of a certain phenotype in the

presence of a specific genotype. This correlation could help in the accurate prediction of prognosis and a better selection of therapeutic strategies for patients.

In the present study genotype-phenotype correlation was restricted to IOP in order to determine its association with the prognosis of the disease. Patients without an objective measurement of these traits were excluded.

#### 4.3.1. Comparison with respect to mean IOP

The patients were divided into two groups - cases with *CYP1B1* mutations [CYP (+)] and cases without *CYP1B1* mutation [CYP (-)]. The mean IOPs were compared between the groups that included the mean IOP at presentation and at different time intervals (Table 4.23). While there was no difference in the mean IOP at presentation, patients who had a follow up of up to 1 year, exhibited a significant difference ( $p= 0.04$ ) in [CYP (+)] group (mean IOP=  $18.0 \pm 8.2$ ) compared to [CYP (-)] group. This difference did not exist in patients with a follow up of more than one year (Table 4.23).

**Table 4.23:** The t-test analysis for [CYP (+)] and [CYP (-)] cases with respect to IOP

<i>Mean IOP (at different time periods)</i>	<i>With CYP1B1 mutation</i>	<i>Without CYP1B1 mutation</i>	<i>P value</i>
At presentation	29.7 $\pm$ 6.6 (n= 123)	28.6 $\pm$ 6.8 (n= 154)	P= 0.16
1 month - 1 year	18.0 $\pm$ 8.2 (n=28)	14.3 $\pm$ 5.5 (n=37)	P=0.04
1-2 years	18.2 $\pm$ 7.9 (n=18)	15.4 $\pm$ 9.2 (n=26)	P=0.29
2-4 years	19.5 $\pm$ 7.8 (n=22)	15.7 $\pm$ 6.9 (n= 31)	P=0.07
4-6 years	16.2 $\pm$ 7.0 (n=11)	15 $\pm$ 4.6 (n=14)	P=0.6
6-10 years	21.4 $\pm$ 6.8 (n=7)	15.4 $\pm$ 6.9 (n=8)	P=0.11
>10 years	22 $\pm$ 2.0 (n=3)	18.9 $\pm$ 8.9 (n=7)	P=0.6

In addition no significant difference ( $p=0.18$ ) was identified in the mean corneal diameter ( $13.25\pm 1.42$ ) of cases with *CYP1B1* mutations and cases without any mutation (mean corneal diameter=  $13.48\pm 1.3$ ) at presentation.

#### 4.3.2 Univariate Cox regression analysis

Univariate Cox regression analysis was done to determine the hazards probabilities of the IOP (Table 4.24). The IOP was taken as continuous variables (covariates) in the Cox regression model. First, the probabilities were calculated for all the patients as a single group. The hazards ratio for IOP at presentation was 1.05 for each unit increment of IOP suggesting it as a significant risk factor. The patients were then divided into two groups - [CYP (+)] and [CYP (-)] in order to determine the hazards probabilities of the factors with respect to *CYP1B1* mutations. It was observed that IOP at presentation was a significant risk factor ( $P= 0.007$ ) with the hazards ratio of 1.08 for each unit increment of IOP in the [CYP (+)] group.

**Table 4.24:** The Univariate Cox regression analysis for PCG cases

Parameters	Hazards ratio (95.0% CI)		
	Overall (including [CYP (+)] & [CYP (-)] cases)	With <i>CYP1B1</i> mutation [CYP (+)]	Without <i>CYP1B1</i> mutation [CYP (-)]
IOP at presentation	1.05 (1.02-1.09) P= 0.005 (n= 201)	1.08 (1.02- 1.15) P= 0.007 (n= 88)	1.03 (0.98 – 1.08) P = 0.26 (n=113)

#### 4.3.3 Survival analysis

Survival curve analysis was performed with respect to IOP using the data on patients who had a minimum follow up of one year ( $n=176$ ). These recordings at different time periods (at presentation, 1 month, 3 months, 6 months, 9 months and 1 year after the surgical intervention) were taken from the medical records of these patients.

The survival curves for the mentioned parameters were plotted using the SPSS software (version 14.0). Analysis of disease outcome was examined as prognosis of the disease with respect to IOP reduction, and was computed by the Kaplan-Meier product limit method. The difference between survivals in each group was evaluated by the log rank test. The plotted survival curves for IOP were different for the patients with *CYP1B1* mutations [CYP (+)] when compared to cases without any *CYP1B1* [CYP (-)] involvement (Fig 4.7). The [CYP (-)] group had higher cumulative survival probability (0.72) when compared to the [CYP (+)] group (0.56), which was found to be statistically significant ( $p= 0.038$ ). It also suggested that 66% ( $n=66/100$ ) of the patients without *CYP1B1* mutations had better prognosis of the disease in terms of IOP reduction on surgical intervention compared to 52.6% ( $n=40/76$ ) of the patients with *CYP1B1* mutations.

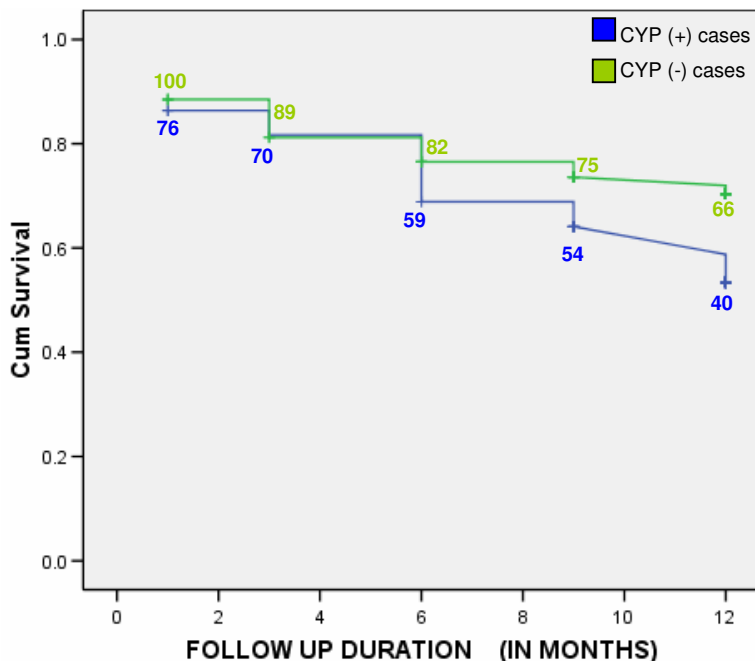


**Figure 4.7:** Survival curve analysis for IOP in [CYP (+)] and [CYP (-)] cases. The X-axis represents the follow up duration of patients whereas the cumulative survival probability is represented on Y-axis. The number of patients at various follow up periods is mentioned along with the respective time periods. The plotted survival curve shows that the cumulative survival probability of [CYP (+)] patients for IOP at the end of 12 months is 0.56 compared to 0.72 for [CYP (-)] patients.

---

## 4.4 SCREENING OF OTHER CANDIDATE GENES IN PCG

### 4.4.1 Mutational analysis of MYOC

*MYOC* screening revealed 5 variations (Table 4.25), which included two missense (Gln48His and Tyr479His) mutations (Fig 4.9) and three silent changes (Gly122Gly, Tyr347Tyr and Gly434Gly). The frequency of *MYOC* mutations was 4.3% (9/210) in the PCG cases. The electropherograms of all the variations identified in *MYOC* are shown in Fig 4.10. None of the unaffected normal controls (n=157) harbored these mutations. The details of the PCG families with *MYOC* mutations are mentioned below:

Gln48His: A heterozygous change from guanine to thymine at position g.804 resulted in the replacement of Glutamine by Histidine at codon 48. This mutation lies in the myosin-like domain of *MYOC* protein and was the most prevalent mutation observed in 3.8% (8/210) cases. One case (PCG095) was heterozygous for the *CYP11B1* mutant allele (Arg368His) and exhibited co-segregation of these two mutant alleles suggesting a possible digenic inheritance of *CYP11B1* and *MYOC* in PCG. None of the normal controls, screened by PCR based restriction digestion using *AccI* enzyme, harbored this mutation. The clinical features of the patients with Gln48His are mentioned in Table 4.25.

#### 4.4.1.1.1 Denaturing high performance liquid chromatography (dHPLC) for Gln48His

The Gln48His mutation was also confirmed by dHPLC. All the patients' samples with heterozygous Gln48His mutation showed the heteroduplex peak formation (Fig.4.8).

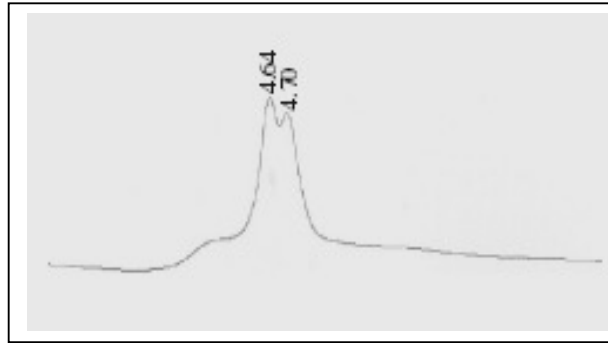


**Figure 4.8:** Heteroduplex peaks obtained in patients with heterozygous Gln48His mutation. The X-axis represents the elution time in minutes whereas the y-axis represents the signal intensity. The sample in the figure showed the heteroduplex peaks with the elution time of first peak at 4.64 minutes and second peak at 4.70 minutes, respectively.

Tyr479His: A novel heterozygous change from thymine to cytosine at position g.17267 resulted in the replacement of Tyrosine by Histidine at codon 479. This mutation lies in the olfactomedin – like domain of the protein and was identified in proband (PCG118) who did not harbor any *CYP1B1* mutation. So far, this mutation has not been reported from any other forms of glaucoma. However, it has been identified in an adult onset POAG case at our centre. None of the normal controls harbored this mutation. The proband with this mutation had bilateral manifestation of the disease since birth and presented with raised IOP and increased C:D ratio in her right eye at the age of 10 months and megalocornea in both the eyes. On surgery the IOP reduced to 10 mm of Hg but she had a visual acuity of 20/163 in both the eyes (Table 4.25).

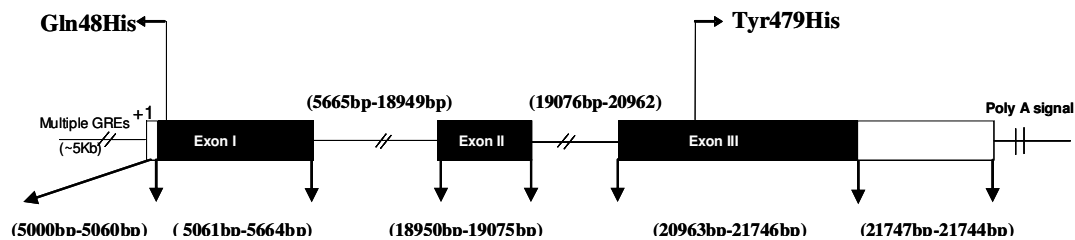


**Figure 4.9:** Schematic representation of the *MYOC* gene (Kubota *et al.*, 1998). The filled boxes represent the region coding for MYOC protein whereas the open boxes represent the untranslated portion of the gene. +1 designates the transcription initiation site. The mutations identified in the present study are indicated by arrows.

#### 4.4.1.6 Synonymous changes in *MYOC*

Apart from the missense mutations 4 silent changes [Gly122Gly (0.5%), Leu166Leu (0.5%), Gly434Gly (0.5%) and Tyr347Tyr (2.4%)] were also identified in *MYOC*. Since these variations were identified in a small proportion of the patients we did not check for their association with the disease phenotype.

**Table 4.25:** Clinical features of patients with *MYOC* mutations

Case ID	Onset	Age at intervention	Nucleotide change	Codon change	Amino acid change	Corneal diameter * OD;OS (mm)	IOP at presentation * OD;OS (mm of Hg)	IOP at final follow up * OD;OS (mm of Hg)	C:D ratio *OD;OS	VA at presentation *OD;OS	VA at final follow up *OD;OS	Treatment
028	Since birth	1 year	g.804 G>T	CAG>CAT	Gln48His	12.5 ; 12.5	24 ; 24	10 ;10	NA;NA	FFL; FFL	FFL; FFL	TRAB & TRAB (OU)
038	Since birth	9 years#	g.804 G>T	CAG>CAT	Gln48His	13.5 ;14	12 ;20	15 ;15	0.3 ; NA	FFL;FFL	20/20 ; 20/50	TRAB & TRAB (OS)
085	4 months	2 years	g.804 G>T	CAG>CAT	Gln48His	13; 15	26 ;12	16 ; 8	No cupping; WNL	FFL; FFL	FFL; FFL	TRAB & TRAB (OD)
095	Since birth	2 years	g.804 G>T	CAG>CAT	Gln48His	12 ;12	38 ;36	32 ;10	0.4; 0.3	FFL; FFL	CF ; PLPR	TRAB & TRAB (OU)
106	6 months	2 years	g.804 G>T	CAG>CAT	Gln48His	15;14	28;26	14;12	0.9;0.9	FFL; FFL	PLPR+; PLPR+	TRAB with mitomycin (OU) somewhere outside LVPEI
278	Since birth	2 months	g.804 G>T	CAG>CAT	Gln48His	13;13	32;28	22;22	Disc excavation ; disc excavation	FL ; FL	20/960; 20/960	TRAB & TRAB (OU)
330	Since birth	1 year	g.804 G>T	CAG>CAT	Gln48His	15;13	26;12	26;10	0.9;0.4	20/630 ; 20/630	NA;NA	Trab (OD)
376	Since birth	3 months	g.804 G>T	CAG>CAT	Gln48His	14;19	14;30	12;12	0.3;No View	20/310; 20/310	FFL; FFL	TRAB outside LVPEI (OU); TSCPC (OS) at LVPEI
118	2 months	10 months	g.17267 T>C	TAC>CAC	Tyr479His	15;13.5	30;22	10;10	0.5;0.2	FFL; FFL	20/163; 20/163	TRAB & TRAB (OU)

# Diagnosed elsewhere and came to our centre for further management; OU-both eyes, VA- visual acuity; CF- counting fingers, PLPR-perception and projection of light, FFL-fixing and following light, FL-follows light TRAB and TRAB-trabectomy and trabeculotomy, TSCPC-transcleral cyclophotocoagulation, NA-not available, WNL-within normal limits

\* OD-right eye, OS-left eye; *MYOC* (Ensembl Human Gene :ENSG00000034971) ([http://www.ensembl.org/Homo\\_sapiens/geneseqview?db=core;gene=ENSG00000034971](http://www.ensembl.org/Homo_sapiens/geneseqview?db=core;gene=ENSG00000034971))



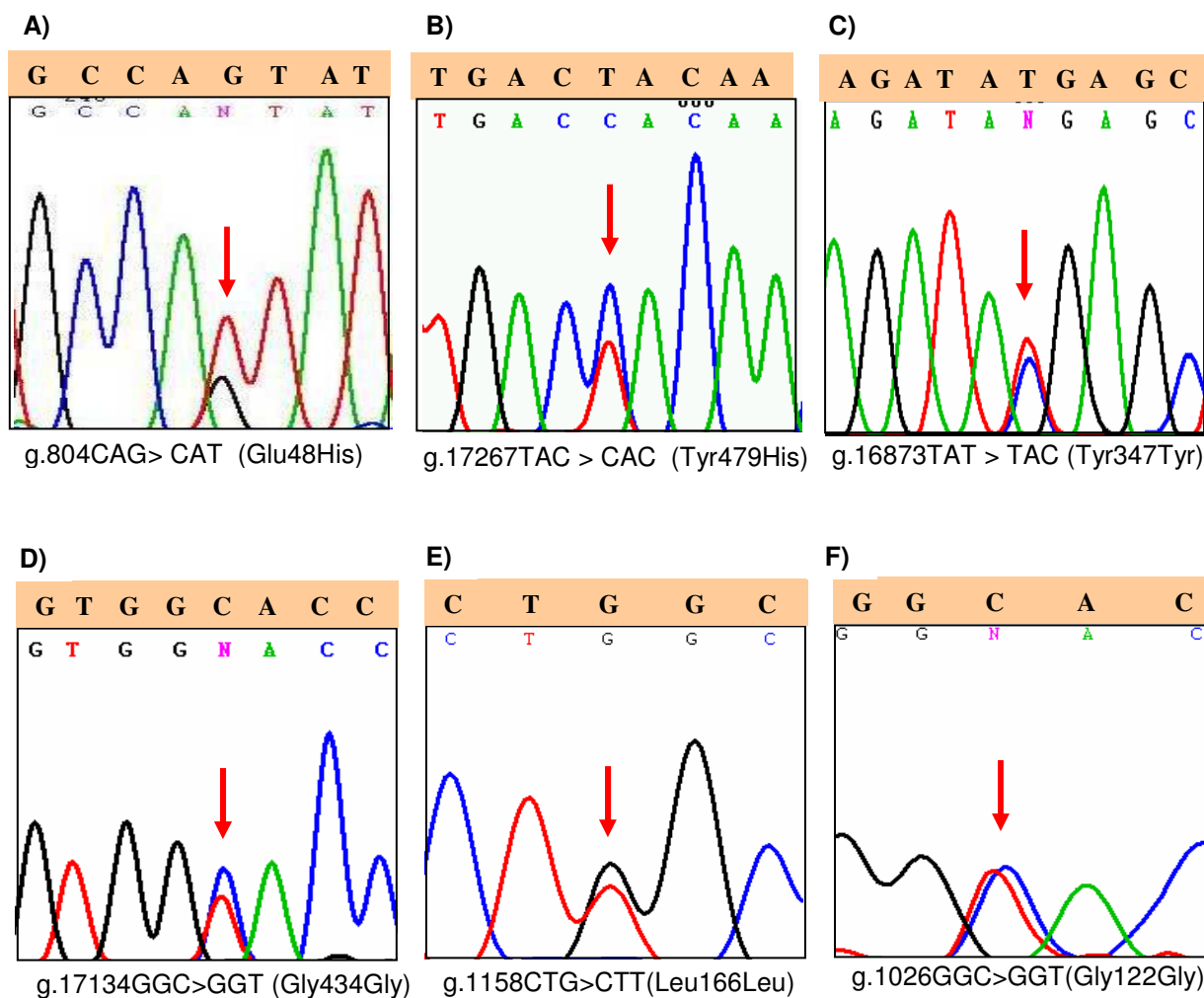


**Figure 4.10:** Electropherograms showing the six *MYOC* variations found in PCG cases. The shaded portions above the electropherograms represent the wild type sequences. The arrow head indicates the site of change. **A)** A heterozygous substitution of CAG> CAT at g.804, resulted in the Gln48His mutation. **B)** A heterozygous substitution of TAC>CAC at g.17267, resulted in the Tyr 479 His mutation. **C)** A heterozygous substitution of TAT>TAC at g.16873, resulted in the synonymous change (Tyr>Tyr) at codon 347. **D)** A heterozygous substitution of GGC>GGT at g.17134, resulted in the synonymous change (Gly>Gly) at codon 434. **E)** A heterozygous substitution of CTG>CTT at g.1158, resulted in the synonymous change (Leu>Leu) at codon 166. **F)** A heterozygous substitution of GGC>GGT at g.1026, resulted in the synonymous change (Gly>Gly) at codon 122.

#### 4.4.1.5 Conservation of the residues

Multiple sequence alignment of MYOC across different species indicated a high degree of conservation for the Glutamine (Q) residue and Tyrosine (Y) residues at codons 48 and 479, respectively (Fig. 4.11.)

	Gln48His ↓	Tyr479His ↓
Mouse MYOC	SGRC <b>Q</b> YTF--	MID <b>Y</b> NPL-- 490
Rat MYOC	SGRC <b>Q</b> YTF--	MVD <b>Y</b> NPL-- 502
Chimpanzee MYOC	SGRC <b>H</b> YTF--	MID <b>Y</b> NPL-- 461
<b>Human MYOC</b>	SGRC <b>Q</b> YTF--	MID <b>Y</b> NPL-- 504
Macaque MYOC	SGRC <b>Q</b> YTF--	MID <b>Y</b> NPL-- 491
Cat MYOC	SGRC <b>Q</b> YTF--	MVD <b>Y</b> NPL-- 498
Microbat MYOC	SGRC <b>Q</b> YTF--	-----
Dog MYOC	SGRC <b>Q</b> YIF--	MID <b>Y</b> NPL-- 497
Xenopus MYOC	SGQC <b>T</b> YSF--	MID <b>Y</b> NPT-- 484
Zebrafish MYOC	NGRC <b>Q</b> YTF--	MVD <b>Y</b> NSA-- 474

**Figure 4.11:** Multiple sequence alignment of human MYOC protein with MYOC protein of 10 different species. The human MYOC protein is underlined. The wild type residues at position 48 and 479 are blocked.

---

#### 4.4.1.3 Segregation of MYOC mutations in PCG families

The segregation of Gln48His mutation in 8 families was determined by PCR based restriction digestion using *AccI* enzyme (Fig. 4.12). The segregation pattern of Gln48His in four PCG families is shown in Fig 4.10. In PCG 028 family, the proband (P1) inherited the mutant allele from her mother (M1) whereas father (F1) harbored the normal allele; in the PCG 038 family, the mother (M2) harbored the normal alleles while father's (F2) DNA sample was unavailable for analysis. In the PCG095 family, the proband (P3) inherited the mutant allele from his father (F3) whereas mother (M3) and proband's sibling (S3) harbored normal alleles. In the PCG 085 family, the parents (M4 and F4) did not harbor the mutant allele indicating a possible *de novo* origin of the mutation in the proband, transmitted through the germline of one of the parents (Fig. 4.10). The probability of a disputed parentage was ruled out by screening the parents and the proband with 16 polymorphic microsatellite markers chosen randomly from chromosomes 1 (DIS450, DIS2890, D1S484 and D1S196), 2 (D2S165, D2S391, D2S337 and D2S126), 3 (D3S1304, D3S1277, D3S1267 and D3S1271), and 4 (D4S412, D4S391, D4S1575, and D4S415) of ABI Prism Linkage mapping set MD-10 panel (version 2.5). In PCG106 and PCG330 families, the probands inherited the mutant allele from their mother, whereas, in PCG278 and PCG376 families, the father was the carrier of the mutant allele. All the parents were unaffected without any signs of glaucoma at presentation. Since Gln48His mutation has been reported in JOAG and POAG cases (Table 2.11) where it was attributed to cause open angle glaucoma through an autosomal dominant transmission. The same could be applied to the PCG families (PCG28, PCG106, PCG278, PCG330 and PCG376) in the present study where all the carrier parents could be the possible suspects of POAG. It could be due

to the recessive mode of inheritance in PCG in these families. The disease manifestation only in the probands could be due to some of the genes that are yet to be characterized.

The segregation of Tyr479His mutation in PCG118 was done by bi-directional sequencing. The proband inherited the mutated allele from his father whereas his mother had both copies of the normal allele. Both the parents were normal without any signs of glaucoma at presentation. As discussed in Gln48His mutation the similar scenario is possible in the carrier father.

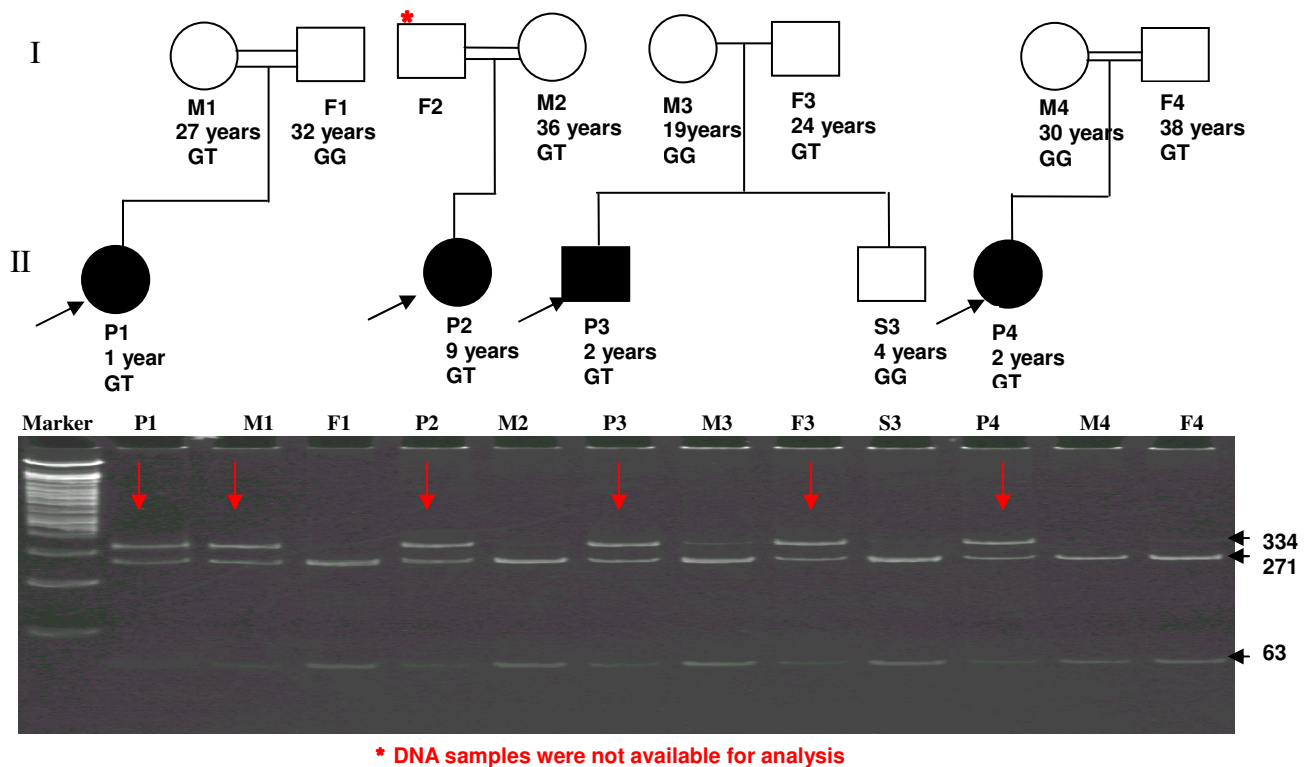


**Figure 4.12:** The segregation of Gln48His mutation in four PCG families by PCR based restriction digestion on a 9% polyacrylamide gel. The filled symbols (circles and squares) indicate the affecteds and the open symbols indicate the normal individuals. The individuals in the pedigree are designated by the letters, which correspond to the lanes in the gel. The ages and genotypes of individuals are shown below their individual letters. The fragments sizes are indicated on the right side of the gel. The heterozygous Gln48His mutation abolished a restriction site for *AccI* enzyme generating three fragments of 334bp, 271bp and 63bp (marked by arrowheads). The wild type presented with two fragments of 271bp and 63bp. The “Marker” represents the 100 bp DNA ladder (GeneRuler™, MBI Fermentas, Lithuania).

---

#### ***4.4.1.4 Digenic inheritance of CYP1B1 and MYOC in PCG***

In PCG095 family, the proband was found to be a carrier of both *CYP1B1* (Arg368His) and *MYOC* (Gln48His) mutant alleles (Fig.4.13). He inherited the Gln48His mutant allele from his father and the Arg368His mutant allele from his mother, whereas, the proband's sibling did not carry either of the two mutant alleles. Both the parents and proband's sibling were unaffected without any signs of glaucoma at presentation. However, as discussed above, the proband's father, who was 24 years of age at the time presentation, could be a suspect of POAG due to the involvement of Gln48His mutation in open angle glaucomas through dominant mode of inheritance. The segregation of the mutations was determined by PCR based restriction digestion using *AccI* and *TaaI* enzymes for Gln48His and Arg368His, respectively (Fig.4.12).

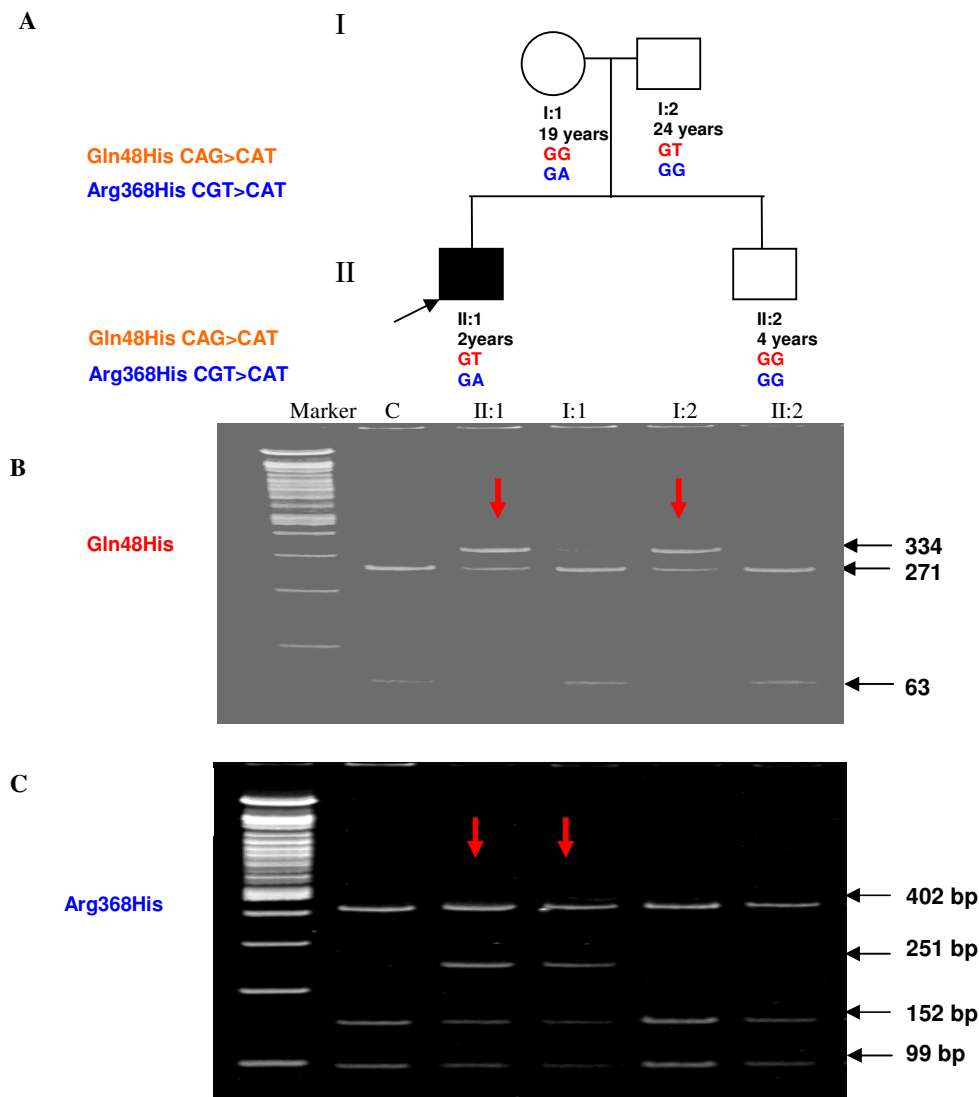


**Figure 4.13:** The segregation of *CYP11B* and *MYOC* mutation in PCG095 family by PCR based restriction digestion on a 9% polyacrylamide gel. The proband was heterozygous for both Gln48His and Arg368His mutation (**A**). The proband inherited the Gln48His mutation from his father and Arg368His mutation from his mother, respectively (**A**). The age and genotype of the individuals are shown below their individual IDs (**A**). The segregation analysis of Arg368His and Gln48His was done by PCR based restriction digestion using *TaaI* and *AccI* enzymes, respectively. The heterozygous Gln48His mutation abolished a restriction site for *AccI* enzyme generating three fragments (334bp, 271bp and 63bp, marked by arrowheads) in proband (II:1) and his father (I:1) as shown in **B**. The wild type presented with two fragments of 271bp and 63bp as seen in mother (I:2) and the control (C) sample (gel image **B**). Similarly, the heterozygous Arg368His mutation abolished a restriction site for *TaaI* generating four fragments (402bp, 251bp, 152bp and 99bp) in the proband (II:1) and his mother (I:1) in the gel image **C**. The wild type allele presented with three fragments (402bp, 152bp and 99 bp) in the father (I:2), sibling (II:2) and control (C) as seen in gel image **C**. The “Marker” represents the 100 bp DNA ladder (GeneRuler™, MBI Fermentas, Lithuania)

#### 4.4.2 Mutation analysis of *FOXC1*

The *FOXC1* gene was also screened in 210 PCG cases unlinked to *CYP11B1* (Table 4.19). Five novel heterozygous *FOXC1* variations were identified in 2.4% (5/210) PCG families. Two of these were missense (His128Arg, and Cys135Tyr), 2 frameshift (g.1086delC and g.1947dup25) and one deletion (g.1155delAAA) (Table 4.26 and Fig. 4.14). Four mutations (His128Arg, Cys135Tyr, g.1086delC and g.1947dupTCAGCCTGGACGGTGCGGATTCCGC) were not identified in the unaffected control (n=157), but the g.1155delAAA was observed in three controls who did not exhibit any signs of glaucoma at presentation.

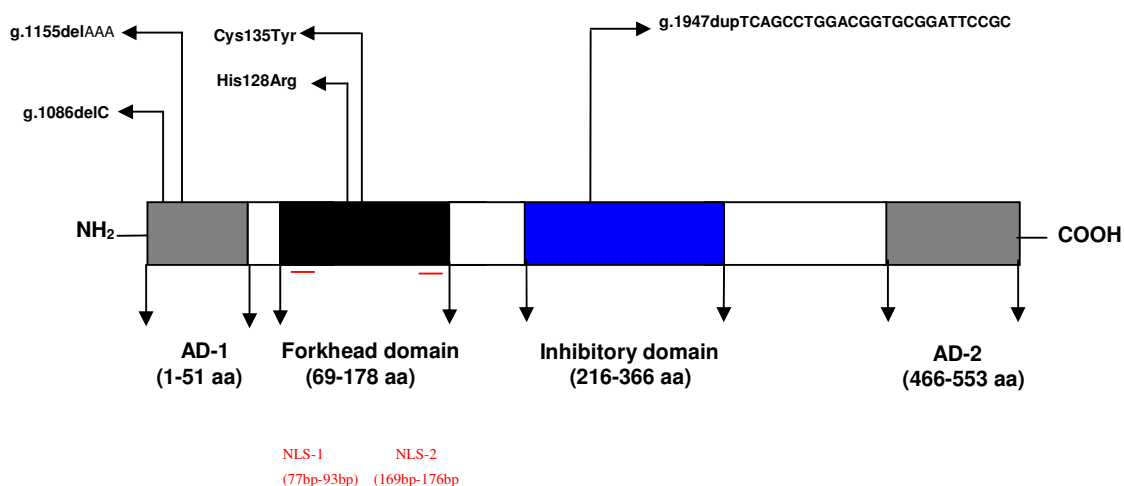


**Figure 4.14:** Schematic representation of the different domains of *FOXC1* protein. The mutations identified in the present study are indicated by arrows. AD-1: activation domain -1, AD-2: activation domain-2, NLS-1: nuclear localization signal 1, NLS-2: nuclear localization signal 2.

##### 4.4.2.1 *FOXC1* mutations identified in PCG

His128Arg: A heterozygous change from adenine to guanine at position g.1457 resulted in the replacement of Histidine by Arginine at codon 128 (Fig.4.15). The His128Arg mutation lies in the Forkhead domain of *FOXC1* protein and was identified in a

---

proband (PCG209) who did not harbor any *CYP1B1* or *MYOC* mutation. The proband had bilateral manifestation of disease since birth and presented with raised IOP and megalocornea and increased C:D ratio (0.9). On surgery the IOP was found to be <21 mm of Hg and he had a visual outcome of 20/130 in both the eyes (Table 4.27).

Cys135Tyr: A heterozygous change from guanine to adenine at position g.2713 resulted in the replacement of Cysteine by Tyrosine at codon 135 (Fig.4.15). The Cys135Tyr mutation lies in the Forkhead domain of FOXC1 protein and was identified in a proband (PCG216), who did not harbor any *CYP1B1* or *MYOC* mutation. The proband had the bilateral manifestation of the disease. He was diagnosed elsewhere and was under treatment. He came to our centre for further management and presented with raised IOP (37 mm of Hg and 40 mm of Hg in the right eye and left eye, respectively), megalocornea (15 mm in both eyes) and increased C:D ratio (0.9:1 in both eyes) at the age of 9 years. The proband had poor prognosis on surgery with raised IOP (30 mm of Hg and 22 mm of Hg in the right and left eye, respectively) and visual acuity of counting fingers in both the eyes (Table 4.27).

g.1086delC: A heterozygous deletion of a single base (C) at position g.1086 resulted in a frame shift after codon 4 and premature termination after 39 amino acids at codon 44 (Fig.4.16). The mutation lies in the AD -1 of the protein and was identified in a proband (PCG100). The proband had bilateral manifestation of the disease since birth and presented with IOP of 22 mm of Hg at the age of 4 months. The IOP in his left eye was elevated at his final presentation (40 mm of Hg) after surgery. However, it reduced to 16 mm of Hg in the right eye. The visual acuity was 20/60 and perception and projection of light in the right and left eye, respectively (Table 4.27). The proband was also heterozygous for a *CYP1B1* mutation (Arg368His).



g.1155delAAA: A heterozygous deletion of 9 bases (CGCGGCGGC) at position g.1155 resulted in the deletion of three alanine residues at codon 28 (Fig.4.16). The mutation lies in the AD -1 of the protein and was identified in a proband (PCG196), who had unilateral manifestation of the disease since birth. She was diagnosed elsewhere and was under treatment. He came to our centre for further management and presented with raised IOP and total cupping at the age of 5 years. The proband is under medication and presently his IOP is reduced to 20 mm Hg and 16 mm Hg in the right and left eye, respectively. There was total cupping (0.9:1) in the glaucomatous eye with a visual acuity of light perception of (Table 4.27). The proband was also heterozygous for a *CYP1B1* mutation (Arg368His).

g.1947dupTCAGCCTGGACGGTGCGGATTCCGC: A heterozygous duplication of 25 bases (TCAGCCTGGACGGTGCGGATTCCGC) at position g.1947 resulted in a frame shift at codon 291 and premature termination after 22 amino acids at codon 313 (Fig.4.16). The mutation lies in the inhibitory domain of the protein and was identified in a proband (PCG044). He had bilateral manifestation of the disease and presented with raised IOP and megalocornea at the age of 2 months. He had a good prognosis with reduced IOP and a visual acuity of 20/20 in both the eyes on surgery (Table 4.27).

**Table 4.26:** Distribution of *FOXC1* gene variations in PCG

	<i>Genomic DNA position</i>	<i>Codon change</i>	<i>Effect on protein</i>	<i>SIFT Score</i>	<i>Affect on protein</i>	<i>Frequency in patients (N=210)</i>	<i>Frequency in controls (n=157)</i>
1	g.1457 A>G	CAC>CGC	His128Arg	0.00	Affect protein function	1 (0.5)	0
2	g.1478 G>A	TGC>TAC	Cys135Tyr	0.02	Affect protein function	1 (0.5)	0
3	g.1086delC	Frameshift after codon 4	Stop 39 amino acids downstream at codon 44	_____	_____	1 (0.5)	0
4	g.1155del9 (CGCGCCGGC)	AAA 28del		_____	_____	1 (0.5)	3 (1.9%)
5	g.1947dup25 (TCAGCCTGGACGGTGCGGATTCCGC)	Frameshift after codon 291	Stop 22 amino acids downstream at codon 313	_____	_____	1 (0.5)	0

*FOXC1* (Ensembl Human Gene : ENSG00000054598)

([http://www.ensembl.org/Homo\\_sapiens/geneseqview?db=core;gene=ENSG00000054598](http://www.ensembl.org/Homo_sapiens/geneseqview?db=core;gene=ENSG00000054598))

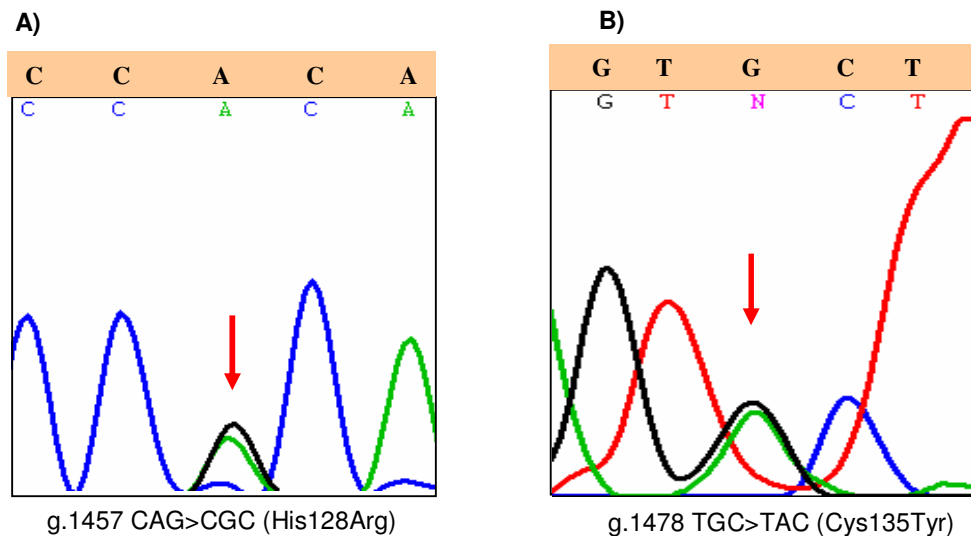


**Figure 4.15:** Electropherograms showing the two missense mutations observed in *FOXC1*. The sequence above the electropherogram in the shaded portion represents the wild type sequence. The nucleotide change is indicated by an arrowhead. **A)** A heterozygous substitution of CAC>CGC at g.1457, resulted in the Histidine to Arginine substitution at codon 128. **B)** A heterozygous substitution of TGC>TAC at g.1478, resulted in the Cysteine to Tyrosine substitution at codon 135.

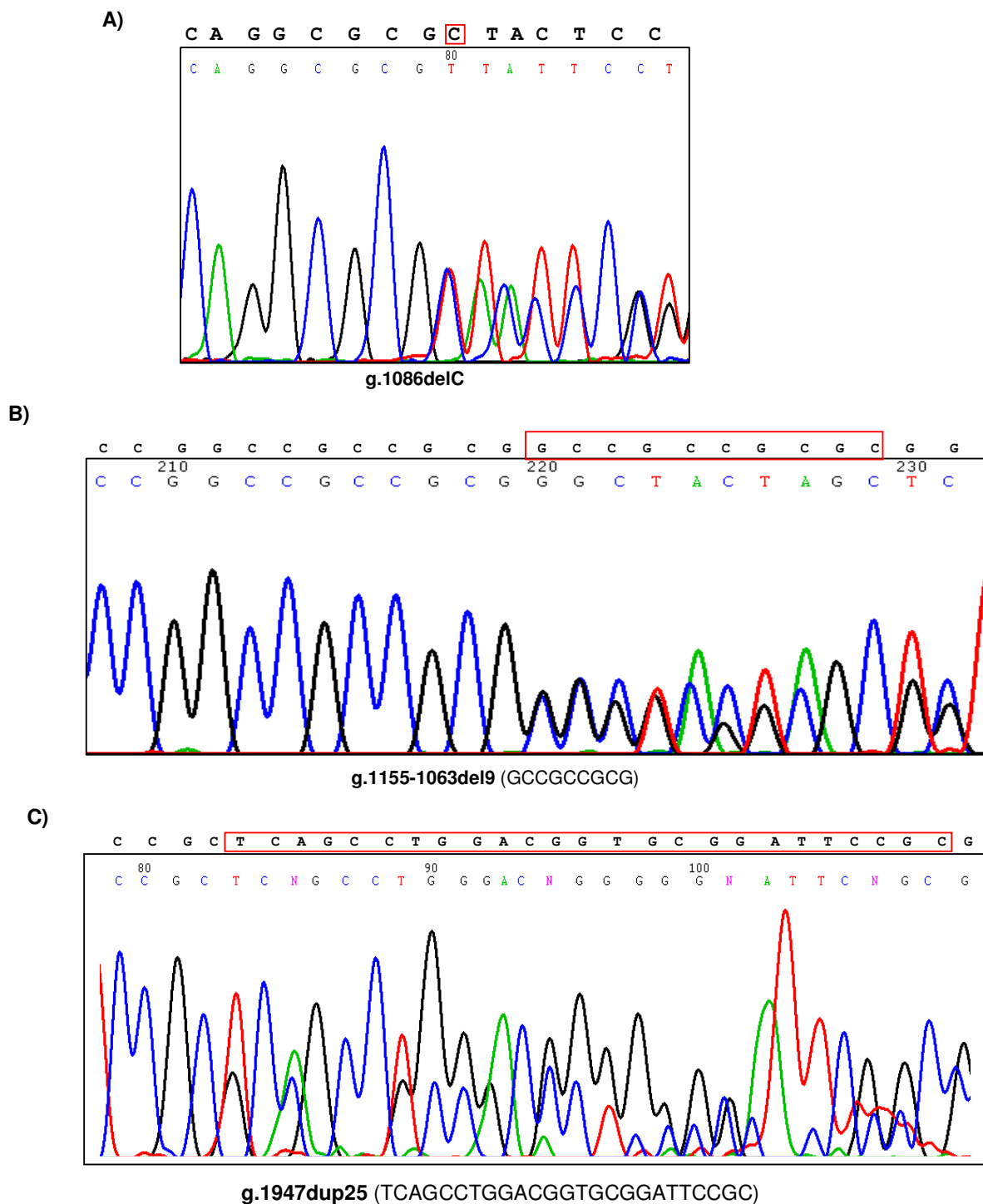


**Figure 4.16:** Electropherograms showing the two frameshift mutations (g.1086delC and g.1947dup TCAGCCTGGACGGTGCGGATTCCGC) and in-frame deletion (g.1155delAAA) identified in *FOXC1*. The deleted or duplicated bases are boxed. **A)** A heterozygous deletion of a single base (C) at g.1086 position. **B)** A heterozygous deletion of 9 bases (GCCGCCGCG) at position g.1155-g.1163. This was the reverse strand **C)** A heterozygous duplication of 25 bases (TCAGCCTGGACGGTGCGGATTCCGC) at position g.1947.

**Table 4.27:** Clinical features of patients with *FOXC1* mutations

<i>Patient ID</i>	<i>Age at onset</i>	<i>Age at intervention</i>	<i>Mutation</i>	<i>IOP at presentation</i> *OD ; OS (mm of Hg)	<i>IOP at final follow up</i> *OD ; OS (mm of Hg)	<i>C:D ratio at presentation</i> *OD ; OS	<i>Corneal diameter</i> *OD ; OS (mm)	<i>Visual outcome at presentation</i> *OD ; OS	<i>Visual outcome at final follow up</i> *OD ; OS	<i>Treatment</i>
PCG209	Since birth	5 years#	His128Arg	32;30	<21;<21	0.9; 0.9	12;13	20/40; 20/40	20/130; 20/130	TSCPC (OU)
PCG216	Since birth	9 years#	Cys135Tyr	37; 40	30; 22	0.9; 0.9	15; 15	20/80; 20/80	CF; CF	TSCPC (OU)
PCG100	Since birth	4 months	g.1086delC	22; 22	16; 40	0.3; 0.3	10.5; 11	FL; FL	20/60; PL+, PR inaccurate	TRAB & TRAB (OU)
PCG196	Since birth	7 months	g.1155delAAA	40; 18	20;16	0.9;0.4	NA	PL+; 20/20	PL+; 20/40	Medication (OU)
PCG044	1 month	2 months	g.1947dup TCAGCCTGGACGGTGCCGATTCCGC	22; 22	12; 10	0.3; 0.3	12; 11.5	NFFL; NFFL	20 / 20; 20 / 20	TRAB & TRAB (OU)

#Diagnosed elsewhere and came to our centre for further management at the age mentioned; TRAB – Trabeculectomy; TRAB & TRAB - Trabeculectomy & Trabeculectomy; OU – both eyes; CF- counting fingers; FL- follows light; NA- not available; PLPR- perception and projection of light, NFFL- not fixing and following light, TSCPC- trans-scleral cyclophotocoagulation

\*OD- right eye; OS- left eye

#### ***4.4.2.2 Segregation of FOXC1 mutations***

His128Arg: The segregation analysis of this mutation was determined by resequencing (Fig.4.17). None of the parents carried the mutant allele suggesting the possible *de novo* origin of this mutation in the proband.

Cys135Tyr: The genetic analysis of this mutation was determined by PCR based restriction digestion using *RsaI* enzyme (Fig.4.18). Both the parents were normal for this change suggesting a possible *de novo* origin of this mutation in the proband.

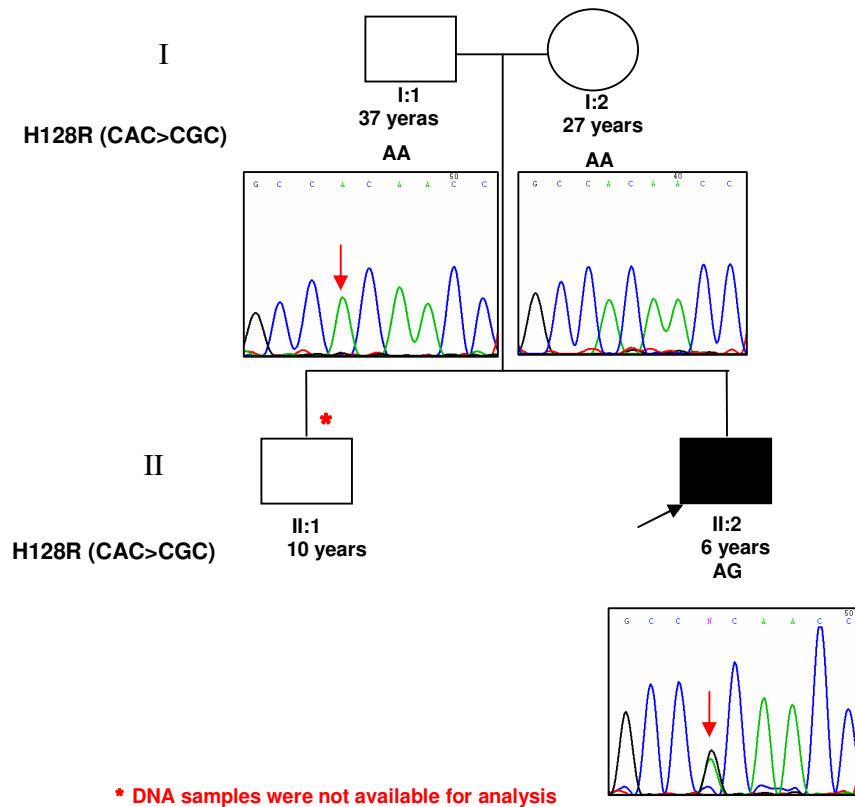


**Figure 4.17:** The *FOXC1* missense (His128Arg) mutation in PCG209 family. The segregation of the His128Arg mutation was determined by resequencing. The proband (II:2) was heterozygous for the mutation, whereas both father (I:1) and mother (I:2) were normal for the variation. DNA sample from the undiagnosed sib (II:1) was not available for analysis (marked by asterisk). The ages of the individuals and genotypes are indicated below their symbols.

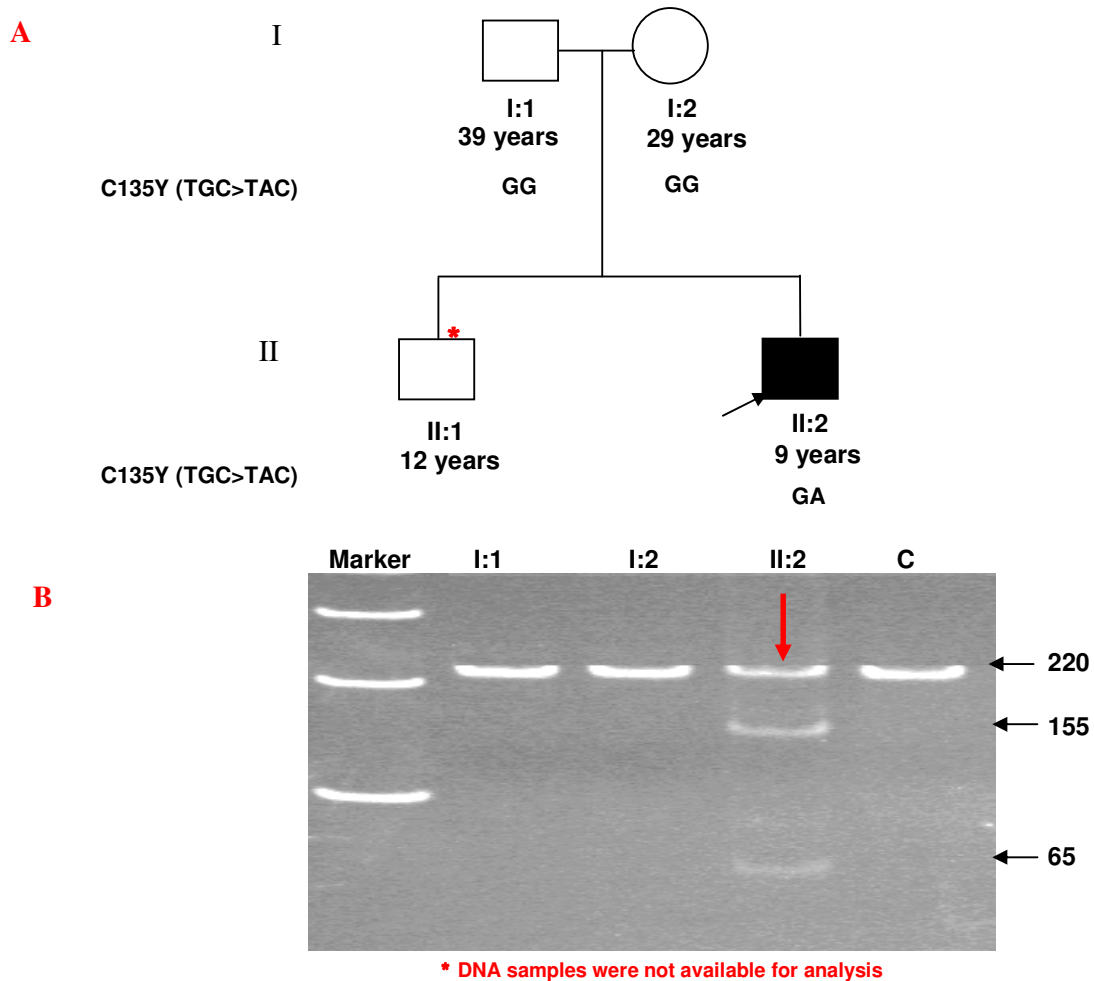
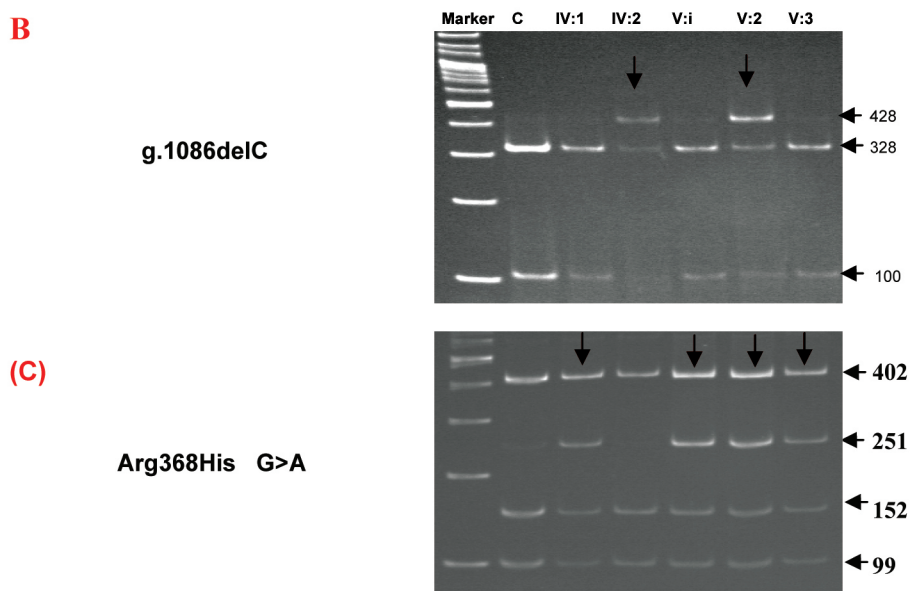
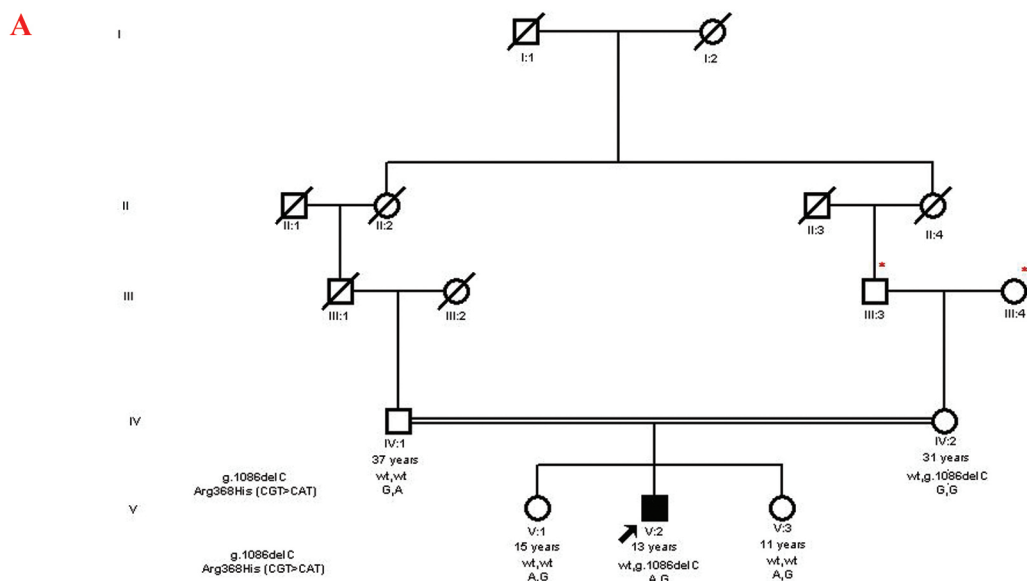


**Figure 4.18:** The *FOXC1* missense (Cys135Tyr) mutation in PCG216 family. The proband (II:2) was heterozygous for the mutation, whereas both father (I:1) and mother (I:2) were normal for the variation. DNA sample from the undiagnosed sib (II:1) was not available for analysis (marked by asterisk). “C” represents a normal unaffected control sample. The ages and genotypes of the individuals are indicated below their symbols (A). The genetic analysis of the Cys135Tyr mutation was done by PCR-based restriction digestion. The heterozygous Cys135Tyr mutation created a site for *RsaI* and generated 2 fragments of 155 and 65 bp along with the undigested PCR amplicon in the proband.(P in gel image B). The wild type allele remained undigested as seen in the unaffected father (I:1), mother (I:2) and the normal subject (C) in gel image B). The Marker represents the 100 bp DNA ladder, (GeneRuler™, MBI Fermentas, Lithuania).



g.1086delC: The segregation of this mutation in family PCG100 was done by PCR based restriction digestion using *PauI* and *TaaI* enzymes for g.1086delC and Arg368His mutations, respectively (Fig.4.19). The proband was found to be a carrier of both *CYP1B1* (Arg368His) and *FOXC1* (g.1086delC) mutant alleles and inherited the *FOXC1* mutation from his mother and *CYP1B1* mutation from his father. His mother was diagnosed to have optic atrophy, superior oblique palsy with raised IOP. The IOP was 34 mm of Hg and 17 mm of Hg with the C:D ratio of 0.9 and 0.6 in the right and left eye, respectively. Both the siblings of proband and his father were carriers of Arg368His allele and did not manifest any signs of glaucoma at presentation.



\* DNA samples were not available for analysis

**Figure 4.19:** The segregation of g.1086delC mutation in *FOXC1* in PCG 100 family by PCR based restriction digestion on a 9% polyacrylamide gel. The proband was heterozygous for both g.1086delC and Arg368his mutation. The present age and genotypes of the individuals are mentioned below their symbols (A). The proband inherited the g.1086delC mutation from his mother and Arg368His mutation from his father, respectively (as shown in A). The segregation of g.1086delC and Arg368His mutations was determined by PCR based restriction digestion using *PauI* and *TaaI* enzymes, respectively. The heterozygous g.1086delC mutation abolished a restriction site for *PauI* generating three fragments (428bp, 328bp and 100bp) in proband (V:2) and his mother (IV:2). The wild type allele generated two fragments (328bp and 100bp) in father (IV:1), two siblings (V:1 and V:3) and the control sample (C) as seen in gel image B. Similarly, the heterozygous Arg368His mutation abolished a restriction site for *TaaI* enzyme generating 4 fragments as described in gel image C). The “Marker” represents the 100 bp DNA ladder (GeneRuler™, MBI Fermentas, Lithuania).

g.1947dupTCAGCCTGGACGGTGCGGATTCCGC: The segregation analysis of this mutation was determined by PCR based restriction digestion using *Hin6I* enzyme (Fig 4.20). The proband's father did not harbor the mutation whereas his mother's and sibling's DNA samples were not available for analysis.

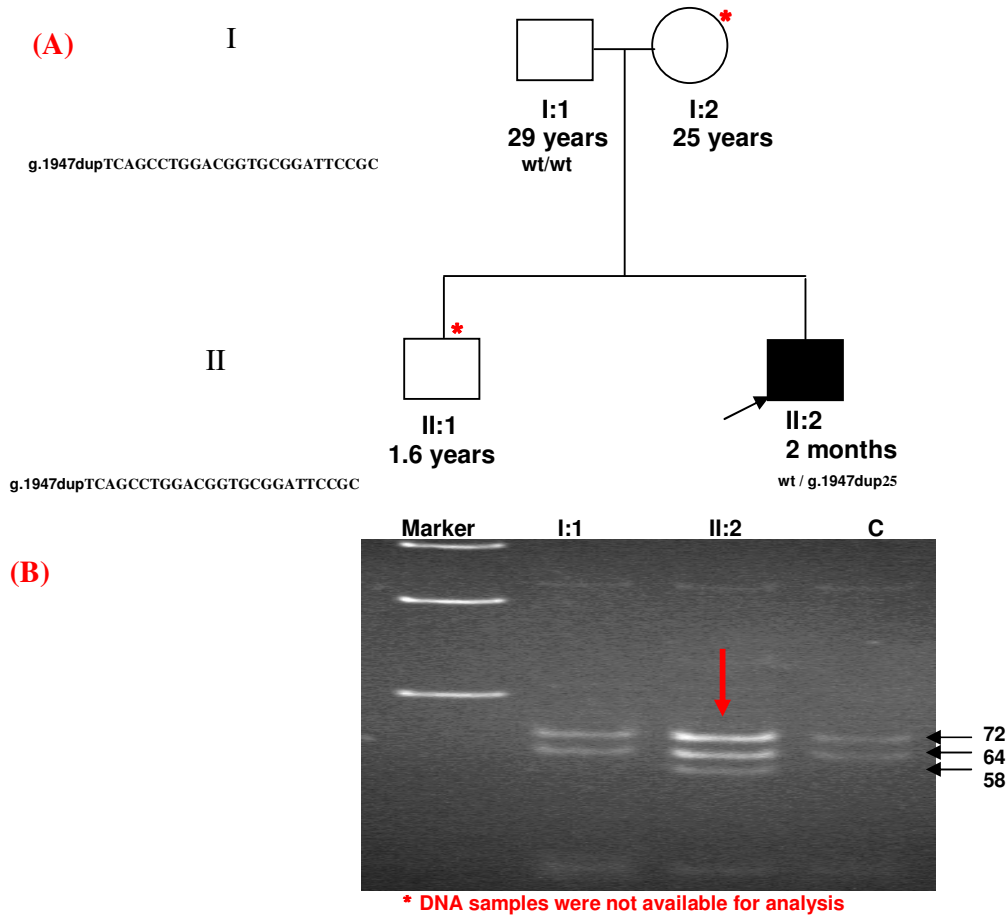


**Figure4.20:** Genetic analysis of a *FOXC1* frameshift (g.1947dupTCAGCCTGGACGGTGCGGATTCCGC) mutation in PCG044 family. The proband (II:2) was heterozygous for the mutation whereas father (I:1) harbor normal alleles. DNA samples from mother (I:2) and sibling (II:1) were not available for analysis (marked by asterisk). The age and genotype of the individuals are indicated below their symbols (A). The “C” in the gel represents a normal control. The g.1947dup25 mutation was screened by PCR-based restriction digestion on 15 % polyacrylamide gel. The heterozygous g.1947dup25 mutation resulted in the creation of a restriction site for *Hin6I* and generated four fragments of 72 bp, 64 bp, 58 bp and 15 bp in the proband (II:2 in gel image B). The wild type presented with 4 fragments of 72 bp, 64 bp, 33 bp and 15 bp as seen in the father (I:1) and the normal control (C in gel image B). The 33bp and 15 bp fragments were not visible on the gel. The Marker represents the 100 bp DNA ladder (GeneRuler™, MBI Fermentas, Lithuania).

g.1155delAAA: The segregation of this mutation was determined by PCR based restriction digestion using *NotI* enzyme (Fig.4.21). Both the parents of the proband along with a younger sib carried the mutation. The proband was also heterozygous for Arg368His and inherited the mutation from his mother while his father and sib were normal for this change. This mutation was identified in three unaffected controls (1.9%), of which two were diagnosed to have senile cataract without any signs of glaucoma at presentation.

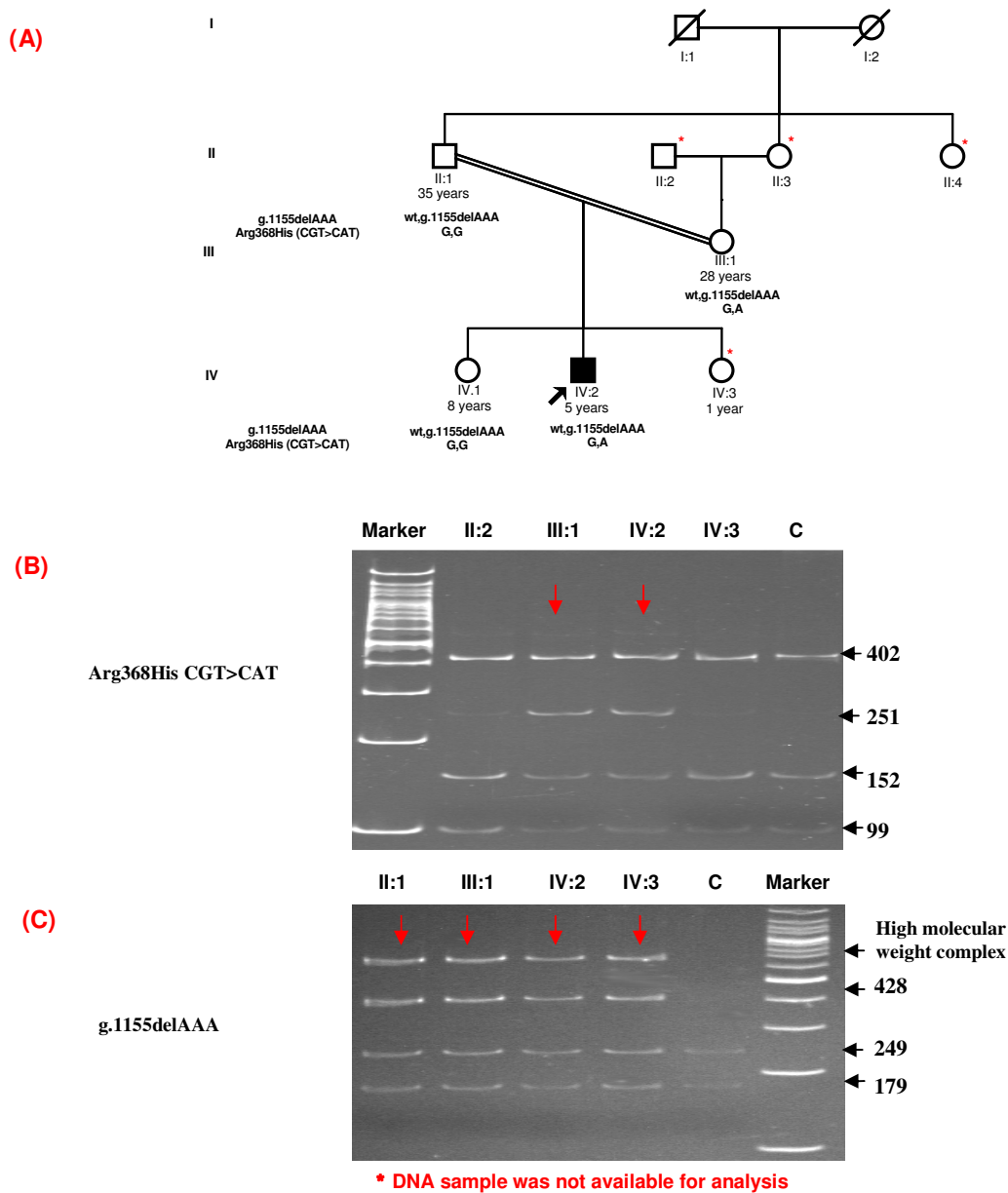


**Figure 4.21:** Segregation of a *FOXC1* (g.1155delAAA) mutation in PCG196 family. The proband was heterozygous for both g.1155delAAA and Arg368His mutation. Both the parents and the younger sibling were also heterozygous for g.1155delAAA (A). The present ages and genotypes of the individuals are mentioned below their symbols. The proband inherited the Arg368His mutation from his mother as shown in gel image (B). The segregation of Arg368His and 1155-1163del9 mutations were determined by PCR based restriction digestion using *TaaI* and *NotI* enzymes, respectively. The heterozygous Arg368His mutation abolished a restriction site for *TaaI* enzyme generating the fragments as described in gel image (B). Similarly, the heterozygous 1155delAAA variation abolished a site for *NotI* enzyme and generated three fragments of 428, 249 and 179bp in all the family members (IV:2, II:1, III:1 and IV:3) as shown in the gel image (C). The wild type allele presented with two fragments of 249bp and 179bp [gel image (C)]. An artifactual band of around 800bp was also observed in case of all the heterozygotes. The Marker represents the 100 bp DNA ladder (GeneRuler™, MBI Fermentas, Lithuania).

#### 4.4.2.4 Conservation of the residues

Multiple sequence alignment of FOXC1 across different species and other related human FOX families indicated a high degree of conservation of the Histidine (H) residue at 128 and Cysteine (C) residue at 135 positions, respectively (Figure 4.22).

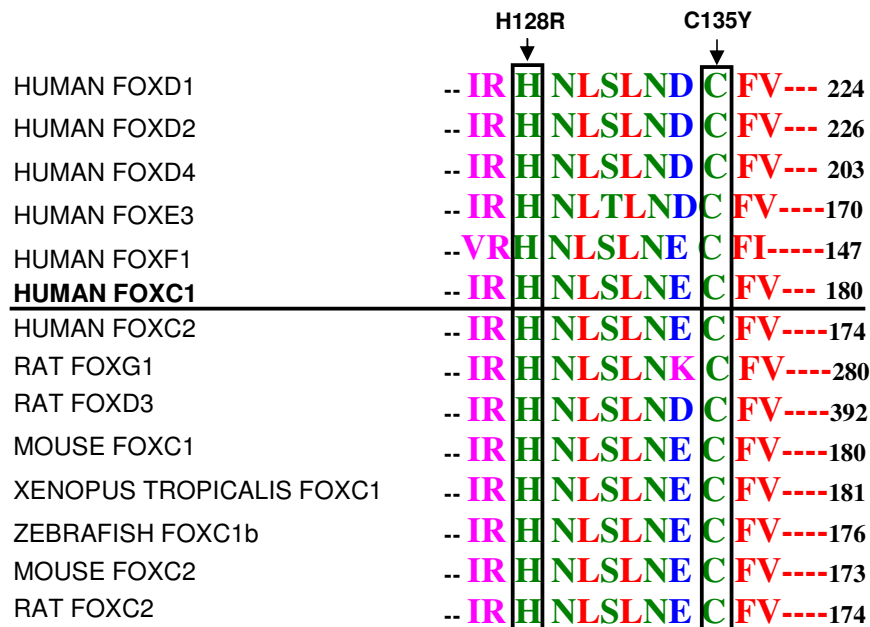


**Figure 4.22:** Multiple sequence alignment of human FOXC1 protein across other 6 members of the FOX family in humans and 6 members from other species. The human FOXC1 is underlined and the wild residues are blocked.

#### 4.4.2.4 FOXC1 polymorphisms

Two previously reported polymorphisms (Mears *et al.*, 1998) were also observed in *FOXC1*. Both the polymorphisms involved the insertion of an extra GGC triplet in two separate GGC repeats at codons 375 and 447, respectively. The first polymorphism (GGC375ins) had 6 GGC repeats in the wild type (GGC<sub>6</sub>) and 7 GGC repeats in the mutant allele (GGC<sub>7</sub>), respectively. Whereas there were 7 GGC repeats in the wild type (GGC<sub>7</sub>) and 8 GGC repeats in the mutant allele (GGC<sub>8</sub>) of the second polymorphism

(GGC447ins). The allele and genotype frequency distribution of these polymorphisms are mentioned in Tables 4.30 and 4.31. There were no significant differences in the allele and genotype frequencies among the cases and controls as evident from Odds ratio and chi square (Tables 4.28 and 4.29) suggesting no association of these polymorphisms with the disease.

**Table 4.28:** Allele frequency distribution of *FOXC1* polymorphisms in cases and controls

<i>FOXC1</i> polymorphism	Allele	Cases (n=210)	Controls (n=110)	P value	Odds ratio (95% CI)
GGC375ins	GGC <sub>6</sub>	0.6	0.59	0.88	—
	GGC <sub>7</sub>	0.4	0.41		0.95 (0.5-1.6)
GGC447ins	GGC <sub>7</sub>	0.66	0.65	0.98	—
	GGC <sub>8</sub>	0.34	0.35		0.95 (0.5-1.7)

**Table 4.29:** Genotype frequency distribution of *FOXC1* polymorphisms in cases and controls

<i>FOXC1</i> polymorphism	Genotype	Cases (n=210)	Controls (n=110)	P value	Odds ratio (95% CI)
GGC375ins	GGC <sub>6</sub> ,GGC <sub>6</sub>	78 (37.1%)	36 (32.7%)	—	1
	GGC <sub>6</sub> ,GGC <sub>7</sub>	98 (46.7%)	58 (52.7%)	0.34	0.77 (0.46-1.3)
	GGC <sub>7</sub> ,GGC <sub>7</sub>	34 (16.2%)	16 (14.5%)	0.96	0.98 (0.48-2.0)
GGC447ins	GGC <sub>7</sub> , GGC <sub>7</sub>	97 (46.2%)	47 (42.7%)	—	1
	GGC <sub>7</sub> , GGC <sub>8</sub>	86 (40.9%)	51 (46.3%)	0.42	0.8 (0.49-1.33)
	GGC <sub>8</sub> , GGC <sub>8</sub>	27 (12.9%)	12 (10.9%)	0.82	1.1 (0.5-2.3)

#### 4.5 OVERALL INVOLVEMENT OF THE CANDIDATE GENES IN PCG

Of the three candidate genes (*CYP11B1*, *MYOC* and *FOXCI*) screened, we identified the maximum involvement of *CYP11B1* mutations [43.8% (132/301)] in our patient cohort (Table 4.30). *MYOC* (4.3%) and *FOXCI* (2.4%) had a relatively lesser contribution to PCG, respectively.

**Table 4.30:** The overall involvement of candidate genes screened in PCG

Genes screened	Mutation			No mutation n (%)
	Homozygous n (%)	Heterozygous n (%)	Compound heterozygous n (%)	
<i>CYP11B1</i> (n= 301)	73 (24.2%)	41 (13.6%)	18 (6.0%)	169 (56.1%)
<i>MYOC</i> (n= 210)	-	9 (4.3 %)	-	201 (95.7%)
<i>FOXCI</i> (n= 210)	-	5 (2.4%)	-	205 (97.6%)



---

**CHAPTER 5: DISCUSSION**

---

Glaucoma comprises a group of heterogeneous optic neuropathies characterized by an excavation of the optic disc and progressive loss of visual field, which results in an irreversible blindness (Flammer *et al.*, 2003). It is the second leading cause of blindness that accounts for 4.5 million people (12.3%) globally (Resnikoff *et al.*, 2004). It presents a heterogeneous condition that is associated with inherited factors and non-genetic factors as well as hypertension, diabetes and cigarette smoking (Fan *et al.*, 2006). The etiology of glaucoma is yet unknown but the disease is often found to cluster in families (Alward *et al.*, 1998).

It has been estimated that by the year 2010, ~60.5 million people will be affected with open angle (OAG) and angle closure (ACG) glaucoma (Resnikoff *et al.*, 2004). The prevalence of POAG and PACG in India ranges from 0.41% - 3.79% and 0.5% - 4.32%, respectively (Table 2.1). The population based epidemiological study, in the state of Andhra Pradesh (Indian), estimated that glaucoma accounts for 8.2% of all blindness in this state (Dandona *et al.*, 2001).

Primary congenital glaucoma (PCG) is the most common form of developmental glaucoma that occurs due to the maldevelopment of the trabecular meshwork (TM) and iridocorneal angle. It manifests in the neonatal or early infantile period with elevated IOP, corneal edema and Haab's striae (Mandal and Netland. 2006). The prevalence of PCG varies across different populations and is highest among the inbred populations (Gencik *et al.*, 1989, Bejjani *et al.*, 1998). In the Indian state of Andhra Pradesh, it has been estimated to be 1 in 3300 live births that accounts for 4.2% of all childhood blindness (Dandona *et al.*, 1998). PCG is inherited as an autosomal recessive disease and three chromosomal loci viz. *GLC3A* (2p21), *GLC3B* (1p36) and

---

*GLC3C* (14q24.3) (Stoilov *et al.*, 1997, Akarsu *et al.*, 1996 and Stoilov *et al.*, 2002a) have been linked to the disease. *CYP1B1* at *GLC3A* (Stoilov *et al.*, 1997) has been characterized with more than 70 different PCG-associated mutations in varying proportions (13.3%-100%) worldwide (<http://www.hgmd.cf.ac.uk/ac/index.php>).

There are very few studies on the molecular genetic analysis of PCG in the Indian population (Panicker *et al.*, 2002, Reddy *et al.*, 2003 and Reddy *et al.*, 2004). The first study (Panicker *et al.*, 2002) reported the involvement of *CYP1B1* in 5 PCG families and devised PCR-based restriction digestion method to detect 5 mutations (ins376A, E229K, P193L, G61E, and R368H). This tool was then used to screen 138 PCG cases that revealed 30.8% of the cases to harbor one of the previously identified mutations. The R368H was the most prevalent mutation in that cohort (Reddy *et al.*, 2003). Further screening of the entire coding region of *CYP1B1* in an independent cohort of 64 PCG cases by resequencing, revealed that *CYP1B1* mutations accounted for 37.5% of PCG cases (Reddy *et al.*, 2004); the R368H was also the most prevalent allele (29.16%). In another study on a south Indian consanguineous family (Ramprasad *et al.*, 2007), the genetic basis of congenital glaucoma was determined by homozygosity analysis, where significant homozygosity for the markers (D2S177 and D2S1346) tightly linked to *CYP1B1* was identified. Further screening of *CYP1B1* in the family revealed the co-segregation of a novel nonsense (Gln110Stop) mutation with the disease in all the affected members. The present study was conducted to determine the extent of *CYP1B1* involvement in a large cohort of patients to understand the broad spectrum of *CYP1B1* mutations underlying PCG. Additionally, two other candidate genes (*MYOC* and *FOXC1*) were screened in the cases that were unlinked to *CYP1B1*, to explore their possible role in PCG.

In the present study the *CYP11B* mutations were identified in 40.7% (90/221) cases. Combining the results of the previous (Reddy *et al.*, 2004) and the present study, *CYP11B* mutations accounted for 43.8% (132/301) of PCG cases (Table 4.19). The frequency of *CYP11B* mutations was similar to populations from Brazil (Stoilov *et al.*, 2002a), Turkey (Bagiyeva *et al.*, 2007) and France (Colomb *et al.*, 2003), but lower than inbred populations from Slovakia (Plasilova *et al.*, 1999), Saudi Arabia (Bejjani *et al.*, 2000), Kuwait (Alfadhli *et al.*, 2006) and Iran (Chitsazian *et al.*, 2007) population (Fig.5.1)

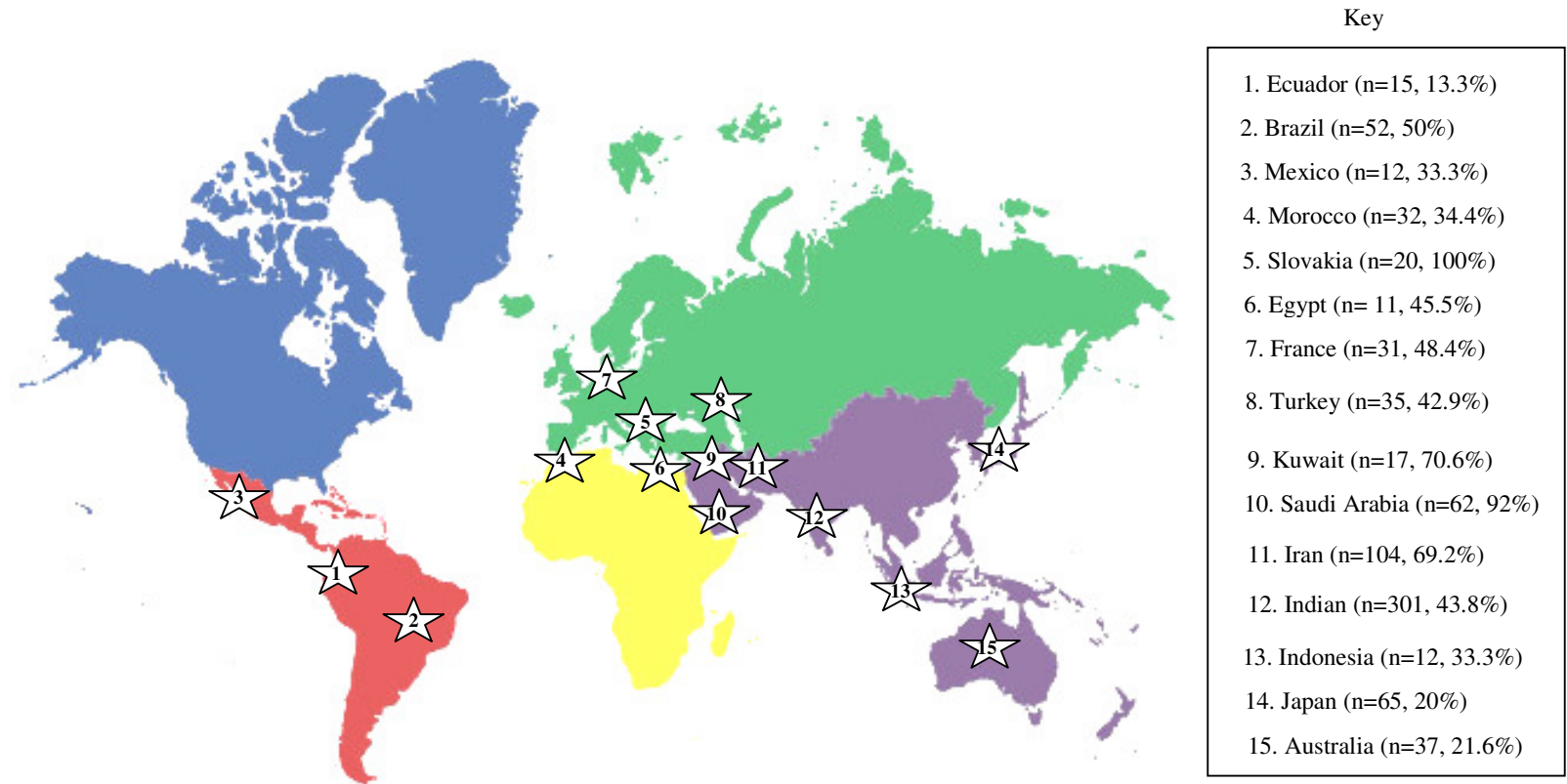


**Figure 5.1:** The involvement of *CYP1B1* mutations in various populations across the globe

Among all the *CYP11B* mutations observed, 24.1% (73/301) were homozygous, 18.5.9% (18/301) compound heterozygous and 13.9% (41/301) were heterozygous for the mutant allele whereas, 56.1% (169/301) cases did not exhibit any mutation. The distribution of PCG cases with different types of mutations in different populations are shown in Table 5.1. The percentage of cases with homozygous mutation ranges between 2.7% - 100%, with the lowest in Australian (2.7%; Dimasi *et al.*, 2007) and highest among the Slovakian Gypsies (100%; Plasilova *et al.*, 1999) and Saudi Arabians (91.9%; Bejjani *et al.*, 2000) followed by Kuwait (70.6%; Alfadhli *et al.*, 2006) and Iranian (69.2%; Chitsazian *et al.*, 2007) populations. The high rate of inbreeding and consanguinity in the latter populations could be attributed to the higher frequency of PCG cases with two mutant *CYP11B* alleles. Among the outbred populations from Japan, Brazil, Indonesia, Australia, Mexico, Morocco and France, the prevalence of PCG-associated *CYP11B* mutations varies from 13.3% to 50% (Table 5.1).

Two other studies that identified a high prevalence of *CYP11B* mutations in PCG comprised a study by Stoilov and co-workers (1998) on 22 PCG families from different ethnic backgrounds (US=2, UK=2, Canada=2 and Turkey=16), in which 16 mutations were identified. All the affected members in these families were found to harbor the mutations indicating 100% involvement of *CYP11B* (Stoilov *et al.*, 1998). The other study by Chavarria- Soley and co-workers (2006) was carried out on 26 PCG cases that exhibited 15 mutations in the gene. The authors sequenced the entire genomic region of *CYP11B* and constructed haplotypes to determine the founder effects for these mutations. It was observed that 8 recurrent mutations (W57X, G61E, E387K, R368H, R469W, c.1064-1076del, c.1200-1209dup and c.1377-1403dup) were identified with an identical haplotype in different individuals, suggesting founder

effects (Chavarria- Soley *et al.*, 2006). But, since this was carried out only on cases known to harbor *CYP1B1* mutations, their results do not depict the actual prevalence of *CYP1B1* in their PCG population.

The cases with one mutant allele in *CYP1B1* range from 3 - 40% worldwide, with the lowest in the Japanese (3%) and highest in the Iranian (40%) population, respectively (Table 5.1). In the present study we found 56.1% (169/301) cases did not harbor any *CYP1B1* mutation. Cases without *CYP1B1* mutation have also been reported from other PCG populations (Table 5.1). The identification of cases with only one copy of the mutant *CYP1B1* allele in PCG indicate that majority of the cases are partially or completely unlinked to *CYP1B1* suggesting the involvement of other candidate genes in PCG.

**Table 5.1:** Worldwide distribution of homozygous, heterozygous and compound heterozygous *CYP1B1* mutations

S. No.	Population	Cases screened (n)	Cases with <i>CYP1B1</i> mutation n (%)	Homozygous n (%)	Heterozygous n (%)	Compound heterozygous n (%)	Cases without any mutation n (%)	Reference
1	Brazil	52	26 (50%)	15 (29%)	4 (7.7%)	7 (13.5%)	26 (50%)	Stoilov <i>et al.</i> , 2002
2	Indonesian/European	21	6 (28.6%)	3 (14.3%)	2 (9.5%)	1 (4.8%)	15 (71.4%)	Sitorus <i>et al.</i> , 2003
3	US/Brazil	21	3 (14.3%)	1 (4.8%)	0	2 (9.5%)	18 (85.7%)	Sena <i>et al.</i> ,2004
4	Slovakian Gypsies	20	20 (100%)	20 (100%)	0	0	0	Plasilova <i>et al.</i> ,1999
5	Japan	65	13 (20%)	1 (1.5%)	4 (6.2%)	8 (12.3%)	7 (63.6%)	Mashima <i>et al.</i> ,2001
6	Saudi Arabia	62	57 (91.9%)	53 (85.5%)	0	4 (6.5%)	5 (8%)	Bejjani <i>et al.</i> ,2000
7	Turkey	35	15 (42.9%)	8 (22.9%)	6 (17.1%)	1 (2.9%)	20 (57.1%)	Bagiyeva <i>et al.</i> ,2007
8	Kuwait	17	12 (70.6%)	9 (52.9%)	1 (5.9%)	2 (11.8%)	5 (29.4%)	Alfadhli <i>et al.</i> , 2006
9	France	31	15 (48.4%)	6 (19.4%)	2 (6.5%)	7 (22.6%)	16 (51.6%)	Colomb <i>et al.</i> ,2003
10	Ecuador	15	2 (13.3%)	1 (6.7%)	0	1 (6.7%)	13 (86.7%)	Curry <i>et al.</i> , 2004
11	Australia	37	8 (21.6%)	1 (2.7%)	2 (5.4%)	5 (13.5%)	29 (78.4%)	Dimasi <i>et al.</i> ,2007
12	Egypt	11	5 (45.5%)	4 (36.4%)	1 (9.0%)	0	6 (54.5%)	El-Ashry <i>et al.</i> , 2007
13	Mexico	12	4 (33.3%)	2 (16.7%)	0	2 (16.7%)	8 (66.7%)	Messina-Bass <i>et al.</i> , 2007
14	Morocco	32	11 (34.4%)	9 (28.1%)	0	2 (6.3%)	21 (65.6%)	Belmouden <i>et al.</i> ,2002
15	Mexico	30	2 (6.7%)	2 (6.7%)	0	0	28 (93.3%)	Zenteno <i>et al.</i> , 2008
16	Iran	104	72 (69.2%)	49 (47.1%)	14 (13.5%)	9 (8.7%)	32 (30.7%)	Chitsazian <i>et al.</i> ,2007
17	India	301	132 (43.8%)	73 (24.3%)	41 (13.6%)	18 (6%)	169 (56.1%)	Present study

---

To the best of our knowledge, the present study exhibited the maximum (n=38) number of different types of mutations compared to other reports from Iran (n=19), Brazil (n=11; Stoilov *et al.*, 2002), Australia (n=10; Dimasi *et al.*, 2007), Saudi Arabia (n=8; Bejjani *et al.*, 2000), Turkey (n=8; Bagiyeva *et al.*, 2007), Japan (n=7; Mashima *et al.*, 2001), Indonesia (n=4; Sitorus *et al.*, 2003), where no more than 20 different types of mutations were observed. This could be attributed to the large sample size (n=301) or due to the large ethnic diversity in our cohort. Some of the mutations identified in the present study have also been reported in other PCG populations (Tables 4.3 and 4.4). However, the proportion of mutations shared across populations varies widely. For example, the Gly61Glu is the most prevalent mutation among PCG patients in Saudi Arabia (69.3%) and Iran (29%); however it is observed in 6%-27% of PCG cases from various other populations like Ecuador (Curry *et al.*, 2004), Morocco (Belmouden *et al.*, 2002), and Egypt (El-Ashry *et al.*, 2007). Similar scenarios are noted for other mutations like Glu229Lys (1.9%-13.3%), Arg469Try (8.6%-12.9%) and g.8037dup10 (1.9%-8.3%) that were observed in varying proportions in other PCG populations in France (Colomb *et al.*, 2003), Iran (Chitsazian *et al.*, 2007), Turkey (Bagiyeva *et al.*, 2007), Australia (Dimasi *et al.*, 2007) and Saudi Arabia (Bejjani *et al.*, 2000). As suggested earlier, the identification of same mutations from different ethnic backgrounds is suggestive of their common founders (Chavarria- Soley *et al.*, 2006).

Majority (75.7%) of the mutations, identified in the present study, were missense (Table 4.3), similar to populations from Saudi Arabia (Bejjani *et al.*, 2000), Iran (Chitsazian *et al.*, 2007), Australia (Dimasi *et al.*, 2007), Japan (Mashima *et al.*, 2001), Turkey (Bagiyeva *et al.*, 2007), Ecuador (Curry *et al.*, 2004), Kuwait (Alfdhli *et al.*, 2006), Indonesia (Sitorus *et al.*, 2003), Mexico (Messina-Bass *et al.*, 2007) and



---

Egypt (El-Ashry *et al.*, 2007). The Arg368His was the most prevalent mutation identified in the present study that accounted for 20.9% (63/301) of all cases. This mutation has also been reported in other populations from Saudi Arabia, Brazil, Iran, Australia and Turkey in minor proportions (Table 5.2).

The relatively high frequency of Arg368His (10.6%) in the Iranian population (Table 5.2) similar to Indian could be attributed to the haplotype sharing across these populations that could be further attributed to common founders or population movements. It was observed that various *CYP1B1* mutations were at a higher frequency [Gly61Glu (29%), Arg390His (19.2%) and Arg469Trp (8.6%)] in the Iranian population. The SNP based haplotype analysis revealed that the identical mutant alleles had independent origins among the familial PCG cases. It suggested that the disease status in such individuals was not attributable to identity by descent but to the high frequency of mutant alleles within this endogamous population (Chitsazian *et al.*, 2007).

Certain *CYP1B1* mutations are uniquely prevalent in certain populations (Table 5.2). These mutations have also been observed in minor proportions in other populations that exhibits a different prevalent mutation. The Gly61Glu in Saudi Arabia (69.3%) and Iran (29%); Glu387Lys in Slovakia (100%) and 4340delG in Brazil (23%), Val364Met in Indonesia (19%) and Japan (6.2%) were identified as the prevalent mutations, respectively (Table 5.2). The recurrence of common mutations in some populations could be attributed to the founder effects (Chakrabarti *et al.*, 2006). The common mutations in different population were found to occur on common haplotype backgrounds (Chakrabarti *et al.*, 2006). Since it is very unlikely that the same mutation would have arisen several times during the course of evolution, therefore, the occurrence of same mutation on the common haplotype background in different

---

geographical regions is probably because of the population movement (Chakrabarti *et al.*, 2006). For example, the E387K mutation, which is the prevalent mutation among the Slovakian Roms (Plasilova *et al.*, 1999), is observed in lower frequencies among the patients in United States and Brazil (Sena *et al.*, 2004). But, in all these populations, E387K is observed on a common haplotype (G-T-C-C-A). This indicates that migrant Roms probably might have carried this mutation to these countries (Chakrabarti *et al.*, 2006). Similarly the immigrants from Saudi Arabia to India might have carried the prevalent mutation (G61E); this is also found on the same haplotype (C-G-G-T-A) in both these populations (Chakrabarti *et al.*, 2006).

A wide spectrum of *CYP11B1* mutations identified in the present study suggests the allelic heterogeneity of the condition. The mutations have been identified throughout the gene, with codon “390” as the hot spot in *CYP11B1*. Three different substitutions (Arg390Ser, Arg390Cys and Arg390His) were identified at this position that jointly accounted for 15.5% (14/90) cases. The mutations at 390 codon have been reported from other populations like Saudi Arabia [Arg390Ser (1.61%); Bejjani *et al.*, 2000], Iran [Arg390His (1.92%); Chitsazian *et al.*, 2007] and Ecuador [Arg390Cys (6.6%); Curry *et al.*, 2004]. In the present study the patients with mutations at Arg390 codon had bilateral manifestation of PCG since birth and presented with raised IOP (range: 22 - 44 mm of Hg) and megalocornea (11 - 15 mm). Similar clinical features have been identified in patients with Arg390Ser from Iran (Chitsazian *et al.*, 2007) whereas the clinical details of the patients from Saudi Arabia (Bejjani *et al.*, 2000) and Ecuador (Curry *et al.*, 2004) were available in the literature.

**Table 5.2:** Distribution of recurrent *CYP1B1* mutations

<i>Population</i>	<i>India</i> (n=301)	<i>Saudi</i> <i>Arabia</i> (n=62)	<i>Brazil</i> (n=52)	<i>Turkey</i> (n=35)	<i>Iran</i> (n=104)	<i>Kuwait</i> (n=17)	<i>Australia</i> (n=37)	<i>Egypt</i> (n=11)	<i>Slovakia</i> (n=20)	<i>Japan</i> (n=65)	<i>Indonesia</i> (n=12)
<i>Mutation</i>											
Gly61Glu	1.7%	69.3%*	----	14.3%	29%*	52.9%	----	27.3%	----	----	----
Val364Met	----	----	----	----	----	----	----	----	----	6.2%*	19%*
Arg368His	20.9%*	1.8%	1.9%	5.7%	10.6%	----	2.7%	----	----	----	----
Glu387Lys	----	----	11.1%	----	----	----	----	----	100%*	----	----
g.4340delG	----	----	23%*	----	----	----	----	----	----	----	----

\* Prevalent mutations

Among the recurring mutations, the Gly229Lys and Tyr81Asn have also been reported from various PCG populations. In the present study, Gly229Lys was identified in 11 PCG families (Table 4.8), of which 10 patients were heterozygous while one patient (PCG264) was compound heterozygous with another missense mutation (Ala443Gly). Gly229Lys has been identified among Iranian [0.96 (1/104); Chitsazian *et al.*, 2007], Australian [2.7% (1/37); Dimasi *et al.*, 2007] and French [6.5% (2/31); Colomb *et al.*, 2003] PCG patients. A single patient from Lebanon was also found to harbor this mutation (Michels-Rautenstrauss *et al.*, 2001). The patients from Australia and France were heterozygous while the patients from Iran and Lebanon were compound heterozygotes with Arg368Cys and Ala443Gly, respectively. Seven patients in the present study had bilateral manifestation of the disease and presented with raised IOP (range: 22 – 38 mm of Hg) and megalocornea (range: 12 – 15 mm). Similar clinical features were noted in patients from Iran and Lebanon, but the clinical details of the patients from Australia and France were not available in the literature.

The Tyr81Asn mutation was identified in 6 PCG families (Table 4.7), of which 2 families (PCG318 and PCG340) were homozygous, 3 heterozygous (PCG104, PCG338 and PCG350) and one was compound heterozygous (PCG281) with another missense mutation (Cys371Phe). Five patients had bilateral PCG and all had presented with raised IOP (range: 24 – 34 mm of Hg) and megalocornea (range: 13 – 17 mm). This mutation has not been reported from any other PCG population so far. However, it was identified in 3 affected individuals in a French POAG family (Melki *et al.*, 2004). Similar to the present study, these affected individuals had bilateral manifestation of the disease and were intervened at 39, 44 and 52 years of age,

respectively. One case presented with high IOP (28 mm of Hg) whereas the clinical details of other two patients were not available in the literature.

Majority of the missense mutations 92% (35/38) in the present study were identified in the cytosolic domain of the protein. This is similar to the data obtained from other populations (Fig.2.18). *CYP11B1* is a membrane bound enzyme, anchored to the endoplasmic reticulum. The cytosolic portion of the protein is responsible for its enzymatic activity, which consists of a set of conserved core structures and signature sequences. These structures include a number of  $\alpha$  helices and  $\beta$  sheets and a "meander region" that are necessary for the heme binding ability of the protein (Stoilov *et al.*, 2001). The structural based analysis of 8 mutations (A115P, M132R, Q144P, P193L, E229K, S239R, R368H, G466D) in the cytosolic domain using molecular dynamic simulations revealed that these mutations have significant effects on the protein's stability, its conformational freedom, dynamics of the substrate access channel and interaction with reductase protein (Achary *et al.*, 2006). Similarly, *in vitro* studies have shown that mutations (G61E and R469W) in the cytosolic domain affect both the stability as well as the enzymatic activity of the protein (Jansson *et al.*, 2001). These observations suggest that mutations in the cytosolic domain interfere with the fundamental properties of the protein and in turn its function that might be resulting in the disease pathogenesis.

Despite a large number of PCG-associated *CYP11B1* mutations, there are very few reports that could convincingly demonstrate the association of *CYP11B1* mutations with the severity of the disease. In the present study, the cases with Arg368His mutation and those harboring other *CYP11B1* mutations were compared with respect to four parameters (age at onset, IOP, C:D and corneal diameter). There were no

significant differences between the two groups with respect to any of these traits, indicating that Arg368His by itself did not confer additional severity of the disease in the patient cohort (Tables 4.21 and 4.22).

The effect of *CYP1B1* mutations on the disease prognosis in terms of IOP reduction was also determined. Univariate Cox regression analysis (Table 4.24) suggested that IOP at presentation was a significant risk factor ( $P= 0.007$ ) with the hazards ratio of 1.08 for each unit increment of IOP in the cases with *CYP1B1* mutations [CYP (+)]. The comparison of mean values of IOP revealed that [CYP(+)] cases had significant ( $p=0.04$ ) reduction in IOP till one year following surgical intervention compared to those that did not harbor any mutation [CYP(-)] cases. The Kaplan-Meier survival analysis exhibited significant differences in the plotted survival curves (Fig.4.7) for IOP between the [CYP (+)] and [CYP (-)] groups suggesting that [CYP(-)] cases had better prognosis of the disease in terms of IOP reduction than the [CYP(+)] patients.

To the best of our knowledge this is perhaps the first report of genotype phenotype correlation based on *CYP1B1* mutations and IOP. One such report is from the Brazilian population where the most prevalent mutation (4340delG) exhibited a severe phenotype (Stoilov *et al.*, 2002a). All the patients with 4340delG were bilateral cases with an age of onset within first month of life and IOP ranged between 25-55 mm of Hg (Stoilov *et al.*, 2002a). Similarly in an earlier study from our centre on 146 Indian PCG patients (Panicker *et al.*, 2004) cases with frameshift mutation (ins376A) were found to have the worst phenotype, (IOP >30 mm Hg, corneal diameter of >13 mm, C: D ratio >0.8, severe corneal edema and presence of Haab's striae). However, these studies considered the IOP at presentation in patients, and hence may not be indicative of a true correlation with the disease prognosis.

Levy and co-workers (2005) determined the prognostic factors for surgical outcomes in cases intervened within first three months of birth and suggested that IOP before surgical procedure was an independent predictive factor for the final outcome. A higher IOP and C: D ratio was found to be associated with the failure of the first surgical procedure. In a study by Kiefer and co-workers (2001), correlation between the postoperative IOP and axial length growth was determined in children who underwent either trabeculotomy or goniotomy. The children with raised IOP after surgery had increased axial length growth while the ones with controlled IOP had either normal or borderline increase in the axial length. Similarly, Law and co-workers (2001) observed that after surgical intervention of the cases with controlled IOP showed a decrease in axial length. These observations suggest that axial length can be used as a good parameter to monitor the control of IOP in congenital glaucoma. In the Indian PCG cases, it was observed that patients who were intervened within 1 month of their age, by combined trabeculectomy and trabeculotomy, had better prognosis in terms of mean IOP reduction, corneal clarity and visual acuity (Mandal *et al.*, 2003).

Hollander and coworkers (2006) tried to correlate *CYP11B1* mutations with the degree of angle dysgenesis in 6 congenital glaucoma patients. Based on histological evaluation the cases were divided into severe (absence of SC, hypoplasia of TM), moderate (the presence of a band of collagenous tissue in TM) and mild goniodysgenesis (deposition of a mucopolysaccharide material in juxtacanalicular tissue). The angle abnormalities were found to vary with different *CYP11B1* mutations like R390H, R117P, C209R and 4340delG, which were associated with severe phenotype whereas, cases with R368H, G61E and E229K mutations had a milder phenotype. These observations suggested a possible classification of *CYP11B1*

---

mutations based on the histological findings, which could be used to correlate with disease severity.

*CYP1B1* mutations have also been shown to exhibit variable penetrance. In an American PCG family, four affected individuals were found to be compound heterozygotes for the E387K and 268del SNF. But only two of them manifested a severe onset of early glaucoma (IOP of 25mm of Hg and 28 mm Hg, respectively and corneal edema), whereas, the other two did not show any symptoms of glaucoma (Sena *et al.*, 2004). The differences in the manifestation of disease could be attributed to the effect of other modifier genes for *CYP1B1*. The low penetrance (50%) with respect to *CYP1B1* mutations was also reported from Saudi Arabian population (Bidinost *et al.*, 2006). In their cohort of 97 individuals, 58 had homozygous or compound heterozygous mutations in *CYP1B1*. However, only 33 of these 58 individuals were affected and 25 did not manifest any clinical features of PCG. These 25 subjects did not exhibit any signs of glaucoma with respect to IOP, corneal diameter and optic nerve cupping. Eight of them with homozygous Gly61Glu mutation had IOPs between 14 – 37 mm of Hg and corneal diameters between 11.5 – 14 mm, respectively. The IOP was above normal limit (>21 mm of Hg) in four cases, of which two had bilateral elevation of IOP (27 and 22 mm of Hg, respectively) while the remaining had unilaterally raised IOP (27 and 37 mm of Hg, respectively). None of these patients received any treatment for glaucoma and their outcomes have not been elaborated any further (Bidinost *et al.*, 2006).

In the present study, 5.9% (18/301) cases were compound heterozygous for *CYP1B1* mutations, of which 3.7% (11/301) had Arg368His as one of the mutant allele (Table 5.3). All these cases had manifestation of the disease since birth except for PCG228 who had an onset at the age of 1 year. All the cases presented with raised IOP (range:



---

22- 42 mm of Hg). The corneal diameter in these patients ranged from 11-16 mm and they had a C:D ratio between 0.2:1-0.9:1, respectively. On surgical intervention their IOP reduced between 8 - 20 mm of Hg. Compound heterozygous cases have also been observed in other PCG populations (Table 5.1). Similar clinical features with bilateral manifestation and raised IOP were observed in the Brazilian (range: 25 - 34 mm of Hg) and Iranian patients (IOP range: 22 - 30 mm of Hg). However, the clinical features of such cases in populations from Japan (Mashima *et al.*, 2001), Saudi Arabia (Bejjani *et al.*, 2000), France (Colomb *et al.*, 2003), Australia (Dimasi *et al.*, 2007) and Morocco (Belmouden *et al.*, 2002) could not be deciphered.

*CYP1B1* mutations have also been implicated in juvenile and adult onset forms of glaucoma, from various ethnic groups as shown in Table 2.7. Most of the *CYP1B1* mutations in JOAG/POAG cases were heterozygous but cases with homozygous and compound heterozygous mutations have also been observed. The association of *CYP1B1* mutations with adult onset glaucomas ranged from 1.3% - 6.0 % (Table 2.7). The involvement of *CYP1B1* in POAG and PCG indicates that it is an important gene in different forms of glaucoma and its association with these glaucomas should be explored further to elucidate its involvement in disease pathogenesis (Vincent *et al.*, 2002). It was observed that open angle glaucoma cases with *CYP1B1* mutations had significantly early age at onset ( $p= 0.023$ ) compared to cases without any mutation (Melki *et al.*, 2004). In the French population, patient with homozygous (269delSNF) and compound heterozygous (g.3979delA & N423Y) mutations have been identified (Melki *et al.*, 2004). Both the cases had severe phenotype in terms of IOP at presentation (42mm of Hg in the patient with compound heterozygous mutation and 40 mm of Hg in the patient with homozygous mutation) compared to the cases with heterozygous *CYP1B1* mutations (IOP ranged between 20 mm of Hg-30 mm of Hg).

---

However, the scenario was not the same in other adult onset glaucoma patients with *CYP1B1* mutations from other populations. In the eastern Indian population, a JOAG case with homozygous *CYP1B1* mutation (R523T) had better prognosis in terms of IOP reduction (16 mm of Hg in both eyes) compared to other JOAG/POAG cases with heterozygous *CYP1B1* mutations where IOP ranged from 14 mm of Hg -31 mm of Hg (Acharya *et al.*, 2006). Similarly, in the South Indian populations, neither of the cases with compound heterozygous *CYP1B1* mutations (M292L and R368H; E229K and P193L) exhibited more severity of the disease compared to cases with heterozygous mutations (Kumar *et al.*, 2007). However, JOAG cases from Iranian population (Bayat *et al.*, 2008) were found to harbor only homozygous *CYP1B1* mutations (3 patients with Gly61Glu and one with Arg368His) suggesting an autosomal recessive mode of inheritance, which was attributed either to the small samples size (n=23) or to the high frequency of *CYP1B1* mutant alleles as discussed earlier (Chitsazian *et al.*, 2007). No differences were observed among the cases with *CYP1B1* mutations compared to the cases with *MYOC* mutations in terms of age at diagnosis and clinical features like IOP and C:D ratio (Bayat *et al.*, 2008). In another study from Indian population the frequency of *CYP1B1* mutations was higher among the POAG cases (18.6%) compared to PACG cases (1.1%). There was a marked allelic heterogeneity with R368H as the prevalent mutation (8.0% in POAG and 5.6% in PACG) cases. The study also showed that ‘C-C-G-G-T-A’ was the risk haplotype associated with *CYP1B1* mutations in POAG and PACG cases similar to that observed in cases with PCG worldwide (Chakrabarti *et al.*, 2007).

In the present study we also screened two glaucoma-associated candidate (*MYOC* and *FOXC1*) genes in PCG cases that were either heterozygous (n=41) or did not harbor any *CYP1B1* mutation (n=169) to determine their possible involvement in PCG.

*MYOC* screening led to the identification of two heterozygous missense (Gln48His and Tyr479His) mutations in 4.3% (9/210) of PCG cases. This was comparable to the global frequency *MYOC* mutation (3-5%) in POAG and JOAG cases (Gong *et al.*, 2004). The Gln48His mutation was identified in 3.8% (8/210) of PCG cases. This mutation has also been reported as a prevalent mutation in POAG in Indian populations (Chakrabarti *et al.*, 2005). For the first time it was identified in two sporadic cases of JOAG and in an adult-onset POAG case from eastern India (Mukhopadhyay *et al.*, 2002). Later this change was also noted in a JOAG family and in a sporadic POAG case from northern and southern India, respectively (Sripriya *et al.*, 2004). These observations clearly establish that Gln48His is a common *MYOC* mutation among Indian glaucoma patients but has not yet been reported from any other population. Although we cannot ascribe causality of all glaucoma phenotypes to the Gln48His mutation alone, it is likely that Gln48His mutation is unique to Indian population and a potential risk factor towards disease predisposition (Chakrabarti *et al.*, 2005). The exact role of this mutation in the disease pathogenesis is unknown. Sripriya and coworkers (2004) have suggested the predicted secondary structure of wild type *MYOC* has extended sheets in the region of 42-45 amino acid position, which were removed in the presence of Gln48His mutation.

The Gln48His mutation co-segregated with a *CYP1B1* (Arg368His) mutation in a PCG family suggesting a possible digenic inheritance of these two genes in the present study. The patient with both *CYP1B1* and *MYOC* mutations exhibited a relatively severe phenotype with respect to IOP at presentation (38 mm of Hg and 36 mm of Hg in the right and left eye, respectively) in comparison to other cases with *MYOC* mutations (IOP at presentation ranged between 12 - 32 mm of Hg suggesting that the effect of two mutant alleles of two different genes in a digenic fashion might

have played a role in the severity of the phenotype (Table 5.3). Comparison of the patient with digenic inheritance to cases harboring compound heterozygous mutations in *CYP1B1*, in terms of age at onset IOP, corneal diameter and C:D at presentation, showed similar clinical features (Table 5.3). Digenic inheritance has also been reported in other ocular disease like retinitis pigmentosa, where mutations in *RDS* (retinal degeneration slow) and *ROM1* (rod outer segment protein) co-segregated with the diseased phenotype (Dryja *et al.*, 1997). But unlike in the present study, there was no effect of digenic inheritance on the disease severity in RP.

The other *MYOC* mutation (Tyr479His) identified in the present study has not been reported with any other type of glaucoma. However, it has been identified in a JOAG patient at our institute who had bilateral manifestation of the disease at the age of 30 years (unpublished data). He presented with raised IOP (34 mm of Hg and 40 mm of Hg in the right and left eye, respectively) with increased C:D ratio (0.9:1 both eyes). On surgical intervention his IOP reduced to 10 mm of Hg and 12 mm of Hg in the right and left eye, respectively with a visual outcome of 20/20. The similar trend was observed in proband (PCG118) of the present study, who had bilateral manifestation of the disease since the age of 2 months and presented with raised IOP (30 mm of Hg and 22 mm of Hg in the right and left eye, respectively) and megalocornea (15 mm and 13.5 mm in the right and left eye, respectively) in both eyes. On surgical intervention, his IOP reduced to 10 mm of Hg in both eyes with a visual acuity of 20/163.

**Table 5.3:** Comparison of the clinical features among the patients with compound heterozygous *CYP1B1* mutations the case with digenic inheritance of *CYP1B1* and *MYOC* in the present study

Patient ID	<i>CYP1B1</i> mutation		Age at onset	Age at intervention	IOP at presentation *OD;OS (mm of Hg)	IOP at final follow up *OD;OS (mm of Hg)	C:D ratio	Corneal diameter *OD;OS (mm)
	Allele 1	Allele 2						
PCG005	Arg368H	Arg390Cys	Since birth	1 year	40;42	14;17	0.3;0.3	12;13
PCG069	Pro193Lys	Glu229Lys	Since birth	2 years	>21;>21	16;16	----	14;16
PCG120	Gly61Glu	Arg368His	Since birth	9 years#	22;32	14;34	0.3;0.9	12;13
PCG144	Arg368H	Arg390Cys	Since birth	1 day	36;30	28;18	0.5;0.3	11;11
PCG190	Arg368H	Arg390His	Since birth	6 months	22;17	15;13	0.8;0.6	13.5;13.5
PCG193	Cys280Stop	His279Pro	Since birth	4 years#	24;24	14;14	0.7;0.7	13;13
PCG206	Arg368H	Arg390Cys	Since birth	4 days	34;12	17;14	----	13;12
PCG212	Arg368H	Val84Phe	Since birth	7 years#	22;28	18;18	0.7;0.8	----
PCG220	Arg368H	Arg390Cys	Since birth	1 month	30;36	14;24	0.5;0.5	12;14
PCG228	Arg368H	Pro442Leu	1 year	3 years	24;28	20;23	----	15;15
PCG251	Arg368H	Ser464Pro	Since birth	1 year	30;27	----	0.8;0.7	14;11
PCG254	Ala54Val	Asn519Ser	Since birth	3 months	28;32	18;18	0.7;0.7	14.5;14.5
PCG258	Arg368H	Arg390Cys	Since birth	1 year	25;24	10;8	0.7;0.6	15;14.5
PCG264	Ala443Gly	Glu229Lys	Since birth	3 months	27;12	8;12	0.3;0.2	13;12
PCG281	Tyr81Asn	Cys371Phe	Since birth	2 months	28;26	12;14	0.2;0.2	14;13
PCG358	Leu97Phe	Ser131Arg	Since birth	2 months	32;38	----	----	13;13.5
PCG369	Arg355Stop	Arg390His	Since birth	2 days	>21;>21	12;12	0.3;0.3	13;13
PCG373	Arg368H	Arg390His	Since birth	1 month	16;22	8;16	0.6;0.6	14;14
PCG095\$	Arg368H	Gln48His	2 months	2 years	38;36	16;14	0.4;0.3	12;12

# Diagnosed elsewhere and was under treatment before coming to our centre for further management;

\* OD-right eye; OS-left eye

\$ Case with digenic inheritance of *CYP1B1* and *MYOC*

To the best of our knowledge the present study is perhaps the first report on the involvement of *MYOC* mutations in PCG (Kaur *et al.*, 2005). Another *MYOC* (g.14710 G>A) mutation was identified in a Chinese family with PCG (Ye-hong *et al.*, 2006). The proband in this family was diagnosed to have bilateral PCG at the age of 1.6 years. He had IOP of 37 mm of Hg, corneal diameter of 14 mm and C:D ratio of 0.8, respectively, in both the eyes. His father had POAG in the right eye and was diagnosed at the age of 36 years with IOP of 36 mm of Hg and C:D ratio of 0.8, respectively. Both the proband and his father were homozygous for *MYOC* mutation whereas proband's mother and his elder sister were heterozygous and were clinically unaffected at the time of presentation. On the basis of identification of *MYOC* mutation in both PCG and POAG patients, the authors suggested the involvement of common biochemical pathway in the disease pathogenesis (Ye-hong *et al.*, 2006). An earlier study also reported the co-segregation of *MYOC* and *CYP11B1* in juvenile onset open angle glaucoma through a digenic mechanism (Vincent *et al.* 2002). It was observed that in a glaucoma family of East Indian (Guyanese) origin. It was observed that individuals with both *CYP11B1* (R368H) and *MYOC* (G399V) mutations had juvenile form of open angle glaucoma with mean age of onset at 27 years, whereas individuals with only *MYOC* (G399V) mutation had adult onset glaucoma with a mean age of onset at 51 years. Based on these observations it was suggested that *CYP11B1* may be a modifier of *MYOC* expression and that these two genes might act through common biochemical pathways. These observations suggest the involvement of *MYOC* mutations in different subtypes of glaucoma (Ye-hong *et al.*, 2006). A similar scenario was observed for the *RDS* gene, where different mutations resulted in different disease phenotypes like the Cys118del resulted in RP whereas Arg172Try and Arg172Gln in macular degeneration, respectively (Wells *et al.*, 1993). Based on

these observations, it was suggested that the functional significance of certain amino acids in *RDS* may be different in cones and rods (Wells *et al.*, 1993).

These observations were remarkably different from the previous reports on *MYOC* mutations where cases with homozygous mutations were found to be asymptomatic. It was shown in a large French-Canadian family that homozygotes for a missense mutation (Lys423Glu) were asymptomatic and heterozygous individuals manifested POAG (Morissette *et al.*, 1998). Based on this observation, it was suggested that *MYOC* mutations act through a dominant negative effect. Similarly, Lam and coworkers (2000) have shown the lack of glaucoma phenotype in a woman with homozygous Arg46Stop mutation confirming the findings of this study. The dominant negative effect of *MYOC* proteins has been supported by several *in vitro* studies. The wild type and mutant myocilin (G367R and K423E) proteins have been shown to interact with each other and form heterocomplexes. Based on these observations it was suggested that progressive accumulation of these abnormal heterocomplexes could lead to the malfunction of myocilin expressing cells like human trabecular meshwork cells, which in turn would result in glaucoma (Gobeil *et al.*, 2004; Kanagavalli *et al.*, 2007). These observations are contradictory to the study by Ye-hong and coworkers (2006), where only the individuals harboring *MYOC* mutations were affected whereas the heterozygous were asymptomatic. Hence, accumulation of a much larger dataset and functional studies might shed more light to decipher the role of *MYOC* in glaucoma pathogenesis.

*FOXC1* screening led to the identification of 5 novel heterozygous (His128Arg Cys135Tyr, g.1086delC g.1155-1163del9 and g.1927dup25 and) mutations in 2.4% (5/210) patients. To the best of our knowledge, this is perhaps the first report on the involvement of *FOXC1* mutations with PCG. Majority (89.1%) of *FOXC1* mutation

(33/37) identified in various anterior segment anomalies have been identified in the FHD (67.5%) or upstream of FHD (21.6%), that included 20 missense, 5 nonsense, 5 deletions and 3 insertion mutations (Table 2.12). In the present study, two mutations (His128Arg and Cys135Tyr) were identified in the FHD, two in AD-1 (g.1086delC and g.1155-1163del9) and one (g.1947dup25) in the inhibitory domain. However, none of the *FOXC1*-associated ARA mutations (Q2X, Q123X and M161K) were observed in the Indian PCG cases and vice versa. Also M161K, the most prevalent mutation identified in 22.2% (2/9) of Indian ARA cases (Komatireddy *et al.*, 2003) was not observed in the present study, suggesting that different *FOXC1* mutations might have resulted in different phenotypes. Involvement of *FOXC1* in PCG suggests its potential role in different glaucoma phenotypes. Hence, screening of *FOXC1* in various glaucomas is warranted to better understand its involvement with these disease conditions.

The co-segregation of *FOXC1* with *CYP11B1* mutations was identified in two PCG (PCG100 and PCG196) families but a clear-cut digenic pattern could not be assessed. In PCG100, the proband inherited the two heterozygous mutant alleles from his respective unaffected carrier parents. Whereas in PCG196, both the unaffected parents along with unaffected sib were heterozygous for the *FOXC1* mutation and he inherited the *CYP11B1* mutation from his mother.

Apart from mutations, two polymorphisms (GGC375ins and GGC447ins) were also identified in the present study. However, none of them were found to be associated with the disease phenotype (Tables 4.28 and 4.29). These polymorphisms have also been reported from other populations in almost similar proportions among cases and controls (Mears *et al.*, 1998, Cella *et al.*, 2006).



A wide range of phenotypic variations have been observed among the patients with *FOXC1* mutations at the intra and inter-familial levels. Honkanen and co-workers (2003) have shown the association of a single *FOXC1* missense (Phe112Ser) mutation with a spectrum of anterior segment anomalies like Axenfeld Reiger's anomaly, Reiger's anomaly and Peter's anomaly suggesting the phenotypic heterogeneity of *FOXC1* mutations. In a study by Khan and coworkers (2008), the proband and his mother harbored the same missense (M161K) mutation; however, the proband was diagnosed with aniridia and congenital glaucoma whereas mother had a spectrum of anterior segment malformations like prominent Schwalbe's line, optic nerve cupping, and iris hypoplasia. Similar phenotypic variations have been identified among the Indian ARA patients with M161K mutation (Komatireddy *et al.*, 2003). This mutation was identified in two ARA families. In one family, the offsprings had better prognosis of the disease in terms of visual acuity (20/80 both eyes) and optic nerve cupping (range: 0.2:1-0.4:1) compared to their affected father harboring the same mutation, who had almost total cupping (0.9:1) in his left eye with a visual acuity of no perception of light and counting fingers in the right and left eye, respectively. But in the other family, all the patients had severe loss of vision (fixing and following light and counting fingers) in the worst eye. However, the IOP was under control (range: 12-18 mm of Hg) with a visual acuity of 20/260 (in the proband) to 20/30 (in the affected father and grandfather) in the better eye despite surgical interventions (Komatireddy *et al.*, 2003). Differences in the phenotypic features were also identified among the cases with *FOXC1* gene duplication compared to the cases with mutations in the *FOXC1* gene (Stungaru *et al.*, 2007). Cases with *FOXC1* gene duplication were found to have iridogoniodysgenesis malformations and higher incidence of raised IOP and glaucoma. In contrast, mutations in *FOXC1* were associated with iris hypoplasia, corectopia, and peripheral anterior synechiae with lower incidence of raised IOP and

glaucoma compared to cases with *FOXC1* gene duplication. Based on these observations it was suggested that patients with *FOXC1* gene duplication had more severe prognosis than the patients with mutations in *FOXC1*. Also the presence of non-ocular findings in the patients with *FOXC1* mutations suggested that *FOXC1* gene duplication eye is particularly sensitive to the duplication of *FOXC1* gene (Stungaru *et al.*, 2007).

Comparison of clinical parameters of the patients with different *FOXC1* mutations in the present study showed similarities in clinical phenotype in the patients. Four patients were had bilateral manifestation of the disease since birth whereas proband (PCG196) had a unilateral disease. Three probands were diagnosed within 7 months of age at our centre while two probands (PCG209 and PCG216) got diagnosed elsewhere and came for further management (Table 4.27). The prognosis was good, in terms of IOP reduction (range: 10-21 mm of Hg) in two patients (PCG44, PCG196) while it was still raised in PCG100 (16 and 40 mm of Hg in the right and left eye, respectively), PCG216 (30 and 22 mm of Hg in the right and left eye, respectively) and PCG209 had hypotony in both eyes.

Similar to the observations of the present study, most of the cases with different anterior segment anomalies harboring *FOXC1* mutations were found to manifest severe form of early onset glaucoma. A patient with Leu86Phe was found to have bilateral manifestation of congenital glaucoma in the right eye leading to complete loss of vision and raised IOP (40 mm of Hg) in the left eye with other associated ocular and systemic abnormalities (Saleem *et al.*, 2003). Similarly, in a study by Fuse and co-workers (2007), the probands with *FOXC1* mutations were found to have congenital glaucoma with associated ocular and systemic features of ARS. Both the probands had bilateral congenital glaucoma and presented with megalocornea and

underwent multiple surgeries. The *FOXC1* mutations are reported have been reported to show phenotypic variability. In a study by Honkanen and co-workers (2003), the proband and his brother had manifested typical features of ARA without glaucoma whereas their maternal uncle harboring the same mutation (Phe112Ser) was diagnosed for congenital glaucoma at the age of 5 months with other associated ocular abnormalities of ARA. Similarly, in a Japanese family, a single mutation was found to result in variable phenotypes (Suzuki *et al.*, 2001). The Pro79Thr mutation was observed in a pair of dizygotic twin boys who had typical ocular and extraocular findings of ARS whereas their 5 year old brother harboring the same mutation was found to have congenital glaucoma (Suzuki *et al.*, 2001). In a study by Mortemousque and co-workers (2004), the proband with *FOXC1* mutation had spectrum of ocular features of ASD associated with raised IOP (26 mm of Hg) without glaucoma whereas his paternal uncle and grandfather's brother harboring the same (Ile91Phe) mutation had bilateral congenital glaucoma associated with other ocular abnormalities. The same scenario was observed in a British family (Ito *et al.*, 2007) where the proband was diagnosed for bilateral ARS with glaucoma at 27 years of age, whereas her son harboring the same mutation (Leu130Phe) was diagnosed for bilateral AR syndrome at the age of 2 months and abnormally high cup-disc ratios (0.8:1 in both eyes). In an earlier study on 6 PCG cases, no mutations were reported in *FOXC1* gene (Nishimura *et al.*, 1998). Thus is apparent that most of these studies had secondary glaucoma associated with both ocular and extraocular abnormalities. This was in contrast to the PCG cases in the present study, where patients did not exhibit any other ocular or systemic abnormalities. These observations suggest the potential involvement of *FOXC1* mutations in the pathogenesis of a wide spectrum of glaucoma phenotypes.

To summarize, the present study provides information on the mutation spectrum of three candidate genes (*CYP1B1*, *MYOC* and *FOXC1*) in PCG that jointly accounted for 48% (145/301) of all cases. However, the remaining 52% of cases did not exhibit any involvement of these genes, which suggested the role of other unidentified candidate loci/genes in PCG pathogenesis. The findings of the present study suggest the involvement of *MYOC* and *FOXC1* in a proportion of PCG cases that are unlinked to *CYP1B1*. The data obtained from the present study provides information on the mutation spectrum of three candidate genes (*CYP1B1*, *MYOC* and *FOXC1*) in a cohort of Indian PCG patients, thereby providing some insights into the molecular genetic defects underlying PCG. It demonstrates the complex nature of PCG in terms of clinical and genetic heterogeneity. It could be helpful in developing a reliable diagnostic method for screening the prevalent mutations in *CYP1B1* in the predisposed families. The involvement of *MYOC* and *FOXC1* in PCG could be explored further in other populations to understand their role in disease pathogenesis.

## CHAPTER 6: CONCLUSIONS OF THE STUDY

Glaucoma comprises a group of clinically and genetically heterogeneous optic neuropathies characterized by an excavation of the optic disc and progressive alteration of the visual field, which if left untreated, results in an irreversible blindness. Primary Congenital Glaucoma (PCG) is the most common form of childhood blindness caused by an unknown developmental defect of the trabecular meshwork and anterior chamber angle. Three chromosomal loci have been mapped to PCG viz. *GLC3A* at 2p21, *GLC3B* at 1p36 and *GLC3C* at 14q24.3, of which the *GLC3A* harbors the Cytochrome P4501B1 (*CYP1B1*) gene. *CYP1B1* is the only member of CYP450 superfamily of heme proteins to be implicated in a developmental anomaly.

The present study dealt with the screening of three candidate genes viz *CYP1B1*, *MYOC* and *FOXC1* in 301 clinically diagnosed PCG cases. So far >70 *CYP1B1* mutations have been implicated in PCG in different ethnic groups. Screening of *CYP1B1* in the present cohort led to the identification of 38 different mutations accounting for 43.8% (132/301) PCG cases, of which, 15 mutations were novel. To the best of our knowledge the present study reports the largest series of PCG cases screened so far. The identified mutations included 8 frameshift (6 deletions, 1 insertion and 1 duplication), 2 nonsense and 28 missense mutations. The novel mutations included 3 deletions and 12 missense mutations. To the best of our knowledge, the present study exhibited the maximum (n=38) number of different types of mutations compared to other reports from Iran (n=19), Brazil (n=11), Australia (n=10), Saudi Arabia (n=8), Turkey (n=8), Japan (n=7), Indonesia (n=4), where not more than 20 different types of mutations have been reported. This could be attributed to the large sample size or due to the high geographical diversity in our population. The proportion of *CYP1B1* mutation in our patient cohort was similar to those reported from Brazil

(50%), Indonesia (33.3%), Turkey (42.9%), France (48.4%), Morocco (34.4%) and Mexico (33.3%). Majority of the identified mutations were missense (73.7%), similar to other populations from Australia (70.0%), Turkey (75%), Kuwait (75%) and Indonesia (75%). Among the missense mutations, 92% (35/38) were identified in the cytosolic domain of the protein, which is similar to that seen in populations from Saudi Arabia (100%), Australia (90%), Japan (91%), Turkey (87.5%), Ecuador (100%), Indonesia (100%), and Mexico (100%). Arg368His was the most prevalent mutation identified in the present study that accounted for 20.9% (63/301) of the cases. However, no significant association was identified between Arg368His mutation and the severity of the disease in terms of age at onset, corneal diameter and IOP at presentation.

Of the 301 PCG cases screened for *CYP1B1*, 169 cases (56.1%) did not harbor any *CYP1B1* mutation. A similar scenario was observed in other PCG populations from Brazil (50%), Japan (63.6%), Morocco (65.6%), France (51.6%), Turkey (57.1%) and Mexico (66.7%). These observations suggest the involvement of other candidate genes in PCG. There were no significant differences between cases with and without *CYP1B1* mutation with respect to IOP at presentation ( $p = 0.16$ ) and mean corneal diameter ( $p = 0.18$ ).

Two candidate genes viz. *MYOC* and *FOXC1* were screened in the cases that were either heterozygous ( $n=41$ ) or without any mutation ( $n=169$ ) in *CYP1B1*. *MYOC* is a candidate gene for juvenile and adult onset forms of Primary open angle glaucoma. On the other hand *FOXC1* is a member of winged helix/forkhead family of transcription factors and is associated with various anterior segment anomalies. Moreover, histologically, the mice with heterozygous null allele (*Foxc1*<sup>+/-</sup>) were found to have anterior segment abnormalities similar to human Axenfeld Reiger anomaly and congenital glaucoma patients. Based on these facts *MYOC* and *FOXC1* were selected as

potential candidates for screening in order to determine their possible involvement in disease pathogenesis.

Screening of *MYOC* led to the identification of two heterozygous missense (Gln48His and Tyr479His) mutations in 4.3% (9/210) cases, which was similar to its global frequency (3-5%) in POAG. To the best of our knowledge, this is the first report on the involvement of *MYOC* that accounted for a small proportion of PCG cases. The Gln48His was the most prevalent mutation (3.8%) in PCG similar to other studies on Indian POAG patients from different geographical regions indicating it to be a potential risk factor in glaucoma pathogenesis. Digenic inheritance of *CYP1B1* and *MYOC* was observed in a PCG family where the proband was heterozygous for both the *CYP1B1* (Arg368His) and *MYOC* (Gln48His) mutations, while his asymptomatic parents carried either of the heterozygous mutant allele. The patient with both *CYP1B1* and *MYOC* mutations exhibited a relatively severe phenotype with respect to IOP at presentation in comparison to other cases with only *MYOC* mutations. The severity of the phenotype in this case could be due to the effect of two mutant alleles in two different genes.

Screening of *FOXC1* gene led to the identification of 5 novel heterozygous mutations (His128Arg, Cys135Tyr, g.1086delC, g.1155delAAA and g.1947dup25) in 2.4% (5/210) cases. The inheritance of *FOXC1* with *CYP1B1* mutations were observed in two PCG families, but a clear-cut digenic pattern could not be established. In one family (PCG100), the proband inherited the *FOXC1* mutation (g.1086delC) from his mother and *CYP1B1* mutation (Arg368His) from his father, respectively. The mother was diagnosed to have optic atrophy, superior oblique palsy with raised IOP. Both the siblings of proband were carriers for Arg368His and were phenotypically normal at presentation. In the second family (PCG196), both the parents along with proband's sibling were heterozygous for the *FOXC1* (g.1155delAAA) mutation. The proband

inherited the *CYP1BI* mutation (Arg368His) from his mother whereas father and sibling were normal for this change. Neither the parents nor the sibling exhibited any signs of glaucoma at presentation. Since this mutation was identified in three unaffected control subjects without any signs of glaucoma at presentation, the association of g.1155delAAA with the disease phenotype could not be assessed. Comparison of clinical parameters of the patients with different *FOXCI* mutations showed similar clinical manifestation.

Genotype phenotype correlation indicated that IOP was as a significant risk factor in patients with *CYP1BI* mutations. These cases had poor prognosis in terms of IOP reduction following surgical intervention up to one year, compared to cases that did not harbor *CYP1BI* mutation. However, no significant difference ( $p>0.5$ ) was observed between the cases with and without *CYP1BI* mutations, in terms of IOP reduction, after 1 year of their surgical intervention.

The current study provides information on the mutation spectrum of three candidate genes (*CYP1BI*, *MYOC* and *FOXCI*) in PCG cases where they jointly accounted for 48% (145/301) of cases. The data obtained from the present study provides a better understanding on the genetic basis of PCG in the Indian context. It would also help in developing a reliable diagnostic method for screening of prevalent mutations in *CYP1BI* in the predisposed families. This study also indicated a potential association of two candidate genes (*MYOC* and *FOXCI*) with PCG. However, screening of *MYOC* and *FOXCI* in other PCG populations is warranted to substantiate their involvement in disease pathogenesis. The genotype-phenotype correlation showed the severity of disease, in terms of IOP reduction, in the cases with *CYP1BI* mutation. However, more studies on other PCG populations are required to validate this finding.



**CHAPTER 7: SPECIFIC CONTRIBUTIONS OF THE STUDY**

The salient findings of the present study in the background of existing literature are listed below:

1. *CYP11B* mutations accounted for 43.8% (132/301) of PCG cases. The frequency of *CYP11B* mutations was similar to the studies from Brazil (50%), Indonesia (33.3%), Turkey (42.9%), France (48.4%), Morocco (34.4%) and Mexico (33.3%) but lower than the inbred populations from Slovakia (100%), Saudi Arabia (92%), Kuwait (70.6%) and Iran (84.6%).
2. A total of 38 different mutations were identified, of which 15 were novel. To the best of our knowledge, the present cohort exhibited the maximum number (n=38) of different types of mutations compared to other reports from Iran (n=19), Brazil (n=11), Australia (n=10), Saudi Arabia (n=8), Turkey (n=8), Japan (n=7), Indonesia (n=4), where not more than 20 different types of mutations have been reported. This could be attributed to the large sample size or due to the high geographical diversity in our population.
3. The vast spectrum of the mutations included missense (73%), deletions (15.8%) and nonsense (5.3%) mutations. The missense mutations were similar to PCG populations from Australia (70.0%), Turkey (75%), Kuwait (75%) and Indonesia (75%).
4. Among the missense mutations, 92% (35/38) were identified in the cytosolic domain of the protein, similar to that observed in other populations from Saudi Arabia (100%), Iran (84.2%), Australia (90%), Japan (91%), Turkey (87.5%), Ecuador (100%), Kuwait (75%), Indonesia (100%) and Mexico (100%).
5. Arg368His was the most prevalent missense mutation that accounted for 20.9% (63/301) of PCG cases. This mutation has also been reported from

various other PCG populations of Saudi Arabia (1.8%), Brazil (1.9%), Iran (10.6%), Australia (2.7%) and Turkey (5.7%) in minor proportions.

6. Genotype-phenotype correlation revealed that cases with *CYP1B1* mutations had poor prognosis of the disease in terms of IOP reduction following surgical intervention.
7. No significant association was identified between Arg368His mutation and the severity of disease condition in terms of age at onset, corneal diameter and IOP at presentation.
8. This study suggested the possible involvement of two other candidate genes (*MYOC* and *FOXC1*) in a smaller proportion of PCG. To the best of our knowledge, this is the first study to show the co-inheritance of *MYOC* and *FOXC1* with *CYP1B1* in PCG.
9. The digenic inheritance of *CYP1B1* and *MYOC* could be established in one PCG (PCG095) family, suggesting that these genes might be interacting through common biochemical pathway.
10. The three candidate genes (*CYP1B1*, *MYOC* and *FOXC1*) jointly accounted for 48% (145/301) of the PCG cases.
11. The information provided by the present study would help in a better understanding of the genetic basis of PCG. However, similar studies are needed to further substantiate the novel findings of the present study.

## LIMITATIONS OF THE STUDY

The work presented in this thesis has provided novel and useful information on the involvement of other candidate genes (*MYOC* and *FOXC1*) with PCG. This information can be helpful for further studies in unraveling the interactions of these genes with the known candidate gene *CYP11B1* in PCG pathogenesis. However, the present study had the following limitations:

- The candidate gene screening was primarily focused on the coding regions of the gene. Screening of the promoter and other regulatory regions of these candidate genes would have provided a comprehensive picture on their association with disease pathogenesis.
- Based on structural variations in the genome, copy number variations (CNV) have become a major tool in understanding the disease pathophysiology. While CNVs have not been analyzed in PCG, this may have provided some clues towards disease association.

## FUTURE SCOPE OF THE WORK

- The present study provided further evidence on the association of *CYP11B1* mutations among Indian PCG cases. The study revealed that *CYP11B1* is a major candidate gene that accounted for 44% of PCG. Hence the functional analysis of the observed mutations could shed some light on the disease pathogenesis.
- The data obtained from the present study would be helpful in designing a reliable diagnostic method for screening the prevalent mutations in *CYP11B1* in populations that can help in a better prognosis of the disease in the predisposed families
- The study also provided novel information on the association of two other candidate genes (*MYOC* and *FOXCI*) in PCG. Whether these genes interact with *CYP11B1* through common biochemical pathways and their effect on expression and function at the cellular level would provide a better understanding of the biochemical pathways in PCG.

## REFERENCES

1. Achary MS, Reddy AB, Chakrabarti S, Panicker SG, Mandal AK, Ahmed N, Balasubramanian D, Hasnain SE, Nagarajaram HA. Disease-causing mutations in proteins: structural analysis of the CYP1B1 mutations causing primary congenital glaucoma in humans. *Biophys J*. 2006; 91: 4329-39.
2. Acharya M, Mookherjee S, Bhattacharjee A, Bandyopadhyay AK, Daulat Thakur SK, Bhaduri G, Sen A, Ray K. Primary role of CYP1B1 in Indian juvenile-onset POAG patients. *Mol Vis*. 2006; 12:399-404.
3. Akarsu AN, Turacli ME, Aktan SG, Barsoum-Homsy M, Chevrette L, Sayli BS, Sarfarazi M. A second locus (GLC3B) for primary congenital glaucoma (Buphthalmos) maps to the 1p36 region. *Hum Mol Genet*. 1996; 5:1199-203.
4. Akillu E, Oscarson M, Hidestrand M, Leidvik B, Otter C, Ingelman-Sundberg M. Functional analysis of six different polymorphic CYP1B1 enzyme variants found in an Ethiopian population. *Mol Pharmacol*. 2002; 61:586-94.
5. Alfidhli S, Behbehani A, Elshafey A, Abdelmoaty S, Al-Awadi S. Molecular and clinical evaluation of primary congenital glaucoma in Kuwait. *Am J Ophthalmol*. 2006; 141:512-6.
6. Allingham RR, Wiggs JL, De La Paz MA, Vollrath D, Tallett DA, Broomer B, Jones KH, Del Bono EA, Kern J, Patterson K, Haines JL, Pericak-Vance MA. Gln368STOP *myocilin* mutation in families with late-onset primary open-angle glaucoma. *Invest Ophthalmol Vis Sci*. 1998; 39:2288-95.
7. Alward WL, Fingert JH, Coote MA, Johnson AT, Lerner SF, Junqua D, Durcan FJ, McCartney PJ, Mackey DA, Sheffield VC, Stone EM. Clinical features associated with mutations in the chromosome 1 open-angle glaucoma gene (*GLC1A*). *N Engl J Med*. 1998; 338:1022-7.
8. Alward WL, Kwon YH, Khanna CL, Johnson AT, Hayreh SS, Zimmerman MB, Narkiewicz J, Andorf JL, Moore PA, Fingert JH, Sheffield VC, Stone EM. Variations in the *myocilin* gene in patients with open-angle glaucoma. *Arch Ophthalmol*. 2002; 120:1189-97.
9. Anderson DR. The development of the trabecular meshwork and its abnormality in primary infantile glaucoma. *Trans Am Ophthalmol Soc*. 1981; 79:458-85.
10. Bagiyeva S, Marfany G, Gonzalez-Angulo O, Gonzalez-Duarte R. Mutational screening of *CYP1B1* in Turkish PCG families and functional analyses of newly detected mutations. *Mol Vis*. 2007; 13:1458-68.
11. Barkan O. Pathogenesis of congenital glaucoma: gonioscopic and anatomic observation of the angle of the anterior chamber in the normal eye and in congenital glaucoma. *Am J Ophthalmol*. 1955; 40:1-11.

12. Bejjani BA, Lewis RA, Tomey KF, Anderson KL, Dueker DK, Jabak M, Astle WF, Otterud B, Leppert M, Lupski JR. Mutations in *CYP1B1*, the gene for cytochrome P4501B1, are the predominant cause of primary congenital glaucoma in Saudi Arabia. *Am J Hum Genet.* 1998; 62: 325-33.
13. Bejjani BA, Stockton DW, Lewis RA, Tomey KF, Dueker DK, Jabak M, Astle WF, Lupski JR. Multiple *CYP1B1* mutations and incomplete penetrance in an inbred population segregating primary congenital glaucoma suggest frequent de novo events and a dominant modifier locus. *Hum Mol Genet.* 2000; 12:367-74.
14. Belmouden A, Melki R, Hamdani M, Zaghoul K, Amraoui A, Nadifi S, Akhayat O, Garchon HJ. A novel frameshift founder mutation in the *cytochrome P450 1B1 (CYP1B1)* gene is associated with primary congenital glaucoma in Morocco. *Clin Genet.* 2002; 62:334-9.
15. Bennett RL, Steinhaus KA, Uhrich SB, O'Sullivan CK, Resta RG, Lochner-Doyle D, Markel DS, Vincent V, Hamanishi J. Recommendations for standardized human pedigree nomenclature. Pedigree Standardization Task Force of the National Society of Genetic Counselors. *Am J Hum Genet.* 1995; 56:745-52.
16. Berk AJ, Sharp PA. Sizing and mapping of early adenovirus mRNAs by gel electrophoresis of S1 endonuclease-digested hybrids. *Cell.* 1977; 12:721-32.
17. Berry FB, Saleem RA, Walter MA. FOXC1 transcriptional regulation is mediated by N- and C- terminal activation domains and contains a phosphorylated transcriptional inhibitory domain. *J Biol Chem.* 2002; 277:10292-97.
18. Bhattacharjee A, Acharya M, Mukhopadhyay A, Mookherjee S, Banerjee D, Bandopadhyay AK, Thakur SK, Sen A, Ray K. Myocilin variants in Indian patients with open-angle glaucoma. *Arch Ophthalmol.* 2007; 125:823-9.
19. Bidinost C, Hernandez N, Edward DP, Al-Rajhi A, Lewis RA, Lupski JR, Stockton DW, Bejjani BA. Of mice and men: tyrosinase modification of congenital glaucoma in mice but not in humans. *Invest Ophthalmol Vis Sci.* 2006; 47:1486-90.
20. Bron AJ, Tripathi RC, Tripathi BJ. *Wolff's anatomy of the eye and orbit.* 8<sup>th</sup> edition. Chapman & Hall. London SE1 8HN, UK. 1997.
21. Buters JT, Sakai S, Richter T, Pineau T, Alexander DL, Savas U, Doehmer J, Ward JM, Jefcoate CR, Gonzalez FJ. Cytochrome P450 CYP1B1 determines susceptibility to 7, 12-dimethylbenz[a]anthracene-induced lymphomas. *Proc Natl Acad Sci U S A.* 1999; 96:1977-82.
22. Caballero M, Rowlette LL, Borrás T. Altered secretion of a TIGR/MYOC mutant lacking the olfactomedin domain. *Biochem Biophys Acta.* 2000; 1502: 447-60.

23. Carpel EF, Engstrom PF. The normal cup-disk ratio. *Am J Ophthalmol.* 1981; 91:588-97.
24. Cella W, Cabral de Vasconcellos JP, Barbosa de Melo M, Kneipp B, Costa F, Longui CA, Costa F, Longui CA, Costa VP. Structural assessment of PITX2, FOXC1, CYP1B1 and GJA1 genes in patients with Axenfeld-Rieger syndrome with developmental glaucoma. *Invest Ophthalmol Vis Sci.* 2006; 47: 1803-9.
25. Chakrabarti S, Devi KR, Komatireddy S, Kaur K, Parikh RS, Mandal AK, Chandrasekhar G, Thomas R. Glaucoma-associated CYP1B1 mutations share similar haplotype backgrounds in POAG and PACG phenotypes. *Invest Ophthalmol Vis Sci.* 2007; 48:5439-44.
26. Chakrabarti S, Kaur K, Kaur I, Mandal AK, Parikh RS, Thomas R, Majumder PP. Globally, CYP1B1 mutations in primary congenital glaucoma are strongly structured by geographic and haplotype backgrounds. *Invest Ophthalmol Vis Sci.* 2006; 47:43-7.
27. Chakrabarti S, Kaur K, Komatireddy S, Acharya M, Devi KR, Mukhopadhyay A, Mandal AK, Hasnain SE, Chandrasekhar G, Thomas R, Ray K. Gln48His is the prevalent *myocilin* mutation in primary open angle and primary congenital glaucoma phenotypes in India. *Mol Vis.* 2005; 11:111-3.
28. Challa P, Herndon LW, Hauser MA, Broomer BW, Pericak-Vance MA, Ababio-Danso B, Allingham RR. Prevalence of myocilin mutations in adults with primary open-angle glaucoma in Ghana, West Africa. *J Glaucoma.* 2002; 11:416-20.
29. Chambers D, Wilson L, Malcolm M, Lumsden A. RALDH-independent generation of retinoic acid during vertebrate embryogenesis by CYP1B1. *Development.* 2007; 134: 1369-83.
30. Chavarria-Soley G, Michels-Rautenstrauss K, Pasutto F, Flikier D, Flikier P, Cirak S, Bejjani B, Winters DL, Lewis RA, Mardin C, Reis A, Rautenstrauss B. Primary congenital glaucoma and Rieger's anomaly: extended haplotypes reveal founder effects for eight distinct *CYP1B1* mutations. *Mol Vis.* 2006; 12:523-31.
31. Chavarría-Soley G, Rautenstrauss BI, Azofeifa J. Glaucoma in Costa Rica. Initial approaches. *Rev Biol Trop.* 2004; 52:507-20.
32. Chitsazian F, Tusi BK, Elahi E, Saroei HA, Sanati MH, Yazdani S, Pakravan M, Nilforooshan N, Eslami Y, Mehrjerdi MA, Zareei R, Jabbarvand M, Abdolahi A, Lasheyee AR, Etemadi A, Bayat B, Sadeghi M, Banoei MM, Ghafarzadeh B, Rohani MR, Rismanchian A, Thorstenson Y, Sarfarazi M. *CYP1B1* mutation profile of Iranian primary congenital glaucoma patients and associated haplotypes. *J Mol Diagn.* 2007; 9:382-93.

33. Choudhary D, Jansson I, Rezaul K, Han DK, Sarfarazi M, Schenkman JB. Cyp1b1 protein in the mouse eye during development: an immunohistochemical study. *Drug Metab Dispos.* 2007; 35:987-94.
34. Coca-Prados M, Escribano J. Role of *MYOC* and *OPTN* sequence variations in Spanish patients with primary open-angle glaucoma. *Mol Vis.* 2007; 13:862-72.
35. Colomb E, Kaplan J, Garchon HJ. Novel cytochrome P4501B1 (*CYP1B1*) mutations in patients with primary congenital glaucoma in France. *Hum Mut.* 2003; 22:496.
36. Curry SM, Daou AG, Hermanns P, Molinari A, Lewis RA, Bejjani BA. Cytochrome P4501B1 mutations cause only part of primary congenital glaucoma in Ecuador. *Ophthalmic Genet.* 2004; 25:3-9.
37. Dandona L, Dandona R, Srinivas M, Giridhar P, Vikas K, Prasad MN, John RK, McCarty CA, Rao GN. Blindness in the Indian state of Andhra Pradesh. *Invest Ophthalmol Vis Sci.* 2001; 42:908-16.
38. Dandona L, Dandona R, Srinivas M, Mandal P, John RK, McCarty CA, Rao GN. Open-angle glaucoma in an urban population in southern India: the Andhra Pradesh eye disease study. *Ophthalmology.* 2000; 107:1702-9.
39. Dandona L, Williams JD, Williams BC, Rao GN. Population – based assessment of childhood blindness in Southern India. *Arch Ophthalmol.* 1998; 116: 545-46.
40. Das J, Bhomaj S, Chaudhuri Z, Sharma P, Negi A, Dasgupta A. Profile of glaucoma in a major eye hospital in north India. *Indian J Ophthalmol.* 2001; 49:25-30.
41. DeLuise VP, Anderson DR. Primary infantile glaucoma (congenital glaucoma). *Surv Ophthalmol.* 1983; 28:1.
42. Dib C, Fauré S, Fizames C, Samson D, Drouot N, Vignal A, Millasseau P, Marc S, Hazan J, Seboun E, Lathrop M, Gyapay G, Morissette J, Weissenbach J. A comprehensive genetic map of the human genome based on 5,264 microsatellites. *Nature.* 1996; 380:152-4.
43. Dimasi DP, Hewitt AW, Straga T, Pater J, MacKinnon JR, Elder JE, Casey T, Mackey DA, Craig JE. Prevalence of *CYP1B1* mutations in Australian patients with primary congenital glaucoma. *Clin Genet.* 2007; 72:255-60.
44. Dolwick KM, Swanson HI, Bradfield CA. In vitro analysis of Ah receptor domains involved in ligand-activated DNA recognition. *Proc Natl Acad Sci, U S A.* 1993; 90:8566-70.
45. Doshi M, Marcus C, Bejjani BA, Edward DP. Immunolocalization of *CYP1B1* in normal, human, fetal and adult eyes. *Exp Eye Res.* 2006; 82:24-32.



46. Dryja TP, Hahn LB, Kajiwarra K, Berson EL. Dominant and digenic mutations in the peripherin/RDS and RDM1 genes in retinitis pigmentosa. *Invest Ophthalmol Vis Sci.* 1997; 38: 1972-82.
47. El-Ashry MF, Abd El-Aziz MM, Bhattacharya SS. A clinical and molecular genetic study of Egyptian and Saudi Arabian patients with primary congenital glaucoma (PCG). *J Glaucoma.* 2007; 16:104-11.
48. Fan BJ, Leung DY, Wang DY, Gobeil S, Raymond V, Tam PO, Lam DS, Pang CP. Novel myocilin mutation in a Chinese family with juvenile-onset open-angle glaucoma. *Arch Ophthalmol.* 2006; 124:102-6.
49. Faucher M, Anctil JL, Rodrigue MA, Duchesne A, Bergeron D, Blondeau P, Côté G, Dubois S, Bergeron J, Arseneault R, Morissette J, Raymond V; Québec Glaucoma Network. Founder TIGR/myocilin mutations for glaucoma in the Québec population. *Hum Mol Genet.* 2002; 11:2077-90.
50. Fingert JH, Heon E, Liebmann JM, Yamamoto T, Craig JE, Rait J, Kawase K, Hoh ST, Buys YM, Dickinson J, Hockey RR, Williams-Lyn D, Trope G, Kitazawa Y, Ritch R, Mackey DA, Alward WL, Sheffield VC, Stone EM. Analysis of myocilin mutations in 1703 glaucoma patients from five different populations. *Hum Mol Genet.* 1999; 8: 899-905.
51. Flammer J. *Glaucoma.* 2nd edition. Gottingen, Germany. Hogrefe & Huber publishers. 2003.
52. Forsman E, Lemmelä S, Varilo T, Kristo P, Forsius H, Sankila EM, Järvelä I. The role of *TIGR* and *OPTN* in Finnish glaucoma families: a clinical and molecular genetic study. *Mol Vis.* 2003; 9:217-22.
53. Fuse N, Takahashi K, Yokokura S, Nishida K. Novel mutations in the *FOXC1* gene in Japanese patients with Axenfeld-Rieger syndrome. *Mol Vis.* 2007; 13:1005-9.
54. Gencik A, Gencikova A, Ferák V. Population genetical aspects of primary congenital glaucoma. I. Incidence, prevalence, gene frequency, and age of onset. *Hum Genet.* 1982; 61:193-7.
55. Gencik A. Epidemiology and genetics of primary congenital glaucoma in Slovakia: description of a form of primary congenital glaucoma in gypsies with autosomal recessive inheritance and complete penetrance. *Dev Ophthalmol.* 1989; 16: 76-115.
56. Gobeil S, Rodrigue MA, Moisan S, Nguyen TD, Polansky JR. Intracellular sequestration of heterooligomers formed by wild type and glaucoma-causing myocilin mutants. *Invest Ophthalmol Vis Sci.* 2004; 45: 3560-67.
57. Gong G, Kosoko-Lasaki, Haynatzki GR, Wilson MR. Genetic dissection of myocilin glaucoma. *Hum Mol Genet.* 2004; 13: R91-R102.

58. Gonzalez FJ, Kimura S. Study of P450 function using gene knockout and transgenic mice. *Arch Biochem Biophys*. 2003; 409:153-8.
59. Granadino B, Perz-Sanchez C, rey-Campos J. Forkhead Transcription factors. *Curr Genomics*. 2000; 1: 353-82.
60. Gu L, Gonzalez FJ, Kalow W, Tang BK. Biotransformation of caffeine, paraxanthine, theobromine and theophylline by cDNA-expressed human CYP1A2 and CYP2E1. *Pharmacogenetics*. 1992; 2:73-7.
61. Guengerich FP, Shimada T. Oxidation of toxic and carcinogenic chemicals by human cytochrome P-450 enzymes. *Chem Res Toxicol*. 1991; 4:391-407.
62. Gupta SP, Mehta P. Average distribution of intraocular pressure in Indians by applanation tonometer. *Indian J Ophthalmol*. 1971; 19:85-90.
63. Hashemi H, Fotouhi A, Mohammad K. The Tehran Eye Study: research design and eye examination protocol. *BMC Ophthalmol*. 2003; 3:8.
64. Hasler JA, Estabrook R, Murray M, Pikuleva I, Waterman M, Capdevila J, Holla V, Christian H, Falck JR, Farrell G, Kaminsky LS, Spivack SD, Boitier E, Beaune P. Pharmacogenetics of cytochromes P450. *Molecular Aspects of Medicine*. 1999; 20: 25-137.
65. Hayashi K. PCR-SSCP: a simple and sensitive method for detection of mutations in the genomic DNA. *PCR Methods Appl*. 1991; 1:34-8.
66. Hollander DA, Sarfarazi M, Stoilov I, Wood IS, Fredrick DR, Alvarado JA. Genotype and phenotype correlations in congenital glaucoma. *Trans Am Ophthalmol Soc*. 2006; 104:183-95.
67. Honkanen RA, Nishimura DY, Swiderski RE, Bennett SR, Hong S, Kwon YH, Stone EM, Sheffield VC, Alward WL. A family with Axenfeld-Rieger syndrome and Peters Anomaly caused by a point mutation (Phe112Ser) in the *FOXC1* gene. *Am J Ophthalmol*. 2003; 135:368-75.
68. Ishikawa K, Funayama T, Ohtake Y, Tanino T, Kurosaka D, Suzuki K, Ideta H, Fujimaki T, Tanihara H, Asaoka R, Naoi N, Yasuda N, Iwata T, Mashima Y. Novel *MYOC* gene mutation, Phe369Leu, in Japanese patients with primary open-angle glaucoma detected by denaturing high-performance liquid chromatography. *J Glaucoma*. 2004; 13:466-71.
69. Ito YA, Footz TK, Murphy TC, Courtens W, Walter MA. Analyses of novel L130F missense mutation in *FOXC1*. *Arch Ophthalmol*. 2007; 125: 128-35.
70. Izumi K, Mashima Y, Obazawa M, Ohtake Y, Tanino T, Miyata H, Zhang Q, Oguchi Y, Tanaka Y, Iwata T. Variants of the myocilin gene in Japanese patients with normal-tension glaucoma. *Ophthalmic Res*. 2003; 35:345-50.

71. Jacob A, Thomas R, Koshi SP, Braganza A, Muliylil J. Prevalence of primary glaucoma in an urban south Indian population. *Indian J Ophthalmol.* 1998; 46:81-6.
72. Jacobson N, Andrews M, Shepard AR, Nishimura D, Searby C, Fingert JH, Hageman G, Mullins R, Davidson BL, Kwon YH, Alward WL, Stone EM, Clark AF, Sheffield VC. Non-secretion of mutant proteins of the glaucoma gene myocilin in cultured trabecular meshwork cells and in aqueous humor. *Hum Mol Genet.* 2001; 10:117-25.
73. Jansson I, Stoilov I, Sarfarazi M, Schenkman JB. Effect of two mutations of human *CYP1B1*, G61E and R469W, on stability and endogenous steroid substrate metabolism. *Pharmacogenetics.* 2001; 11:793-801.
74. Jansson M, Marknell T, Tomic L, Larsson LI, Wadelius C. Allelic variants in the *MYOC/TIGR* gene in patients with primary open-angle, exfoliative glaucoma and unaffected controls. *Ophthalmic Genet.* 2003; 24:103-10.
75. Johnson DH. Myocilin and glaucoma: A TIGR by the tail? *Arch Ophthalmol.* 2000; 118:974-8.
76. Kakiuchi-Matsumoto T, Isashiki Y, Ohba N, Kimura K, Sonoda S, Unoki K. *Cytochrome P450 1B1* gene mutations in Japanese patients with primary congenital glaucoma. *Am J Ophthalmol.* 2001; 131:345-50.
77. Kanagavalli J, Krishnadas SR, Pandaranayaka E, Krishnaswamy S, Sundaresan P. Evaluation and understanding of *myocilin* mutations in Indian primary open angle glaucoma patients. *Mol Vis.* 2003; 9: 606-14.
78. Kanagavalli J, Pandaranayaka PJ, Krishnadas SR, Krishnaswamy S, Sunderesan P. In vitro study on the secretion of the Gly367Arg mutant myocilin protein. *Mol Vis.* 2007; 13: 1161-8.
79. Kanski JJ. *Clinical Ophthalmology: A systematic approach.* 5th ed. Butterworth-Heinemann. 2003.
80. Kaur K, Reddy ABM, Mukhopadhyay A, Mandal AK, Hasnain SE, Ray K, Thomas R, Balasubramanian D, Chakrabarti S. Myocilin gene implicated in primary congenital glaucoma. *Clin Genet.* 2005; 67: 335-40.
81. Kawase C, Kawase K, Taniguchi T, Sugiyama K, Yamamoto T, Kitazawa Y, Alward WL, Stone EM, Nishimura DY, Sheffield VC. Screening for mutations of Axenfeld-Rieger syndrome caused by *FOXCI* gene in Japanese patients. *J Glaucoma.* 2001; 10:477-82.
82. Kiefer G, Schwenn O, Grehn F. Correlation of postoperative axial length growth and intraocular pressure in congenital glaucoma- a retrospective study in trabeculotomy and goniotomy. *Graefes Arch Clin Exp Ophthalmol.* 2001; 239: 893-9.

83. Kim BS, Savinova OV, Reedy MV, Martin J, Lun Y, Gan L, Smith RS, Tomarev SI, John SW, Johnson RL. Targeted Disruption of the Myocilin Gene (*MYOC*) Suggests that Human Glaucoma-Causing Mutations Are Gain of Function. *Mol Cell Biol*. 2001; 21:7707-13.
84. Klein BE, Klein R, Linton KL. Intraocular pressure in an American community. The Beaver Dam Eye Study. *Invest Ophthalmol Vis Sci*. 1992; 33:2224-8.
85. Komatireddy S, Chakrabarti S, Mandal AK, Reddy AB, Sampath S, Panicker SG, Balasubramanian D. Mutation spectrum of *FOXC1* and clinical genetic heterogeneity of Axenfeld-Rieger anomaly in India. *Mol Vis*. 2003; 9:43-8.
86. Krawczyński MR, Czarny-Ratajczak M, Pecold K, Latos-Bieleńska A. Study of TIGR gene in patients with primary open angle glaucoma. *Klin Oczna*. 2004; 106:564-8.
87. Kubota R, Kudoh J, Mashima Y, Asakawa S, Minoshima S, Hejtmancik JF, Oguchi Y, Shimizu N. Genomic organisation of the human myocilin gene (*MYOC*) responsible for primary open angle glaucoma (*GLC1A*). *Biochem Biophys Res Commun*. 1998; 242:396-400.
88. Kubota R, Mashima Y, Ohtake Y, Tanino T, Kimura T, Hotta Y, Kanai A, Tokuoka S, Azuma I, Tanihara H, Inatani M, Inoue Y, Kudoh J, Oguchi Y, Shimizu N. Novel mutations in the myocilin gene in Japanese glaucoma patients. *Hum Mutat*. 2000; 16:270.
89. Kumar A, Basavaraj MG, Gupta SK, Qamar, Ali AM, Bajaj V, Ramesh TK, Prakash DR, Shetty JS, Dorairaj SK. Role of *CYP1B1*, *MYOC*, *OPTN*, and *OPTC* genes in adult-onset primary open-angle glaucoma: predominance of *CYP1B1* mutations in Indian patients. *Mol Vis*. 2007; 13:667-76.
90. Lam DS, Leung YF, Chua JK, Baum L, Fan DS, Choy KW, Pang CP. Truncations in the TIGR gene in individuals with and without primary open angle glaucoma. *Invest Ophthalmol Vis Sci*. 2000; 41:1386-91.
91. Lee JS, Lee SH, Oum BS, Chung JS, Cho BM, Hong JW. Relationship between intraocular pressure and systemic health parameters in a Korean population. *Clin Experiment Ophthalmol*. 2002; 30:237-41.
92. Leske MC, Connell AM, Wu SY, Hyman L, Schachat AP. Distribution of intraocular pressure. The Barbados Eye Study. *Arch Ophthalmol*. 1997; 115:1051-7.
93. Levy J, Carmi R, Rosen S, Lifshitz T. Primary congenital glaucoma presenting within the first three months of life in a Bedouin population: prognostic factors. *J Glaucoma*. 2005; 14:139-44.
94. Lewis DFV, Gillam EMJ, Everett SA, Shimada T. Molecular modelling of human *CYP1B1* substrate interactions and investigation of allelic variant effects on metabolism. *Chemico-Biological Interactions*. 2003; 145: 281-95.

95. Leydhecker W, Akiyama K, Neumann HG. Intraocular pressure in normal human eyes. *Klin Monatsblatter Augenheilkd Augenarztl Fortbild.* 1958; 133:662-70.
96. Libby RT, Smith RS, Savinova OV, Zabaleta A, Martin JE, Gonzalez FJ, John SW. Modification of ocular defects in mouse developmental glaucoma models by tyrosinase. *Science.* 2003; 299:1578-81.
97. Llobet A, Gasull X, Gual A. Understanding trabecular meshwork physiology: A key to the control of intraocular pressure? *News Physiol Sci.* 2003; 18: 205-9.
98. López-Garrido MP, Sánchez-Sánchez F, López-Martínez F, Aroca-Aguilar JD, Blanco-Marchite C, Coca-Prados M, Escribano J. Heterozygous CYP1B1 gene mutations in Spanish patients with primary open-angle glaucoma. *Mol Vis.* 2006; 12:748-55.
99. Lopez-Martinez F, Lopez-Garrido MP, Sanchez-Sanchez F, Campos-Mollo E, Coca-Prados M, Escribano J. Role of MYOC and OPTN sequence variations in Spanish patients with primary open-angle glaucoma. *Mol Vis.* 2007; 13:862-72.
100. Mabuchi F, Yamagata Z, Kashiwagi K, Tang S, Iijima H, Tsukahara S. Analysis of myocilin gene mutations in Japanese patients with normal tension glaucoma and primary open-angle glaucoma. *Clin Genet.* 2001; 59:263-8.
101. Mandal AK, Netland PA. The pediatric glaucomas. Elsevier's Butterworth Heinemann. 2006.
102. Mandal AK, Gothwal VK, Bagga H, Nutheti R, Masoori T. Outcome of surgery on infants younger than 1 months with congenital glaucoma. *Ophthalmology.* 2003; 110: 1909-15.
103. Mashima Y, Suzuki Y, Sergeev Y, Ohtake Y, Tanino T, Kimura I, Miyata H, Aihara M, Tanihara H, Inatani M, Azuma N, Iwata T, Araie M. Novel cytochrome P4501B1 (CYP1B1) gene mutations in Japanese patients with primary congenital glaucoma. *Invest Ophthalmol Vis Sci.* 2001; 42:2211-6.
104. Mataftsi A, Achache F, Héon E, Mermoud A, Cousin P, Mettetz G, Schorderet DF, Munier FL. MYOC mutation frequency in primary open-angle glaucoma patients from Western Switzerland. *Ophthalmic Genet.* 2001; 22:225-31.
105. Maumenee EA. The pathogenesis of congenital glaucoma: a new theory. *Trans Am Ophthalmol Soc.* 1958; 56:507-70.
106. Mears AJ, Jordan T, Mirzayans F, Dubois S, Kume T, Parlee M, Ritch R, Koop B, Kuo W-L, Collins C, Marshall J, Gould DB, Pearce W, Carlsson P, Enerback S, Morissette J, Bhattacharya S, Hogan B, Raymond V, Walter MA. Mutations of the Forkhead/winged helix gene, FKHL7, in patients with Axenfeld-Rieger anomaly. *Am J Hum Genet.* 1998; 63: 1316-28.

107. Melki R, Colomb E, Lefort N, Brézin AP, Garchon HJ. *CYP1B1* mutations in French patients with early-onset primary open-angle glaucoma. *J Med Genet.* 2004; 41:647-51.
108. Melki R, Idhajji A, Driouiche S, Hassani M, Boukabboucha A, Akhayat O, Garchon H, Belmouden A. Mutational analysis of the *Myocilin* gene in patients with primary open-angle glaucoma in Morocco. *Ophthalmic Genet.* 2003; 24:153-60.
109. Messina –Bass OM, Gonzalez-Huerta LM, Chima-Galan C, Kofman-Alfaro SH, Rivera-Vega MR, Babayan –Mena I, Cuevas-Covarrubias SA. Molecular analysis of *CYP1B1* gene: identification of novel truncating mutations in patients with primary congenital glaucoma. *Ophthalmic Res.* 2007; 39: 17-23.
110. Michels-Rautenstrauss K, Mardin C, Wakili N, Jünemann AM, Villalobos L, Mejia C, Soley GC, Azofeifa J, Ozbey S, Naumann GO, Reis A, Rautenstrauss B. Novel mutations in the MYOC/GLC1A gene in a large group of glaucoma patients. *Hum Mutat.* 2002; 20:479-80.
111. Michels-Rautenstrauss KG, Mardin CY, Zenker M, Jordan N, Gusek-Schneider GC, Rautenstrauss BW. Primary congenital glaucoma: three case reports on novel mutations and combinations of mutations in the *GLC3A* (*CYP1B1*) gene. *J Glaucoma.* 2001; 10:354-7.
112. Mirzayans F, Gould DB, Héon E, Billingsley GD, Cheung JC, Mears AJ, Walter MA. Axenfeld-Rieger syndrome resulting from mutation of the *FKHL7* gene on chromosome 6p25. *Eur J Hum Genet.* 2000; 8:71-4.
113. Mitchell P, Smith W, Attebo K, Healey PR. Prevalence of open-angle glaucoma in Australia. The Blue Mountains Eye Study. *Ophthalmology.* 1996; 103:1661-9.
114. Morissette J, Clepet C, Moisan S, Dubois S, Winstall E, Vermeeren D, Nguyen TD, Polansky JR, Cote G, Anctil JL, Amyot M, Plante M, Falardeau P, Raymond V. Homozygotes carrying an autosomal dominant TIGR mutation do not manifest glaucoma. *Nat Genet.* 1998; 19: 319-21.
115. Mortemousque B, Amati-Bonneau P, Couture F, Graffan R, Dubois S, Colin J, Bonneau D, Morissette J, Lacombe D, Raymond V. Axenfeld-Rieger anomaly: a novel mutation in the forkhead box C1 (*FOXC1*) gene in a 4-generation family. *Arch Ophthalmol.* 2004; 122:1527-33.
116. Mukhopadhyay A, Acharya M, Mukherjee S, Ray J, Choudhury S, Khan M, Ray K. Mutations in MYOC gene of Indian primary open angle glaucoma patients. *Mol Vis.* 2002; 8:442-8.
117. Murphy TC, Saleem RA, Footz T, Ritch R, McGillivray B, Walter MA. The wing 2 region of the *FOXC1* forkhead domain is necessary for normal DNA-binding and transactivation functions. *Invest Ophthalmol Vis Sci.* 2004; 45:2531-8.

118. Murray GI, Melvin WT, Greenlee WF, Burke MD. Regulation, function, and tissue-specific expression of cytochrome P450 CYP1B1. *Annu Rev Pharmacol Toxicol.* 2001; 41:297-316.
119. Nema HV, Nema N. *Diagnostic Procedures in ophthalmology.* 1st ed. Alpha Science International. 2002.
120. Nishimura DY, Searby CC, Alward WL, Walton D, Craig JE, Mackey DA, Kawase K, Kanis AB, Patil SR, Stone EM, Sheffield VC. A spectrum of *FOXC1* mutations suggests gene dosage as a mechanism for developmental defects of the anterior chamber of the eye. *Am J Hum Genet.* 2001; 68:364-72.
121. Nishimura DY, Swiderski RE, Alward WLM, Searby CC, Patil SR, Bennet SR, Kanis AB, Gastier JM, Stone EM, Sheffield VC. The forkhead transcription factor FKHL7 is responsible for glaucoma phenotypes which map to 6p25. *Nat Genet.* 1998; 19: 140- 7.
122. Oefner PJ. Surface-charge reversed capillary zone electrophoresis of inorganic and organic anions. *Electrophoresis.* 1995; 16:46-56.
123. Ohtake Y, Tanino T, Suzuki Y, Miyata H, Taomoto M, Azuma N, Tanihara H, Araie M, Mashima Y. Phenotype of cytochrome P4501B1 gene (CYP1B1) mutations in Japanese patients with primary congenital glaucoma. *Br J Ophthalmol.* 2003; 87:302-4.
124. Orita M. Single-strand conformation polymorphism analysis. *Nippon Rinsho.* 1990; 48:170-5.
125. Pang CP, Leung YF, Fan B, Baum L, Tong WC, Lee WS, Chua JK, Fan DS, Liu Y, Lam DS. TIGR/MYOC gene sequence alterations in individuals with and without primary open-angle glaucoma. *Invest Ophthalmol Vis Sci.* 2002; 43:3231-5.
126. Panicker SG, Reddy AB, Mandal AK, Ahmed N, Nagarajaram HA, Hasnain SE, Balasubramanian D. Identification of novel mutations causing familial primary congenital glaucoma in Indian pedigrees. *Invest Ophthalmol Vis Sci.* 2002; 43:1358-66.
127. Panicker SG, Reddy AB, Mandal AK, Ahmed N, Nagarajaram HA, Hasnain SE. Correlation between genotype and phenotype in Indian primary congenital glaucoma patients. *Invest Ophthalmol Vis Sci.* 2004; 45: 1149-56.
128. Papadopoulos M, Cable N, Rahi J, Khaw PT; BIG Eye Study Investigators. The British Infantile and Childhood Glaucoma (BIG) Eye Study. *Invest Ophthalmol Vis Sci.* 2007; 48:4100-6.
129. Plášilová M, Feráková E, Kádasi L, Poláková H, Gerinec A, Ott J, Ferák V. Linkage of autosomal recessive primary congenital glaucoma to the *GLC3A* locus in Roms (Gypsies) from Slovakia. *Hum Hered.* 1998; 48:30-3.

130. Plášilová M, Stoilov I, Sarfarazi M, Kádasi L, Feráková E, Ferák V. Identification of a single ancestral *CYP1B1* mutation in Slovak Gypsies (Roms) affected with primary congenital glaucoma. *J Med Genet.* 1999; 36:290-4.
131. Povoia CA, Malta RF, Rezende Mde M, de Melo KF, Giannella-Neto D. Correlation between genotype and phenotype in primary open angle glaucoma of Brazilian families with mutations in exon 3 of the TIGR/MYOC gene. *Arq Bras Oftalmol.* 2006; 69: 289-97.
132. Quigley HA, Broman AT. The number of people with glaucoma worldwide in 2010 and 2020. *Br J Ophthalmol.* 2006; 90:262-7.
133. Quigley HA. Number of people with glaucoma worldwide. *Br J Ophthalmol.* 1996; 80:389-93.
134. Ramakrishnan R, Nirmalan PK, Krishnadas R, Thulasiraj RD, Tielsch JM, Katz J, Friedman DS, Robin AL. Glaucoma in a rural population of southern India: the Aravind comprehensive eye survey. *Ophthalmology.* 2003; 110:1484-90.
135. Ramprasad VL, George RJ, Sripriya S, Nirmaladevi J, Vijaya L, Kumarmanickavel G. Molecular genetic analysis of consanguineous south Indian family with congenital glaucoma: relevance of genetic testing and counseling. *Ophthalmic Genet.* 2007; 28:17-24.
136. Ramprasad VL, Sripriya S, Ronnie G, Nancarrow D, Saxena S, Hemamalini A, Kumar D, Vijaya L, Kumaramanickavel G. Genetic homogeneity for inherited congenital microcoria loci in an Asian Indian pedigree. *Mol Vis.* 2005; 11:934-40.
137. Raychaudhuri A, Lahiri SK, Bandyopadhyay M, Foster PJ, Reeves BC, Johnson GJ. A population based survey of the prevalence and types of glaucoma in rural West Bengal: the West Bengal Glaucoma Study. *Br J Ophthalmol.* 2005; 89:1559-64.
138. Raymond V. "Molecular genetics of the glaucomas: Mapping of the first five "GLC" loci,". *Am J Hum Genet.* 1997; 60: 272-277.
139. Reddy AB, Kaur K, Mandal AK, Panicker SG, Thomas R, Hasnain SE, Balasubramanian D, Chakrabarti S. Mutation spectrum of the *CYP1B1* gene in Indian primary congenital glaucoma patients. *Mol Vis.* 2004; 10:696-702.
140. Reddy AB, Panicker SG, Mandal AK, Hasnain SE, Balasubramanian D. Identification of R368H as a predominant *CYP1B1* allele causing primary congenital glaucoma in Indian patients. *Invest Ophthalmol Vis Sci.* 2003; 44:4200-3.
141. Resnikoff S, Pascolini D, Etya'ale D, Kocur I, Pararajasegaram R, Pokharel GP, Mariotti SP. Global data on visual impairment in the year 2002. *Bull World Health Organ.* 2004; 82:844-51.



142. Ritch R, Shields MB, Krupin T. *The Glaucomas*. Basic sciences. Second edition. Mosby-Year book, St. Louis, Missouri. USA. 1996.
143. Rojas B, Ramírez AI, de-Hoz R, Salazar JJ, Remírez JM, Triviño A. Structural changes of the anterior chamber angle in primary congenital glaucoma with respect to normal development. *Arch Soc Esp Ophthalmol*. 2006; 81:65-71.
144. Rose R, Karthikeyan M, Anandan B, Jayaraman G. Myocilin mutations among primary open angle glaucoma patients of Kanyakumari district, South India. *Mol Vis*. 2007; 13: 497-503.
145. Rotchford AP, Johnson GJ. Glaucoma in Zulus: a population-based cross-sectional survey in a rural district in South Africa. *Arch Ophthalmol*. 2002; 120:471-8.
146. Saccone S, De Sario A, Della Valle G, Bernardi G. The highest gene concentrations in the human genome are in telomeric bands of metaphase chromosomes. *Proc Natl Acad Sci, U S A*. 1992; 89:4913-7.
147. Saleem RA, Banerjee-Basu S, Berry FB, Baxevanis AD, Walter MA. Structural and functional analyses of disease-causing missense mutations in the forkhead domain of *FOXC1*. *Hum Mol Genet*. 2003; 12:2993-30053.
148. Sambrook J, Fritsch EF, Maniatis T: *Molecular cloning: a laboratory manual*: 2nd ed. Cold Spring Harbor (NY): Cold Spring Harbor Press.1989.
149. Sanger F, Coulson AR. A rapid method for determining sequences in DNA by primed synthesis with DNA polymerase. *J Mol Biol*. 1975; 94:441-8.
150. Sarfarazi M, Akarsu AN, Hossain A, Turacli ME, Aktan SG, Barsoum-Homsy M, Chevrette L, Sayli BS. Assignment of a locus (GLC3A) for primary congenital glaucoma (Buphthalmos) to 2p21 and evidence for genetic heterogeneity. *Genomics*. 1995; 30:171-7.
151. Sarfarazi M, Stoilov I. Molecular genetics of primary congenital glaucoma. *Eye*. 2000; 14:422-8.
152. Sena DF, Finzi S, Rodgers K, Del Bono E, Haines JL, Wiggs JL. Founder mutations of CYP1B1 gene in patients with congenital glaucoma from the United States and Brazil. *J Med Genet*. 2004; 41:e6.
153. Shaffer RN, Weiss DI. *Congenital and pediatric glaucomas*. St.Louis, CV Mobsby.1970.
154. Shaffer RN. Pathogenesis of congenital glaucoma; gonioscopic and microscopic anatomy. *Trans Am Acad Ophthalmol Otolaryngol*. 1955; 59: 297-308.

155. Shields MB, Buckley E, Klintworth GK, Thresher R. Axenfeld-Reiger syndrome. A spectrum of developmental disorders. *Surv Ophthalmol.* 1985; 29: 387-409.
156. Shields MB. *Textbook of glaucoma.* 5<sup>th</sup> edition. Baltimore; Williams and Wilkins.2005.
157. Shimada T, Gillam EM, Sutter TR, Strickland PT, Guengerich FP, Yamazaki H. Oxidation of xenobiotics by recombinant human cytochrome P450 1B1. *Drug Metab Dispos.* 1997; 25:617-22.
158. Shimada T, Hayes CL, Yamazaki H, Amin S, Hecht SS, Guengerich P, Sutter TR. Activation of chemically diverse procarcinogens by human cytochrome P-4501B1. *Cancer Research.* 1996; 56: 2979-84.
159. Shimada T, Watanabe J, Inoue K, Guengerich FP, Gillam EMJ. Specificity of 17 $\beta$ -oestradiol and benzo (a) pyrene oxidation by polymorphic human cytochrome P4501B1 variants substituted at residues 48,119 and 432. *Xenobiotica.* 2001; 31: 163-76.
160. Shimizu S, Lichter PR, Johnson AT, Zhou Z, Higashi M, Gottfredsdottir M, Othman M, Moroi SE, Rozsa FW, Schertzer RM, Clarke MS, Schwartz AL, Downs CA, Vollrath D, Richards JE. Age-dependent prevalence of mutations at the GLC1A locus in primary open-angle glaucoma. *Am J Ophthalmol.* 2000; 130:165-77.
161. Shiose Y, Kawase Y. A new approach to stratified normal intraocular pressure in a general population. *Am J Ophthalmol.* 1986; 101:714-21.
162. Sihota R, Tuli D, Dada T, Gupta V, Sachdeva MM. Distribution and determination of intraocular pressure in normal pediatric population. *J Pediatr Ophthalmol Strabismus.* 2006; 43: 14-18.
163. Sitorus R, Ardjo SM, Lorenz B, Preising M. CYP1B1 gene analysis in primary congenital glaucoma in Indonesian and European patients. *J Med Genet.* 2003; 40:e9.
164. Smith RS, Zabaleta A, Kume T, Savinova OV, Kidson SH, Martin JE, Nishimura DY, Alward WL, Hogan BL, John SW. Haploinsufficiency of the transcription factors FOXC1 and FOXC2 results in aberrant ocular development. *Hum Mol Genet.* 2000; 9:1021-32.
165. Soley GC, Bosse KA, Flikier D, Flikier P, Azofeifa J, Mardin CY, Reis A, Michels-Rautenstrauss KG, Rautenstrauss BW. Primary congenital glaucoma: a novel single-nucleotide deletion and varying phenotypic expression for the 1,546-1,555dup mutation in the *GLC3A (CYP1B1)* gene in 2 families of different ethnic origin. *J Glaucoma.* 2003; 12:27-30.

166. Sripriya S, Uthra S, Sangeetha R, George RJ, Hemamalini A, Paul PG, Amali J, Vijaya L, Kumaramanickavel G. Low frequency of myocilin mutations in Indian primary open-angle glaucoma patients. *Clin Genet*. 2004; 65:333-7.
167. Steger G. Thermal denaturation of double-stranded nucleic acids: prediction of temperatures critical for gradient gel electrophoresis and polymerase chain reaction. *Nucleic Acids Res*. 1994; 22:2760-8.
168. Stoilov I, Akarsu AN, Alozie I, Child A, Barsoum-Homsy M, Turacli ME, Or M, Lewis RA, Ozdemir N, Brice G, Aktan SG, Chevrette L, Coca-Prados M, Sarfarazi M. Sequence analysis and homology modeling suggest that primary congenital glaucoma on 2p21 results from mutations disrupting either the hinge region or the conserved core structures of cytochrome P4501B1. *Am J Hum Genet*. 1998; 62:573-84.
169. Stoilov I, Akarsu AN, Sarfarazi M. Identification of three different truncating mutations in cytochrome P450 1B1 (*CYP1B1*) as the principal cause of primary congenital glaucoma (buphthalmos) in families linked to the *GLC3A* locus on chromosome 2p21. *Hum Mol Genet*. 1997; 6:641-47.
170. Stoilov I, Jansson I, Sarfarazi M, Schenkman JB. Role of cytochrome P-450 in development. *Drug Metabol Drug Interact*. 2001; 18: 33-55.
171. Stoilov IR, Costa VP, Vasconcellos JP, Melo MB, Betinjane AJ, Carani JC, Oltrogge EV, Sarfarazi M. Molecular genetics of primary congenital glaucoma in Brazil. *Invest Ophthalmol Vis Sci*. 2002a; 43:1820-27.
172. Stoilov IR, Sarfarazi M. Third genetic locus (*GLC3C*) for primary congenital glaucoma (PCG) maps to chromosome 14q24.3. *Invest Ophthalmol Vis Sci*. 2002b; 43 E- Abstract 3015.
173. Stone EM, Fingert JH, Alward WL, Nguyen TD, Polansky JR, Sunden SL, Nishimura D, Clark AF, Nystuen A, Nichols BE, Mackey DA, Ritch R, Kalenak JW, Craven ER, Sheffield VC. Identification of a gene that causes primary open angle glaucoma. *Science*. 1997; 275:668-70.
174. Strungaru MH, Dinu I, Walter MA. Genotype-phenotype correlations in Axenfeld-Rieger malformation and glaucoma patients with *FOXC1* and *PITX2* mutations. *Invest Ophthalmol Vis Sci*. 2007; 48:228-37.
175. Sutter TR, Tang YM, Hayes CL, Wo YYP, Jabs EW, Li X, Yin H, Cody CW, Greenlee WF. Complete cDNA sequence of a human dioxin-inducible mRNA identifies a new gene subfamily of cytochrome P450 that maps to chromosome 2. *J Biol Chem*. 1994; 269: 13092-99.
176. Suzuki R, Hattori Y, Okano K. Promoter mutations of myocilin gene in Japanese patients with open angle glaucoma including normal tension glaucoma. *Br J Ophthalmol*. 2000; 84:1078.

177. Suzuki T, Takahashi K, Kuwahara S, Wada Y, Abe T, Tamai M. A novel (Pro79Thr) mutation in the FKHL7 gene in a Japanese family with Axenfeld-Rieger syndrome. *Am J Ophthalmol*. 2001; 132: 572-75.
178. Suzuki Y, Shirato S, Taniguchi F, Ohara K, Nishimaki K, Ohta S. Mutations in the TIGR gene in familial primary open-angle glaucoma in Japan. *Am J Hum Genet*. 1997; 61:1202-4.
179. Tamm ER. Myocilin and glaucoma: facts and ideas. *Prog Retin Eye Res*. 2002; 21: 395-428.
180. Tanaka Y, Sasaki M, Kaneuchi M, Shiina, Igawa M, Dahiya R. Polymorphisms of the CYP1B1 gene have higher risk for prostate cancer. *Biochem Biophys Res Commun*. 2002; 296: 820-26.
181. Tang YM, Wo YY, Stewart J, Hawkins AL, Griffin CA, Sutter TR, Greenlee WF. Isolation and characterization of the human cytochrome P450 CYP1B1 gene. *J Biol Chem*. 1996; 271:28324-30.
182. Tomarev SI, Wistow G, Raymond V, Dubois S, Malyukova I. Gene expression profile of the human trabecular meshwork: NEIBank sequence tag analysis. *Invest Ophthalmol Vis Sci*. 2003; 44: 2588-96.
183. Vasconcellos JP, Melo MB, Costa VP, Tsukumo DM, Bassères DS, Bordin S, Saad ST, Costa FF. Novel mutation in the MYOC gene in primary open glaucoma patients. *J Med Genet*. 2000; 37:301-3.
184. Vázquez CM, Herrero OM, Bastús BM, Pérez VD. Mutations in the third exon of the MYOC gene in spanish patients with primary open angle glaucoma. *Ophthalmic Genet*. 2000; 21:109-15.
185. Vijaya L, George R, Paul PG, Baskaran M, Arvind H, Raju P, Ramesh SV, Kumaramanickavel G, McCarty C. Prevalence of open-angle glaucoma in a rural south Indian population. *Invest Ophthalmol Vis Sci*. 2005; 46:4461-7.
186. Vincent AL, Billingsley G, Buys Y, Levin AV, Priston M, Trope G, Williams-Lyn D, Héon E. Digenic inheritance of early-onset glaucoma: CYP1B1, a potential modifier gene. *Am J Hum Genet*. 2002; 70:448-60.
187. Wang WH, McNatt LG, Shepard AR, Jacobson N, Nishimura DY, Stone EM, Sheffield VC, Clark AF. Optimal procedure for extracting RNA from human ocular tissues and expression profiling of the congenital glaucoma gene *FOXC1* using quantitative RT-PCR. *Mol Vis*. 2001; 7: 89-94.
188. Watanabe J, Shimada T, Gillam EM, Ikuta T, Suemasu K, Higashi Y, Gotoh O, Kawajiri K. Association of *CYP1B1* genetic polymorphism with incidence to breast and lung cancer. *Pharmacogenetics*. 2000; 10: 25-33.
189. Weih LM, Mukesh BN, McCarty CA, Taylor HR. Association of demographic, familial, medical, and ocular factors with intraocular pressure. *Arch Ophthalmol*. 2001; 119:875-80.

190. Weisschuh N, Dressler P, Schuettauf F, Wolf C, Wissinger B, Gramer E. Novel mutations of *FOXC1* and *PITX2* in patients with Axenfeld-Rieger malformations. *Invest Ophthalmol Vis Sci*. 2006; 47:3846-52.
191. Weisschuh N, Neumann D, Wolf C, Wissinger B, Gramer E. Prevalence of *myocilin* and *optineurin* sequence variants in German normal tension glaucoma patients. *Mol Vis*. 2005; 11:284-7.
192. Wells J, Wroblewski J, Keen J, Inglehearn C, Jubb C, Eckstein A, Jay, Arden G, Bhattacharya S, Fitzke F. Mutations in the human retinal degeneration slow (RDS) gene can cause either retinitis pigmentosa or macular dystrophy. *Nat. Genet*. 1993; 3:213-8.
193. Werck-Reichhart D, Feyereisen R. Cytochromes P450: a success story. *Genome Biol*. 2000; 1: 3003.1-3.
194. Whitlock JP Jr. Genetic and molecular aspects of 2, 3, 7, 8-tetrachlorodibenzo-p-dioxin action. *Annu Rev Pharmacol Toxicol*. 1990; 30:251-77.
195. Wiggs JL, Allingham RR, Vollrath D, Jones KH, De La Paz M, Kern J, Patterson K, Babb VL, Del Bono EA, Broome BW, Pericak-Vance MA, Haines JL. Prevalence of mutations in *TIGR/Myocilin* in patients with adult and juvenile primary open-angle glaucoma. *Am J Hum Genet*. 1998; 63:1549-52.
196. Wo YY, Stewart J, Greenlee WF. Functional analysis of the promoter for the human *CYP1B1* gene. *J Biol Chem*. 1997; 272:26702-7.
197. Yen YC, Yang JJ, Chou MC, Li SY. Identification of mutations in the *myocilin (MYOC)* gene in Taiwanese patients with juvenile-onset open-angle glaucoma. *Mol Vis*. 2007; 13:1627-34.
198. Yoon SJ, Kim HS, Moon JI, Lim JM, Joo CK. Mutations of the *TIGR/MYOC* gene in primary open-angle glaucoma in Korea. *Am J Hum Genet*. 1999; 64:1775-8.
199. Zenteno JC, Hernandez-Merino E, Mejia-Lopez H, Metias-Florentino M, Michel N, Elizondo-Olascoaga C, Kordu-Ortega V, Casab-Rueda H, Garcia-Ortiz JE. Contribution of *CYP1B1* mutations and founder effect to primary congenital glaucoma in Mexico. *J Glaucoma*. 2008; 17: 189-92.
200. Zheng W, Xie DW, Jin F, Cheng JR, Dai Q, Wen WQ, Shu XO, Gao YT. Genetic polymorphism of cytochrome P450-1B1 and risk of breast cancer. *Cancer Epidemiol Biomarkers Prev*. 2000; 9:147-150.
201. Zhuo YH, Wang M, Wei YT, Huang YL, Ge J. Analysis of *MYOC* gene mutation in a Chinese glaucoma family with primary open –angle glaucoma and primary congenital glaucoma. *Chin Med J*. 2006; 119: 1210-14.

## ANNEXURES

### ANNEXURE I

#### *Reagents used in DNA extraction*

Reagents	Methods of preparation
Phosphate buffer saline (PBS)	8 grams of sodium chloride (NaCl), 0.2 grams of potassium chloride (KCl) and 1.44 grams of sodium biphosphate (Na <sub>2</sub> HPO <sub>4</sub> ) were added to 800 milliliters (ml) of double distilled water. The pH of the solution was adjusted to 7.4 with 1M hydrochloric acid. The final volume of the solution was made to 1000 ml with autoclaved double distilled water. The final concentration of the solution was 10X. The working solution of 1X was prepared by diluting the stock solution with autoclaved double distilled water.
Extraction buffer	1 ml of 10 mM Tris chloride buffer (Tris Cl) (pH 8.0), 20 ml of 0.5 M ethylene diamene tetra acetate (EDTA) and 5 ml of 0.5 % sodium dodecyl sulphate (SDS) was added to 78.5 ml of autoclaved double distilled water to make the final volume to 100 ml.
RNase	100 milligrams (mg) of of Rnase (powdered form) was added to 10 ml of double distilled water to make a solution of concentration 10 mg / ml.
Proteinase K	100 mg of of proteinase K (powdered form) was added to 5 ml of autoclaved double distilled water to make a solution with a concentration of 20 mg / ml.
Saturated phenol	The phenol was melted at 68°C. To the melted phenol equal volume of 0.5 M Tris Cl was added. The solution was mixed thoroughly on a magnetic stirrer for 15 minutes. The solution was allowed to stand till the phases were separated. After the separation of the two phases the upper phase of Tris Cl was aspirated. Equal volume of 0.1 M Tris Cl was added to the phenol and again mixed thoroughly on a magnetic stirrer to separate the two phases. The final pH of the phenolic phase (lower phase) was 8.0.
10 mM of ammonium acetate	760 mg of ammonium acetate salt was added to 80 ml of autoclaved double distilled water. The solution was mixed thoroughly on a magnetic stirrer and the final volume was made up to 100 ml
Developing solution	3 ml of 10N NaOH, 400 µl of formaldehyde were added to 96.6 ml of distilled water to make a final volume of 100 ml.

**ANNEXURE II*****Reagents used in Agarose gel electrophoresis***

Reagents	Methods of preparation
Tris Borate Ethylene Diamine Tetra Acetate (TAE- 50X)	242g of Tris base, 57.1 ml of glacial acetic acid and 100 ml of 0.5M EDTA were added to 800 ml of autoclaved double distilled water. The solution was mixed thoroughly on a magnetic stirrer and the final volume was adjusted to 1000 ml with autoclaved double distilled water.
Ethidium bromide (EtBr- 1000X)	50 mg of EtBr was added to 100 ml of autoclaved double distilled water to make a stock solution of concentration 0.5mg/ml. This stock solution was diluted 1000 times with double distilled water to make the working solution of 0.5 ug/ml. EtBr was kept in glass bottle covered with aluminum foil because of its light sensitive nature.

## ANNEXURE III

**Reagents used in SSCP**


Reagents	Methods of preparation
39:1 acrylamide	Thirty-nine grams of acrylamide (Sigma – Aldrich, St. Louis, USA) and 1 gram of bisacrylamide ( were added to 100 ml of autoclaved distilled water. The solution was mixed thoroughly on a magnetic stirrer for 15 minutes. The final volume was adjusted to 200 ml with autoclaved distilled water and solution was kept at 4°C for further use.
10 X Tris Boric EDTA (TBE)	108 grams of Tris base, 55 grams of boric acid and 40 ml of 0.5M EDTA (ethylene diamine tetra acetate) were added to 700 ml of autoclaved distilled water. The solution was mixed thoroughly on a magnetic stirrer for 15 minutes. The final volume was adjusted to 1000 ml with autoclaved distilled water. The working solution of 0.5X was prepared by diluting the stock solution (10X TBE) with autoclaved double distilled water.
10% APS (Ammonium persulphate)	10 grams of APS was dissolved in 100 ml of autoclaved distilled water to make a 10% solution and stored at –20°C for further use.
2% silver nitrate solution	2 grams of silver nitrate was added to 80 ml of autoclaved distilled water. The solution was mixed thoroughly on a magnetic stirrer for 10 minutes. The final volume was adjusted to 100 ml with autoclaved distilled water.
10N sodium hydroxide solution (10 N NaOH)	55 grams of sodium hydroxide pellets were dissolved in 70 ml of autoclaved distilled water and the final volume was adjusted to 100 ml with autoclaved distilled water.
Fixative	10 ml of absolute alcohol and 0.5 ml of glacial acetic acid were added to 89.5 ml of distilled water to make a final volume of 100 ml.
Developing solution	3 ml of 10N NaOH, 400 µl of formaldehyde were added to 96.6 ml of distilled water to make a final volume of 100 ml.



**ANNEXURE IV*****Reagents used in dHPLC***

Reagents	Methods of preparation
Buffer A (0.1M TEAA with pH 7)	50 ml of 2M TEAA and 250 µl of acetonitrile were added to 900ml of HPLC graded water (Ranbaxy fine chemicals Ltd. New Delhi). The solution was transferred to an inverting flask (1000 ml KIMAX <sup>R</sup> , Kimble USA). After proper mixing the final volume was adjusted to 1 liter with HPLC grade water (Ranbaxy fine chemicals Ltd. New Delhi).
Buffer B (0.1M TEAA + 25% acetonitrile)	50 ml of TEAA and 250 ml of acetonitrile were added to 900ml of HPLC water. The solution was transferred to an inverting flask (1000 ml KIMAX <sup>R</sup> , Kimble USA). After proper mixing the final volume was adjusted to 1 liter with HPLC grade water.

## PUBLICATIONS

1.  *Molecular Vision* 2004; 10:696-702 <<http://www.molvis.org/molvis/v10/a84>>  
Received 27 July 2004 | Accepted 30 September 2004 | Published 30 September 2004

©2004 Molecular Vision

### Mutation spectrum of the *CYP1B1* gene in Indian primary congenital glaucoma patients

Aramati Bindu Madhava Reddy,<sup>1</sup> Kiranpreet Kaur,<sup>1</sup> Anil Kumar Mandal,<sup>2</sup> Shirly George Panicker,<sup>1</sup> Ravi Thomas,<sup>2</sup> Seyed Ehtesham Hasnain,<sup>3</sup> Dorairajan Balasubramanian,<sup>1</sup> Subhabrata Chakrabarti<sup>1</sup>

(The first two authors contributed equally to this publication)

#### Short Report

2. Myocilin gene implicated in primary congenital glaucoma

Kaur K, Reddy ABM, Mukhopadhyay A, Mandal AK, Hasnain SE, Ray K, Thomas R, Balasubramanian D, Chakrabarti S. Myocilin gene implicated in primary congenital glaucoma.

*Clin Genet* 2005; 67: 335–340. © Blackwell Munksgaard, 2005

3.  *Molecular Vision* 2005; 11:111-3 <<http://www.molvis.org/molvis/v11/a12>>  
Received 15 November 2004 | Accepted 4 February 2005 | Published 4 February 2005

©2005 Molecular Vision

3. Gln48His is the prevalent myocilin mutation in primary open angle and primary congenital glaucoma phenotypes in India

Subhabrata Chakrabarti,<sup>1</sup> Kiranpreet Kaur,<sup>1</sup> Sreelatha Komatireddy,<sup>1</sup> Moulinath Acharya,<sup>2</sup> Koilkonda R. Devi,<sup>1</sup> Arijit Mukhopadhyay,<sup>2</sup> Anil K. Mandal,<sup>3</sup> Seyed E. Hasnain,<sup>4</sup> Garudadri Chandrasekhar,<sup>3</sup> Ravi Thomas,<sup>3</sup> Kunal Ray<sup>2</sup>

**4. Globally, *CYP1B1* Mutations in Primary Congenital Glaucoma Are Strongly Structured by Geographic and Haplotype Backgrounds**

*Subhabrata Chakrabarti,<sup>1</sup> Kiranpreet Kaur,<sup>1</sup> Inderjeet Kaur,<sup>1</sup> Anil K. Mandal,<sup>2,3</sup> Rajul S. Parikh,<sup>3</sup> Ravi Thomas,<sup>2,3</sup> and Partha P. Majumder<sup>4</sup>*

Investigative Ophthalmology & Visual Science, January 2006, Vol. 47, No. 1  
Copyright © Association for Research in Vision and Ophthalmology

**5. Glaucoma-Associated *CYP1B1* Mutations Share Similar Haplotype Backgrounds in POAG and PACG Phenotypes**

*Subhabrata Chakrabarti,<sup>1</sup> Koilkonda R. Devi,<sup>1</sup> Sreelatha Komatireddy,<sup>1</sup> Kiranpreet Kaur,<sup>1</sup> Rajul S. Parikh,<sup>2</sup> Anil K. Mandal,<sup>2</sup> Garudadri Chandrasekhar,<sup>2</sup> and Ravi Thomas<sup>2</sup>*

Investigative Ophthalmology & Visual Science, December 2007, Vol. 48, No.  
Copyright © Association for Research in Vision and Ophthalmology

## PRESENTATIONS

Presented a paper (**Oral**) entitled “Molecular Genetics of Primary Congenital Glaucoma –Indian Scenario” for the Young Scientist Award Competition at the XXXIII Annual conference of the ISHG and International symposium on Genetics Revisited: the Genomics and Proteomics advantage, Andhra University, Visakhapatnam, AP, February 11 –13, 2008.

Presented a paper (**Poster**) entitled “Identification of *FOXC1* variations in Indian Primary Congenital Glaucoma (PCG) cases” at the 2<sup>nd</sup> World Glaucoma Congress held on 18<sup>th</sup> -21<sup>st</sup> July , Singapore, 2007.

Presented a paper (**Oral**) entitled “The C-G-G-T-A is the most predominant CYP1B1 haplotype associated with mutations in Primary Congenital Glaucoma” at the 14<sup>th</sup> Indian Eye Research Group Meet, Hyderabad July 2005.

Presented a paper (**Poster**) entitled "Phenotypic heterogeneity in Primary Congenital Glaucoma due to *MYOC* and *CYP1B1* gene mutations" at the International symposium on Human origins and genes, evolution and complex diseases held on 17<sup>th</sup> -19<sup>th</sup> February, 2005 at National Centre for Biological Sciences, Bangalore.

Presented a paper (**Poster**) entitled "Myocilin in PCG" at the 24<sup>th</sup> Annual Conference of Indian Society of Human Genetics held On 8<sup>th</sup>-11<sup>th</sup> January, 2004 at National Institute of Mental Health & Neurosciences, Bangalore.

Presented a paper (**Oral**) entitled "Involvement of Myocilin gene in Primary Congenital Glaucoma" at the 13<sup>th</sup> Indian Eye Research Group Meet, Chennai August 2004.

Presented a paper (**Oral**) entitled “Molecular Genetics of Primary Congenital Glaucoma: Impact of SNPs on haplotype background in Indian population” in the 12<sup>th</sup> Indian Eye Research group meet, Hyderabad.

## **AWARDS**

Recipient of the **Travel fellowship** provided by **Association of International Glaucoma Societies (AIGS)** to attend the World Glaucoma Congress meet held in Singapore, 2007.

Recipient of **Centre for Scientific and Industrial Research-Senior Research (CSIR-SRF) fellowship** (2005-2008)

**Qualified the Nation wide joint Centre for Scientific and Industrial Research / University Grant Commission / National Entrance test (CSIR/UGC/NET) and awarded with UGC-JRF scholarship, 2002.**

Recipient of **Gold medal** for securing 1<sup>st</sup> rank in post graduation **from Human dept, Guru Nanak Dev University, 2002.**

Recipient of **Gold medal** for securing 1<sup>st</sup> rank in graduation **from Human Genetics dept, Guru Nanak Dev University, 2000.**

**BRIEF BIOGRAPHY OF THE CANDIDATE**

KiranpreetKaur has been working at Kallam Anji Reddy Molecular Genetics Laboratory at LV Prasad Eye Institute for past five years. She joined this institute after her academic training (M.Sc. Human genetics) at Guru Nanak Dev University, Amritsar. She has been conferred with the University **'Gold Medal'** for her graduation and post graduation courses.

After joining LVPEI, she was involved in research related to 'Molecular Genetic Analysis of Primary Congenital Glaucoma'. She was also involved in teaching the graduate students at the Bausch and Lomb School of Optometry, LVPEI.

Her PhD work has been published in International journals of repute. She has presented her work in national and international scientific meetings. She presented her work at the **World Glaucoma Congress'07**, Singapore and was awarded with the **Travel Fellowship** by **Association of International Glaucoma Societies (AIGS)**.

## **BRIEF BIOGRAPHY OF THE SUPERVISOR**

Dr. Subhabrata Chakrabarti (b.1972) is a Research Scientist at the L.V. Prasad Eye Institute, Hyderabad, India, for the last 7 years. He obtained his Ph.D. in human genetics and was also a visiting scientist at the prestigious National Eye Institute at NIH, USA (2006). He has done some pioneering work in the area of molecular genetics of eye diseases in India. His main thrust lies in understanding the molecular mechanisms underlying complex ocular diseases like glaucoma, anterior segment disorders, age-related macular degeneration (AMD) and myopia.

Dr. Chakrabarti collaborates widely with his peers within and outside the country and has lectured at all the major eye institutes in the world. All his research works have been done in India and published in peer reviewed international journals. He is an editorial board member for two journals and a reviewer for 13 other international journals and various granting agencies. His research work has been funded through competitive extramural research grants from various international and national funding agencies. He has organized scientific conferences, chaired sessions, conducted workshops and presented widely at the international and national levels.

His research works been widely acknowledged and the Association of International Glaucoma Societies (AIGS) gave him the Clinician Scientist Award in 2005. He has also been awarded with the Associateship of the Indian Academy of Sciences (2004), Indian National Science Academy (INSA) medal for Young Scientist (2006) and the Platinum Jubilee Award of the National Academy of Sciences India (2007).

Dr. Chakrabarti is a Ph.D. examiner and supervisor for the University of Melbourne, Australia, BITS, Pilani and the University of Hyderabad, Hyderabad. He has supervised three Ph.D. candidates and a post-doctoral fellow. He is a member of several national and international professional bodies, notable among them being the advisory board member of the World Glaucoma Association and executive council member of the Indian Society of Human Genetics. Currently he is a chair of the scientific committee and a member of the ethics committee of the Institutional Review Board.